Investigation of Corrosion Protection Systems for Bridge Stay Cables

Volume Two

by

Homer Robert Hamilton III, B.S.C.E., M.E.

Dissertation

Presented to the Faculty of the Graduate School of

The University of Texas at Austin

in Partial Fulfillment

of the Requirements

for the Degree of

Doctor of Philosophy

The University of Texas at Austin

December 1995

Investigation of Corrosion Protection Systems for Bridge Stay Cables

Approved by
Dissertation Committee:

_____
John E. Breen, Co-Supervisor

_____
Karl H. Frank, Co-Supervisor

_____
Harovel G. Wheat

_____
Michael D. Engelhardt

_____
Richard E. Klingner

to Nancy

Acknowledgments

This dissertation is based on research conducted for the Texas Department of Transportation and the Federal Highway Administration at the Phil M. Ferguson Structural Engineering Laboratory at the University of Texas at Austin. The assistance and support provided by Lisa Carter-Powell and Jeff Wouters from TxDOT are greatly appreciated.

I would like to thank Richard Klingner and Mike Engelhardt for serving on my committee and providing guidance with my dissertation, and Harovel Wheat for sharing her expertise in the field of durability and for providing guidance in corrosion testing techniques. I would also like to thank Karl Frank for sharing his experience with stay cables and for his knowledge of the "nuts and bolts" of experimental work. A special thanks goes to Jack Breen for his patience and gentle, ever-present pressure to push myself beyond my present limits. His enthusiasm for engineering and life in general is infectious to all who are fortunate enough to work with him. I am especially grateful for his special understanding of the difficulties of juggling graduate school and family responsibilities and for the support he provided with that task.

This research project required many hours of manual labor, many of which were performed in the heat of the storage building ("the oven"). I am indebted to Driss Najah, Mark Clarke and David Vliet for the use of their strong backs, but more importantly for their good humor and helpful suggestions that made laborious tasks somewhat more pleasant. I would also like to thank those who "volunteered" to help with injecting the grout. It was a dirty, lackluster job that required more time for clean-up than anything else.

Research project 1264 had several areas of focus, each assigned one or more graduate students. As a member of "Team 1264" I had the pleasure of working with Rodney Davis, William Kittleman, and Rene Vignos. I enjoyed working with these guys and value the friendships that we developed during that time.

I have found the students here at Ferguson Laboratory to be a "breed apart." It was most enjoyable to work in an atmosphere of cooperation and communal effort. Help was always there for the asking. The many friendships made during this journey, I know, will last a lifetime. While I can't name everyone that I would like here, I especially value the friendships I've developed with Wayne Clendennen, Reed Freeman, Todd Helwig, Willy Ramirez, Carin Roberts, and Karen Ryals.

I would like to express my gratitude to Blake Stasney, Pat Ball, Wayne Fontenot, Wayne Little, Ryan Green, and Ray Madonna for their helpfulness and advice. I am also grateful to April Jenkins and Sharon Cunningham for their helpful assistance. A special thanks goes to Laurie Golding who so skillfully navigates the treacherous waters of equipment purchasing.

My deepest appreciation goes to my parents who have provided much needed encouragement and reassurance during this endeavor.

Saving the best for last, I want to thank my best friend, Nancy (she also happens to be my wife). Although, somehow my "thank you" pales in comparison to the sacrifices she made in allowing me to pursue this dream. I can still remember the shocked look in her eyes when I told her that I wanted to quit my job, sell our house, live in a tiny apartment and to graduate school. It's a wonder I'm still alive; but never a complaint. In fact, she made what could have been a miserable experience into a fantastic adventure for our family, the memories of which I cherish as the best in my life. I dedicate this work to Nancy for her endless patience, understanding, support, and sacrifice without which this would not have been even remotely possible, and to the two wonderful sons she has given me, Travis and Logan, who have brought much joy to my life.

Austin, Texas Trey Hamilton
August, 1995

Table of Contents

Appendix A
Stay Cable Survey Data

A.1 Sample Questionnaire (see Figure A.1 on page 291)

A.2 Results of Survey

A.3 List of Respondents (see Figure A.31 on page 375)

Figure A.1 - Sample Survey

Figure A.2 - Response to Question 1.1.

Figure A.2 - Response to Question 1.1.

Figure A.2 - Response to Question 1.1.

Figure A.3 - Response to Question 1.2.

Figure A.3 - Response to Question 1.2.

Figure A.3 - Response to Question 1.2.

Figure A.4 - Response to Question 1.3.

Figure A.4 - Response to Question 1.3.

Figure A.4 - Response to Question 1.3.

Figure A.5 - Response to Question 1.4.

Figure A.5 - Response to Question 1.4.

Figure A.5 - Response to Question 1.4.

Figure A.5 - Response to Question 1.4.

Figure A.5 - Response to Question 1.4.

Figure A.5 - Response to Question 1.4.

Figure A.6 - Response to Question 1.5.

Figure A.7 - Response to Question 1.6.

Figure A.8 - Response to Question 2.1.

Figure A.8 - Response to Question 2.1.

Figure A.8 - Response to Question 2.1.

Figure A.9 - Response to Question 2.2.

Figure A.9 - Response to Question 2.2.

Figure A.9 - Response to Question 2.2.

Figure A.10 - Response to Question 2.3.

Figure A.10 - Response to Question 2.3.

Figure A.10 - Response to Question 2.3.

Figure A.11 - Response to Question 2.4.

Figure A.11 - Response to Question 2.4.

Figure A.11 - Response to Question 2.4.

Figure A.12 - Response to Question 2.5.

Figure A.12 - Response to Question 2.5.

Figure A.12 - Response to Question 2.5.

Figure A.12 - Response to Question 2.5.

Figure A.13 - Response to Question 2.6.

Figure A.14 - Response to Question 2.7.

Figure A.15 - Response to Question 2.8.

Figure A.15 - Response to Question 2.8.

Figure A.15 - Response to Question 2.8.

Figure A.16 - Response to Question 3.1.

Figure A.16 - Response to Question 3.1.

Figure A.16 - Response to Question 3.1.

Figure A.17 - Response to Question 3.2.

Figure A.17 - Response to Question 3.2.

Figure A.17 - Response to Question 3.2.

Figure A.18 - Response to Question 3.3.

Figure A.18 - Response to Question 3.3.

Figure A.18 - Response to Question 3.3.

Figure A.18 - Response to Question 3.3.

Figure A.19 - Response to Question 3.4.

Figure A.20 - Response to Question 4.1.

Figure A.20 - Response to Question 4.1.

Figure A.20 - Response to Question 4.1.

Figure A.21 - Response to Question 4.2.

Figure A.21 - Response to Question 4.2.

Figure A.21 - Response to Question 4.2.

Figure A.22 - Response to Question 4.3.

Figure A.22 - Response to Question 4.3.

Figure A.22 - Response to Question 4.3.

Figure A.23 - Response to Question 4.4.

Figure A.23 - Response to Question 4.4.

Figure A.23 - Response to Question 4.4.

Figure A.24 - Response to Question 4.5.

4.5 If you use or specify cement grout as a blocking compound, indicate whether admixtures are specified and indicate what admixtures you have used or approved.

Grout Admixture	No. of Times Mentioned
Low Bleed	5
Sika 300SC	3
Presy 317.10	2
Conbex 208	2
Water reducing.	2
Tricosal 181	3
W/R Grace plasticizer	1
WRDA-19	3
Expansive agent	7
Retardant	1
Corrosion Inhibitor	2
Grace Darvair	1
Master Builders MBVR	1
Beto-kem Invert	1
Flow Cable (Master Builders)	1
Halliburton grout system.	1
Use performance specification requiring strength, pumpability, and bleed limit	1
Would not specify a cement grout	4
No Admixture	2

Figure A.25 - Response to Question 5.1.

Figure A.26 - Response to Question 5.2.

Figure A.27 - Response to Question 6.1.

Figure A.27 - Response to Question 6.1.

Figure A.27 - Response to Question 6.1.

Figure A.28 - Response to Question 6.2.

Figure A.29 - Response to Question 6.3.

6.3 What stay cable suppliers and systems do you recognize or have you used?

Manufacturers listed by respondents are presented below along with the number of times the name was mentioned:

Manufacturer	No. of Times Mentioned
VSL	38
BBR	27
DSI	26
Freyssinet	23
Stronghold	14
Bridon	6
Shinko Wire	5
SEEE Shin-kozogijutsu	4
New PWS Nippon Steel	4
Stahlton (BBRV)	4
Thyssen	3
Nippon Steel	3
British Ropes	3
Arbed	2
Pfeifer	2
Prescon	2
Mitsubishi Steel Co. of Japan	1
Trefilunion	1
Kobe Steel Co.	1
Wire Rope Industries	1
McCalls SP	1
FKK	1
PSC	1

Many systems and components were listed in this section. To reduce the volume without losing the essence of the response the system descriptions have been abbreviated to the description of the tension element:

Parallel strand	44
Epoxy-coated strand	3
Greased and sheathed strand	3
Parallel wire	16
Galvanized wire	6
Long lay parallel wire	2
Parallel bar	9
Locked-coil	5

Figure A.30 - Response to Question 7.1.

7.1 Please list past/recent experience, positive or negative, with stay cable projects related to any of the above items 1 through 6.

In this question it was intended that the respondent relate their project experience with the systems they had listed in question 6.3. I most cases the respondents simply listed their experience with cable stayed bridges in general. Selected excerpts of these comments are presented below:

- Hi-Am is expensive but saves money in erection costs.
- Epoxy coating : Does not work as a barrier; wedges don't bite at low stress levels; epoxy tears at wedges; epoxy quality is variable.
- Greased and sheathed system: question safety index relative to bonded system.
- Corrosion inhibiting capability of VSL non-grout system is somewhat doubtful.
- Prefabricated long lay galvanized wire cable with directly extruded PE jacket is becoming mainstream in Japan. All properties provided: length tolerance, fatigue, corrosion resistance.
- Long life experience with suspension systems of all types leads to the conclusion that the best approach is to use 110 years of successful experience as establishing the validity of (?) practices, modified as required to (?) the added requirements for the service. Prestressed concrete practice is not a good guide in this case.
- Difficult to get good information from some manufacturers during design.
- Installation done by structural steel erector who had no appreciation for care required in handling HDPE pipes.
- Fabricator had difficulty getting repeatable results for epoxy resin/steel ball flexural and compressive tests.
- Good experience with locked coil (galvanized).
- In Portugal two bridges use galvanized greased and sheathed strand with out external pipe but cables are noisy. Strands clap together.
- Feel that epoxy coating system is flawed.
- Using epoxy coated (Flo-Fil) and greased and sheathed system. Feel these increase the level of protection.
- Cement grout composition should be further studied to eliminate possible corrosive action.

- Research is needed in Anchorage area fill mix in the ? of wedge anchoring system is needed.

- Very difficult to convince workers of importance of careful handling of stay (erection, grouting, and tensioning).

- Farø Bridge (1985) - Oscillation problems. These are typical of sheathed heavy grouted stays.

- Wye Bridge (1966) - Complete stay replacement at 20 years due to inability to inspect/maintain inner strands.

- Survey does not address rain vibration and HDPE shapes which might solve this problem.

- Stahlton system: Needs strengthening at neoprene washers in steel trumpets. Only small relative movement between PE and neoprene will cause overheating and melting of PE. stainless steel sheet and PTFE is used. Inspection limited.

- Locked coil needs painting regularly. Not easy in windy or rainy conditions.

- Generally stay vibration is a problem. Most big bridges seem to require damping/stiffening of stays. Suppliers should be more aware of this problem and develop suitable details.

- Quincy - First use of epoxy strand pushed in strand by strand.

- Dame Point - Bars with steel sheathing. Fabricated on site and installed as a unit no problems. Short time.

- Alamillo Bridge - Epoxy coated (Flo-Fil) with HDPE sheathing. No filling in free length zone. Expensive installation procedure of cable. Fabricated on site before installation.

- Paterna Bridge - Cables with waxed monostrands and red HDPE sheathing. No filling material in free length., Easy installation of prefabricated cable with spreader beams.

- Clark Bridge - Epoxy coated, cement grout, HDPE sheathing, saddles. Problems in first fatigue tests. Field problems due to minimum supplier involvement.

- Parallel prestressing wire cable with alloy socket. Nippon steel. Dolson Grand Bridge, South Korea.

- Parallel strand, Freyssinet, West Sea Great Bridge.

- Parallel wire, Hi-Am: Advantages: High stress range, very reliable. Disadvantages: Usually with cement grouting (negative) can so far only be supplied with Black PE Pipe (aesthetics).

- Locked Coil: Advantages: Smallest diameter, Easy to paint any color. Disadvantages: Delicate as far as corrosion protection of anchorage zone is concerned. In large cables the outer layer of "Z" wires may jump out of position thus losing the natural corrosion protection.

- Strands: Advantages: Most economical, permits individual stressing. Disadvantages: Stress range somewhat smaller than wire. The very thin wires forming the strands are very susceptible to corrosion if not properly protected.

- Bars: Advantages: Relatively good natural corrosion resistance (large diameter; lower grade of steel). Disadvantages: Can only be supplied on drums when bar diameter is less than 16 mm or else must be coupled (negative).

- Experience with Dwidag good except with field control of coupler installation.

- Parallel strand, cement grout, HDPE (VSL): Problems meeting full size fatigue test criteria.

- Strand, cement grout, HDPE (Stronghold): Problems with pushing strand at site, sheath diameter too small, strand snaked contractor insolvency.

- BBR parallel wire, cement grout, HDPE: Good experience, expensive.

- Bridon long lay galvanized bridge strand, wax blocking HDPE sheathing: Good system, problems in quality control during socketing.

- Nippon long lay galvanized bridge strand wax HDPE sheath: Excellent.

- Galvanized Bridge Strand in HDPE sheath: Excellent condition 26 years after installation.

- Two cable stayed bridges have good experience. Had problems with slippage on wedges but increased pressure which solved problem.

- British manufacturers use hot-dip galvanizing. There have been no known cases of hydrogen embrittlement.

- Due to vibrations from wind, bending fatigue tests are performed. Dampers are installed.

- At design stage have found it necessary to keep options open to permit use of alternate systems.

- Galvanized parallel prestressing wire covered by PE is produced in the factory and transported to the site. It is important not to hurt during erection. In this case the diameter of PE pipe is less than that of injection type.

Figure A.31 - List of Respondents to Stay Cable Survey.

Jean-Phillipe Fuzier
Freyssinet International
Vélizy, France

Ronald J. Bonomo
Dywidag Systems Intl. USA, Inc.
Bolingbrook, IL
USA

D.C.C. Davis
Acer Consultants Pte. Ltd.
Surrey, Great Britain

Lau Joo Meng
Housing and Development Board
Signapore

Jim Roberts
California Dept. of Transportation
Sacramento, CA
USA

Steinmann
Tallahassee, FL
USA

Alan Matejowsky
Texas Dept. of Transportation
Austin, TX
USA

Maurice D. Miller
Howard, Needles, Tammen and Bergendoff
Kansas City, MO
USA

Juan Murillo
T.Y. Lin International
San Francisco, CA
USA

Mark J. Sofia
Vijay Chandra
Parsons Brinckerhoff
Ft. Myers, FL
USA
Allan H. Walley

Washington State Dept. of Transportation
Olympia, WA
USA

David Goodyear
DGES
Olympia, WA
USA

Arvid Grant
Arvid Grant & Associates, Inc.
Olympia, WA
USA

Walter Podolny, Jr.
Federal Highway Administration
Washington, D.C.
USA

Daniel Tassin
J. Muller International
San Diego, CA
USA

Ki-Chul, Cho
Dae-Lim Industrial Co. Ltd.
Seoul, Korea

Hugh S. G. Knox
Bridge Engineering Consultant
North Yorkshire, Great Britain

J.L. Canclo Martins
Rua Ricardo Espirito Santo 9
Lisboa, Portugal
Robin Sham
Maunsell Consultancy Services, Ltd.
London, England
United Kingdom

Anton Petersen
COWI Consult A/S
Lyngby-Copenhagen, Denmark

Johs Holt
Wdm. Thranes Gr.75

Oslo, Finland

Jorge M. Schlaich
Schlaich, Bergemann und Partner
Stuttgart, Germany

S. Strathopoulos
Domi SA
Athens, Greece

Torsten Lunabba
Finnish Road Administration
Helsinki, Finland

Gemeetewerken Rotterdam
Rotterdam, Netherlands

Clifford L. Freyermuth
Clifford L. Freyermuth, Inc.
Phoenix, AZ
USA

Kent Preston
Wiss, Janney, Elstner & Assoc.
Moorestown, NJ
USA

Peter Marti
Swiss Federal Institute of Technology
Zürich, Switzerland

Walther René
Ècole Polytechnique Fèdèrale de Lausanne
Lausanne, Switzerland
James P. McCafferty
Scott Wilson Kirkpatrick
Glasgow, Scotland

Mr. Donzel
Swiss Federal Highways Office
Bern, Switzerland

Franz A. Zahn
VSL International Ltd.
Berne, Switzerland

Shoji Ikeda
Yokoham National University
Yokohoma, Japan

Shoshi Kashima
Tsuyoshi Matsumoto
Honshu-shikoku Bridge Authority
Tokyo, Japan

Makoto Kanamori
Nihon Tetsudo Kensetsu Kodan
Tokyo, Japan

Tadayoshi Ishibashi
Higashinihon Ryokyaku Tetsudo Co.
Tokyo, Japan

Tsutomu Sato
Tetsudo Sogo Gijutsu Kenkyu-sho
Rosen Kouzou Kenkyu-shitsu
Tokyo, Japan

Shigenori Nakahara
JR Higashi Nihon Consultants Co.
Tokyo, Japan

Toshio Ichihashi
Taisei Corporation
Tokyo, Japan

Munetaka Kubota
Kajima Corporation
Tokyo, Japan
Motohiko Suzuki
Oriental Kensetsu Co.
Tokyo, Japan

Akibumi Masuda
Shinko Kosen Kogyo Co.
Amagasaki, Japan

Y. Nojiri
Kasima Technical Research Institute
Tokyo, Japan

Louis A. Garrido
Baton Rouge, LA
USA

Heinrich Hochreither
Dyckerhoff & Widmann, AG
Munich, Germany

Ernst H. Petzold III
Sverdrup Corporation
St. Louis, MO
USA

H.S. Russell
Construction Technology Laboratory
Skokie, IL
USA

Morris Schupack
Schupack Suarez Engineers, Inc.
South Norwalk, CT
USA

Khaled Shawwaf
Dywidag Systems International USA, Inc.
Flushing, NY
USA

Holger S. Svensson
Leonhardt, Andra und Partner
Stuttgart, Germany

Yoshito Tanaka
Shinko Wire Company Limited
Amagasaki, Japan
N. Winkler
Bureau BBR Ltd.
Zurich, Switzerland

David T. Swanson
VSL Corporation
Campbell, CA
USA

Niels Gimsing
ABK, Dth
Lyngby, Denmark

Ray Wedgewood
Roads and Traffic Authority
Sydney NSW
Australia

Bernard Shepherd
Corcoran Shepherd
Box Hill VIC
Australia

Rex Atkins
VIC Roads
Kew VIC
Australia

Peter R. Taylor
Buckland & Taylor, Ltd.
N. Vancouver B.C.
Canada

Appendix B
Portland Cement Grout Series-Test Methods

B.1 General

This section describes in detail the procedures used to perform the grout tests discussed in Chapter Five. "Mix" or "mix number" indicates a specific mix design which has a unique combination of materials. These mixes are presented in Table 5.1 in Chapter Five. A "test" or "test number" refers to a test conducted using a particular mix. The test is assigned a number which matches the mix number. Letters are appended to the mix number to indicate subsequent tests. For example, if four tests were conducted with mix 19, then they would be assigned test numbers 19, 19a, 19b, 19c.

B.2 Grout Preparation

All specimens in a test were grouted at the same time from the same grout mix using the following procedures:

1. Water, cement and admixture quantities were measured by weight prior to initiation of mixing.
2. Quantities of grout depended on which tests were being conducted. When all test methods were to used to test the grout mix then 7 liters (l) of grout were mixed using a five gallon (18.9 l) bucket with the HS type mixer blade turning at 1700 rpm. When only the grout pressure test was conducted then 1.9 l of grout was mixed in a 6 x 12 (152-mm diameter x 305-mm long) concrete cylinder mold using PS type mixer turning at 1200 rpm. Because of the small quantity of grout it was necessary to reduce the mixing speed to prevent splashing.
3. The water was placed in the mixing container and the Sikament 300SC (when used) admixture was added. The mixer was started and the addition of the cement was started immediately. The cement was added slowly enough to allow thorough mixing to occur. Silica fume (when used) was blended with the cement prior to adding to the mixing water.
4. Following addition of the cement any other admixtures to be used were added in accordance with the manufacturers' instructions. Total mixing time was 2-3 minutes.

B.3 Grout Pressure Test

B.3.1 Test Setup

B.3.1.1 Original Test Method

A bleed test was developed by Schupack which evaluates the bleed properties of the grout under pressurized conditions.[101] The test was designed to simulate the conditions of the grout at the bottom of 61-m tall post-tensioning ducts in nuclear cooling towers.

The test apparatus consisted of a 47-mm diameter filtration funnel with a 200-ml capacity and was manufactured by Gelman Sciences (Figure B.1). The filter is manufactured for use in rapid batch filtration of bacteriological or cell culture media, food fluids, viscous oils, hydraulic fluids, or lubricants. The filter funnel had a stainless steel screen to support the filter paper which was placed in the bottom of the filter. Funnel stems were provided to connect the air supply to the funnel in order to pressurize the grout. Borosilicate glass fiber filters (Gelman Type A/E) were placed in the bottom of the funnel to provide the media for filtering the water out of the grout. The filters have a nominal retention rating of 95% of all solids with a diameter greater than 1 μm.

The original test concept was to simulate the filtering action that occurs when the bleed water seeps into the space between the wires of the strands. A sample of grout is placed in the filter funnel and air pressure of 552 kPa is applied to the grout. The filter paper simulates the filtering action that the strand wires have on the grout. The level of pressure used in the filtration test was based on the net pressure at the bottom of a 61 m vertical tendon.

B.3.1.2 Modified Test Method

PTI *Recommendations for Stay Cable Design, Testing and Installation* restricts the maximum vertical height of grout lifts in polyethylene pipe to 38 m.[28] This is less than the 61 m tendon height assumed for the original test procedures. As a result, the pressure at which the grout was rated was reduced correspondingly. Figure B.2 shows the derivation of the pressure at which the amount of bleed from each mix was compared. The grout unit weight for a water and cement mixture with a w/c ratio of 0.40 is 1950 kg/m^3. The net fluid pressure which exists at the interface between the grout and bleed water can be calculated by subtracting the unit weight of grout from water. If it is assumed that the strand acts as a filter which prevents cement particles from entering the wire interstices but allows water to pass freely, then the net pressure at the interface between the water and grout is 354 kPa.

Currently there are no recommendations which specify a maximum amount of bleed allowed in the grout pressure test. The PTI *Recommended Practice for Grouting of Post-Tensioned Prestressed Concrete* suggests that the bleed in a test similar to the ASTM C940 test method be no more than 2% of the volume of the sample.[128] Due to the lack of recommendations available for the maximum amount of bleed under pressure, it was decided that the amount recommended by the PTI specification would be adopted. That is, the total bleed water must be less than or equal to 2% of the sample volume of grout at the end of the 3 minute hold period at 354 kPa in the bleed under pressure test. This created a standard which was used to develop and objectively select the optimum anti-bleed grout mix (OAG).

B.3.2 Test Procedure

1. Place filter media in filter funnel. Insert screen first then filter (woven side against filter paper) and finally the PTFE gasket. Screw cap on hand tight.
2. Fill with 200 ml of freshly mixed grout.
3. Place filter funnel on top cap hand tight.
4. Place filter funnel in frame. Make sure air supply valve is off and connect air supply.
5. Test pressure regulator up to 552 kPa and back down to zero.
6. Ten minutes after filling with grout, open air supply valve and increase pressure in 69.0 kPa increments and hold for 3 minutes at each increment. Record volume of bleed after each increment.
7. Stop at 552 kPa and hold pressure steady for 30 minutes.

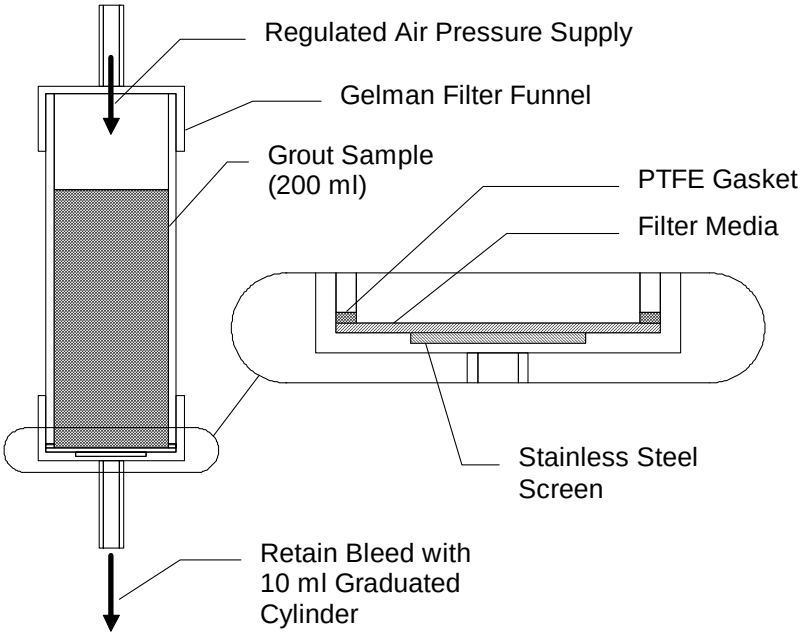

(a) Gelman Pressure Filter.

(b) Grout Pressure Test Setup.

Figure B.1 - Grout Pressure Test.

8. Record pressure at which bleed first occurs and volume of bleed water at 15 and 30 minutes after reaching 552 kPa.
9. Terminate test after 30 minutes at 552 kPa or when sample can not hold pressure. This is indicated by a hissing sound from the mouth of the funnel and foaming.

B.4 ASTM Expansion and Bleed Test

As a comparison for the results of the grout pressure test the ASTM standard test method for bleed was chosen. This test gives additional data on the bleed properties of the grout under atmospheric conditions. The test method was modified slightly by placing a bundle of strand in the graduated cylinder.

B.4.1 ASTM Standard Test Method

ASTM C940-87 *Expansion and Bleeding of Freshly Mixed Grouts for Preplaced-Aggregate Concrete in the Laboratory* gives a simple method for determining bleed of grouts which are not under pressure.[13] The method requires filling a 1000 ml graduated cylinder with 800 ± 10 ml of fresh grout. The top level of the grout is monitored for bleed water over a specified time period. In an effort to more closely simulate the conditions under which the grout will be used, a modification to this method was made.

B.4.2 Modified ASTM Test Method

The standard test method was modified by placing three 0.5-inch diameter 7-wire strand bundled together inside the graduated cylinder immediately after the grout had been introduced. The volume of grout added to the cylinder was adjusted slightly to prevent overflow when the strands

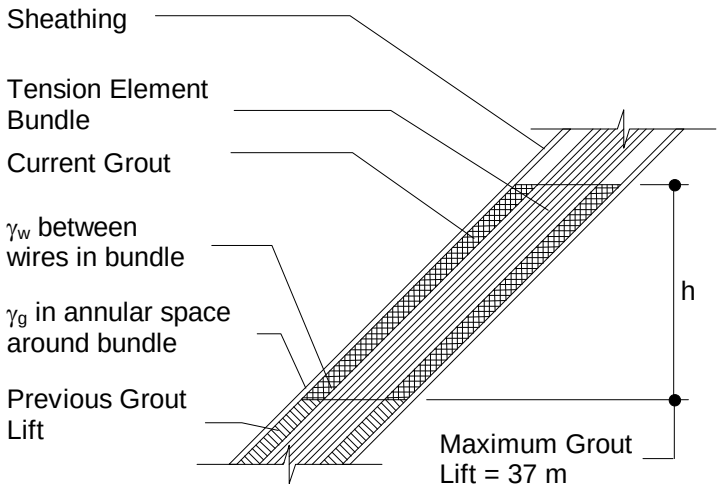

γ_g = Density of Grout (1950 kg/m^3)
γ_w = Density of Bleed Water (1000 kg/m^3)
h = Height of Lift (38 m)
Net pressure, p, at the base of the grout column can be calculated from:

$$p = h(\gamma_g - \gamma_w) = 354\ kPa$$

Figure B.2 - Derivation of Pressure for Grout Pressure Test.

were placed in the cylinder. Inserting the strands in the grout intensified the tendency of the grout to bleed. Ghorbanpoor and Madathanapalli performed similar bleed tests by filling a 2-in. diameter plexiglass tube with 39.4 in high column of grout.[52] A bundle of three strands were placed in the grout immediately after filling. Measurements were taken at intervals specified in the ASTM test method.

The revised test method is as follows:

1. Fill graduated cylinder to 700 ml ±10 ml with freshly mixed grout.
2. Place the three-strand bundle in graduated cylinder.
3. Record volume of sample and time.
4. Place strand centering device on strands.
5. Take readings at 15, 30, 45 min. and 1, 2, hr. etc. until two successive readings show no further expansion or bleeding. Two volumes are to be taken at each interval. The volume at the top of sample and the volume at the interface between the bleed water and grout.
6. Decant bleed water into graduated cylinder and record volume.
7. Retain bleed water in appropriate container.

B.5 Flow Cone Test

ASTM C 939-87 *Standard Test Method for Flow of Grout for Pre Placed-Aggregate Concrete (Flow Cone Method)* was used to test the flowability of the grout in the fresh state.[12] The flow cone used to perform this test is of aluminum construction and was placed in a wood frame during the test performance. The grout was placed in the flow cone at some time after mixing. The discharge of the cone was opened and the grout was allowed to pour out of the cone. The timer was started when the discharge was opened. The timer was stopped when a break in the stream of the flow cone was noted. When the inside of the cone was inspected and light could be seen through the discharge hole then the test was considered successful. However, if the grout was too thick and did not completely evacuate the cone then the tests was null. There were other standard test methods available for testing highly viscous grouts. However, pumpability of the grout is questionable if the grout does not give a valid test in the flow cone. Therefore, it was decided that this test would serve as a benchmark of the flowability of the grout. If the grout could not be tested using the flow cone method, then the mix design was eliminated from consideration.

B.6 Initial Set

Although not of primary importance in grout for post-tensioning and stay cable applications, it is a minimum requirement that the grout remain fluid for a length of time necessary to complete mixing and injection with a little extra time for contingencies such as equipment failure. However, the grout must not delay set for too long.

ASTM C191-92 *Time of Set for Hydraulic Cement by Vicat Needle* was used to evaluate the initial time of set for the grout.[11] This gave an indication of the accelerating or retarding nature of the admixtures in the grout test mixes. In lieu of the final set and to give an indication of early strength gain, compressive strength tests were run at 24 hours. In a similar manner to grouting multiple lifts, the previous lift would be checked for strength prior to placement of the next lift.

B.7 Compressive Strength

ASTM C109-90 Compressive Strength of Hydraulic Cement Mortars (Using 2-in. or 50-mm Cube Specimens) was used to determine the compressive strength of the grout.[10]

B.8 pH Test

Alkalinity of the fresh grout was tested using pH paper with the range of 12.5-14. This test was not a part of the regular bank of tests run on each grout. The pH was taken only on selected tests.

B.9 Cement Mill Reports

Cement was obtained in bulk from the Balcones Plant of the LaFarge Corporation located in New Braunfels, Texas. There were two different batches of cement used in the test program. The first batch (Figure B.3) was used in all of the grout development tests presented in Chapter Five. This batch was also used to mix the grout for specimens LS-1 through 4 of the large scale test series presented in Chapters 7-9. The second batch of cement (Figure B.4) was used to mix the grout for the Modified ACTM in Chapter Six and specimens LS-5 through 8 of the large scale test series.

B.10 Strand Material Properties

Results of chemical tests performed on all of the prestressing strand used are given in Table B.1 and Table B.1. Mill certificate test results are listed in Table B.2. Strand from reel 1 was used for large scale tests LS-1 through 4 and for a portion of the Modified ACTM tests (see Chapter Six for details). Strand from reel 2 was used in specimen LS-5.

Figure B.3 - Cement Mill Test Report for First Batch.

Figure B.4 - Cement Mill Test Report for Second Batch

Table B.1 - Results of Chemical Analysis of Strand (% by weight).

Elements	Bare Strand Reel 1		Bare Strand Reel 2		Galvanized Strand	
	Center wire	Outer wire	Center wire	Outer wire	Center wire	Outer wire
Carbon	0.82	0.81	0.78	0.76	0.81	0.81
Manganese	0.83	0.83	0.68	0.75	0.78	0.71
Phosphorus	0.007	0.012	0.006	0.012	0.006	0.007
Sulfer	0.009	0.011	0.005	0.010	0.011	0.005
Silicon	0.22	0.25	0.26	0.16	0.022	0.20
Nickel	0.05	0.03	0.04	0.03	0.02	0.03
Chromium	0.03	0.18	0.03	0.16	0.01	0.01
Molybdenum	0.01	0.01	< 0.01	< 0.01	0.01	< 0.01
Copper	0.08	0.08	0.10	0.08	0.05	0.06
Aluminum	< 0.005	< 0.005	< 0.005	< 0.005	< 0.005	< 0.005
Vanadium	0.054	0.065	0.077	0.059	0.043	0.039
Niobium	< 0.005	< 0.005	< 0.005	< 0.005	< 0.005	< 0.005
Boron	< 0.0005	0.0005	< 0.0005	< 0.0005	< 0.0005	< 0.0005

Table B.1 - Results of Chemical Analysis of Strand (% by weight).

Elements	Epoxy-Coated		Epoxy-Coated and Filled		Greased and Sheathed	
	Center wire	Outer wire	Center wire	Outer wire	Center wire	Outer wire
Carbon	0.82	0.80	0.79	0.80	0.78	0.80
Manganese	0.84	0.83	0.76	0.86	0.77	0.76
Phosphorus	0.015	0.019	0.007	0.005	0.012	0.011
Sulfer	0.010	0.014	0.010	0.008	0.012	0.010
Silicon	0.20	0.23	0.24	0.24	0.28	0.25
Nickel	0.02	0.02	0.03	0.02	< 0.01	< 0.01
Chromium	0.04	0.05	0.03	0.03	0.19	0.18
Molybdenum	< 0.01	< 0.01	0.01	< 0.01	< 0.01	< 0.01
Copper	0.01	0.01	0.09	0.07	< 0.01	0.01
Aluminum	0.032	0.051	< 0.005	< 0.005	0.035	0.031
Vanadium	0.055	0.068	0.044	0.48	0.080	0.076
Niobium	< 0.005	< 0.005	< 0.005	< 0.005	< 0.005	< 0.005
Boron	< 0.0005	< 0.0005	< 0.0005	< 0.0005	< 0.0005	< 0.0005

Table B.1 - Results of Chemical Analysis of Helical Spacer (% by weight).

Elements	Helical Spacer Wire
Carbon	0.80
Manganese	0.77
Phosphorus	0.014
Sulfer	0.010
Silicon	0.24
Nickel	0.02
Chromium	0.28
Molybdenum	<0.01
Copper	0.02
Aluminum	0.029
Vanadium	<0.005
Niobium	<0.005
Boron	<0.0005
Titanium	0.018

Table B.2 - Mechanical Properties of Strand From Mill Certificates.

Parameter	Reel 1	Reel 2	Epoxy-Coated	Epoxy-Coated and Filled	Galvanized	Greased and Sheathed
Breaking Load (kN)	190.4	193.5	193.5	193.5	194.7	183.7
Load at 1% extension (kN)	178.8	179.9	179.9	179.9	175.9	165.3
Ultimate Elongation	5.47%	5.09%	5.09%	5.09%	5.21%	3.6% min.
Modulus of Elasticity (MPa)	194400	197200	197200	197200	198600	197900

Appendix D
Proposed Revisions to the PTI Stay Cable Recommendations

D.1 Introduction

The Post-Tensioning Institute's *Recommendations for Stay Cable Design, Testing, and Installation* currently has no rational basis for selection of the stay cable corrosion protection system.[28] Material requirements as well as qualification tests for various elements of a typical corrosion protection system are presented. However, no guidelines are given as to how and to what extent these elements are to be combined to form the corrosion protection system. In fact, there is no specific requirement which categorically states that corrosion protection must be provided for a stay cable. Apparently, one could erect a stay system composed of bare strand only and still be in compliance with the current PTI Recommendations! While this example is somewhat extreme, it points out the need for a section which explicitly requires that corrosion protection be used. In addition, a rational selection process is needed in which corrosion protection system can be tailored to the site conditions and level of importance of the bridge. Therefore, it is proposed that the following paragraphs be added to section 9.0 Corrosion Protection in the PTI Recommendations:

9.0 Corrosion Protection

This section covers the design of the corrosion protection system for the stay cable. The Corrosion Protection Demand Factor (CPD), defined in Section 9.2, is calculated from factors reflecting the site environment, bridge use, and stay redundancy. The Corrosion Protection Effectiveness Factor (CPE), defined in Section 9.3 is calculated from factors associated with the effectiveness of the corrosion protection system selected for the stay cable. The effectiveness factor of the selected corrosion protection system must satisfy the following equation:

$$CPE \geq CPD$$

or Protection $\geq$ Demand

9.1 Bridge Environment

The aggressiveness of the environment in which the bridge is situated shall be categorized by the level of chlorides and pollutants present in the atmosphere and whether salts may be applied to the bridge deck in the winter. This categorization is then used as a consideration in selecting the

level of corrosion protection for the stay which is appropriate for the site. If the bridge is located at a site in which any one of the following environmental conditions exist then the bridge shall be considered to be in a *harsh* environment:

- Aggressive chemical or industrial atmosphere
- Sea-water environment (within 50 miles of sea-coastal area)
- Road salts are applied to the bridge deck regularly in the winter months

If the bridge is not located in any one of these environments then the bridge shall be considered to be in a *mild* environment.

9.2 Corrosion Protection Demand Factor

The Corrosion Protection Demand Factor (CPD) shall be calculated from the factors given in Table D.1 and Table D.2 using the formula:

$$CPD = I + R + E$$

9.3 Corrosion Protection Effectiveness Factor

There are a number of corrosion protection systems available for use in stay cables. In general, a typical stay cable system has an external sheathing surrounding the tension elements. The sheathing may have a blocking agent injected. In addition, the tension elements can have individual barriers to provide additional levels of protection as needed. Thus, the corrosion protection system is composed of nested barriers which provide a level of corrosion protection redundancy. Increasing the number of effective barriers increases the redundancy and thus improves the corrosion protection system. This is reflected in the increasing value of the Corrosion Protection Effectiveness Factor as additional barriers are added. The Corrosion Protection Effectiveness Factor (P) shall be calculated with the equation

$$CPE = EB + IB_1 + IB_2 + BA$$

Table D.1 - Importance Factor.

Type of Road	ADTT	Truck Loading	Importance (I)
Freeways, Expressways, Major Highways and Streets (or Rail Bridge)	2,500 or more	2,000,000	10
Freeways, Expressways, Major Highways and Streets	less than 2,500	500,000	8
Other highways and streets not included in the above categories	n/a	100,000	5

* Average Daily Truck Traffic.

Table D.2 -Redundancy and Environment Factors.

Redundancy (R)	Nonredundant stay design ..... 10 Redundant stay design 5
Environment (E)	Harsh ..... 10 Mild 3

using the factors obtained from Table D.3. Note that two individual barriers can be combined to increase the factor. One example is greased, sheathed and galvanized strand, with a corrosion protection demand factor of 22.

9.4 Temporary Stay Cable Protection

Temporary corrosion protection for the tension elements shall be provided continuously from the point of manufacturing until the full corrosion protection system is in place.

For bridges in a mild environment, where protection is not provided by an individual protection system, an approved corrosion inhibitor shall be used to provide temporary corrosion protection to the bare tension elements. The individual bare wires, strands or bars shall be coated with an approved water soluble corrosion inhibitor prior to their insertion into the sheathing.

Appropriate polarization and exposure tests shall be conducted by an approved testing laboratory to determine the effectiveness of the

Table D.3 - Factors for Calculating Protection.

Location	Type of Protection..... Factor	Quality Control Covered in Section:
External Barrier (EB)	PE sheath (w/ Tape) 10	3.4.3
	Steel sheath (painted) 15	3.4.2
Individual Barrier (IB)	None 0	
	Epoxy-coated strand (not filled) 4	not covered
	Epoxy-coated wire or bar 10	not covered
	Epoxy-coated and filled strand 10	6.5
	Greased and sheathed strand 10	6.6
	Galvanized wire, bar, or strand 12	not covered
Blocking Agent (BA)	None 0	
	PC Grout 5	3.5
	Polyurethane 8	not covered
	Petroleum Wax 9	not covered
	Grease 8	not covered

corrosion inhibitor to provide corrosion protection. The polarization tests shall conform to ASTM G5, “Standard Reference Test Methods for Making Polarization Measurements.” If integrity of the bond between the injected grout and main tension elements is a major design consideration, bond testing shall be performed to prove that the proposed corrosion inhibitor does not impair the bond significantly. During and after cable threading operation, water, rain, or snow shall not be allowed to enter the external barrier. Within three months following threading installation and prior to

grouting operation, the corrosion inhibitor shall be reapplied by re-application from the top of the external barrier.

For bridges in a harsh environment, a permanent individual barrier protection system with a factor of 8 or higher as shown in Table D.3 shall be used. Additional measures shall be taken to provide continuous protection of the tension elements at the anchorage region where the individual protection system can be disturbed.

9.5 Anchorage Protection

If an individual barrier protection system is required in the overall stay cable corrosion protection system, special measures are required to provide protection of the tension element at the anchorage. In general, penetration and/or removal of the individual barrier is necessary in this area to connect the tension element to the anchorage. Special procedures shall be utilized to ensure the integrity of the corrosion protection system in the anchorage region. Details shall be approved by the engineer. An approved blocking agent other than pc grout shall be used in this area. If pc grout is to be used in the free length, precautions shall be taken to ensure that the pc grout will not leak into the anchorage region during injection.

9.6 Test Requirements

If the bridge is to be located in a harsh environment, accelerated corrosive qualification testing of a representative shortened full size system shall be conducted to ensure that the various levels of corrosion protection are compatible in the completed system.

D.2 Design Example

An example of the selection of a corrosion protection system using the proposed method is presented. An environment is assumed and several combinations of corrosion protection methods are checked.

Bridge: Major interstate highway with ADTT > 2500 located in an environment where it crosses salt water and deicing salts are applied. Design of the stay cables allows removal and replacement of one stay at a time.

DEMAND

I	Importance I	10
R	Redundant design	5
E	Harsh environment	10

$$CPD = I + R + E = 10 + 5 + 10 = 25$$

Required Corrosion Protection Effectiveness $CPE \geq CPD \geq 25$

$$CPE = EB + IB_1 + IB_2 + BA$$

PROTECTION

system #1

EB	PE sheath	10	
IB	none	0	
BA	pc grout	5	
CPE		15	n.g.

system #2

EB	steel sheath	15	
IB	none	0	
BA	pc grout	5	
CPE		20	n.g.

system #3

EB	PE sheath	10	
IB	epoxy-coated/filled (or greased and sheathed) strand	10	
BA	pc grout	5	
CPE		25	ok

system #4

EB	PE sheath	10	
IB	galvanizing	10	
BA	pc grout	5	
CPE		25	ok

system #5

EB PE sheath 10
IB galvanizing.....12
BA wax..... 9
CPE .....31 ok

system #6
EB PE sheath 10
IB galvanized, greased and sheathed strand 22
BA pc grout..... 5
CPE .....37 ok

system #7
EB PE sheath 10
IB epoxy-coated bar.....10
BA pc grout..... 5
CPE .....25 ok

Chapter One
Introduction

Historical Development of Cable-Stayed Bridges

The development of the modern cable-stayed bridge technology began in post World-War II Germany. It was estimated that some 15,000 bridges had been destroyed during the war. The scarcity of raw materials and advancing techniques of structural analysis made the use of the highly material efficient system of cable-stayed bridges very attractive. While long spans (500-1500 m) have generally been the domain of the suspension bridge, cable-stayed bridges are much more efficient than girder bridges for midrange spans (150-500 m). In recent years another aspect of the cable-stayed bridge has increased its use. Cable-stayed bridges are aesthetically pleasing as well as monumental in form. Their attractiveness has caused local populations near the bridge sites to be more receptive to cable-stayed bridges than to more traditional girder bridges.

Cable-stayed bridges are not a recent development, but rather a bridge system that is very old.[122] However, cable-stayed bridges have not seen widespread application until recently. Inclined stays were first introduced in England in the early part of the nineteenth century. A number of bridges with these inclined stays failed, thus diminishing confidence in this form of construction. The failures are now attributed mainly to the designers' misunderstanding of the actual structural behavior of stayed bridges. Stays saw a resurgence in the second half of the nineteenth century when John A. Roebling used them in the construction of such bridges as the Niagara Falls Bridge and the Brooklyn Bridge. Both of these bridges were considered suspension bridges but Roebling utilized inclined stays to carry a portion of the gravity load and to stiffen the structure. Roebling understood very well that the stayed system provides a much stiffer structure than does the suspension system.

The first part of the twentieth century saw a few examples of pure inclined stay bridges constructed. However, the true growth in the use of cable-stayed bridges began with the construction of what is generally agreed to be the first modern cable-stayed bridge. The Strömsund Bridge was completed in 1956 in Sweden. It had a main span of 183 m and side spans of 75 m.[53, 90, 122, 125] The Strömsund Bridge utilized stay cables which were constructed with groups of helical strands.[53]

The use of cable-stayed bridges in the US began in 1971 when the construction of the Sitka Harbor Bridge in Alaska was completed. There are currently 19 cable-stayed bridges in the United States with a large portion of those completed in the last ten years. There are currently two cable-stayed bridges in Texas. One of these, the Houston Ship Channel Crossing, is shown in Figure 0.1.

Figure 0.1 - Houston Ship Channel Crossing.

Classifications and Definitions of Components

Cable-stayed bridges have a distinct structural form that can be divided into the components shown in Figure 0.2. Stay cables are by necessity connected or anchored to the stiffening girder. However, the stay can be anchored at the tower or it can be continuous through the tower over a saddle (see Figure 0.3).

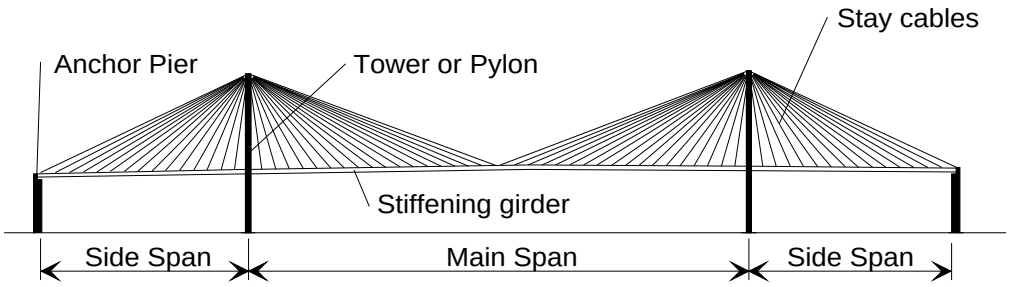

Figure 0.2 - Basic Components of a Typical Cable-Stayed Bridge.

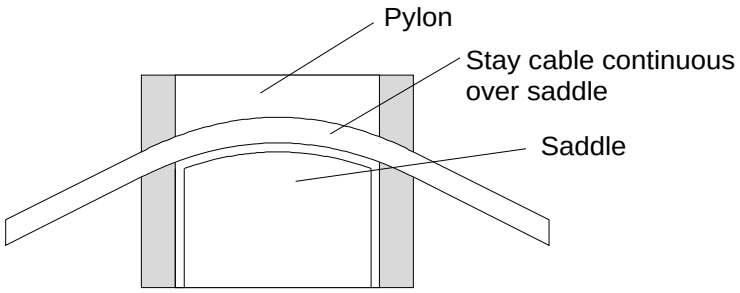

(a) Saddle Connection at Pylon.

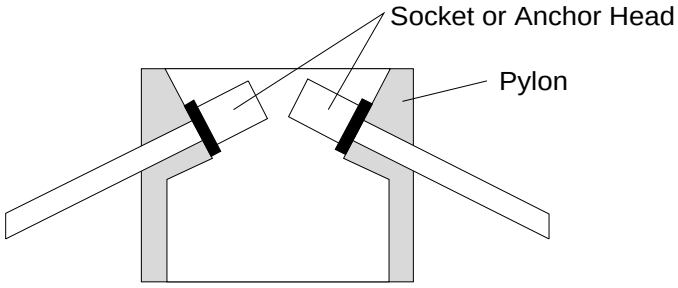

(b) Stay Anchored at Pylon.

Figure 0.3 - Two Types of Connections at Pylon.

Stay cable systems can be divided into several basic components depending on the type of stay cable and how it is to be manufactured and installed. The following definitions describe the various components:

STAY CABLE: the complete stay cable system including anchorages, main tension elements, sheathing and all corrosion protection materials and devices.

ANCHORAGE: device comprising all components and materials required to retain the force in a stressed stay cable and to transmit this force to the towers and to the superstructure.

SOCKET: one type of end anchoring device for the tension elements (see Figure 0.4). It typically consists of a steel cylinder with a conical cavity into which the tension elements are inserted. One type of socket (normally used with structural rope, strand, or helical locked-coil main tension elements) uses a metallic alloy fill to lock the cable in place, usually molten zinc alloy. Another popular type of socket system is the patented HIAM system that is marketed by Bureau BBR, Ltd. The socket is filled with a zinc dust, steel balls, and epoxy resin binder. Parallel prestressing wires are usually used with this type of anchorage.

Figure 0.4 - Socket Type Anchor.[53]

ANCHOR HEAD: end anchoring device commonly used with prestressing strand main tension elements. Prestressing wedges are generally used to connect the strand to the anchor head. It is very similar to the standard anchorage devices used in post-tensioning applications (see Figure 0.5) .

SADDLE: stay cable detail at tower or pylon for those bridges which utilize a continuous stay cable passing over the tower without tower anchorages.

Figure 0.5 - Anchor Head Anchorage Device.[90]

MAIN TENSION ELEMENT: the fundamental tension carrying element in the stay cable. Various types are:

1. Structural rope -- manufactured cable consisting of many strands helically wound around a core composed of a strand or another rope -- may be galvanized or non-galvanized (see Figure 0.7).

2. Helical locked coil strands -- manufactured cable consisting of interlocking steel elements arranged to lock together when in place around the core -- may be galvanized or non-galvanized (see Figure 0.8).
3. Structural strand -- an arrangement of wires helically placed about a center wire to produce a symmetrical section excluding, however, prestressing quality strand (see Figure 0.6).
4. Parallel prestressing wire cables -- cables assembled from individual prestressing wires using either zinc alloy or HIAM type sockets (see Figure 0.8).
5. Parallel prestressing strand cables -- cables assembled from individual seven wire prestressing strands (see Figure 0.8). These cables can be further subdivided according to the strand corrosion protection system:
    (1) Bare strand
    (2) Galvanized strand
    (3) Epoxy coated strand with no coating around center wire or interstices
    (4) Epoxy coated strand with an additional epoxy coating around center wire filling all interstices
    (5) Individually greased and sheathed monostrands
6. Parallel prestressing bar cables -- cables assembled from individual prestressing bars (see Figure 0.8). These cables can be further subdivided as:
    (1) Uncoupled
    (2) Coupled
    (3) Glued coupled

SHEATHING: the outer enclosure for the tension element to provide rigidity and/or confinement for the corrosion protection system. Common sheathings include steel pipe and high-density polyethylene (PE) pipe. In a few cases, sheathings such as copper and stainless steel have been used.

CORROSION PROTECTION SYSTEM: the assemblage of materials used to provide long term durability and corrosion resistance to the cable. Corrosion protection systems can include various combinations of:

(a) Galvanizing
(b) Cementitious grouts with or without admixtures

Figure 0.6 - Structural Strand Main Tension Element.[90]

Figure 0.7 - Structural Rope Main Tension Element.[90]

Figure 0.8 - Other Types of Main Tension Elements.[125]

(c) Epoxy grouts

(d) Epoxy coatings

(e) Corrosion inhibiting greases and waxes

(f) Plastic sheathing around individual wires, strands and bars

(g) Sheathing

(h) Tedlar tapes

(i) Other materials

(j) Cathodic protection

(k) Inert gas pressurized systems

(l) Electrical isolation systems

BLOCKING COMPOUND: The material used to fill the void between the tension elements and the outer sheathing. It may be an integral part of the corrosion protection system. Examples are cement or epoxy grouts, greases and waxes.

Corrosion Protection Systems

The most popular stay cable system currently used in the United States is the parallel strand system.[112] The following list categorizes the stay cables used in 19 bridges which have been completed to date in the US. They are listed as Sheath-Main Tension Element-Blocking Compound:

- Steel sheath - bars - portland cement (pc) grout 1
- Steel sheath - prestressing strands - pc grout 2
- PE sheath - prestressing strands - pc grout 7
- PE sheath - epoxy-coated prestressing strands - pc grout 3
- PE sheath - prestressing wires - pc grout 2
- None - Galvanized structural strand - none 3

It is clear that the most popular main tension element is prestressing strand and the most popular sheath is PE. The only blocking agent that has been used in the US is pc grout. Not counting the structural strand, over eighty percent of the bridges rely on the sheath and pc grout for corrosion protection.

The first application of the sheath and pc grout corrosion protection was in the Schillersteg Pedestrian Bridge in Stuttgart, Germany completed in 1961.[98] The Schillersteg stays were composed of up to 90 6-mm diameter wires inside a PE sheath with a helical spacer of 2.5-mm diameter. The stays were injected with pc grout for corrosion protection.

Large-scale application of this system was not realized until the completion of the Mannheim-Ludwigshafen (a.k.a. North Bridge or Kurt-Schumacher) Bridge in 1972 across the Rhine. This marked the first use of parallel wire stay cables on a major cable-stayed bridge.[53] The

stays contained 295 wires of 7 mm diameter and were anchored in a new type of socket called the HIAM.

Other major bridges such as the Brotonne Bridge in France (completed in 1977), Zarate-Brazo Largo bridges over the Parana in Argentina (completed in 1977), and the Pasco-Kennewick Bridge in the United States (completed in 1978) followed closely behind.[53, 70, 125] The Brotonne Bridge used a steel pipe for sheathing while the Parana and Pasco-Kennewick used PE pipe.

Since 1961, at least 62 cable-stayed bridges have been constructed with this type of corrosion protection system; none of the cables has ever been replaced.[98] However, the system is not very old when compared to the expected life of these structures. The oldest traffic bearing bridge with this system is a little over twenty years old. Because none of the stays has been replaced, it is not conclusively known how well the systems are performing because the main tension element is not visible. Several field evaluations have been performed to determine the effectiveness of the systems.

Field Evaluation of Grout as Corrosion Protection for Stay Cables

Schillersteg Bridge [98]

The corrosion protection system for the Schillersteg bridge was investigated after 9, 13, and 18 years of service. During each inspection windows were cut in the sheathing to inspect the grout. In all cases the grout was solid with no detectable cracking. Tests indicated that the grout had not carbonated significantly. Several areas were chipped out and the underlying wires were examined. The wires were found to be smooth with no apparent corrosion.

In 1974 and 1979 sections of PE were taken from the stay cables and were tested for tensile strength and ductility. The results showed no significant changes in properties from the original material. It should be noted that the PE pipe was exposed to direct sunlight and was not covered with tape.

Pasco-Kennewick Bridge [55]

In May 1990, the Pasco-Kennewick Bridge was inspected to determine the condition of the stays after 13 years of service. Twelve of the 144 cables were “opened” by making small cuts in the PE sheathing and then removing the grout (see Figure 0.9). No visible signs of corrosion were found on the wires in the areas that were uncovered. In addition, no major voids, cracking, or spalling were noted during the investigation. However, small closely spaced cracks perpendicular to the axis of the stay were noted in the grout (see Figure 0.9). These were caused, most likely, by live-load tensile strains in the stay. The cracking is similar in size and geometry to cracks normally found on the grout surface of a fatigue test specimen following the fatigue test.[98]

Figure 0.9 - Sheathing and Grout Removed Locally from Pasco-Kennewick Stay Cable. Note Narrow Grout Cracks at 6¾-, 7¾-, 8½-, and 9½-inch marks.

Problems with Corrosion Protection

Cables in Trouble

In 1987 Watson and Stafford conducted an informal "world condition survey" of existing cable-stayed bridges.[110] The survey consisted of visiting bridge sites and making limited visual inspections of nearly 100 cable-stayed bridges. Based on their external observations they indicated that "most of the nearly 200 cable stayed bridges that have been built around the world in the past few decades are in serious danger because corrosion is attacking their cables." They went on to say that "...nearly all [corrosion protection] methods [specified] have failed to one extent or another." In another article the same authors indicated that cable-stayed bridges have "serious design shortcomings that unless they are resolved can significantly shorten the useful life of any stayed girder, particularly those in marine environments and in spans in excess of 100 meters." [109]

They indicated that one problem in design is that cables are sometimes grouped together so closely that access for inspection is very difficult. The Maxau Bridge over the Rhine (completed 1967) was cited as an example of this problem. Photographs were shown of the locked-coil cable group which showed signs of corrosion along the free length and near the anchorages.

Another example given was the Mannheim-Ludwigshafen Bridge in Mannheim, Germany (completed 1972). The cables were originally constructed by embedding a bundle of ungalvanized wires in polyurethane with zinc-chromate.[53] The bundle was then wound with a polyester film and covered with a 4-mm thick polyurethane covering. Finally, the cable was painted. Watson and Stafford included photographs that depict severe pitting corrosion of the underlying wires in areas where the outer coating had been removed for inspection. At the time the paper was written (1988) an official investigation of the corrosion problems was being conducted.

Watson and Stafford also expressed concern about cable vibration and cited bridges that have had damping mechanisms installed to reduce vibration problems. However, no failures or durability problems resulting from the vibrations were reported. Fretting fatigue was also suggested as a problem peculiar to modern systems, but no examples of failures were given. The authors also cited a Japanese study in which 22 bridges in Japan were analyzed. It was found that the stays had elongated under load a maximum of 12% in the 3-5 years after the bridges were completed. Watson and Stafford believed that this behavior could severely affect the performance of the corrosion protection systems.

As a repair method for existing stays Watson and Stafford recommend the application of a tinned copper jacket to the outside of the stay. This system was used to repair the stays at the Mannheim-Ludwigshafen bridge. For new systems, a continuous titanium grade stainless coated carbon steel tubing with a 3 mm thickness is suggested. This tube would be extruded onto the erected cable on-site and subsequently injected with pc grout.

In summary the Watson and Stafford report on the performance of stay cables included the following specific examples: [110]

- Four bridges with examples of heavy corrosion on the locked-coil strand stay cables.
- One bridge in which the tape wrapping for PE sheath had failed.
- Several examples of bridges in which the stay cables had excessive vibrations.
- Two bridges in which the PE sheath had cracked in service.

Watson and Stafford's report was very controversial. In a subsequent staff article published in *Civil Engineering* it was stated that "no single article in the editors' recent memories has stirred as much comment" as this article by Watson and Stafford.[27] One response came from Blair Birdsall, who wrote: "In my opinion such phrases as 'in danger of sudden collapse,' 'in serious danger,' and 'in a state of very serious premature distress,' overstate the problem. What we're discussing here is not really bridges that are in imminent danger of disastrous failure. We are simply discussing ways of achieving the minimum life cycle cost of maintaining the bridges. To this end there is a

fascinating worldwide discussion in progress, searching for the optimum answers."[19] While the comments from the engineering community ranged from highly critical to very complimentary, most agreed that the article opened a necessary dialog concerning the corrosion protection of bridge stay cables.

Lake Maracaibo Bridge[98]

The Lake Maracaibo Bridge was completed in 1962 in Venezuela. It has five main spans each of which are identical in length (235 m). Each half span is supported by a single set of cables on each side of the bridge girder concentrated in a single line. The cable bundle supports the bridge girder at 80 m from the tower centerline. Each cable consists of 16 locked-coil ropes each with a 74-mm diameter. The original corrosion protection system consisted of bare wires with an inner filling of redlead and linseed oil. The exterior was covered with two base coats of redlead and resin, each with a thickness of 50 μm. Two finishing coats of ironglimmer and linseed oil, each with a thickness of 50 μm were also applied.

An inspection of the bridge in 1978 indicated that more than 500 wires had broken (see Figure 0.10). By early 1979, 3 ropes had failed completely and collapse was imminent.[85] The cause was determined to be lack of maintenance and the failure to replace the neoprene boots that protected the anchorage area. Replacement of the cables was very difficult because of the lack of redundancy in the system. In addition, the original stay cables were cast into the pylon so that use of the original anchorage system was not possible. At great expense, a new anchorage system was constructed on the top of the pylons and the cables were removed and replaced individually. The process was time-consuming and costly, with a total cost of $50 million. The replacement cables are locked-coil strand and are also now in a serious state of deterioration due to lack of maintenance.[74]

saul and svensson

Figure 0.10 - Broken Wires on Locked-Coil Cables of Lake Maracaibo Bridge.[98]

Köhlbrand Bridge [98]

The Köhlbrand Bridge, located in Hamburg, Germany, was completed in 1974. The bridge had a total of 88 locked-coil strands which had essentially the same corrosion protection system as the Lake Maracaibo Bridge cables. The cables ranged in size from 54

to 104-mm in diameter.

Twenty-five broken wires were found during a 1976 inspection (see Figure 0.11). Several factors contributed to the wire failures:

- Misalignment of the anchorages introduced bending stresses into the stay
- The area where the cable entered the socket was not well protected
- Lead collars were used to prevent contact with the steel anchor beam. Because lead is cathodic to steel, the cable corroded preferentially
- The cables were not designed specifically for fatigue
- The cables vibrated excessively under live loads
- The dead load stresses in the stay cable were very small which allowed the locking Z-wires on the outer barrier to relax. This allowed the ingress of moisture, salts, and pollutants
- Salts were heavily used on the bridge deck

The primary cause of deterioration was probably the salts because all of the wire breaks found were near the bridge deck. Because of the extensive damage, all of the stays had to be replaced.

Luling Bridge

Investigation of Cracked PE, February 1986[70]

The Luling Bridge was opened in October, 1983. The stays consisted of parallel wire main tension elements and PE sheath injected with pc grout. HIAM type sockets were used at the anchorages. The stays were injected with grout between July and September 1983. In April 1985 cracks in the PE sheath were detected in two cables on the side span (backstays). They were

Figure 0.11 - Broken Wires at Lower Cable Anchorage on Köhlbrand Bridge.[98]

subsequently repaired by PE welding. However, new cracks soon developed at the repair welds. In November and December of 1985, new cracks were detected in the sheath of three cables on the main span (forestays). In March 1986 a broken butt weld was detected in a cable sheath and rust stains were visible. In February 1986, an investigation was undertaken to determine the cause of the problems and propose repairs.

Before installation of the stay cables, 35 sheath crack repairs were made on 21 out of the total of 72 cables. Most of the cracks had occurred in the PE sheath at the butt welds and were transversely oriented. It was believed that a combination of faulty sheath welding combined with the stresses induced by coiling for transportation to the site were the cause of the cracking. Other findings of the investigation were:

- Backstay sheath cracking was caused by overstressing of the sheathing during grouting. The cause of overstressing was not addressed in the report.
- Forestay cables were not overstressed during grouting. Conjectures for the cause of cracking were as follows;
  - Grouting during hot weather
  - Elevated temperatures during the life of the cable
  - Very low temperatures at the time of cracking
- Failed butt welds were attributed to incomplete shop welding and/or handling during cable installation.
- Poor quality pipe with reduced ductility. Some of the polyethylene used in the sheath was found to be of marginal quality in that it did not meet the specified ductility requirements.

The proposed repair method consisted of filling all cracks with a polyurethane grout and applying a Tedlar tape over the full length of each stay with a 50% overlap.

Field Inspection, January 1990[112]

Swait and Funahashi performed a field investigation of the Luling Bridge in February 1990. A visual inspection showed transverse cracks in the sheathing at some locations. In addition, a 51 mm x 51 mm section of sheath was cut and removed at two locations. One location was near a pre-existing sheathing crack and the other was away from any pre-existing sheathing cracks. The grout was removed in these areas and a total of five underlying wires were exposed.

At the location where the sheathing was cracked, one of the wires showed uniform surface corrosion and "microscopic corrosion pits" were observed. The grout was cracked in the transverse and longitudinal directions with some corrosion product visible in the cracks. At the other location there was no corrosion encountered and the wires were found to be bright and untarnished.

The cover plate over one of the HIAM anchorages at the bridge deck level was removed for inspection. When the plate was removed, rust-colored water ran out. The lower portion of the anchorage inside the socket was heavily corroded. The button heads of the wires did not show corrosion and were covered with "some hard grease, plastic or epoxy type material."

Half-cell measurements were taken of the cable at selected locations using a copper/copper-sulfate reference electrode (CSE). It was not specified if the measurements were open-circuit or if the voltmeter was grounded to the cable. The readings were taken in four places and are shown in Table 0.1 along with readings vs. saturated calomel electrode:

Location A: at a pre-existing break in the sheathing where the pipe was cracked around the entire circumference. Four readings were taken, one at each quadrant on the exposed surface of the grout.

Location B: location where corroded wires were found. Three readings were taken along the split.

Location C: same as the second location where grout was removed but no corrosion was found.

Location D: in an area where there was no cracking of the sheath.

Table 0.1 - Half-Cell Values Taken on Surface of Grout During Luling Stay Cable Inspection.

Location	$-mV_{CSE}$	$-mV_{SCE}$
A	248(bottom), 140, 121(top), 204	180(bottom), 70, 50(top), 130
B	351, 280, 415,	280, 210, 350
C	98, 134	30, 60
D	124, 161	50, 90

Carbonation tests were conducted at locations B, C, and D. Carbonation had occurred at the surface of the grout in Location B but the depth was not determined. Carbonation was not detected at Locations C and D.

The results from the large-scale tests reported in Chapters 7, 8, and 9 can be used to interpret these half-cell readings. It was found in the large-scale tests that:

- Corrosion was found in areas where the readings were more negative than $-250\ mV_{SCE}$.
- Corrosion may or may not have been found when the reading was above $-250\ mV_{SCE}$.

Using these results as a criterion to evaluate the readings taken from the Luling Bridge, the indication would be that active corrosion would probably be found under Location B with two out of the three readings found to be more negative than -250 mV_{SCE}. Field observations agree with this evaluation in that corrosion was found on the underlying wires. Although there were no readings in the large-scale tests that were in the -30 to -60 mV_{SCE} range, many readings (with no active corrosion) ranged between -100 and -150 mV_{SCE}. It is generally accepted that the more positive the half-cell value the less likely that active corrosion is present. This would indicate that the probability of active corrosion was low with the readings taken at Location C. Again, field observations agree with this evaluation in that no corrosion was found on the underlying wires.

Fatigue Acceptance Tests

In compliance with the PTI *Recommendations for Stay Cable Design, Testing, and Installation*, fatigue acceptance tests (FAT) are conducted on full-scale specimens prior to the construction of a cable-stayed bridge.[28] The following are descriptions of FAT that were conducted for specific bridges and in which corrosion occurred during the test. The FAT specimens are generally very carefully fabricated and kept in a laboratory environment for their entire service life. No corrosion would be expected to occur during this test. The FAT, in essence, requires that the stay be cycled at a given stress range for $2x10^6$ cycles with no more than 2% of the number of wires fracturing during the fatigue test. At the end of the test, the specimen is tested statically and must reach 95% of its guaranteed ultimate tensile strength.

Baytown Bridge, Houston, Texas[48]

In one of the fatigue acceptance test conducted for the Baytown Bridge, severe corrosion was found on the strands after the tests. The specimen was composed of 55 15.2-mm diameter prestressing strands in a PE sheath. Several wire failures occurred at corrosion sites.

Clark Bridge, Alton, Illinois[30, 32, 33]

The components of the stay cable test specimens were:

- 17-, 37-, and 46-strand 15.2-mm diameter, epoxy-coated, grit-impregnated strand (coated, not filled) stay cables
- Special prestressing wedges plus bond socket
- Plastic caps protecting ends of strands

Two of the FAT were axial tests and one was an axial-flexural test (for bridges with saddles). All FAT specimens passed the PTI requirements.

17 strand: Trapped water was found inside top socket and corrosion stains were found on the inside surfaces of both top and bottom sockets.

46 strand: Water came out of strand at bottom when cap was removed. Corrosion was found on the inside face of socket. Examination of broken strands found that, in most cases, some corrosion was evident on the center wire. A small amount of water came out of several of the strands when they were removed from stay. Corrosion was noted in the area of 14 of the total of 16 strands where wire breaks occurred. Water was found in five strands.

37 strand: The weld between the PE pipe and PE sleeve failed during the test, exposing the grout underneath. After grout injection the grout cap was removed and strands were saw cut. Water was observed coming out of some of the strand ends. Dry, pressurized air was then used to remove moisture from inside the epoxy-coated strand.

Burlington Bridge, Burlington, Iowa[31]

In June 1991 FAT tests were conducted on specimens for the Burlington Bridge over the Mississippi River at Burlington, Iowa.[31] The 31-strand test specimen failed to meet the PTI requirement for the number of wire breaks during the fatigue test. It also did not reach the minimum load level during the ultimate static test. The test specimen consisted of 31 15.2-mm diameter epoxy-coated (not filled) strands. HIAM type sockets were used at the anchorage. A short section of the stay adjacent to the socket was filled with epoxy compound with zinc dust. A coal-tar epoxy transition material was placed between this and the pc grout in the free length. The epoxy coating was stripped from the strand in the socket to ensure complete bonding between the strand and socket compound. PE sheath was used in the free length.

The stay specimen was injected with grout and tested in the vertical position. Dissection revealed corrosion on the inside face of the steel transition pipe near the bottom anchorage. However, no corrosion was found inside the steel pipe at the top anchorage. Corrosion was also found on the strands in the short length adjacent to the socket that was filled with the epoxy/zinc compound. There were 24 wire breaks in this area. Of these, ten were clearly ductile, while the remaining breaks had fatigue or shear fracture surfaces. Corrosion was also found on strands near the top anchorage but it was less extensive. Strands under the coal-tar epoxy had only localized corrosion.

A detailed investigation was performed to determine the cause of the corrosion.[95] The investigation indicated that many of the brittle fractures were due to fretting fatigue and that all but a

few were located in areas of, or near, corrosion in the epoxy/zinc area near the socket. The fractured wires were examined for hydrogen to determine if hydrogen embrittlement was a problem. No significant levels of hydrogen were detected. Chlorides were detected but the location and quantities were not specified in the report. The report suggested that additives in the grout or bleed water from the grout might be combining with excess epoxy hardener and causing corrosion. It also suggested that bleed water should be prevented from entering the area adjacent to the socket. Another suggestion was to eliminate the use of grout.

In subsequent tests the epoxy/zinc mixture and coal-tar epoxy were replaced with a polyurethane fill. The remainder of the sheathing was filled with grout.

Bayview Bridge, Quincy, Illinois[116, 117]

A total of three specimens were tested as a part of the FAT program for the Bayview Bridge (37-, 44-, and 61-strand stays with epoxy-coated and unfilled strand). Approval of the cable system required that two of the specimens perform satisfactorily under specified fatigue loading and the remaining specimen under specified static loading. The specimens were vacuum grouted in the horizontal position and regrouted three times within intervals of 25 minutes after the initial grouting. Reports on the performance of the 37- and 44-strand specimens indicated that they had satisfied the specified fatigue and static loading requirements specified for this bridge. Wire fatigue failures did occur in both specimens. Subsequent post-mortem examination revealed that fatigue cracks had formed consistently in the outer wires either at the point of contact with an adjacent wire or on the face exposed to the interstitial space that was found to contain moisture and was corroded. It was concluded that the cut epoxy-coated strand ends should be sealed to prevent the penetration of bleed water into the interstitial space of the strands.

Other

Tanabe and Hosokawa reported that corrosion was found in the cables of the cable-net roof system of the Yoyogi Indoor Stadium in Tokyo twelve years after construction.[114] The roof has two main cables, each composed of 37 bare spiral ropes inside steel pipe, filled with portland cement grout. The corrosion (described as heavy) was found on the spiral ropes. The extent of corrosion was not given. However, the corrosion had progressed sufficiently to cause the grout to delaminate. The investigators indicated that the cause, among other things, was that water had permeated into the grout. Their opinion was that the problems would not have occurred if the strands had been galvanized. The investigators also suggested that all wires in bridge stay cables should be galvanized and the use of cement grout is not desirable. Their view was that visual inspection of the

final fabrication process is very important and that this is not possible during the injection of pc grout.

Field Evaluation of Stay Cables

There was very little information found in the literature on the nondestructive testing of stay cables. Swait and Funahashi indicated that the only instrument available today to detect loss of cross-section is the magnetic perturbation method.[112] However, they also state that the instrument was successful in detecting wire *breaks* but not loss of section due to corrosion. While locating wire breaks is useful, the critical problem is that a small amount of corrosion can initiate a fatigue crack.

Other Stay Cable Durability Tests

Matsui and Fukumoto [75]

The effect of thermal cycling on the corrosion of prestressing wire and rod embedded in cement grout was investigated. The specimen set-up is shown in Figure 0.12. The test variables were:

- Wires: Parallel wire strands, galvanized and ungalvanized. There were two sizes of strand formed. One was formed by bundling seven 5-mm diameter wires into the shape of a seven-wire strand. The second strand was formed in the same manner with seven 7-mm wires.
- Grouts: Portland cement grout with w/c = 0.3, 0.4, and 0.5; "Nonbleeding mortar" (manufactured by Shinko-Kousen Co.); Polyurethane grout (manufacturer not specified).
- Defects of various configurations intentionally made in the grout.
- Defects in the pipe made after grout had set.

There were two identical specimens for each variable. One set of specimens was exposed to 110 cycles of temperature change between 5° and 60°C at a constant humidity of 60% while the other set was cycled similarly 300 times. The extremes were achieved in an environmental

Figure 0.12 - Specimen Schematic for Environmental Tests.[75]

chamber.

The amount of corrosion found on the specimens cycled 110 times was less than the amount of corrosion found on the specimen cycled 300 times that indicated a correlation with the number of cycles. In all cases in which the duct was filled with cement grout, significant corrosion was found on the center wire of the bare wire strand specimens in the areas where the grout had not penetrated. No corrosion was found on the center wire of the galvanized strands. Corrosion was found on bare strand specimens at the grout defects. No corrosion was found on the galvanized strand specimens with similar grout defects.

Tanaka and Haraguchi [115]

Exposure tests were conducted to determine the effectiveness of the blocking agent in providing adequate corrosion protection if the sheathing is damaged. These tests were conducted using several different blocking agents injected into a PE sheathing. The sheath of each of the specimens was subsequently broken and the specimens were subjected to weathering (type of weathering was not specified). The variables and results were:

- Portland cement grout: After two years of exposure small cracks were observed in the grout at the opening in the PE sheath. Steel was not corroded.
- Polymer cement grout: After two years of exposure the results were the same as above.
- Polybutadiene: After two years of exposure the exposed surface of the blocking agent changed color and had extensive cracking. However, steel was not corroded.
- Grease: After two years of exposure the exposed surface of the blocking agent became dark and dry. The steel was not corroded.

Summary and Comment

The most positive impact of the controversial article by Watson and Stafford was that it motivated the design community to look critically at the current methods used for corrosion protection of stay cables. It is generally agreed that the use of locked-coil strand with no galvanizing can be a severe problem as was shown in the Köhlbrand and Lake Maracaibo Bridges. However, there is still some disagreement as to the level of protection that is provided by the pc grout and PE sheathing system or the “two-barrier system.”

Field evaluations of the two-barrier system have been conducted on several bridges. While no problems were found at the Pasco-Kennewick and Schillersteg, the Luling bridge showed some corrosion problems both in the free length and at the anchorages. In addition, these evaluations only examined small locations on a few selected stays in each of the bridges. Because the corrosion

protection system completely encases the main tension elements, visual inspection and verification of performance is impossible. Thus, there is no other proven inspection technique to determine how well the stay is performing other than complete removal and thorough examination.

Some engineers question the use of PE sheath and grout at all. Schupack, who has extensive experience in prestressed and post-tensioned concrete, is against the use of pc grout injected into a PE sheath.[27] He maintains that there are several problems with this system. One is that a multiwire tendon cannot be effectively grouted with all of the spaces between the wires filled with grout. Another problem is that the coefficient of thermal expansion of PE sheath is incompatible with that of the grout. Birdsall also questions the use of PE sheath injected with pc grout.[27] He is of the opinion that the grout will not be durable under the action of live loads and temperature changes.

Recent fatigue acceptance tests cited in this chapter have suggested a problem with corrosion of the cables. Even in the sealed environment of the PE sheath, stays have corroded during the relatively short-term fatigue test, leading to the initiation of fatigue cracks. This has been especially true when using epoxy-coated unfilled strand for the main tension element. The bleed water seeps into the interstitial spaces in the strands and causes corrosion which initiates fatigue cracks under the cyclic loading.

One method to evaluate the various corrosion protection systems available for stay cables is by accelerated corrosion testing. While there has been extensive work conducted in the area of corrosion protection for reinforced and prestressed concrete, there has been very little work done in the area of stay cables. Two experimental programs were cited in this chapter in which experiments were conducted specifically to test the effectiveness of the corrosion protection systems for stay cables. Matsui and Fukumoto's work looked at the effect of temperature fluctuations on the effectiveness of protection while Tanaka and Haraguchi's work examined the effect of breaking the sheathing and exposing the blocking agent to ambient weathering conditions. Matsui and Fukumoto indicated that there were problems with the corrosion protection provided by pc grout while Tanaka and Haraguchi indicated that pc grout provided adequate protection for over two years.

Objectives of Research

No failures or severe performance problems have been detected in in-service two-barrier corrosion protection systems. However, this is really the only statement that can be made about the system because of the lack of data available. The experimental research described here was designed to investigate the two-barrier system and to attempt to resolve some of the questions concerning the effectiveness of its corrosion protection. The objectives were as follows:

- Develop and implement a rational and objective evaluation of the two-barrier corrosion protection system.
- Evaluate several improved corrosion protection systems.
- Provide a basis for continued objective research in this area.

Experimental Program

Because of its current popularity and widespread use, the experimental program was designed around stay cable systems that use seven-wire prestressing strand. All of the tests performed in the program utilized 12.7-mm diameter seven-wire strand with a guaranteed ultimate strength of 1860 MPa.

The research was almost purely experimental and consisted of several test series. The experimental program flow chart is shown in Figure 0.13. The portland cement grout series consisted of selecting trial mix designs and testing the fresh properties of various mixes. The best basic mix was then selected for use in the Modified Accelerated Corrosion Test Method (ACTM) and the first four specimens of the large-scale tests. In addition, the fresh properties of the basic grout mix were tested to determine the effect of adding corrosion inhibitors. A silica fume grout was also developed. The effectiveness of the corrosion protection provided by these “improved” grout mixes was tested with the Modified ACTM. The grout that performed the best in the Modified ACTM was selected for use in Specimen LS-5 in the large-scale test series.

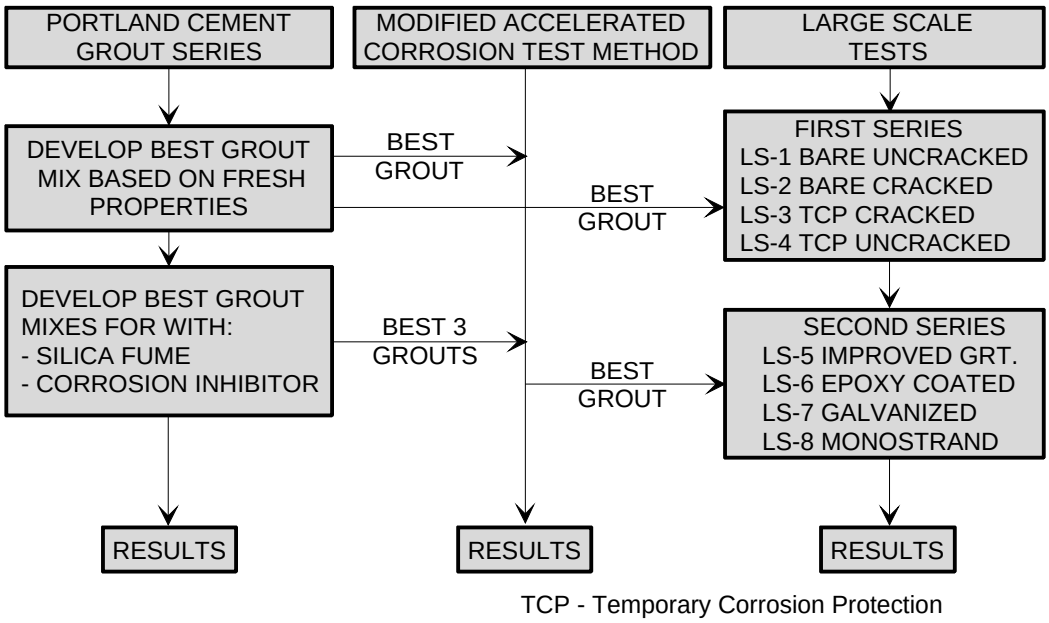

Figure 0.13 - Flow Chart for Experimental Program.

Organization of Dissertation

This dissertation is essentially divided into chapters covering specific aspects of the test program. Chapter Two covers corrosion of prestressing steel. The standard background material covering the corrosion of reinforcing steel in concrete is discussed. Also covered are topics related especially to prestressing steel such as hydrogen embrittlement, stress corrosion cracking, and fretting fatigue.

Chapter Three reviews the current corrosion protection systems available for bridge stay cables. Much of this chapter is spent addressing the use of portland cement grouts. Other types of blocking agents are discussed as well as individual protection systems for the strand such as epoxy-coating, galvanizing and greasing and sheathing.

Chapter Four covers a worldwide survey of opinion on the issue of design, construction, and installation of stay cables. Chapter Five covers the pc grout series while Chapter Six covers the results of the Modified ACTM tests.

Chapters Seven, Eight and Nine cover the large-scale tests. Chapter Seven covers the test concept and design. In addition, it covers the assembly, grout injection and load testing of the specimens. Chapter Eight details the accelerated corrosion test method and results. Chapter Nine provides further analysis of the data from the accelerated corrosion tests and draws conclusions as

well. Finally, Chapter Ten gives a summary and the overall conclusions and recommendations of this study.

Chapter Two
Corrosion of Prestressing Steel

2.1 Introduction

As noted in Chapter One the current technology in stay cable construction is relatively young. The oldest major installations which used portland cement grout (pc grout) and polyethylene (PE) pipe for corrosion protection were constructed only a little more than twenty years ago. None of the bridges which have these types of stays have been demolished or have had stays replaced. While there have been several field inspections performed on these types of stays, the effectiveness of the protection cannot be fully assessed until the stays are taken out of service and fully disassembled and examined.

An extensive amount of experimental work has been performed relating to the durability of prestressing strand and wire. In addition, many field studies have been performed on prestressed concrete structures in service. Because of certain similarities in the use of strand in stay cables and in prestressing, it was useful to examine the problems that are specific to the durability of prestressing strand and wire to gain some understanding of the problems and failure mechanisms involved. This understanding could then be applied to the special problems which might be encountered in the durability of stay cables.

The fundamental mechanisms for corrosion of prestressing steel in concrete or grout are essentially the same as those for reinforcing bars.[73] High-strength steel is somewhat more reactive than mild steel and highly stressed steel is more reactive than steel that is not stressed. However, the fundamental mechanisms and causes are the same. Accordingly, the fundamental aspects of corrosion will be presented here as they relate to strand in pc grout.

In addition to the traditional corrosion damage of reinforcing bars, prestressing strand and wire have increased susceptibility to other kinds of damage that are not usually of concern for mild steel. Damage from hydrogen embrittlement, stress corrosion cracking, fretting fatigue and corrosion fatigue will be discussed.

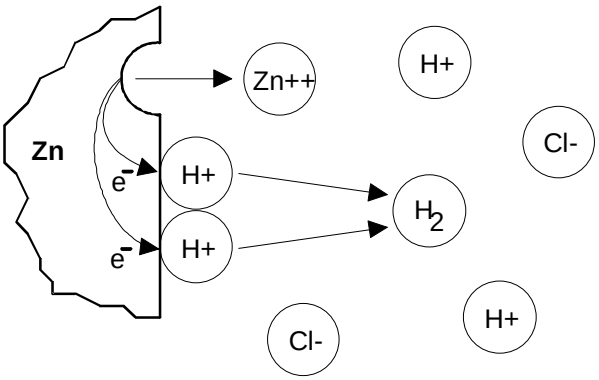

Figure 2.1 - Electrochemical Reactions During Corrosion of Zinc in Air-Free Hydrochloric Acid.[47]

2.2 Corrosion of Steel in Grout

2.2.1 Background

Corrosion is defined as the destructive attack of a material through a reaction with its environment.[47, 123] The material can be metallic or nonmetallic. While there are a variety of processes that can cause the destruction of nonmetallic materials, corrosion of metallic materials is largely *electrochemical* in nature.

Any electrochemical reaction can be divided into two reactions: anodic and cathodic. The corrosion process can be illustrated as in Figure 2.1 by the reactions that occur during corrosion of zinc (metal) in hydrochloric acid (electrolyte). The reactions are:

Anodic reaction (oxidation): $Zn \rightarrow Zn^{2+} + 2e$

Cathodic reaction (reduction): $2H^{+} + 2e \rightarrow H_2$

Note that electrons flow from the anodic reaction site to the cathodic reaction site. In order to conserve charge the reaction rate of the anode must always equal the reaction rate of the cathode.

When unprotected steel is exposed to moisture and oxygen the following electrochemical reaction occurs:

Anodic reaction: $Fe \rightarrow Fe^{2+} + 2e$

Cathodic reaction: $2H_2O + O_2 + 4e \rightarrow 4(OH^{-})$

These same reactions can occur when unprotected steel is surrounded by concrete or cement grout. In Figure 2.2 the surface of a prestressing strand is shown surrounded by cement grout. The anodic site is where the iron is oxidized. The electrons from that reaction flow to the reduction site (cathode) and combine with oxygen and water to produce the hydroxyl ions. If the grout is a sufficiently conductive electrolyte, the hydroxyl ions are transported to the anodic site. The iron ions, in the presence of the hydroxyl ions, form $Fe(OH)_3$ or the familiar red-brown rust.

In sound, uncracked and uncontaminated grout these reaction rates are depressed to a sufficiently low level because of the protective oxide layer that forms over the surface. The amount of iron lost to corrosion is insignificant over the life of a typical structure.[99] An environment with an elevated pH (>13) and oxygen is required for this protective or passive layer to form. The presence of sodium, potassium, and calcium hydroxides derived from the reactions between the mix water and portland cement particles provides an environment suitable for the passivation of the steel. Consequently, grout can provide excellent corrosion protection in two ways. One is to maintain the alkaline environment surrounding the surface of the grout necessary to passivate the steel. The other is to provide a tough barrier to the exterior elements. However, the problems begin when the grout is no longer sound and/or uncontaminated.

2.2.2 Chlorides

It has been well established that the presence of chlorides in concrete or grout, in the presence of sufficient moisture and oxygen, can cause corrosion of reinforcing steel. However, the exact mechanism is not universally agreed upon. Several theories have been put forth to explain the mechanism that causes the corrosion in the presence of chlorides.[60, 66] The most popular of these is the theory based on the assumption that there is a passive oxide film formed around the steel that normally protects the steel from corrosion. When the chlorides reach a certain concentration at the film, it is dispersed and accelerated corrosion begins in the unprotected area. That chlorides will cause a drastic increase in corrosion is rarely disputed. However, the critical level of chlorides required at the surface of the strand to cause corrosion is not agreed upon.

After an extensive literature search and analysis, Kahhaleh indicated that there was a wide range of chloride contents (in concrete) that researchers had found to be critical levels.[66] The critical range typically fell between 0.14% and 0.35% by weight of cement. These values can vary depending on the alkalinity of the surrounding concrete. As the pH decreases the level of chlorides necessary to initiate corrosion decreases.[99]

Another effect of an elevated chloride content is the shift in potential at the steel surface.[71] It has been shown that this potential shift is due to the presence of sufficient chlorides and can

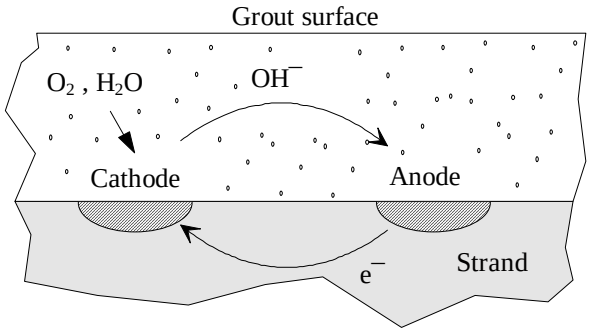

Figure 2.2 - Schematic Representation of Corrosion in Grout.

be as much as 200 mV with respect to the copper-copper sulfate reference electrode.

Some investigators have theorized that the chloride ions reduce the pH of the pore solution in the concrete surrounding the steel. The depressed pH causes a loss of the passive film and leads to accelerated corrosion.

Chlorides generally migrate to the surface of the steel either by diffusion through the grout or at a crack or defect in the grout. A certain amount of chlorides can be chemically and physically bound in the matrix of the grout so that the time to reach the critical level of chlorides is increased. The ability of the grout to bind the chlorides depends on the cement composition and the amount of cement per unit volume. The rate at which the chlorides will diffuse through the grout decreases with a decreasing water/cement ratio.[99] In addition, a well consolidated grout (few air pockets or voids) provides a more dense structure that slows the rate of chloride diffusion.

The other common mode in which the chlorides migrate to the steel is through cracks in the grout. Figure 2.3 shows the effect of a crack in grout on the concentration of chlorides at the surface of the steel. There has been much debate about the role that cracking has in the corrosion of steel in concrete.[111] Beeby is of the opinion that there is no good evidence to support the idea that cracking leads to corrosion problems any more severe than in uncracked concrete of similar quality.[15] In addition, he indicates that if cracks are present the crack width has little influence on corrosion. Mehta and Gerwick indicate that, for concrete in a marine environment, the presence of a few cracks transverse to the reinforcing can lead to a self-perpetuating corrosion process in which corrosion is initiated at the base of the crack.[78] This corrosion product expands and causes further opening of the crack and initiation of additional corrosion that is accompanied by further expansion and cracking. The researchers also indicate that the cathodic areas away from the cracks must have a sufficient supply of oxygen and moisture to support the anodic reaction at the cracks.

ACI Committee 222 indicates that there are two viewpoints with respect to the effect of cracking on corrosion of reinforcing in concrete.[1] The first is that cracks severely reduce the service life of the structure by permitting the access of chloride ions, moisture, and oxygen to the reinforcing steel. Thus, the cracks accelerate the onset of corrosion and aid in the process by providing a space for the corrosion products to be deposited. The other viewpoint is that while cracks may accelerate the onset of corrosion, such corrosion is localized. Because the chlorides will eventually penetrate the concrete over time and initiate widespread corrosion, the result after a few years service is that there is little difference between the amount of corrosion in cracked and uncracked concrete.

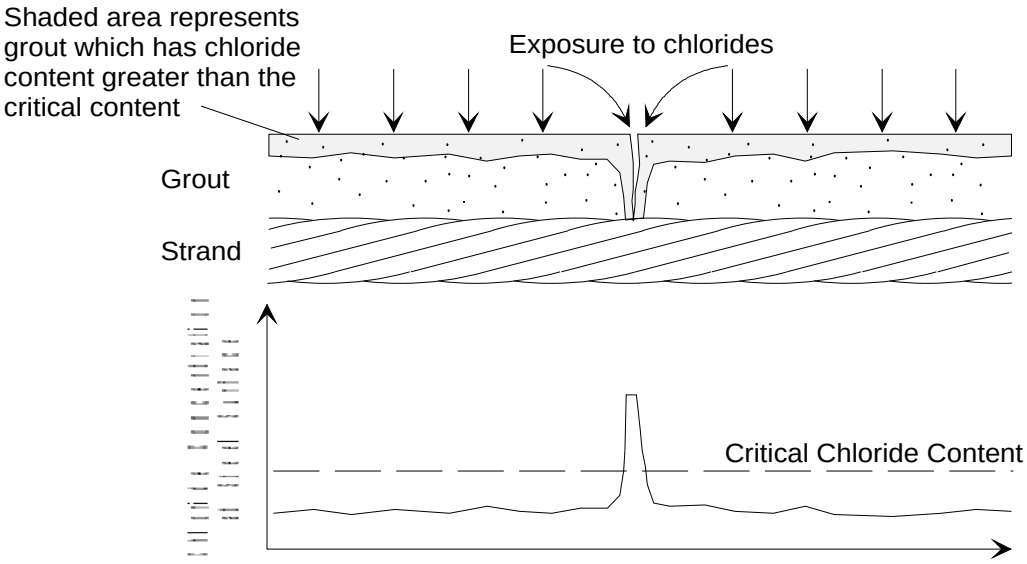

Figure 2.3 - Chloride Concentration at the Surface of the Strand Near a Crack.

The concentration of chlorides at the base of a crack can lead to a phenomenon known as pitting corrosion. While the electrochemical theory explaining pitting corrosion is still the subject of much research and discussion, there are a few basic principles that are generally agreed upon.[47, 99] Figure 2.4 shows the formation and propagation of a pit. Pitting generally describes a unique type of anodic reaction that is autocatalytic or self-propagating in nature. The process is initiated by the arrival of sufficient quantities of chloride ions at the surface of the steel to disturb the passive layer and initiate active corrosion. When the oxygen available locally is depleted, the reduction reaction ceases in the pit and begins at sites adjacent to the pit that have oxygen available for the reduction reaction. The dissolution of iron ions continues, producing an excess of positive charge in the pit region. The negatively charged chloride ions are drawn to the iron ions in the pit which results in the increased concentration of ferric chloride that hydrolyses, producing insoluble rust and free acid:

$$FeCl_2 + H_2O \rightarrow Fe(OH)_2 + H^+Cl^-$$

With the production of free acid, the potential in the region becomes more negative. The adjacent sites produce hydroxyl ions that increase the pH at the cathodic sites.

2.2.3 Carbonation

Carbon dioxide, over time, penetrates concrete and grout through the pore structure.[66, 99, 22] The carbon dioxide combines with the moisture in the pore structure to form carbonic acid. This neutralizes the alkalinity of the grout by reducing the pH to less than 9, increasing the susceptibility to corrosion. The following simplified equation describes the process:

$$Ca(OH)_2 + CO_2 \rightarrow CaCO_3 + H_2O$$

Figure 2.4 - Effect of Corrosion Product Hydrolysis and Recycling Cl^- on Pitting Corrosion.[99]

in the presence of H_2O and NaOH

As shown in Figure 2.5, the carbonation process begins at the surface and migrates inward as the carbon dioxide continues to diffuse, creating a "carbonation front" behind which the grout pH has dropped below 9. Carbonation in sound concrete with adequate cover proceeds at a slow enough rate so that in most conditions the design life of the structure will be shorter than the time necessary for the carbonation front to reach the steel and possibly initiate corrosion.

In cracked grout the carbon dioxide has a direct path to the grout surrounding the steel at the base of the crack. The carbonation proceeds from the surface of the crack face inward causing a drop in pH along the face of the crack. Figure 2.5 shows this effect schematically. One thing to note is that the penetration of carbonation decreases with the depth of the crack because the narrower crack width inhibits the access of the carbon dioxide to the face of the crack. Following one of the natural wet cycles which the exposed grout might experience, the base of the crack is the last to dry out, thus further inhibiting the diffusion of the carbon dioxide.

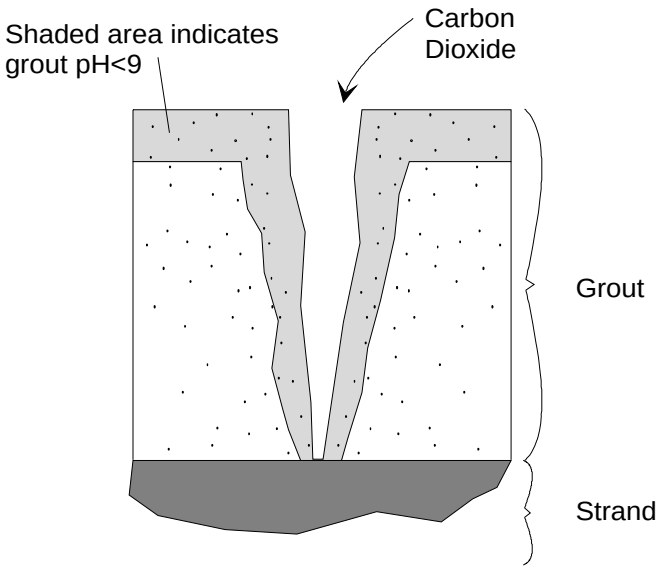

Figure 2.5 - Carbonation of Crack in Grout.

2.2.4 Area Effect

The intensity of the anodic and cathodic reactions depend, in part,

on the ratio of the surface areas over which these reactions occur.[123] If the cathodic to anodic area ratio is high then an unfavorable condition is created. One example of the area effect might be the prestressing strands in a stay cable. If the stay cable protection is breached in an isolated location and chlorides penetrate to the strand in this location, corrosion will be initiated. If the remainder of the cable remains protected from chlorides, then it can act as the cathode while the area under the break is the anode. The cathodic reaction occurring on the remainder of the stay provides a very large flow of electrons to the anodic site to support that reaction. Because the area of the anodic site is small and the current is large, there is a large current density flowing to the site. Not only is the corrosion rate increased, but because the area of the anode is limited, the direction of corrosion will likely be *into* the strand and not along the length. This will lead to a much faster loss in cross-sectional area.

2.2.5 Other Controlling Factors

In addition to the presence of chlorides, the two primary factors that control the rate of corrosion are oxygen availability and conductivity of grout.[77, 99] In order for the pitting corrosion process to continue, the cathodic sites must have an uninhibited supply of oxygen. In addition, the grout must have sufficient conductivity to promote the ionic flow necessary to complete the corrosion process.

In uncracked concrete, oxygen diffusion is controlled primarily by the quality of the concrete and the thickness of cover. With increasing cover thickness and lower water-cement ratios the diffusion rate decreases. Reducing the water cement ratio from 0.6 to 0.4 reduces the diffusion rate of oxygen through concrete by a factor of two.[77] It has also been shown that for a given cover and water cement ratio, the diffusion rates in mortar were 2.5 times higher than in corresponding concretes.

The conductivity of the grout is proportional to the pore water content of the grout.[47, 99] Reducing the water saturation of concrete from 100% to 20% can increase the resistivity (inverse of conductivity) from 7 x 10^3 Ω-cm to 6 x 10^6 Ω-cm, a factor of 1000. Observations of existing structures indicate that corrosion of embedded steel is not a problem in practice as long as the resistivity is above 50-70 x 10^3 Ω-cm.[77] In addition to moisture content, the resistivity of the grout can be affected by the ionic concentration in the pore water solution.

2.3 Modern Corrosion Theory

The following is a brief summary of the electrochemical basics of thermodynamics and mixed-potential theory as they relate to corrosion. The summary is of basic principles generally understood and accepted in the corrosion engineering community and is based on references 47, 64,

76, and 123, unless noted otherwise. These principles are presented in order to lay the groundwork for the anodic polarization tests conducted as a part of this research and reported in Chapter Six.

2.3.1 Thermodynamics

The concept of applying thermodynamics to the study of corrosion has been widely accepted for many years.[47] To gain an understanding of how thermodynamics can be used to determine the tendency of a reaction to occur, an idealized example will be used. Figure 2.6 shows two electrodes in an electrolyte solution which contains the electrodes' ions at unit activity. The solutions are connected by a salt bridge which allows ionic transfer without mixing of the solution. Because each solution is at unit activity, the rate of the anodic reaction r1 is equal to the rate of the cathodic reaction r2. Thus there is no net loss in metal. If the electrodes are connected by a high-resistance voltmeter the reading will indicate the difference in the electrical energy level or

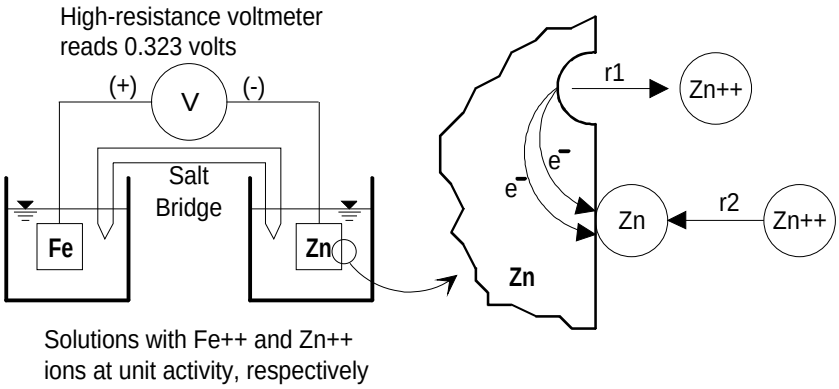

Figure 2.6 - Iron and Zinc in Solutions with their Ions at Equilibrium.[47]

electromotive force (EMF) between the two reacting (but not corroding) electrodes.

Since electrical energy is the driving force in any electrochemical reaction, this difference in potential gives an indication of the "tendency" for corrosion to occur should the electrodes be placed in an environment conducive to corrosion. The energy state of a reversible reaction is usually defined with reference to a standard potential as its *half-cell potential*. Table 2.1 presents the standard potential of several pertinent reactions. These potentials are also known as the standard EMF series.

Table 2.1 - Standard EMF Series.[123]

Reaction	Standard Potential (Volts vs. SHE[b])
$O_2 + 4H^+ + 4e = 2H_2O$ (pH = 0)	+1.229
$O_2 + 2H_2O + 4e = 4OH^-$ (pH = 7)[a]	+0.82

$Hg_2^{2+} + 2e = 2Hg$	+0.788
$O_2 + 2H_2O + 4e = 4OH^-$ (pH = 14)	+0.401
$2H^+ + 2e = H_2$	0.000
$Fe^{2+} + 2e = Fe$	-0.440
$Zn^{2+} + 2e = Zn$	-0.763
$2H_2O + 2e = H_2 + 2OH^-$	-0.828

[a] Not a standard state.
[b] Standard hydrogen electrode

Unfortunately, the half-cell potential of any reaction or electrode can only be measured in a full cell relative to another half-cell. This necessitates defining a reference half-cell potential or reference electrode. The most commonly used reference electrode is the Standard Hydrogen Electrode (SHE). However, there are other reactions which make convenient reference electrodes when used in experimental measurement of unknown half-cell potentials. Several are listed in Table 2.2 including the saturated calomel electrode (SCE) which is commonly used in research related to corrosion of reinforcing in concrete. The reference half-cell name and reaction are shown along with its potential relative to SHE.

When an electrochemical reaction occurs, an associated drop in the free energy of the system occurs. This phenomenon can be used in conjunction with the half-cell potential of each of

Table 2.2 - Potential Values for Common Secondary Reference Electrodes.[47]

Reference Electrode Name	Reaction	Potential vs. SHE (volts)
Mercury-Mercurous Sulfate	$HgSO_4 + 2e = 2Hg + SO_4^{2-}$	+0.615
Copper-Copper Sulfate	$CuSO_4 + 2e = Cu + SO_4^{2-}$	+0.318
Saturated Calomel	$Hg_2Cl_2 + 2e = 2Hg + 2Cl^-$	+0.241
Silver-Silver Chloride (Saturated)	$AgCl + e = Ag + Cl^-$	+0.222
Standard Hydrogen	$2H^+ + 2e = H_2$	0.000

the electrodes in the system to determine the direction which the reaction will take. The change in free energy in any electrochemical reaction or corrosion process can actually be calculated using the cell potential of the particular reactions and the following equation:

$$\Delta G = - nFE$$

where ΔG is the change in free energy, n is the number of electrons exchanged in the reaction, F is Faraday's constant, and E is the total cell potential:

$$E = E_{ANODE} - E_{CATHODE}$$

where E_{ANODE} and $E_{CATHODE}$ are the half-cell potentials of the respective reaction in its equilibrium state.

In a metal/electrolyte system, the spontaneous direction of an electrochemical reaction will be the direction that reduces the system energy. Depending on the constituents of the reaction, metal loss may or may not occur. A reduction in system energy results in a negative value for ΔG. Because F and n are always positive, the spontaneous direction of the reaction can be determined by computing E for each possible reaction. The algebraic combination of each possible half-cell potential which results in the most negative value for E is the direction the reaction will occur. The equilibrium or standard state values of half-cell are used to calculate E.

This principle can be illustrated by electrically connecting the electrodes in Figure 2.6 with a low-resistance wire. Since the cells are no longer in equilibrium, the reaction will spontaneously occur in one of two directions. One direction would be to assume that the iron is the anode and the zinc is the cathode. This would make $E_{Fe/Fe2+}$ = -0.440 V and $E_{Zn/Zn2+}$ = -0.763 V and thus E = 0.323 V. However, E is positive so the reaction will not occur in this direction but rather in the direction in which zinc is the anode and iron is the cathode. The total cell potential in this case would be -0.323 V. It can also be said that, in general, the metals with the less negative half-cell potential are more noble than the metals with the more negative half-cell potential and that the more active metals will corrode sacrificially to the more noble metals.

In summary, thermodynamics can be used to state a criterion for corrosion. Corrosion will not occur unless the spontaneous direction of the reaction indicates metal oxidation. In any electrochemical reaction, the most negative or active half-cell tends to be oxidized (corrode), and the most positive or noble half-cell tends to be reduced.

2.3.2 Electrode Kinetics

While the use of thermodynamic theory can indicate the spontaneous direction of the reaction, it does not provide any indication of the *rate* of the reaction. From an engineering perspective, corrosion rate is the most valuable information regarding corrosion of a metal because it gives an indication of useful life of a structure. The prediction of corrosion rate requires the use of electrode kinetics which establishes a relationship between the potential of a reaction and the corrosion rate. In order to understand electrode kinetics it is necessary to define several terms and relationships.

In Figure 2.6 each electrode is in equilibrium with the surrounding unit activity solution. The electrons flow through the metal from the anodic reactions to the cathodic reactions. Corrosion rate is defined as the loss of mass per unit area per time. Since no electrons can leave the electrode,

the law of conservation of charge requires that the "rate" of the cathodic (r2) and anodic (r1) reactions be equal. This "rate" of corrosion is proportional to the flow of electrons by Faraday's law:

$$r_{cathodic} = r_{anodic} = \frac{i_o a}{nF}$$

where i_o is the *exchange current density* and a/nF is constant. Current density is the current divided by the exposed surface area and is generally presented as μAmp/cm^2. This parameter is commonly used in defining the electron consumption of the anodic reaction and is also directly proportional to the amount of metal lost to corrosion. Just as the important parameter in thermodynamics is half-cell potential, so the exchange current density is the primary kinetic parameter.

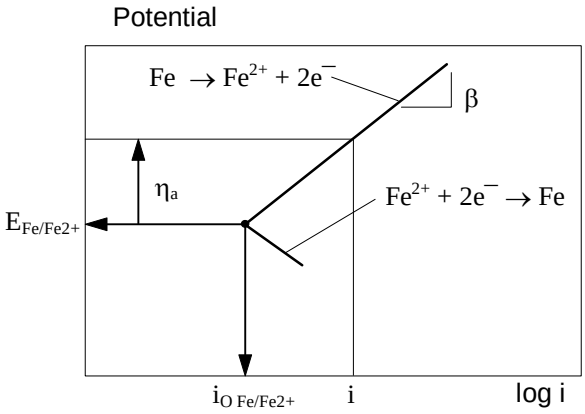

Figure 2.7 - Activation Polarization Curve for Iron.

Assume that the iron half-cell in Figure 2.6 is completely disconnected from the zinc. If the iron half-cell, which is currently in equilibrium, is electrically disturbed from that equilibrium by some means, then one of two things will happen. Either more iron will dissolve than is plated resulting in loss of metal, or more ions will plate resulting in a gain of metal. This deviation from equilibrium is defined as *polarization*.

This polarization or displacement of electrode potential normally results in a net current flow. If the reaction is under *activation* polarization, then the relationship between polarization and corrosion current can be illustrated as shown in Figure 2.7. Activation polarization generally occurs when the reaction is controlled by a slow electrode reaction. Polarization is usually termed overvoltage and is designated by the variable η while the accompanying current is designated as *i*. As shown in Figure 2.7, the overvoltage is measured relative to the standard half-cell potential. The relationship between the current and overvoltage can be represented by the equation:

$$\eta_a = \pm \beta \log \frac{i}{i_o}$$

where η_a is the overvoltage and β is the slope of the polarization curve. β is experimentally determined for each reaction in a particular environment. Note that the exchange current density i_o corresponds to the half-cell potential of the reaction and that it corresponds to a reversal in the direction of the reaction. The exchange current density is also experimentally determined. The equation is called the Tafel equation and β is termed the Tafel slope or Tafel constant.

Concentration polarization normally controls in systems which have a very high reaction rate. One example of concentration polarization is the depletion of oxygen concentration at the cathode. If the reaction rate is very rapid but the diffusion of oxygen to the cathode is slow the anodic reaction will be impeded. Figure 2.8 shows a schematic of the cathodic portion of a concentration polarization curve. Note that as the reaction rate (corrosion current i) increases a limiting rate is approached which is known as the limiting diffusion coefficient (i_L). The equation describing this reduction process is given by:

$$\eta_c = 2.3\frac{RT}{nF}\log\left(1-\frac{i}{i_L}\right)$$

Both activation and concentration polarization are usually present (see Figure 2.9). Combined polarization can be characterized by the sum of the two equations for overvoltage:

$$\eta_T = \eta_a + \eta_c$$

where η_T is the total overvoltage.

Up to this point only single electrode systems have been examined. When two or more electrodes are combined for an electrochemical reaction, the polarization curves for each of the electrodes can be combined to characterized the parameters of the system. A combined system is analyzed using mixed-potential theory.

2.3.3 Mixed-Potential Theory

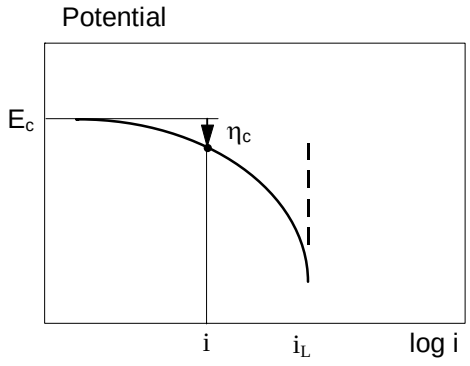

Figure 2.8 - Typical Concentration Polarization Curve

When the two electrodes in Figure 2.6 are electrically isolated they remain in equilibrium at $E_{Fe/Fe2+}$ and $E_{Zn/Zn2+}$, their standard half-cell potentials. However, when the half-cell electrodes in the zinc-iron example are short-circuited the spontaneous direction of the reaction results in corrosion of zinc and deposition of iron on the surface of the iron electrode. Both electrodes are polarized to the *free corrosion potential* (E_{CORR}). Figure 2.10 shows schematically the result of short circuiting the two electrodes. The cathodic reaction of the iron electrode is polarized an amount equal to the difference between the iron free corrosion potential and the free corrosion potential of the mixed electrodes $E_{CORR.}$ Conversely the zinc electrode is polarized anodically. This polarization is a result of the natural potential difference between the electrodes. This potential difference could be called the driving force in the corrosion process. The corrosion rate is the location where the polarization

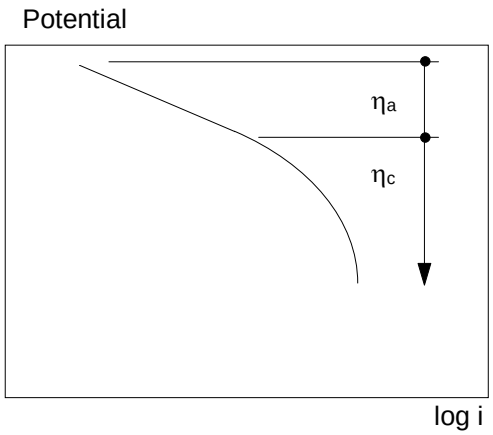

Figure 2.10 - Combination of Concentration and Activation Polarization.

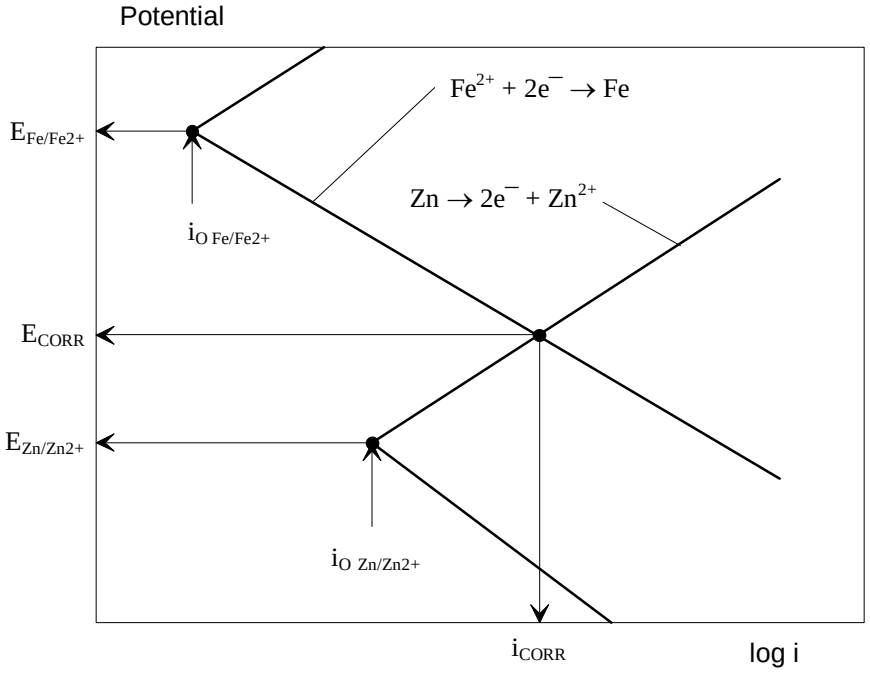

Figure 2.9 - Schematic of Mixed-Electrodes Iron and Zinc.

curves intersect. If β, E, and i_O are known for each metal then E_{CORR} and i_{CORR} can be determined.

The degree of polarization and the resistance of the electrolyte limits or controls the magnitude of the current produced. Controlling factors for corrosion in grout can be illustrated using mixed-potential theory as shown in Figure 2.11.[1]

When the magnitude of the polarization of the anodic reaction is large compared to that of the cathodic reaction then the reaction is said to be anodically controlled. If the reverse is true then it is cathodically controlled.

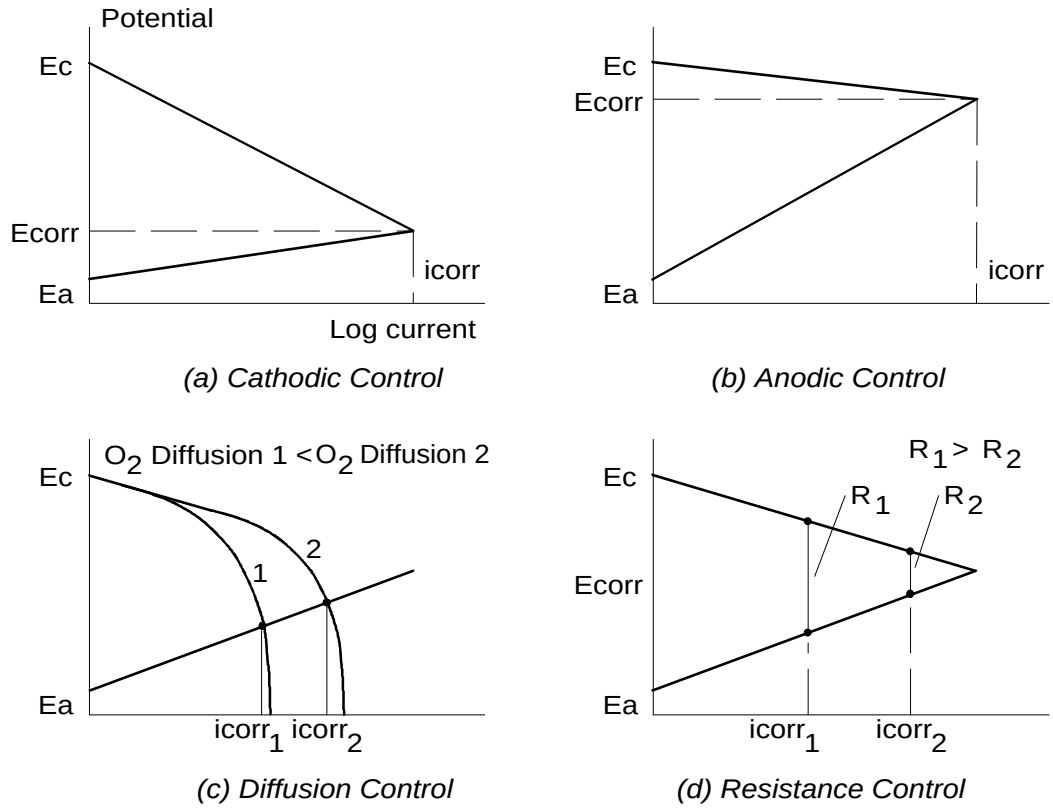

Figure 2.11 - Corrosion Control Mechanisms.[1]

In grout there are two types of controlling mechanisms that usually control. One is known as cathodic diffusion (Figure 2.11c).[1] This occurs when concentration polarization controls the cathodic reaction. As the diffusion of oxygen is reduced the cathodic reaction comes under concentration polarization and the corrosion rated is reduced correspondingly. Another mechanism is the resistance of the grout. If the electrolyte (grout) separating the anode and cathode is of high resistance then the reaction is said to be resistance-controlled. Figure 2.11d shows that increasing the resistance of the grout reduces the corrosion rate.

2.4 Anodic Polarization

Modern test methods and mixed-potential theory can be used to characterize an electrochemical reaction. Figure 2.12 shows a schematic of a potentiostat which has the ability to apply a constant potential to the working electrode (WE) by varying the current based on the potential sensed at the tip of the reference electrode (RE). The cathodic reaction occurs at the auxiliary electrode (AE). The material for the AE is usually an inert metal such as platinum.

The potentiostat can be used to develop the polarization curve for the WE in a particular electrolyte. The test procedure essentially consists of varying the potential and measuring the current flowing from the AE to the WE. This current flow is then plotted as the anodic polarization curve (see Figure 2.13). The measured current represents the difference between the corrosion currents for the anodic reaction at WE and the cathodic reaction AE. When the set potential approaches E_{CORR} then the magnitude of the anodic and cathodic currents become comparable. However, when the set potential is greater than E_{CORR} the anodic current becomes much larger than the cathodic current and the measured current approaches that of the anode.

One major difficulty in this type of test is the influence that the electrolyte resistance can have on the test results.[56] The potentiostat adjusts the applied potential based on the measurement of potential at the tip of the reference electrode. However, the RE is physically separated from the surface of the WE. Depending on the resistance of the electrolyte, the difference between the potential at the RE and WE may be significant. This phenomenon is known as "IR drop." It is undesirable because it causes incorrect measurements to be made. If the error is significant it can cause the corrosion rate to be underestimated. In addition, it can result in incorrect polarization curves. [56]

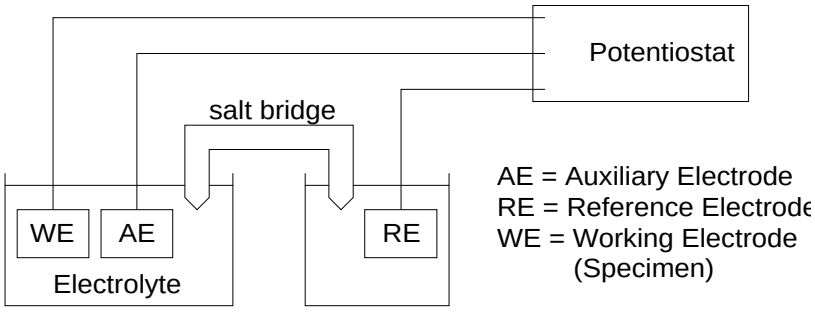

Figure 2.12 - Schematic of Anodic Polarization with Potentiostat.

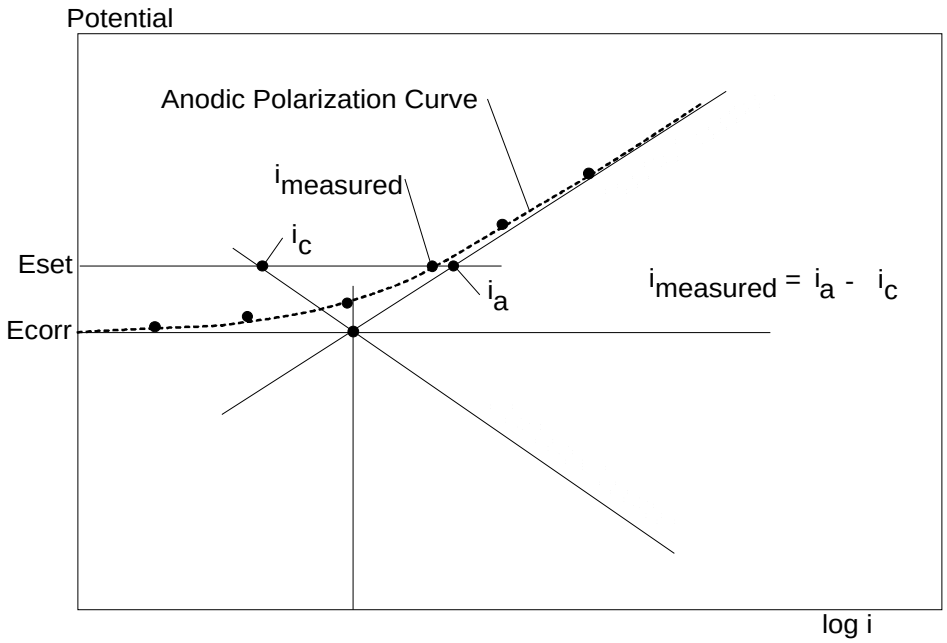

Figure 2.13 - Anodic Polarization Curve.

There are several methods to minimize the effect of IR drop.[56] The resistance of the electrolyte can be reduced or the geometry can be adjusted so that the RE is closer to WE. Another method is to measure the IR drop and adjust the data accordingly. One popular method of measurement is called current interruption. When the current is turned off, the cell potential will immediately drop by an amount equal to the IR drop. Depolarization of the WE takes some time due to capacitance effects. This procedure can be done electronically so that the user need not manually make corrections.

Chapter Six describes the procedures and results using anodic polarization to accelerate corrosion of a short section of prestressing strand embedded in a layer of pc grout. The test setup is as shown in Figure 2.12 with a saturated calomel reference electrode placed directly in the electrolyte which was 5% (by weight) NaCl solution. The test procedure was to crack the grout and then immerse the grout in the electrolyte. The salt solution was not allowed to contact the strand directly. Thus the test gave an indication of the level of protection provided by the grout against the ingress of chlorides. The strand was polarized to +600 mV_{SCE} and allowed to remain at that level until the chlorides reached the surface of the strand and initiated corrosion.

2.5 Hydrogen Embrittlement (HE)

When exposed to atomic hydrogen some metals can experience nonductile fracture when stressed in tension. HE can also play a role in crack growth for fatigue loading.[47] While most steels

are to some extent susceptible to HE, it is the high-strength steels which are most susceptible to HE.[64] The type of steel also affects the tendency toward HE. There are three main types of prestressing steels:[62]

- Hot-rolled, stretched and stress-relieved bars
- Quenched and tempered martensitic wires/bars
- Cold-drawn, stress relieved wire/strand

Of these three, the cold-drawn, stress relieved wire/strand (prestressing wire/strand) is the most resistant to HE cracking.[57]

Probably the most prominent failure caused by HE was the 1980 collapse of the Berlin Congress Hall.[63] The collapse was precipitated by HE of quenched and tempered prestressing rods. It is believed that the HE was caused by hydrogen evolution during corrosion attack. Schupack and Suarez recently conducted a survey which indicated good performance of prestressing strand/wire in the US.[100] They reported receiving information on 50 corrosion incidents (40% of them were parking structures which had deicing salts applied) of which there were 10 cases of probable brittle failure. This low number suggests that prestressing strand/wire has been performing well in service. There have been no reports of problems with prestressing wire or strand in stay cables.

There are many theories which purport to explain the mechanism of HE.[47] One such theory proposes that atomic hydrogen diffuses into the lattice of the metal and accumulates near slip dislocation sites or microvoids. The dissolved hydrogen then interferes with the slip mechanism reducing the ductility of the metal. Regardless of the mechanism, it has been shown that the presence of atomic hydrogen in significant quantities can promote nonductile behavior in high-strength steels.

The remainder of this section covers the phenomenon of HE as it relates to high strength prestressing steels, specifically prestressing strand and wire. In order for HE to occur, atomic hydrogen must somehow be evolved near the surface of the metal so that it can be adsorbed. In general HE can be associated with hydrogen-producing cathodic reactions occurring on the surface of the steel. However, there are also other possible sources of hydrogen. The following sections discuss the various methods by which hydrogen can be evolved.

2.5.1 Corrosion-Generated Hydrogen

One possible source of hydrogen is at the base of a corrosion pit which is corroding in the presence of chlorides. As discussed previously, pitting corrosion is an autocatalytic process in which the pH of the solution in the pit can drop significantly. Novokshenov suggests that this pH can be as low as 1.5 to 5.0 and that this results in a shift in the corrosion potential in the pit below the

reversible hydrogen potential.[84] H_2O inside the pit dissociates at the anode site inside the pit to form H protons which migrate to the cathode site inside the pit where they are discharged to atomic hydrogen (with electrons freed during iron dissolution) and adsorbed into the steel. As the pH continues to decrease the combining of electrons and hydrogen protons tends to replace the cathodic reaction occurring outside the pit and the process continues with atomic hydrogen collecting in the imperfections in the steel.

Other investigators have suggested that promoters such as sulfur, arsenic or thiocyanate are necessary at the base of the pit for the atomic hydrogen to form.[62]

2.5.2 Cathodic Protection

If concrete or grout surrounding prestressing strand or wire is contaminated with chlorides, cathodic protection can be applied to prevent further corrosion of the steel. Cathodic protection essentially consists of cathodically polarizing the prestressing steel with reference to a sacrificial anode. This forces the anode material to corrode sacrificially to protect the cathode. Depending on the level and extent of corrosion, an impressed current may need to be applied to the systems to sufficiently polarize (and protect) the steel. If the applied protection potential is low then the predominant cathodic reaction is:[62]

$$1/2O_2 + H_2O + 2e \rightarrow 2OH^-$$

If the cathodic protection exceeds the equilibrium hydrogen potential value, then water is reduced as follows:

$$H_2O + e \rightarrow H_{ADS} + OH^-$$

where H_{ADS} denotes adsorbed atomic hydrogen. The equilibrium potential of the hydrogen cell depends on the pH. At the typical grout pore water pH of 12.6 to 14.6, the hydrogen evolution values can range from -730 to -840 mV standard hydrogen electrode (SHE). Isecke and Mietz suggest that the actual potential required to support the significant evolution of hydrogen is lower than this (200 to 300 mV_{SHE} more negative than the equilibrium potential).[62] The significance is that reinforced concrete cathodic protection is typically no more negative than -400 mV_{SHE}. They also indicate that the hydrogen recombination reaction in which gas is formed competes with uptake of dissolved hydrogen, further inhibiting the reaction.

Several researchers have investigated HE in association with cathodic protection (polarization) and brittle fracture of prestressing steels. Parkins et al. reported that enhanced cracking occurred at potentials less negative than -900 mV_{SCE} , but that enhanced cracking was seen at all potential levels if the environment was acidic.[86] Hartt et al. indicated that in tests using notched and smooth wire, and with different values of pH, Cl^-, and precharging time, HE was observed in

specimens polarized more positive than -900 mV_{SCE}.[58] However, some of the notched specimens showed susceptibility to HE even at potentials less negative than -900 mV_{SCE}. Funahashi et al. found that hydrogen was generated on steel embedded in mortar at potentials more negative than -970 mV_{SCE}.[50] They also found that hydrogen could be generated near -750 mV_{SCE} when the pH was near 9.0.

Although the results differed somewhat, the recommendations from these investigations were in general agreement. Parkins et al. concluded that HE risk could be kept low by using polarization values less negative than -500 mV_{SCE} while use of potentials more negative than -900 mV_{SCE} can result in HE. Hartt et al. suggested that excessive protection can cause HE of the prestressing steel (more negative than -900 mV_{SCE}). The severity and extent of corrosion present on the steel can have an effect on the risk of HE when applying cathodic protection. In the potential range -500 to -900 mV_{SCE} the presence of sharp pits or defects can increase the tendency for HE. Funahashi et al. suggested a lower limit on potential of -720 mV_{SCE}. These potentials should be adjusted to remove the IR Drop from the potential reading. In addition, because most cathodic protection systems are current controlled, it was suggested that the equipment be provided with a current-off potential limitation to prevent very negative polarization values.

2.5.3 Galvanizing and Grout

Zinc, used in galvanizing prestressing strand and wire, if in contact with fresh portland cement grout reacts with the alkali ingredients and evolves hydrogen:[130]

$$Ca(OH)_2 + Zn \rightarrow Ca(Zn(OH)_4) + H_2$$

Although not confirmed conclusively experimentally, there is concern that the hydrogen evolved in this reaction may enter the steel lattice and embrittle the wire. There is little data concerning the relationship between the volume of adsorbed hydrogen and the brittleness of the steel.[130]

Federation Internationale de la Precontrainte (FIP) recommends the use of ammonium thiocyanate (NH_4SCN) solution to determine the susceptibility of prestressing wire to stress corrosion cracking (SCC). However, researchers have indicated that the failure induced by this method is HE rather than SCC.[130]

Tests were conducted by Yamaoka et al. on 5-mm diameter drawn prestressing wires.[130] The behavior of bare wires was compared with that of galvanized wires and galvanized wires which had been redrawn after galvanizing. Examination of the microstructure indicated that the galvanizing on the surface of the wire which had not been redrawn was crack free. However, the wire which had been redrawn had microcracks in the zinc layer. These cracks extended down to the

steel surface. The specimens were dipped in a 35% aqueous solution of NH_4SCN for 65 hours. Tensile and torsion tests were conducted along with measurement of adsorbed hydrogen.

The results indicated that the bare wire suffered a reduction in ductility while the galvanized wire did not lose any ductility. The galvanized and redrawn wire suffered some loss in ductility but not as much as the bare wire. The zinc layer adsorbed the hydrogen and prevented it from penetrating into the steel. However, wire which had been redrawn after galvanizing had cracks which allowed the hydrogen localized access to the surface of the wire. Measurement of hydrogen absorption confirmed these findings. The investigators indicate that the microstructure of the zinc is very similar to titanium which is a known hydrogen adsorber. The zinc has a large volume of interstitial space which can adsorb a large quantity of hydrogen. Based on the results of their work, Yamaoka et al. concluded that the hydrogen formed during contact of zinc with fresh grout should not cause hydrogen embrittlement.

Other research has confirmed that hydrogen released in the reaction between the zinc and wet grout is effectively prevented from entering the steel by the zinc barrier.[34]

2.6 Stress Corrosion Cracking (SCC)

For a brittle failure to qualify as stress corrosion cracking (SCC) the metal must be under tensile stress and simultaneously exposed to a corrosive environment.[47] Several theories have been proposed to explain the SCC mechanism. One theory is that the process starts with a small corrosion pit (Figure 2.14). The stress concentration at the bottom of the pit causes deformation along a slip plane. This deformation exposes new metal which is active compared to the surrounding pit and is immediately corroded to form a new pit. This process continues until the section fractures. Klodt indicates that of the many possible combinations of environments which cause SCC in iron-base alloys, the only environment which prestressing steel might be exposed to in service is H_2S.[68]

Klodt performed experimental studies in which cold-drawn prestressing wire was placed in 3.5% NaCl and $CaCl_2$ solutions at 93°C for 340 hours.[68] The stress levels were 1210, 1380, and 1550 MPa. There were no failures in any of the specimens which led to the conclusion that SCC was not a problem in a chloride environment. Klodt also cited other research work that indicated that SCC of cold-drawn steel in concrete contaminated with chlorides was not a problem

Figure 2.14 - Schematic of Progression of Stress Corrosion Cracking.[129]

Cherry and Price conducted a series of tests on cold-drawn prestressing wire (1800 MPa ultimate tensile strength) to determine if sodium chloride solutions of varying pH (10, 12, 14) would cause SCC.[25] There were two tests conducted. The first was a long-term constant strain test which lasted over a year. The tests were conducted at 1500 MPa stress level. The second test was an "ultra-slow stress corrosion cracking test" at a strain rate of $2x10^{-6}$ s^{-1}. Wires fractured in both tests. However, the failures were attributed to loss of section due to corrosion and not SCC.

Parkins et al. conducted a similar set of tests for SCC and HE. In addition to the parameters used by Cherry and Price, Parkins et al. also lowered the pH of the solution with HCl.[86] They found that at applied potentials more positive than -0.600 V (SCE), SCC is present in the form of dissolution at the tip of the crack rather than being caused by hydrogen evolution. The main difference is that in the Parkins et al. study the wires were notched, while they were not in the tests conducted by Cherry and Price.

Yamaoka and Tanaka gave two examples of field failures which were attributed to SCC. One was a prestressing strand which was left stressed and ungrouted in a post-tensioning duct for 7-months. Another was a prestressing wire wrap for a pipe which failed after six years of service.

2.7 Fretting Fatigue

Fretting fatigue is a corrosion-related phenomenon which can affect prestressing strand/wire used in post-tensioned applications. Fretting fatigue is an extension of fretting corrosion which occurs at the contact area between two materials. There are some basic conditions which must be satisfied in order for the damage to be considered fretting corrosion (as opposed to wear):[47]

- The interface must be under load
- Repeated relative motion between the two surfaces must occur
- The load and relative motion on the interface must be sufficient to produce relative slip and deformation on the surface

The relative motion necessary to produce fretting corrosion is extremely small and can be as little as 10^{-7} mm. It occurs only on surfaces that are subjected to repeated small relative

displacements. The relative motion of the surfaces in the presence of oxygen causes wear and corrosion at the interfaces.

It has been shown that the process which causes fretting corrosion can also cause fatigue cracking in prestressing strand used in post-tensioned girders.[97] This process has been referred to as fretting fatigue. In post-tensioning ducts, strands are in close contact with one another. This contact along with cyclic loading can lead to premature fatigue failures due to fretting. At deviation points in curved duct the strands which are in contact with the duct material which can experience fretting. Fatigue cracks can be initiated prematurely from the combination of surface damage (from the fretting corrosion) and the very high local contact stresses.

PTI *Recommendations for Stay Cable Design, Testing and Installation* require that the helical wire spacer on stay cable systems be coated with epoxy or polyethylene to prevent fretting fatigue from occurring between the wire and outside layer of wires or strands in the bundle.[28] Premature wire failures have been noted in stay cable fatigue test which have been attributed to fretting fatigue between adjacent wires.[113] Other stay cable fatigue tests have had wires fracture due to fretting fatigue between the strands and bare wire used for a helical spacer.[48]

2.8 Corrosion Effect on Fatigue Performance

A metal that progressively cracks on being stressed cyclically is said to fail by fatigue.[123] The number of cycles required to cause fracture is known as the fatigue life. The fatigue life can be reduced when the specimen is subjected to a selected environment during cycling. This phenomenon is known as *corrosion fatigue*. While corrosion fatigue of steel is well documented and studied, there has not been much study devoted to the corrosion fatigue of prestressing strand/wire.

2.9 Summary

Providing a durable corrosion protection system for strands in stay cables is a unique problem. Prestressing strand was developed for and is largely used in prestressed concrete. This application provides the rigid and tough environment of the outer layers of the prestressed concrete member as the first line of protection against the corrosive elements. The use of strand in stay cables has removed them from the protective environment of the concrete and placed them more at the mercy of the elements. In addition, there are special problems associated with the corrosion of prestressing strand that are not an issue with mild reinforcing steel. A number of these elements were discussed in this chapter. The following summarizes the key points of the chapter:

- Localized corrosion on prestressing strand at the base of a crack in the pc grout has the potential to be much more damaging for a strand in a stay cable than for mild steel

embedded in concrete. Loss of section for high-strength steel under tension is much more critical than for lower strength mild steel reinforcing. The same loss of section for the two systems produces a much larger loss of capacity for the high-strength steel than for the mild steel.

- Hydrogen generated at the base of a pit in a strand corroding in the presence of chlorides has been discussed as a possible mechanism for hydrogen embrittlement. Experimental work is lacking in this area.
- In recent years research has been conducted on the effect of cathodic protection on prestressing steels. While protection potential levels have been established, the industry is still cautious in proceeding with implementation. One of the reasons is the fear of hydrogen embrittlement. It has been shown that there is the possibility for atomic hydrogen production on the surface of a prestressing strand when the protection potential is too negative. This can lead to hydrogen embrittlement. It is unlikely that cathodic protection would be considered a viable option for stays because the elements are so long that maintaining an even current distribution would be very difficult.
- Atomic hydrogen is also produced when zinc galvanizing is in contact with fresh grout. It has been shown experimentally that in prestressing wires which were hot-dipped galvanized, the zinc layer actually adsorbs the hydrogen produced by this reaction. In wires which were drawn after galvanizing, the hydrogen migrated to the wire through cracks in the zinc layer caused by the drawing process.
- Comparison of several experimental studies suggests the lack of a clear consensus on the performance of prestressing strand with respect to stress corrosion cracking (SCC). However, there does seem to be agreement that the presence of chlorides in an environment similar to that provided by grout is not a problem. The accepted method for testing for SCC susceptibility utilizes an ammonium thiocyanate solution environment coupled with a constant strain rate loading. The problem with this test is that it does not really represent typical field conditions. Its primary purpose is to provide a reference standard of quality for prestressing steel.
- Fretting fatigue is another failure mechanism to which prestressing strand is susceptible. Avoidance or this particular form of damage should be a primary consideration when designing stay systems. Eliminating steel-on-steel points of contact between the strands and other components should be given special consideration during design and construction.

- Corrosion fatigue has not really been investigated as a possible cause of the wire breaks in the stay cable fatigue test specimens cited in Chapter One. It is possible that a combination of the constituents of the grout and the excess water from the grout combine to form an environment which under cyclic loading could contribute to premature failure of the strands.

Chapter Three
Corrosion Protection of Stay Cables

Introduction

In recent years there has been a great increase in the number of methods and materials available for corrosion protection of the main tension elements in bridge stay cables. These systems have been developed and heavily promoted by prestressing suppliers with little or no objective evaluation of their effectiveness of the systems to perform as claimed.

In this chapter the various materials and methods which are available for use in corrosion protection are identified and described. Previous evaluations of the materials and methods are also discussed if available. While most of the corrosion protection systems discussed herein may be applicable to other types of prestressing such as bar or wire, the emphasis will be on the use of these protection schemes to improve the durability of the prestressing *strand* in stay cables.

Philosophy of Protection

The lack of effective nondestructive test methods available to periodically inspect stay cables in place has led, in part, to two choices concerning the corrosion protection of stay cables. These choices were defined succinctly by Buergi:[20]

- Use of multiple robust protection barriers to provide a redundant system with several backup protective barriers.
- Design for ease of inspection (easier detection of failure), at the expense of robustness, reliability, and life expectancy.

Birdsall has indicated that inspectability should be a priority.[27] That philosophy is based in part on the success that suspension bridges have had in the last one-hundred years using galvanized wires open to inspection. He also thinks grouted systems should not be used, in part because it restricts access for visual inspection. On the other hand Arvid Grant argues that the more robust systems (namely PE sheathing with pc grout injected) when properly installed provide adequate corrosion protection.[27]

In the survey presented in Chapter Four the responses indicated that the multiple barrier system with less inspectability was more favored than the reduction in the number of barriers to improve inspectability.

Code and Standard Requirements

There are currently two sets of recommendations available for cable-stayed bridge design and construction. One is *Recommendations for Stay Cable Design, Testing and Installation,* published by the Post-Tensioning Institute's Committee on Cable-Stayed Bridges.[28] The other is *Guidelines for the Design of Cable-Stayed Bridges,* published by the American Society of Civil Engineers (ASCE) Committee on Cable-Stayed Bridges. The PTI document provides recommendations only for the stay cables while the ASCE document covers the complete bridge. The PTI document provides detailed recommendations for the design and construction of stay cables while the ASCE document covers the types of stays only briefly. Stay cables utilizing the helical or locked-coil strands, or wires ropes are not addressed in the PTI recommendations. The types of cables covered include parallel wire, strand and bar cables enclosed in a sheath and injected with a protective filler.

One significant requirement of the PTI Recommendations is that bridge stay cables be designed in a "redundant" manner. This requires that the loss of a single stay will not cause significant structural damage. In addition, the bridge should be designed to allow the replacement of a stay cable without damage to the bridge.

The PTI recommendations indicate standard test methods and material property requirements for the individual components of a stay cable. Some procedures and methods are also given for the installation of the stay. Full-scale fatigue testing is also required for the proposed stay system to be used.

Sheathing

<u>High-Density Polyethylene (PE) Sheathing</u>

PE is a highly dense, non-reactive material which provides excellent protection from moisture intrusion. A 6-mm thick layer of PE has approximately the same permeability as a 11-m thick concrete wall.[112] However, the PE must remain undamaged in order to provide this protection.

PE which is not properly protected from ultraviolet (UV) radiation can have a significant reduction in ductility as shown in Figure 0.1.[98, 112] The weathering is a combination of accelerated UV exposure and moisture exposure. The addition of carbon black to PE has been shown to prevent its embrittlement when exposed to accelerated weathering conditions. Five thousand hours of

accelerated exposure has been correlated with 25 years of outdoor exposure. In addition, there have been other tests conducted on PE exposed in field conditions:[98]

- Bell Telephone Co., 1969: 27 years outside exposure in Florida coastal region. No significant degradation of mechanical properties
- Schillersteg Pedestrian Bridge with PE sheathing, 1979: 18 years of exposure with no significant degradation

Figure 0.1 - Accelerated Weathering Results on PE.[112]

The color of PE sheathing with carbon added is black. Solar radiation can cause the temperature on the surface of black sheathing to reach as high as 65°C while a white sheathing under similar circumstances would reach only 40°C.[112] In addition, PE has a thermal coefficient of expansion approximately six times that of pc grout or steel. Therefore, the control of thermal fluctuations from the solar radiation on the sheathing is critical to maintaining the long-term performance of the PE sheathing. Typically, a light-colored tape is applied to the surface of the sheathing to reduce the magnitude of the temperature fluctuations.

Overpressure during the grouting operation is another potential problem with PE sheathing. The grout injection is executed in lifts from the bottom of the stay. As the lift rises in the sheathing the hoop stresses build up in the sheathing with a maximum near the bottom of the lift. When the grout hardens, the stresses are locked into the sheathing. Because of the incompatible thermal expansion coefficient, the contraction of the sheathing under lower temperatures is restrained by the grout. This results in appreciable increases in the hoop strains. If large enough these will cause the sheathing to split. This phenomenon is thought to be at least partly responsible for the cracks in the sheathing at the Luling Bridge.[112]

PTI recommendations now restrict the lift height to a maximum of 38 m and the diametrical expansion of the sheathing at the injection point to 2% of the original diameter. In addition, the temperature of the sheathing can be no greater than 38°C during injection. PE sheathing material properties are also specified as shown in Table 0.1. These provisions are intended to prevent occurrences such as those on the Luling Bridge. The PTI Recommendations require that the PE sheathing wall thickness shall be sufficient to withstand grouting pressures. The maximum allowable Standard Dimension Ratio (SDR = ratio of outside diameter to minimum wall thickness) is 18. This value is valid as long as the specified grout injection procedures are followed and the bridge service temperature is not expected to be lower than -29°C. If the bridge service temperature significantly lower then the specified SDR may not be appropriate.

Table 0.1 - Acceptable PE Sheathing Material Properties.[28]

Property	ASTM test method	Value
Density, gm/cm^3	D1505	0.941-0.955
Melt Index	D1238	Max of 1.0
Flexural Modulus	D790	552-1103 MPa
Tensile Strength at Yield	D638	21-28 MPa
Environmental Stress Crack Resistance: Test condition Test duration Failure, max, %	D1639	 C 192 hours 20%
Hydrostatic Design Basis	D2837	8.62-110.3 MPa

PE sheathing is not continuously extruded for use in stay cables. Rather, it is manufactured in standard lengths and fusion welded together to form a continuous length of sheathing. Fusion welding consists of heating the squared ends of two sections of PE sheathing up to the melting point.[6] After the proper melt has been attained, the ends of the two sections are forced together and allowed to cool while maintaining the proper applied force. To produce a joint with adequate bond, a specific temperature range (which is material dependent) must be maintained. In addition, the force required to hold the ends together depends on the fusion temperature and material. Finally, proper use of an alignment jig is necessary to ensure that the sheathing is not kinked after welding. If the stays are field assembled then the fusion welding must be performed in the field where inspection and quality control can be difficult. However, if the stays are factory assembled then the welding can be performed in a more controlled environment.

One concern with prefabricated stays is that they must be coiled onto reels for transporting to the site. If the coil diameter is too small then the stresses in the PE can cause cracking. This operation has been claimed to be partly responsible for sheathing cracking problems on at least two

bridges: the Luling and the Zarate-Brazo Largo.[53, 70] Since then studies have been conducted to determine the minimum coiling diameter which should be used with prefabricated stays.[112] However, it should be noted that the quality of the polyethylene material and welds affects the diameter to which the PE can be coiled.

There is evidence to indicate that stress concentrations at damaged areas such as cuts or abrasions may lead to the shortening of the PE service life.[112]

Steel Pipe Sheathing

Three bridges in the United States have used steel pipe: Dame Point Bridge in Florida, Sunshine Skyway Bridge in Florida, and the C & D Canal Bridge in Delaware. ASTM A53, Grade B, black steel pipe is generally used with the pipe being connected by butt welding in the field.[31] FHWA does not allow the pipe to be considered in the strength design of the stay. However, if grout is injected, there is bond and load transfer between the grout and pipe. The pipe will experience the same fatigue loading as the strands. This raises some concerns about the fatigue performance over the life of the structure at the butt welds. Another concern is the possibility of dissimilar metal corrosion between the main tension element and the steel sheathing.[112]

Stainless Steel and Copper Encapsulation

Stafford and Watson have suggested a unique repair method for existing stays by applying a tinned copper jacket to the outside of the existing stay.[109] This system was used to repair the stays at the Mannheim-Ludwigshafen bridge. Another unique system suggested for new stays was a continuous titanium grade stainless coated carbon steel tubing with a 3-mm thickness. This tube would be extruded onto the erected cable on-site and subsequently injected with grout.

Tape Protection for Sheathing

As a part of the investigation into the cracking of PE sheathing at the Luling Bridge, studies were conducted on the durability and strength of tapes used for wrapping PE sheathing.[70] The study gave the following reasons for use of tape:

- Seal cracked sheathing against water and air
- Strengthen sheathing against bursting pressures
- Reduce PE temperature due to solar heating

The study compared several different types of tape:

- Filament Tape: Polyester film with glass yarn reinforcement (0.2 mm) manufactured by 3M
- Tedlar Tape: Polyvinyl Fluoride film (0.09 mm) manufactured by 3M
- Coroplast Tape: Polyvinyl Chloride film (0.2 mm) manufactured in Germany
- CMC Tape: Tedlar tape with glass yarn reinforcement made in Germany
- Raychem Tape: Polyethylene heat-shrink film (1 mm) made in the United States
- Aluminum tape: Aluminum film (0.13 mm film/0.13 mm backing) made by 3M

The direct tensile strength of the tape was tested. In addition, the tensile strength was tested using a taped undamaged PE sheathing and a taped split PE sheathing in which an increasing bursting pressure was applied until the tape failed in tension. The tape adhesion was tested as well. The testing was performed on specimens which had been exposed in a weather-o-meter which accelerates the effect of ultra-violet degradation. Unexposed specimens were also tested. The results were ranked in accordance with their performance. The results indicated that Coroplast, Filament, Tedlar, and CMC performed the best and at about the same level. Other test results have confirmed that the Tedlar tape performs well in accelerated weathering tests.[108]

Portland Cement Grout

Bridge stay cables which use pc grout as a blocking agent have many of the characteristics of an external tendon of a post-tensioned box girder that has been removed from the box girder cavity and placed outside in the environment. In external post-tensioning tendons the grout serves two purposes. One is to provide some bond transfer between the tendon and the bridge at the deviators. The other and major reason is to surround the strand with an alkaline environment to prevent corrosion and to serve as a barrier to the entrance and transport of deleterious substances into and through the duct. Consequently, in both stay cables and external post-tensioning tendons, the grout is injected principally to provide a physical barrier and an alkaline environment.

As a result, the external tendon and stay are protected against corrosion by the combined actions of the duct and pc grout. The principal difference between these two applications is that the external tendon is usually placed inside the cavity of the box girder where the environment is innocuous. On the other hand, the stay cable is necessarily directly exposed to the elements because of the inherent geometry of the bridge. There is no prestressed concrete surrounding the duct (either in direct contact or indirectly) to provide the additional robust layer of protection afforded to the post-tensioning tendons. This makes the effectiveness of the protection provided by the sheathing and pc grout for the stay much more critical than in post-tensioned concrete. In fact, it could be said

that in most post-tensioned applications the corrosion protection ability of the duct and pc grout will never be fully tested while the duct and grout in the stay cable are put to the test from the day the stay is erected.

While the ability of intact PE duct to act as a moisture barrier has been proven, it follows that if the sheathing is in some way damaged then the grout must be able to provide an effective back-up system to the sheathing. To this end, a literature review was conducted on pc grouts for post-tensioned and stay cable applications. The following subsections present the findings of this review.

It should be noted that the majority of the literature covered methods and materials and how they affect injection of the pc grout. While this is a crucial aspect of grouting, it was surprising to find that there was very little information available on the effectiveness of grouts in slowing or preventing corrosion.

Grout Performance

Performance of stay cables is discussed in Chapter One. There have been no known failures or major problems in actual structures of bridge stay cable systems which have used pc grout for corrosion protection. Some corrosion has been found in several pc-grouted fatigue test specimens. Similarly, Schupack indicates that catastrophic failures of bonded post-tensioning tendons in post-tensioned systems have been rare when reasonable quality control is used during grout injection.[105] However, there have been a significant number of reports of bonded tendon failures occurring where there was no grout or very little grout in the duct. Schupack also reports that in some cases contaminants have entered through unsealed anchorages and sometimes traveled the full length of the tendon through bleed voids created in the top of the tendon. Other examples of problems were the penetration of chlorides through the concrete, attacking the metal duct and eventually the prestressing steel.

In 1985 the Ynys-y-Gwas Bridge in South Wales, a single span segmental post-tensioned concrete structure, collapsed.[127] The bridge was constructed in 1953 and had a simply supported segmental post-tensioned webs deck with a clear span of 18.3 meters. The tendons were composed of 5-mm diameter wires. The segmental joints were 25 mm in length and were filled with a very porous mortar which tested very high in chlorides. The failure was attributed to corrosion of the tendons at the porous joints. This construction is not typical of modern segmental construction which utilize match cast joints sealed with epoxy.

Grouting Recommendations

Post-Tensioning Institute (PTI)

Post-Tensioning Ducts: Recommendations for grouting of post-tensioning ducts have not changed over the years. In 1971 the PCI Committee on Post-Tensioning published the "Recommended Practice for Grouting of Post-tensioned Prestressed Concrete."[87] A number of the key recommendations from this committee are listed as follows:

- Use a grout pump able to produce a minimum outlet pressure of 1.0 MPa gage. Pumping pressure at the tendon inlet should be kept less than 2.1 MPa gage.
- Equipment used to mix grout should be able to mix batch within 1½ to 3 minutes.
- Grouting equipment should be used which can complete grouting of the largest duct on the project in less than 20 minutes.
- Use Type I or II portland cement with a water/cement ratio of no more than 0.45.
- When tested using Corps of Engineers Method CRD-C79, minimum efflux time should be 11 seconds.

The recommendations included in the 5th edition of the *Post-Tensioning Manual* for grouting post-tensioned ducts have not changed significantly from the original version.[91] In fact, all of the key points listed above remain unchanged in the current edition of the grouting recommendations. There are no requirements for testing the corrosion protection effectiveness of the grout mix designs. PTI has recently formed a committee to review and rewrite their grouting standards to include the latest materials and methods.

Stay Cables: PTI *Recommendations for Stay Cable Design, Testing, and Installation* provide recommendations for pc grout which are very similar to the recommendations for the post-tensioning ducts.[28] However, the stay cable recommendations prescribe physical properties for the grout as shown in Table 0.2. In addition, a qualification test is required in which these physical properties are tested by an independent agency and reported to the engineer. To inspect for air pockets, a full size specimen (3 m in length) is to be grouted and autopsied 7-14 days later to check for voids or adverse corrosion effects. Finally, polarization testing is required using the anodic polarization method discussed in Chapter Six. However, no limits of performance are given with which to compare the results of the test.

Table 0.2 -PTI Grout Property Requirements for Stay Cables.[28]

Property	Test Values	Test Method
Water-cement ratio	0.40 maximum	
Compressive strength (28 days) (Average of three cubes)	34.5 MPa minimum	ASTM C109
Initial set of grout	90 minutes minimum	ASTM C266
Bleeding	2% of grout volume at 3 hours after mixing	reference [A116]
Fluid consistency (efflux time from cone)	11 seconds minimum	ASTM C939 or Corps of Engineers CRP-C611

Precompression of grout is also cited as a possible means of improving the corrosion protection of the grout.

FIP Grouting of Tendons in Prestressed Concrete[128]

The FIP recommendations are much more specific and detailed than those produced by PTI. More stringent requirements are given for testing the grouts to be used in the field. Laboratory tests and field trial mixes are suggested for normal projects. Full-scale site tests are suggested for special projects where adequacy of equipment, grout mix, or methods are in question. Specific laboratory tests are recommended for flowability, expansion and bleeding, resistance to freezing, and strength in order to develop a reasonable mix design. Water-cement ratio maximum of 0.40 is recommended with a maximum of 0.45 for special cases of hot weather or evaporation during mixing. Site equipment for testing viscosity, expansion and bleeding, compressive strength and temperature are suggested.

The FIP Guide is also more detailed regarding the injection of the grout. Methods are suggested for the use of vents and re-grouting. Grout agitation is recommended until it is injected. Use of a high-speed mixer capable of 1500 rpm with a high-speed compulsory blade is recommended with a mixing time of 2-4 minutes.

There are no recommendations for testing the effectiveness of the grout in providing corrosion protection.

Concrete Society's Design Group Working Party[29]

After the failure of Ynys-y-Gwas bridge in Wales in 1985, the Department of Transport in Great Britain announced a moratorium on grouted post-tensioned concrete bridges. The Concrete Society Design Group formed a working party, with the support of the Concrete Bridge Development Group, to examine the use of post-tensioning in bridges. One sub-group of this party

drafted a revised specification for grouting, particularly for the structures for which construction was imminent.

In general this working group took the then current recommendations and guidelines and made a few modifications to the existing Department of Transport requirements. Similar to FIP, the fluidity, bleeding, volume change, and strength are to be tested. Limits are given for each of the properties. Admixtures are not specified directly but more as a performance recommendation: allow low w/c but still impart good fluidity, minimum bleed, and volume stability or expansion.

While no tests for corrosion were specified, the recommendations did address the possibility that admixtures may cause corrosion.

Study by Thompson, Lankard, and Sprinkel[120]

A comprehensive study of the state-of-the-art in grouting of post-tensioned bridge structures in the US was undertaken in 1990. The study focused on the current available recommendations and the specifications of the surveyed state departments of transportation (DOT). Consultants, grouting material suppliers, and contractors were also contacted.

The document most frequently cited by state DOT's regarding specifications for grouts for post-tensioned construction was the PTI *Recommended Practice for Grouting of Post-Tensioned Prestressed Concrete* (Grouting Recommendations).[91] However, the state DOT's made additions and modifications to the guidelines as appropriate for their particular needs. Those changes are discussed in the following paragraphs.

The PTI Grouting Recommendations allow the use of Type I, II, and III portland cement. However, some DOT's permit the use of Type II only. The PTI Grouting Recommendations allow the use of pozzolans or aggregates, but give no other guidelines for their use. Most DOT's do not require the use of pozzolans or sand. However, the Washington DOT allows the use of fly ash; Florida DOT requires the use of fly ash and sand; and Caltrans does not allow the use of any pozzolans or aggregates.

In general, DOT's do not require the use of an admixture. Rather, they require that the admixture impart the properties of good flowability, minimum bleed, and expansion while maintaining a low water/cement ratio. The only corrosion related requirement by a DOT is that the chloride content of the admixture be below 0.5 percent.

Maximum water-cement ratios permitted by the DOT's ranged from 0.35 to 0.53 with the most common being 0.44.

Grout fluidity requirements, as measured by the Flow-Cone Method (ASTM C939), were generally more restrictive than those of the PTI Grouting Recommendations. The following efflux times were cited:

- Washington DOT: 15-20 seconds.
- Oregon DOT: 11-19 seconds.
- California DOT: at 20 minutes after mixing the efflux time should not increase by more than 3 seconds.

Although some DOT's have compressive strength requirements for grouts, most do not. None of the DOT's had a requirement for bleeding or permeability.

Grouting Tests for Luling Bridge Stays [106]

Schupack developed a pc grout mix which had reduced bleed for possible use in the Luling bridge stays. A 0.44 w/c grout with 1.5% (by weight of cement) Conbex 208 was used in the test. The test setup consisted of a 1.5-meter long, 89-mm diameter transparent acrylic tube with 70 6.4-mm diameter wires bundled to simulate the bundle in the stay cable. A 6.4-mm diameter seven-wire strand helical spacer was also used. Water soluble oil was introduced into the sheathing prior to grout injection. The grout was gravity injected using a grout head of 3.7 m with the specimen at an angle of 35 degrees. One hundred percent of the injected volume was wasted out of the top of the specimen. The findings were as follows:

- Grout readily displaced the oil.
- Oil was entrapped against the top side of the sheathing.
- Grout was porous in the area where the spacer and sheathing were in close contact.
- There was incomplete coverage of the helical spacer where it was in close contact with the sheathing
- Longitudinal flaws appeared on the top side of the specimen and appeared to be filled with oil.
- Three days after grouting the ends were opened and 65 ml of oil drained out from the wire bundle. Longitudinal "voids" 150 to 300 mm long and approximately 1.5-mm wide were found against the top side of the duct. Some of the voids exposed underlying wires.

- Cuts made through the specimen perpendicular to the axis indicated that practically no grout had penetrated to the spaces between the inner wires.

It is not indicated in Schupack's report if the grout mix used in the tests was actually used in the Luling bridge or if subsequent tests developed a grout which proved to be more successful.

Voids

One of the primary problems in injecting pc grout into post-tensioning ducts or stay cables is voids. Woodward and Miller found during one inspection of a post-tensioned concrete bridge in the United Kingdom that voids were present in over half the ducts examined and in many these cases the tendons were exposed by the voids.[126] They also reported that a bridge in Japan had voids in 35% of the ducts examined and 10% were less than half full of pc grout. Schupack found during the demolition of a 35-year old bridge that many of the tendon ducts were ungrouted.[102] Some were suspected to have contained water which froze and caused the webs to crack along the duct.

Generally, voids occur in the top of the ducts and tend to concentrate at the high points of the duct profiles.[126] There are two possibilities for the formation of a void: Air pockets trapped in the ducts during the injection of the grout, and the collection of bleed water at the high points of the duct profile which is then drawn back into the grout after it has set. One full-scale test conducted by Woodward and Miller indicated a void was formed in one of the specimens because the grout was too stiff and did not allow the air to travel to the vent at the top of the duct profile. Conclusions of the study were that the important parameters necessary for successful injection are proper equipment and well trained personnel along with a fluidity of the grout mix suitable for pumped injection and cohesion sufficient to suppress bleeding. No mention was made of expansive admixtures.

Expansive admixtures are sometimes used to reduce or eliminate voids.[105] Usually the expansion is caused by a gas forming agent added to the grout before injection. The vents at the high points of the tendon profile are left open. The air pockets trapped during injection make their way to vents and are pushed out by the expansion of the grout. Use of expansion admixtures is discussed in section 3.5.7 Admixtures.

Bleed

In grouting ducts or stay cables which have large changes in elevation, significant pressure can be developed at the bottom of the column. Previous work has indicated that this pressure can cause a segregation of the water and cement which is also known as "bleeding."[101, 103, 104] It was suggested that this bleeding is promoted by the bundle of prestressing strand or wire present inside the duct or sheathing. When a pc grout bleeds the cement particles settle to the bottom of the column

and the water rises to the top. When a strand or wire bundle is present the water seeps into the interstices, leaving the cement particle outside the bundle. This water, because its density is less than that of the pc grout, rises to the top of the column and forms a layer of water which is normally drawn back into the grout as it cures. This behavior in itself is not detrimental to the protective layer of grout. The problem occurs when the bleed water does not rise all the way to the top of the grout column. Instead it can form "lenses" of bleed water at random locations along the length of the column.[101, 103, 104] The bleed water is subsequently drawn back into the grout leaving a length of the strand or wire bundle unprotected.

In 1971 Schupack conducted qualitative tests on grouts for use in long vertical ducts.[104] It was found that when a 3-m long clear plastic tube, oriented vertically, was filled with a neat cement containing no admixtures and then pressurized to 350 to 700 kPa, water came to the top but also formed intermediate lenses of bleed water. In addition, it was discovered that when prestressing strands were placed in the conduit with the grout that the amount of bleed was increased. This was labeled "water transport mechanism" and was thought to be a filtering process in which the space between the outer six wires of the strand allowed water to enter the space between the outer wires and inner wires, but did not allow the cement to enter. Since the specific gravity of the grout is approximately twice that of water it forces the bleed water to the top of the column.

As a part of the test program Schupack developed a gelling agent which was a combination of soluble cellulose along with an expansive agent. Laboratory tests indicated that the admixtures eliminated the bleeding and provided sufficient expansion to eliminate voids. Two 9-m long 1500-mm diameter plexiglas tubes with six 35-mm diameter prestressing bars were injected with grout using the new admixture. Visual inspection indicated that there was no significant segregation or bleeding. After the test the specimens were cut into sections to check if the space between the bars had been filled. It was found that the grout would not penetrate between the wires in a prestressing wire tendon. However, it was found that the spaces between the strand were completely filled.

In 1974 Schupack reported additional tests performed on the new gelling admixture.[101] Tests were conducted on the bleed, pumpability, water retention, and penetrability of the grout which used the gelling admixture. The bleed tests were conducted under pressure using a filter funnel with a fine weave filter paper (the details of this test are covered in Chapter Five). The pumpability was tested by pumping the grout through a 9-m long 64-mm diameter flexible metal duct with constricted end fittings. It was found that the pump could be started and stopped with no problems. In addition, there were no leaks of bleed water or grout through the joints in the flexible duct. Penetrability tests were made by strapping 19 12.7-mm diameter strands together inside a 100-mm diameter opaque duct. The penetration of the grout between the strands was checked by cross-cutting the stay and

examining the sections. It was found that the grout successfully filled all of the spaces between the strands at the locations where the cuts were made.

Grouting of the post-tensioned bridge over Alsea Bay in California required a special test program to develop a grout admixture which satisfied the requirements of the project.[5] Concern was expressed over the possibilities of voids in the ducts. Several types of cellulose based anti-washout admixtures (similar in behavior to Schupack's gelling agent) were considered for use in the grout. Two types of anti-bleed admixtures were tested: Sikamix SC which was a combination of Sikament 300 a superplasticizing, water-reducing admixture, and Kelco, a natural polymer which provides the anti-bleed property; and Celbex 208 which is a cellulose based additive which provides anti-bleed properties. Batches of each mix were initially prepared a slow paddle mixer. This led to rapid stiffening of the Celbex mix while the Sikament mix remained somewhat fluid and pumpable. From these preliminary results it was decided to abandon the Celbex and use the Sikament for grouting the large-scale tests. The large-scale tests proved to be successful in that no voids were found in the mock-up when it was cored one week after injection.

Cracking

None of the papers reviewed which dealt with grout for post-tensioning addressed the issue of grout cracking and its effect on corrosion protection. However, Bruce indicated that in post-tensioned rock anchors all installations are permanent.[82] Therefore, the corrosion protection is crucial to the long-term performance. Bruce points out that the major difference in the US and foreign practice is that in foreign practice pc grout is not considered as an acceptable barrier to corrosion. It carries the potential for microfissuring under load and these can be as severe as 2.5 mm wide at 100 mm spaces which he claims can quickly lead to corrosion. Foreign practice considers an acceptable barrier one which can be inspected prior to installation. He goes on to conclude that a tendon incorporating a plastic sheathing and grouted in place would be considered single protection by foreign practice while it would be considered a two-barrier system in the US Bruce does not specify what is considered "foreign practice."

Admixtures

Expansive Admixture

Currently there is no consensus among those involved in the field of grouting regarding the need for expansive additives in grouts for post-tensioning ducts.[118] Ideally a pc grout would not shrink or expand at any time during the life of the structure. However, this degree of control is very difficult to attain because of the variety of admixtures and mechanisms of expansion. There have been a number of expansive admixtures developed using different mechanisms to counteract the

natural tendency of the grout to shrink. Corps of Engineer Specification CRD-C-621-89 categorizes these non-shrink grouts as follows:

Gas-liberating - Contains ingredients that react to generate or release gases such as hydrogen, oxygen, or nitrogen. Expansion continues until either the gas-liberating mechanism has been exhausted or the grout mixture has solidified.

Metal-Oxidizing - The increase in volume comes from the increase in volume of oxidizing metal. The grout generally contains an oxidizable metal and an oxidation-promoting ingredient.

Gypsum-Forming - Reaction of calcium sulfate hemihydrate (CSH or plaster of paris) and water. Expansion continues until all the plaster of paris has been converted to gypsum or until all the water has been used.

Expansive-Cement - May or may not contain a metallic aggregate. These grouts derive their non-shrink properties from the expansive nature of the cementitious system. The expansive cement may be one involving a reaction to produce ettringite.

The most popular expansive admixture used in post-tensioning is the metal oxidizing type and is usually composed of aluminum. The obvious problem with this type of admixture is that the expansion ceases after the grout has set.

A study completed in 1977 on a variety of post-tensioned concrete applications in California found that the elimination of the expansive admixtures did not affect the quality of the grout.[119]

The Concrete Society's Design Group (in Great Britain) recommendations suggest that there is some debate concerning the usefulness of expansive admixtures as well as the possibility for hydrogen embrittlement from the hydrogen gas.[29] The Design Group indicated that In Germany their use is permitted; in France it is prohibited. The Design Group found no evidence to corroborate the fear of HE and did not ban their use.

In Texas, the use of expansive admixtures which produced hydrogen was not permitted in the pc grout for the Baytown Bridge stay cables.[48]

Silica Fume

Silica fume is a by-product of the fabrication of silicon or ferrosilicon alloys.[4] During the reduction of quartz by coal in the submerged electric arc furnace, SiO vapors are formed. When these vapors come in contact with the oxygen they are oxidized, and condense in the form of very fine particles of amorphous silica. The particles generally have a mean diameter of 0.10 to 0.15 μm which is about 50 to 100 times finer than cement particles. Silica fume is a very reactive pozzolan which reacts with the lime liberated during the hydration of the portland cement. The

result has been found to drastically increase the compressive strength of concrete as well as significantly reduce its permeability. In addition, the use of silica fume in cement paste significantly reduces the chloride diffusion rate when compared to concretes without the silica fume.[51]

Several studies have claimed that the use of silica fume reduces the bleed of the pc grout.[101, 103, 104] They indicate that the water retentivity was improved and the bleeding was eliminated. However, it should be noted that none of the bleed tests were performed under pressure nor did they include strand in order to test the water transport mechanism

It is claimed that the spherical silica fume particles with a diameter of 0.02 to 0.05 μm bind the mix together due to the large surface forces. In addition, they act as ball bearings between the rough cement particles which are approximately 100 times larger.[38] Up to 15% silica fume by cement weight was used in tests of pc grouts for use in post-tensioning ducts in reactor pressure vessels which have an elevated operating temperature. Bleed tests under pressure were not conducted. However, 75-mm diameter by 1600-mm long pipes oriented both vertically and horizontally were filled with grout and checked for bleed. All of the grout mixes tested bled to a certain degree under these conditions.

Other experimental work completed on silica fume modified grouts included flow behavior, microstructure and strength.[107] Viscosity measurements were taken on grouts with and without silica fume. The silica fume was added up to 15% by cement weight. The results of the tests on flow characteristics indicated that the silica fume mix performed better than the neat cement mix. Bleed was examined by filling vertical and 30° sloped plexiglass tubes (75-mm diameter by 1600-mm long) with the various grout mixes. It was observed that the silica fume had considerably less bleeding than the mixes without silica fume.

Extensive work on the formulation of a silica fume grout mix was completed by Hope and Ip.[61] Two mixes were developed and tested. No bleed tests were done. The constituents were Type I cement, fly ash, aluminum powder, and calcium nitrite. However, only the results of the tests on the silica fume grout were reported in the reference. The results indicated that the electrical resistivity in the silica fume modified grout was higher than that of the control grout. In addition, the chloride permeability was found to be very low. The resistivity increased as the amount of silica fume increased. Expansion occurred in the first thirty minutes with the uncoated aluminum while the coated aluminum expanded for the first hour after mixing.

Extensive work in testing different grout formulations by Ghorbanpoor and Madathanapalli found that the best mix design was Type I portland cement grout, 20-25 percent silica fume by cement weight, and a superplasticizer.[52] Various additives tested were: Latex, fluidifying/expansive agents, anti-bleed, and superplasticizer. The tests included expansion and shrinkage, bleeding

characteristics, compressive strength, flow time, permeability, pH of bleed water, setting time, and surface corrosion observations of the post-tensioning steel surrounded by each mix tested.

Calcium Nitrite

Calcium nitrite has been used as a corrosion inhibitor in reinforced concrete for more than twenty years.[16] However, its use in pc grout for post-tensioning is only now being investigated.[52, 118]

Calcium nitrite was first introduced to the United States in 1979 from Japan where it had been used for approximately ten years.[88] The nitrite ion acts by quickly oxidizing the ferrous metal ion to form an insoluble ferric-oxide coating on the steel surface. This occurs at any location where the natural oxide coating has become permeable enough to allow migration of the ferrous ions. As the chloride content near the surface of the steel increases causing additional penetrations of the oxide coating, the ability of a given amount of calcium nitrite to maintain passivity is decreased because the nitrite ions are gradually consumed.

Comments

Serious consideration has been given to the use of pc grout in post-tensioned concrete. Most of the work has been directed at the improvement of the fresh properties so that placement can be more effective. Field evaluations of existing systems indicate that this is an important aspect of grouting. However, very little of the work on grout for post-tensioning ducts has addressed the effectiveness of the corrosion protection provided by the pc grout. It seems that the underlying sentiment is that this is not an issue. The perceived issue is that the duct should be completely filled to preclude the entrance and transport of water and contaminants along the length of the tendon. This is probably due to the field experience with post-tensioning ducts in which some inspected ducts have either been empty or partially filled with grout. Corrosion problems are then a result of the absence, rather than the poor performance of pc grout.

It is reasonable to expect that all of the structural components of a bridge which are intended to last the design lifetime will be provided with a consistent level of durability. If this is the case, then the required performance of a stay cable is much higher than that of an internal tendon or an external tendon placed in the cavity of a box girder. Thus, a higher level of performance would be expected from the pc grout in a stay cable than in post-tensioned concrete. However, this higher expectation as well as the special problems inherent in grouting a stay cable have not been addressed in the literature.

The only grout tests specifically for stay cables found in the literature were that of Schupack's for the Luling Bridge. Unfortunately, the results of the tests were quite distressing. The tests indicated that grout did not fill the space between the wires with grout. Presumably in the

actual bridge, moisture from the grout would gather in the spaces between the wires and possibly cause corrosion. These tests should have been a red flag to those involved in stay cable construction to at least conduct additional tests to determine if this problem could be alleviated.

The use of a metal-oxidizing expansive admixture in a stay cable is questionable at best. Expansive admixtures work best when they are used to push bleed water and air out of the vents at the high-points of tendon profiles. The inherent straight shape and sloped geometry of the stay make the use of an expansive agent unnecessary. Moreover, it is likely that the hydrogen bubbles would rise to the top side of the stay and gather around the strands or wires producing a porous grout. In addition, there is still the possibility for hydrogen embrittlement with hydrogen producing admixtures.

The addition of calcium nitrite and silica fume is likely to improve corrosion resistance of the grout. They have been used successfully in concrete for a number of years. However, grout cracking and the effect that cracking has on corrosion protection have not been addressed.

Because of the potential for lens formation along the length of a stay, it is imperative that the bleed of the pc grout be reduced to a minimum. While some of the research reviewed suggested that silica fume could perform this function, the results were conflicting. In addition, none of the tests in which the grout was claimed to be anti-bleed were performed under pressure. Neither were the tests conducted using a bundle of strand to enhance bleed.

Other Blocking Compounds

Petroleum Wax

Petroleum wax was first used in France in external prestressing ducts in 1984, and has been successfully used in several projects since that time.[23, 24] It was also used in grouting the Tampico cable-stayed bridge in Mexico.[112] Unlike grease, petroleum wax is a micro-crystalline and homogeneous material, reversible at any temperature. Other advantages of the material are that it has a lower density than pc grout and it can be injected in the plant when the cable is assembled. The wax actually lubricates contact points to reduce fretting and can be used with galvanized strand without fear of hydrogen embrittlement. The wax remains crack-free under compressive and tension loads. Injection of the material requires that the wax be heated to 85-105°C so that it is liquid enough to inject. When heated it has the consistency of a fine motor oil so that any defect in the sheathing will cause a leak which is difficult to stop.

Buergi reports results of tests on petroleum wax for use in the anchorage region on the Kemijoki River Bridge, in Rovaniemi, Finland.[20] The harsh environment prompted the use of a

robust system produced by VSL in which the strands are greased and sheathed inside a PE sheath which is subsequently filled with pc grout.

The anchorage was to be filled with a material other than cement grout to protect the exposed portion of the strands where the sheathing had been removed. A total of fifteen different products of various types were examined with tests of the complete anchorage at temperatures between -50° and +50°C. Also, compatibility with the other materials used in the anchorage (polyethylene, cement grout and grease on strands) was tested. The results indicated that "wax-like" (material name was not given) materials tended to crack at low temperatures, especially around adjacent components such as the protection cap or anchor head. The wax appeared to pull away from the surrounding components at low temperatures. In addition, the cracks did not close again upon reheating to ambient temperature. One of the candidates was a cold applied material (material name not given) which held a constant viscosity through a wide range of temperatures and is reportedly pumpable down to -18°C. The material does shrink at low temperatures but does not pull away from the components. It forms internal voids which close when returned to ambient temperature. At high temperatures the material expands. This problem has been solved by the use of an expansion volume integrated into the protection cap.

Polyurethane

Custom nonpozzolanic chemical grouts have been developed for use in ground stabilization as well as structural repair and sealing[82] Two component hydrophobic polyurethane has been used to seal cracks in the concrete which encased pipes which were leaking. It proved to be an effective repair.

Grease or Oil

Greiner, Inc. has applied for a patent on a system which has a corrosion-resistant liquid retained in the cable sheathing. A liquid flow-control device drains condensation or purges the corrosion-resistant liquid to-and-from each sheath in response to temperature changes. It is claimed to be able to maintain the ability to verify the continued presence of a corrosion-resistance system. The system has not been used yet but a feasibility study is currently being conducted for a Korean bridge project.[80]

Individual Strand/Wire Protection

Temporary Corrosion Protection

PTI *Recommendations for Stay Cable Design, Testing and Installation* requires that temporary corrosion protection (TCP) be provided for the period of time between installation of the

stay cable and final grout injection. The type varies with the exposure conditions. PTI recommendations suggest that bare tension elements are to be coated with an appropriate water soluble corrosion inhibitor prior to erection and then it is to be reapplied at least every three months until grout is injected.

Kittleman tested a number of water soluble oils and found that their ability to provide short term corrosion protection was good.[67] It was found that the reapplication of the oils would be necessary for maintaining corrosion protection. However, there is evidence that this "maintenance" item is not always performed.[112] TCP was applied to the main tension element prior to erection but no additional application of TCP was made on either the James River or Luling Bridges.[112] The cables were up for 1-1/2 years on the James River Bridge and 1 year on the Luling Bridge before they were grouted.

Figure 0.2 - Epoxy-Coated Strand[45]

Epoxy Coating

Epoxy-Coated strand is manufactured by Florida Wire and Cable, Inc under the trade names of *Flo-Gard* and *Flo-Fil* (see Figure 0.2). Flo-gard is seven wire prestressing strand which has a thick epoxy coating on the exterior circumference of the external wires. Flo-fil in addition to the external coating has the interstices between the outer wires and the inner wire filled with epoxy also.

Epoxy-coated strand is manufactured to meet the requirements of ASTM A882-92[7] Standard Specification for Epoxy Coated Seven-Wire Prestressing Steel Strand and ASTM A416.[8] The final coating thickness of the strand, according to the ASTM A882, can range from 0.63 to 1.14 mm. However, the design thickness for the strand is usually 0.76 mm.[79]

PTI *Recommendations for Stay Cable Design, Testing and Installation* requires that the epoxy coating thickness be within the range from 0.63 to 1.00 mm.[28] Unlike the ASTM standard, the PTI Recommendations suggest a coating thickness tolerance of ±0.063 mm (see section 8.4 for further discussion). This control is necessary to ensure that the teeth of the wedges evenly penetrate the epoxy and grip the strand. In addition, the PTI recommendations require that "epoxy coated strand shall be of the type in which the interstices of the strand are filled with epoxy."

The coating is a thermo-setting, fusion-bonded epoxy applied in a continuous process to the bare strand.[65, 79] The manufacturing process starts with strand which meets ASTM A416. The strand

is mechanically cleaned and then preheated to 300°C prior to application of the coating. The strand is then run continuously through a fluidized bed of electrostatically charged epoxy particles. As the electrically grounded strand passes through the bed the charged particles are attracted to the surface of the strand. To manufacture the coated and filled strand the outer six wires are separated from the inner wire just prior to entering the fluidized bed. This results in epoxy fill in the interstitial space between the wires.

Although the strand is manufactured using low-relaxation strand, relaxation tests of the strand show a 60% greater relaxation than that of uncoated strand in 1000 hour tests.[79] Florida Wire and Cable, Inc. conducted a series of tests on the strand to determine its effectiveness in providing corrosion protection. The program included the following:

- Bond, transfer and pull-out tests on grit impregnated strand
- 3000 hour salt spray tests
- Chemical reactivity
- Heat effects of bond transfer properties of grit impregnated strand
- Fatigue characteristics of post-tensioned assemblies
- Long-term creep characteristics of grit impregnated strand
- Chloride permeability of coating
- Impact resistance of coating

The salt spray and chemical reactivity tests indicated that the epoxy provided excellent protection without suffering any damage during the course of the tests. Fatigue tests indicated no difference in fatigue life from the uncoated strand and no loss of integrity of the coating. Chloride permeability was tested by immersion in 5% NaCl solution while being subjected to a constant voltage of 6 volts. After four years of continuous exposure, no corrosion was found. Selected specimens were tested with their coatings intentionally damaged. While corrosion was noted at the break, there was no undercutting or loss of bond noted in the coating.

The use of epoxy coated strand in stay cables and other post-tensioning applications requires the use of special wedges which will bite through the epoxy coating and into the underlying strand. Other details of installation and stressing procedures are included in the PCI report on the use of epoxy-coated strand.[94]

The first cable-stayed bridge to use epoxy-coated strand was the Bayview Bridge completed in 1987 over the Mississippi river at Quincy, Illinois.[112] Since then epoxy-coating has been used in two other bridges recently constructed: Burlington Bridge in Iowa and the Clark Bridge in Illinois.

Greased and Sheathed

Greased and sheathed strand has been used almost exclusively in parking and office structures. However, in recent years VSL and Freyssinet have been marketing a greased and sheathed strand system for their stay cables.

VSL uses a system which incorporates a bare strand coated with a lubricating grease which has "wire cable rust and corrosion inhibition additives." A tightly fitting high-density polyethylene sheath is then extruded over the strand. The greasing process used in manufacturing this type of strand is shown in Figure 0.3. Standard prestressing strand is de-stranded, greased and re-stranded. The excess grease is removed and a high-density polyethylene sheathing is extruded over the strand. This prevents any relative movement between the sheathing and strand during assembly or stressing. This differs from the heavily greased strand in an oversized plastic sheathing which is typically present in unbonded single strand tendons used in parking garage and office structures. The tight extrusion also reduces the likelihood of voids in the grease in the annular space between the strand and sheathing. The grease meets the requirements of PTI corrosion preventive coating for unbonded single strand tendons.

Figure 0.3 - De-stranding and Application of Grease to Strand Prior to Extrusion of Sheathing. (Courtesy of VSL)

Freyssinet uses a strand which is similar except that a petroleum wax is used instead of a grease and the strand is galvanized before the wax and sheathing are applied.[49] The wires used to produce the strand are hot-dipped galvanized prior to the last drawing operation before stranding. The strand is then coated with and the interstices are filled with a petroleum wax. A high-density polyethylene sheathing is then extruded tightly over the surface of the strand (see .Figure 0.4).

Figure 0.4 - Schematic of Strand Used in Freyssinet Stay Cables.[49]

PTI *Recommendations for Stay Cable Design, Testing and Installation* provides specific material and performance requirements for greased and sheathed strands which are to be used in stay cables.[28] Although there have been no bridges constructed in the United States using this type of corrosion protection system, it is currently popular in Europe and Mexico and is likely to be seriously considered for use in the US in the near future. PTI recommendations give performance requirements for the grease and sheathing as well as minimum material standards. This standard was developed to cover the typical “parking garage” type monostrand.

It has been claimed that one of the distinct advantages of the greased and sheathed system is that, should it be necessary, the strands in the stay can be replaced individually. Buergi indicates that when individually greased and sheathed strand are used that the strands can be replaced by detensioning and pulling the strand out of the sheathing.[20] While removing the strand a replacement strand can be fed into the sheathing. Freyssinet indicates that their monostrand system (strands individually galvanized, waxed, and sheathed) provides sufficient protection so that an outer sheathing and blocking material are not necessary.[49] They suggest that this provides the added benefit of inspectability and replaceability. Using their isotension method of individually stressing the strands, the stay cable can be replaced strand-by-strand with lightweight equipment and no disruption to traffic.

Note that when using monostrand type cables special protection techniques are required in the anchorage region because the sheathing must be removed under the anchor head so that the grips can be in direct contact with the strand.

Galvanizing

Hot-dipped galvanizing is the most common method of zinc application.[35] After being thoroughly cleaned, the wire is drawn through a molten bath of zinc at temperatures of 450-460°C. When the wire exits the bath a pure layer of zinc coating forms over several layers of iron-zinc alloy. The relative thickness of the layers and the total thickness depends on the bath temperature, time of immersion, speed of withdrawal, and silicon content. Careful quality control is required in order to ensure that the coating is ductile and the base metal quality is not reduced.

Zinc provides protection by sacrificially corroding in place of steel when exposed to a corrosive environment. Zinc is anodic to steel in the EMF series and will corrode sacrificially to steel when there is electrical contact and a sufficiently conductive electrolyte is present. The advantage of a sacrificial protection system is that it theoretically does not have to completely cover the protected part. Nicks and abrasions in the zinc should not cause corrosion of the underlying steel.

Zinc has been used to protect exposed steel from atmospheric corrosion for many years. It has also been used to protect reinforcing steel in concrete for a number of years.[35] However, there are special problems encountered when using zinc-coated steel, especially high-strength steel, in contact with cement paste. In the presence of a high-alkaline environment such as that of wet pc grout the corrosion rate of zinc is very high. One product of this corrosion is hydrogen gas. It is feared that this can cause hydrogen embrittlement of the underlying wire or strand. Results of testing in this area were discussed in Chapter Two.

The use of galvanizing on prestressing strand is currently prohibited by the Federal Highway Administration and as a result is not readily available for use in the US. However, the use of galvanizing in stay cables is very popular in Europe as well as Japan. It is used in Europe both in the form of galvanized strand and galvanized wire. In Japan the more popular system seems to be the galvanized wire system.

Galvanized prestressing strand for use in a stay cable is normally produced by applying zinc to the wire before the final drawing process so that the loss of strength of the wire from the high temperature zinc bath is regained by the drawing operation. The wire is then stranded to the final configuration. This also allows close tolerances to be kept on the dimensions of the strand..

Anchorage Protection

While the general configuration of anchorages can be specified in the construction documents, the detailed design of the anchorage region of the stay cable is usually performed by the prestressing supplier who has been selected to supply the stay cables for a particular bridge. By

necessity, prestressing suppliers have standardized their own proprietary anchorages and unless there are unusual project requirements will supply one of their standard anchorages. In that light, the state-of-the-art anchorages of four prestressing companies will be presented to give an overview on the available technology relating to corrosion protection at the anchorage.

Bureau BBR Ltd.[21] BBR advocates the use of their patented HIAM or DINA sockets with prestressing wire main tension elements (see Figure 0.5 and Figure 0.6). The BBR system is completely factory assembled. The HIAM socket uses a filler made up of hardened steel balls, zinc dust, and epoxy resin while the DINA uses a mixture of resin and hardener compound in the anchor head.

The socket type anchorage has the advantage that the area where load is transferred from the wires to the anchor head is completely sealed with the compound. This combined with the cathodic protection provided by the zinc dust provides a robust corrosion protection system. This socket system can be used with bare or galvanized wires.

Figure 0.5 - BBR HIAM Socket.[21]

Figure 0.6 - BBR DINA Socket.[21]

The remaining three state-of-the-art systems utilize wedge type anchorages which have several potential problems. The potential for dissimilar metal corrosion is a problem in the anchorage region especially in the contact area between the strand and wedges.[112] In addition, epoxy-coated as well as the greased and sheathed systems are “compromised” at the anchorage. The sheathing on the greased and sheathed system must stop at the anchor head to allow contact between the strand and wedges. Even though the epoxy is not removed from the coating system in the epoxy-coated strand, the wedges still must bite through the epoxy to connect the strand to the anchor head. This local break in the epoxy must be protected from corrosion.

If a pc grout is to be injected into the main sheathing, then care must be taken to ensure that a watertight seal is made between the anchor head and the individual sheathing. This prevents water from intruding into the grip region of the anchor head during grout injection.

Dywidag[41] The state-of the-art system promoted by Dywidag is shown in Figure 0.7. There is a steel socket assembly at the anchorage which is intended to provide bonded performance for live loads. This anchorage is known as high fatigue resistance or HFR-Anchorage. The entire length of the stay is grouted with pc grout, including the anchorage. In addition to bare strands, this systems can make use of grit-impregnated, epoxy-coated strand; galvanized strand; tar-coated strand; or as greased and individually sheathed strand.

Figure 0.7 - State-of-the-Art Stay Cable Anchorage Developed by Dywidag.[41]

Freyssinet [49] The state-of-the-art system utilizes the greased and sheathed (and galvanized if desired) strand for the stay system. The entire anchorage area, including the transition, is injected with petroleum wax. This necessitates the installation of a stuffing box assembly which seals the transition region from the free length (see Figure 0.8).

VSL[124] The state-of-the-art system provided by VSL, shown in Figure 0.9, is similar to that of Freyssinet except that the strand sheathing is sealed against the anchor head with a "separation tube." A separation tube is provided for each strand in the stay. This allows the pc grout (if used) to enter the transition length. The area under the anchor cap and inside the anchor head is filled with a corrosion protective material similar to that used around the strands.

Figure 0.8 - State-of-the-Art Stay Cable Anchorage Developed by Freyssinet.[49]

Figure 0.9 - State-of-the-Art Stay Cable Anchorage Developed by VSL.[124]

Prestressing Wire Systems

Wire and Grout

BBR stay cable systems are factory assembled parallel (or with a slight pitch) wire stays utilizing the BBR Hi-Am type socket.[21] The stay is then grouted with pc grout for corrosion protection.

The prefabricated prestressing wire system with the Hi-Am type anchorage is used quite frequently in Japan. In some cases galvanized wires have been used in the stays in contact with the pc grout.

Other Wire Systems

A unique stay cable corrosion protection system was used on the Papineau-Leblanc Bridge opened in Montreal in 1969.[36] The corrosion protection system was unique for its day because it provided several levels of protection rather than the usual galvanizing and painting. There were two lines of cables descending from either side of the tops of the towers. Each line consisted of 24 bridge strands arranged in bundles of twelve. Each individual wire of the bridge strand was galvanized. The strand was covered with a 5-mm thick PE coating which was extruded directly onto the strand in the factory. The strands were prestretched prior to passing through an extension die where the PE coating was applied. The strands were then cut to proper length and socketed.

Tanabe and Tawaraya describe a recently developed system which they call NEW-PWS.[114] It consists of galvanized wires bundled and then given a slight twist so that they are not parallel but not so much twist that the strength is reduced. The galvanized wires are wrapped with a filament tape and a PE sheathing is extruded directly over the bundle. The anchorage is a combination of zinc cast and epoxy resin.

Pfeifer Seil- und Heberechnik GmbH & Co manufacture a cable known as “Hicore.” The cable is composed of 7-mm diameter galvanized prestressing wire bundled with a slight twist. The bundle is filled and coated with a polyurethane grout.

The Japanese have historically favored prefabricated bundled parallel or near-parallel wire (bare or galvanized) systems inside PE sheathing injected with grout or other noncementitious material.[72, 114] However, in recent years the trend in Japan seems to be toward galvanized wires with the sheathing extruded directly onto the bundle or with some noncementitious material injected into PE sheathing.[114]

Other Systems

Encapsulation/Electrical Isolation

Schupack has patented an electrically isolated post-tensioning system. He has suggested its use in an electrically isolated stay system. The stay would be completely encased from end to end with a dielectric sheathing to prevent the ingress of harmful substances and to minimize the possibility of stray currents. This type of system has been used in parking garage monostrand tendons but has never been used in a stay cable.

Cathodic Protection

Cathodic protection (CP) has been developed over the last 20 years for reinforced concrete.[26] It has been demonstrated successfully on a number of full-scale projects. As a result CP is being considered for use with prestressed concrete. The significant problems that CP faces with use in prestressed concrete are:

- Lack of electrical continuity in prestressing steel
- Danger of hydrogen embrittlement from the cathodic reaction
- Difficulty in monitoring corrosion activity
- Difficulty in ensuring an even distribution of protection current
- Lack of appropriate performance criteria

Recent research has examined these issues and found that there are still major questions which need to be addressed before CP can be used routinely on prestressed structures. Until further research resolves the problems with CP in prestressed concrete it is unlikely that CP will even be considered for use in protecting stay cables.

Chapter Four
Stay Cable Survey

4.1 Introduction

In May 1993, a survey was undertaken to sample the opinions of the industry on the design, fabrication, installation, and long term durability of stay cables and to determine current trends. The survey was carried out on an international level with the assistance of a grant from a cable stay supplier and was not part of the work sponsored by the Texas Department of Transportation or the Federal Highway Administration.

4.2 Purpose and Scope

One of the purposes of the survey was to provide the sponsor with information which would be useful in developing and marketing components and systems for stay cables. However, in conducting the survey, the University of Texas was not restricted in publishing the results in any appropriate open forums. Therefore, it could be seen that there were other significant benefits to be gained from the survey other than the marketing purposes of the sponsor. Because the cable-stayed bridge industry is at a critical stage, there is a need for a compilation of the knowledge and expectations of those involved in the design, assembly, erection and maintenance of stay cables. The data gathered in this survey will be made available to specification writing committees to help bring the industry's opinion to bear in the code writing process.

The scope of the survey encompasses only the stay cable and does not address any other aspect of the cable-stayed bridge. The questions posed involve strength, fatigue resistance, durability, cost, constructability and aesthetics of various stay cable components and systems. Surveys were sent to 190 owners, contractors, design consultants, suppliers, and research institutes covering North America, Europe, Asia and Australia.

4.3 Description of Survey

The survey was composed of three parts: cover letter, stay cable terminology for survey, and stay cable questionnaire. A sample of the survey questionnaire is located in Appendix A. The cover letter introduces the survey to the subject and describes why the survey was being conducted and how the information to be gathered would be used. The stay cable terminology is a glossary of

terms used in the survey which may have been unfamiliar to the respondent. The questionnaire is divided into eight sections:

0. Addressee Information.
1. Design.
2. Corrosion Protection.
3. Inspectability/Durability.
4. Installation.
5. Aesthetics.
6. Marketing.
7. Past Experience.

Each section contains several questions which are related to the section topic. The majority of the questions are in a format that provides several alternatives which were to be numerically rated by the respondent using the following scale:

10 ..... meaning excellent or clear first choice
8 ..... meaning very good or desirable
6 ..... meaning good or acceptable
4 ..... meaning marginal or questionable
2 ..... meaning poor or objectionable
0 ..... meaning very bad or totally objectionable

In addition, several yes/no questions were asked as well as essay and fill-in-the-blank questions.

4.4 Survey Distribution

The first mailing of surveys was made in February 1993 in which approximately 190 surveys were distributed. The cover letter requested that the surveys be returned within one month's time. As of March 16, 1993, 32 replies had been received. At that time, a preliminary report of the results was prepared and furnished to the sponsor. As of June 22, 1993, 46 replies had been received. A thank you letter was then sent to those who had participated in the survey. In addition, approximately 50 second copies of the survey were sent to selected names on the list with a follow-up letter to remind them that a survey had been sent and that their participation would be appreciated. The follow-up names were selected in an attempt to provide a more diverse geographical distribution of responses since many of the responses in the first mailing were from the United States. A follow-up letter without a survey was also sent to all others who had not replied. The follow up process was moderately successful. At the time the survey was closed at the end of

November 1993 a total of 83 replies had been received. Of these replies, 62 completed the survey (respondents) while the remaining replies declined to participate due to lack of experience or knowledge. Throughout this chapter, the terms "respondent(s)" and "response(s)" will be used to denote those who completed the survey and their responses, respectively. A list of the respondents is given in Appendix A.

4.5 Presentation of Results

In order to make interpretation and comparison of data as simple as possible, the results have been assembled into a graphical format. The results for each question are presented for all responses ("All" category) and then are divided into categories of geography and industry sector. The three geographical categories selected were North America, Europe and Asia/Australia. The four industry sector categories selected were Supplier, Owner/Authority (Owner), Design Consultant/Research and Development (Designer), and Contractor. The figures illustrating the results are included in Appendix A.

4.5.1 Distribution of Respondents

A database was formed using the results of the numerically rated questions and yes/no questions. The database was then used to extract the distribution of the respondents according to geography and industry sector as is shown in Figure 4.1. The geographical distribution of responses is reasonably balanced with North America having the highest percentage. However, the distribution of industry sector is weighted heavily toward the Designer category at 55% with Owner category having 25% of the responses. This is not surprising considering that this represents roughly the distribution of the industry categories in the mailing list.

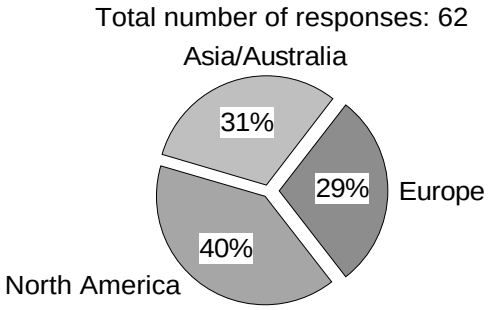

(a) Distribution of Responses by Geographical Categories.

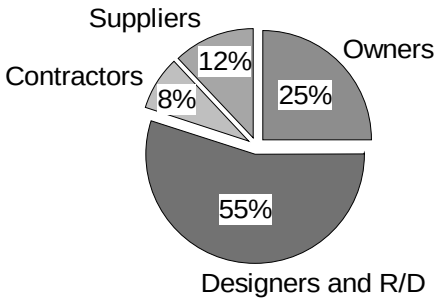

(b) Distribution of Responses by Industry Categories.

Figure 4.1 - Distribution of Responses.

4.5.2 Development of Graphical Presentation

Presentation of the numerically rated questions is made by graphical means. This was accomplished by extracting the numerical

responses from the database for the particular category of geography or industry sector. The extracted numerical responses were then summed and divided by the total number of responses multiplied by 10. This gave the percentage of the maximum possible approval rating (which is 100%) for each given selection in the question. For example, if the particular selection was given a 100% approval rating, this would mean that all respondents had given that selection a rating of ten.

A bar chart was then compiled which compares the approval rating for each of the possible selections for a given question. This resulted in a bar chart for each category of each numerically rated question. In general, the results for each question were placed in subsets of figures. The (a) figure has the results for the All respondents category. In addition, a compilation of comments made by respondents as well as "other" selections for that particular question are also located in the (a) figure. The (b) figure shows the ratings by geographical category and the (c) figure shows the ratings by industry category.

A departure from this scheme was made for two of the questions requiring rating. In question 1.4 (Figure A.5), in addition to the format previously described, an additional format was developed in which to present the results. For each of the categories, the stress range which received the highest rating was summarized into a bar chart. This chart presents the percentage of respondents which gave their highest rating to a particular stress range. Figure A.5(d), -(e), and -(f) contain these additional charts in the order as previously described. The second is question 2.5 (Figure A.12) which is developed in the same manner as other rating questions. However, the location of the categories within the figure is different because it was necessary to list the possible responses in a key rather than in the bar chart. The All respondents category is placed in Figure A.12(a). The geographical categories are presented in Figure A.12(b), all industry categories except Contractor are presented in Figure A.12(c), and Contractor along with "other" selections and comments are presented in Figure A.12(d).

The yes/no questions are also presented in a bar chart format. For each category, the percentages of yes and no answers based on the total number of responses for that category are presented in a bar chart. All respondent categories are presented in a single chart for each question along with reasons for yes/no response. "Common" reasons are those that have been used by more than one respondent. "Individual" reasons are those that have been given by a single respondent only.

Question 1.3 asked for the three most important performance aspects/requirements for a stay cable. The response styles and lengths for this question were quite varied. During the initial review of the answers to this question, keywords were selected which matched or described the responses given. Many of these keywords were appropriate for more than one response. In this

manner ten keywords were developed which were used to characterize an important aspect/requirement for a stay cable. The keywords and their general definition are as follows:

Durability - Ability of stay cable to successfully resist corrosive elements.

Fatigue - Ability of stay cable to successfully resist cyclic loading.

Strength - Ability of stay cable to successfully resist static loading.

Replace - Stay cable can be easily replaced.

Install - Stay cable can be easily installed.

Monitor - Stay cable can be easily monitored.

Stiffness - High axial stiffness of stay cable.

Vibration - Reduced problems with vibration.

Cost - Low cost.

Weight - Low weight.

Any other responses were given "other" as a keyword. Three of the keywords which closely matched the response given in each question were then entered into the database. The database was then searched for the number of times the keyword was used for each category. These results were then placed in a bar chart for each category (Figure A.4). The bar chart lists the keywords and shows the number of times that keyword is used in the form of a percentage of the total number of questions for that particular category. This results in a total possible percentage of 300% (if the percentage for all keywords is summed) since there are three keywords for each question. Answers which belonged in the "other" category were listed on the bottom of the page with the figure. As with the numerically rated questions, the All Respondents category is presented in the (a) figure accompanied by the "other" responses while the geographical and industry categories are presented in the (b) and (c) figure respectively.

The answers to question 3.3.1 and 3.3.2 were given in terms of years. In order to present this question in a graphical manner it was necessary to develop several ranges of years to which the results could be matched. For a given category, the number of responses which fit into a particular range of years was extracted from the database. These numbers are presented in a bar chart as a percentage of the total number of responses. In addition, an average expected life in each category was calculated using the years given in 3.3.1. The All respondents category is presented in the (a) figure while the geographical and industry category are presented in the (b) and (c) figures respectively. The average expected life of a stay cable without replacement is presented in the (d) figure.

4.6 Summary of Results

This section presents the graphical results of the survey. The figures are placed in the order of the appearance of the questions on the questionnaire as Figure A.2 to A.30. In the sample questionnaire included in Appendix A, the number of the figure in the text which displays the results is shown in brackets. All definitions of terms given in the results or the following sections are as defined in the "Stay Cable Terminology for Survey" which was included in all survey forms and is shown in Appendix A. To assist in reviewing the data a partial table of contents is presented below:

4.7 Discussion of Results

The purpose of this section is to provide an overview as well as a discussion of the significance of the results. The following subsections discuss the results and present any significant trends or results as they relate to the particular area of the survey. In interpreting the results it is important to recognize that no costs or relative costs between various alternatives were given to the respondents in the survey documents.

4.7.1 Design

Question 1.1 Structural Performance (Figure A.2) - Parallel strand was given the highest rating in the All category at 83% while parallel wire was rated second highest at a somewhat surprising 80%. It was surprising because so many bridges now seem to use parallel strand. Helical locked coil strand received a relatively high rating (greater than 60%) while prestressing bars have a very low rating (less than 40%) in the All category. Ratings for strand and for wire are close for Europe and Asia/Australia but wire lags behind strand in N. America (76% to 85% respectively). Helical locked coil strand is rated higher in Europe (75%) than in N. America and Asia/Australia (50% and 63% respectively). It is interesting to note that the Owner category gives wire a slightly higher rating than strand while all other industry categories rate strand slightly higher.

Question 1.2 Anchorage Systems (Figure A.3) - Hi-Am type sockets were most preferred (86%) and wedges alone were least preferred (63%) for the All category. In addition, wedge type anchorage with bonding of the tension elements in a socket received a rating of (75%). This trend is typical for all other categories.

Question 1.3 Important Aspects/Requirements for Stay Cable (Figure A.4) - In nearly all categories the Durability and Fatigue keywords are rated very high as compared to all other keywords. The only dissension is the Contractor category which rates Install and Fatigue as the two highest rated keywords. The ratings of the remaining keywords are not consistent among the various categories. Strength is rated third for the All category and for N. America and Asia/Australia while Replace and Monitor are rated at third for Europe. Strength and Replace are both rated third by the Owner category while all other industry categories rate Strength third.

While all agree that durability and fatigue strength are two of the most important aspects of a stay cable there is some disagreement about the third aspect. For the Owner category, replaceability is as important as strength while Europe felt replaceability and monitorability were equally important as the third choice.

Question 1.4 Fatigue Stress Range (Figure A.5) - All categories gave a top rating to the stress range of 200 MPa (28 ksi). One respondent indicated that the answer would depend on the percentage of the live load for the individual project while another indicated that it depends on the type of bridge, traffic loading and stay material. This trend holds when examining figures (d), (e), and (f) which present the selection which the respondent gave their highest rating. In the All respondent category 47% gave 200 MPa (28 ksi) their highest rating. Both N. America and Europe follow this trend with 46% and 64% for 200 MPa (28 ksi) respectively. However, Asia/Australia are evenly divided between 150 MPa (21 ksi) and 200 MPa (28 ksi) at 33 percent. It is interesting to note that the Designer category is less conservative with 250 MPa (35 ksi) receiving the highest percentage of top ratings while all other industry categories give 200 MPa (28 ksi) the highest percentage of top ratings.

Question 1.5 Saddles (Figure A.6) - In all categories the majority of the respondents do not favor the use of saddles. It is interesting to note that Asia/Australia has the least objection to saddles (53% no), Europe has the most objection (76% no) while N. America is between the two with 58 percent. It is also interesting to note that the Designer category has the least objection to saddles while all other industry categories have much stronger objections.

Question 1.6 Analysis for Bending Stresses (Figure A.7) - Under lateral loads and wind or traffic vibration stay cables can develop bending stresses which may be significant. Forty-one percent of the respondents did not perform a specific analysis for these bending stresses while 35%

ran some type of analysis to determine stresses. There was no clear agreement on the methods used to perform these analyses. Some discussed beam/column theory while others mentioned using non-linear computer programs to analyze the stays. Twenty-four percent did not feel they had the experience to answer the question.

4.7.2 Corrosion Protection

Question 2.1 Material Configuration (Figure A.8) - The All category rates parallel wire as the highest for ease and reliability of corrosion protection with a 79% rating while parallel strand is close behind with 77%. The ratings for strand and wire are slightly higher in structural performance (83% and 80%) than in this question (77% and 79%). Prestressing bar is treated more favorably for corrosion protection with a rating of 70% as compared to a rating of 40% for structural performance. As with structural performance, Europe (72%) rates helical locked coil strand higher than N. America (55%) or Asia/Australia (66%). Strand is rated slightly higher than wire in N. America while both Europe and Asia/Australia rate wire slightly higher than strand. Suppliers rate strand higher than wire (93% to 83%). However, all other industry categories rank wire higher than strand.

Question 2.2 Protection Systems (Figure A.9) - Monostrand with galvanized tension element has the highest rating in the All category with 84% while epoxy-coated and filled element is slightly lower with 76%. It is interesting to note that in the All category epoxy-coating and cement grout have nearly the same rating (58% and 56% respectively). It is also interesting to note the N. America category rated the epoxy-coated and filled element the highest (82%) while both Europe and Asia/Australia rated the galvanized monostrand the highest (85% and 88% respectively). The N. America category rates the galvanized monostrand very close to the top with 81%. In all categories there is a significant difference between galvanized and ungalvanized monostrand. The results are particularly surprising since most bridges completed to date have used cement grouted bare tension elements which finished fairly low in the survey. This system seems popular mostly with the supplier category.

Question 2.3 Blocking Compound (Figure A.10) - All selections except for "no blocking compound" were rated very close within a range of 59% to 66% by the All category. This could mean that no significant differences were seen between the possible choices. The N. America category rates cement grout the highest (68%) and Asia/Australia rates it close to the top (67%) while Europe rates it relatively low (48%). Europe prefers the two-part epoxy system while Asia/Australia prefers polyurethane. In the industry categories it is interesting to note that the Owner category prefers cement grout while the Designer category prefers the two-part epoxy system.

Question 2.4 Sheathing System (Figure A.11) - HDPE sheathing is preferred unanimously among all categories. Although other sheathing systems had strong support, most respondents feel sheathing must be provided.

Question 2.5 Corrosion Protection Systems (Figure A.12) - The most highly rated choice in the All category is the monostrand with galvanized tension elements and external sheath at 74%. Close behind are monostrand with bare elements, cement grout and external HDPE (70%) and galvanized tension elements with wax and external HDPE sheath (73%). The distribution of ratings both according to geography and industry are similar to the All category. N. America and Asia/Australia (73% and 74% respectively) rate the epoxy-coated system more favorably than Europe (56%). The All category rates the traditional "suspension bridge" type corrosion protection of exposed galvanized elements at 38%. This low value tends to hold for the other categories as well. It is interesting to note that the bare tension element with cement grout and HDPE sheath is 59% for the All category.

Although this question offered nine stay cable systems which were to be rated by the respondent for corrosion protection, there are many combinations of stay cable systems. The selections given are intended to represent a good cross-section of the available systems and components. However, several suggestions for alternative systems were made by respondents not satisfied with the selections given. One suggestion is galvanized strand, individually sheathed with external HDPE sheath extruded or fitted tightly on bundle. Another option is galvanized wire tension element with an external HDPE sheath extruded over the bundle.

Question 2.6 Portland Cement Grout Blocking Compound (Figure A.13) - In all categories except Europe the majority of the respondents believe that a portland cement grout blocking compound is an adequate corrosion protection system. Several respondents qualify their response by saying that the grout should be used in a HDPE sheath, while one said that he considered the HDPE sheathing to be the main corrosion protection. The reasons given in support of the cement grout blocking system were that it provides an alkaline environment around the steel, experience has shown it works, and some answered yes even though they were not completely convinced. Some reasons given for answering no to this question were that cracks from vibration and live load stresses are unavoidable.

Question 2.7 Grout Encasement (Figure A.14) - All categories had a majority answer yes when asked if they believe that the tensile elements are completely encased in grout. Reasons given for answering yes are that experience to date has been good or that they were not really convinced but answered yes anyway. Reasons given for answering no are that one can't really have ideal

grouting conditions and there are going to be voids from bleeding. Designers are least convinced with 56% responding yes while the Owner category had the most positive responses 87%.

Question 2.8 Temporary Protection Systems (Figure A.15) - The All category rated galvanizing, epoxy coated and filled, and greased and sheathed monostrand as the top choices (77%, 76%, and 72% respectively). The top rated choices varied geographically. N. America rated epoxy-coated and filled as the top choice at 80% while Europe and Asia/Australia rate galvanizing as the top choice at 84% and 74% respectively. Top choices also varied according to industry category. The Supplier category rated epoxy-coating and filling top at 83% while all other categories rated galvanizing as the top choice. Water soluble oils and desiccants were rated substantially lower.

4.7.3 Inspectability/Durability

Question 3.1 Inspectability versus Protection (Figure A.16) - In general, all categories were willing to settle for limited visual inspectability if multiple protection was provided.

Question 3.2 Replacement of Stay Cables (Figure A.17) - All categories overwhelmingly rated replacement of the entire stay as desirable over replacement of individual steel elements.

Question 3.3 Design Life (Figure A.18) - The results of this question are somewhat confusing. The question asks what design life is expected from: (a) a stay without an expected replacement and (b) if one replacement is expected during the life of the bridge. From a purely logical point of view the design life given for the stay which is to be replaced should be lower than that of the stay that is to be replaced once for a given life of a bridge. The results do not reflect this trend which indicates that the respondents may have misunderstood the question. Nevertheless, the results from the question can be useful in determining the life respondents expect to get from a stay cable. As can be seen in part (d) of this figure the All category expects a life of 60 years from a stay that is not intended to be replaced. The Owner category expects the longest life (76 years) while the Contractor category expects the shortest life (33 years). N. America and Asia/Australia are close in their expectations (67 and 65 years respectively) while Europe expects a much lower life at 45 years.

Question 3.4 Need for Replacement (Figure A.19) - In all categories excluding supplier a majority of the respondents agreed that there would need to be a replacement of a stay cable or component during the life of the structure. Some reasons given for the positive response were: only for accidental events, include the cost of replacement in maintenance. Those that disagreed indicated either that no structure should be designed with the aim of replacing it or that it should only be for accidental events.

4.7.4 Installation

Question 4.1 Installation of Stay Cable (Figure A.20) - All categories excluding the Contractor category prefer a fully shop prefabricated stay cable as compared to a stay assembled in place or assembled at the site. The Contractor category prefers a stay assembled in place.

Question 4.2 Stressing Procedure (Figure A.21) - All categories except Contractor rate stressing of the stay as a unit as the best method for stressing. The Contractor category rates both selections equally. Another option given by a respondent is to stress the individual strands initially to a low level and then stress the stay to the final level as a unit.

Question 4.3 Installation of Blocking Compound (Figure A.22) - Injection or grouting after stay cable installation is the method most highly rated by the All category (72%). Injection of grouting before installation using a flexible blocking compound is close behind (70%). Both N. America and Asia/Australia rate the in place installation highest while Europe rates preinjection with a flexible blocking compound higher.

Question 4.4 Installer (Figure A.23) - Results tend to differ for the question of who will install the stay cable. In the All category an 81% rating is given to the main contractor installation with supervision of the supplier. For the geographical categories N. America and Asia/Australia give the highest rating to the same choice. However, Europe rates installation by the stay supplier highest (77%). In the industry categories the Contractor and Supplier give their highest rating to installation by stay cable supplier. Owner and Designer rate installation by the main contractor with supervision by the stay supplier the highest.

Question 4.5 Grout Admixtures (Figure A.24) - A number of admixtures are mentioned in this question. The main concern seems to be to provide a grout which has nonshrink, low bleed, and pumpable properties. Also mentioned are no admixtures or not to use a portland cement grout at all.

4.7.5 Aesthetics

Question 5.1 Color Selection (Figure A.25) - For all categories it was important to the majority of the respondents to be able to select the color of the stay cable.

Question 5.2 Stay Diameter (Figure A.26) - For All, N. America, Asia/Australia, Owner, Designer, and Contractor categories the majority of the respondents felt it was not important to have the smallest diameter stay cable diameter. However, the majority of the Europe and Supplier category felt it was important to minimize the stay diameter. The reasons given for a yes answer were better response to wind forces or easier to handle while some reasons for no were that other factors more important or that it is only important for longer spans where wind response may be a problem. It is interesting to note that a large majority (74%) of the N. America category responses

are no while 75% of the Europe category are yes. A similar trend is noted between the Supplier (57% yes) and Owner (67% no) categories.

4.7.6 Marketing

Question 6.1 Documentation (Figure A.27) - The All category rates the need for "technical documentation on system and design/installation documentation and design/installation support" very close (80% and 79%) while "stay cable system documentation only" is rated at 62%. This trend holds for all categories except Europe which rates "technical documentation on system and design/installation" at 81% while the other two choices are less than 74%.

Question 6.2 Meetings Concerning Stay Cables (Figure A.28) - A large majority of the respondents in all categories expressed an interest in regular contacts/meetings between authorities, designers, contractors, and stay cable suppliers.

Question 6.3 Suppliers and System Familiarity (Figure A.29) - The question asked what stay cable suppliers and systems do you recognize or have you used. A total of 23 stay cable suppliers were listed with VSL, BBR, DSI, and Freyssinet taking the top four positions when considering the number of times they were mentioned. It should be noted that a higher ranking does not necessarily indicate that the products of the companies are preferred but rather recognized. In the second part of the question, many different stay cable systems were listed. To simplify the tabulation of systems, the list is broken into various groups based on the description of the tension element. The systems most often mentioned are parallel strand at 44, while parallel wire is mentioned 16 times and parallel bar is mentioned 9 times. Also mentioned are epoxy-coated strand, greased and sheathed strand, galvanized wire, long lay wire, locked coil and structural strand.

4.7.7 Past Experience

Question 7.1 Past Experience (Figure A.30) - Comments made in this section are extensive and cover many different aspects of stay systems. The comments do not generally following a particular theme or idea. Rather, they are a collection of the respondents' good and bad experiences with stay cable systems. Several comments are even directly contradictory such as in the use of epoxy coating. One respondent suggested that epoxy coating does not work as a barrier while another suggests that it increases the level of protection.

4.8 Trends

It is unwise to make recommendations or draw conclusions concerning the use of stay cables based solely on a mail survey of this nature. However, many respondents made a great deal of effort to express their opinions and experiences. The compilation of this information can certainly

indicate trends. In view of the scattered information in this area, such trends can be highly useful to the stay cable community.

4.8.1 Design

From a structural performance aspect the following items are very highly rated in the All category of respondents:

- Parallel strand or parallel prestressing wire.
- Hi-Am type anchorage.
- Place anchorages at towers (no saddles).
- Use fatigue stress range: 200 MPa (28 ksi).
- Three most important aspects of stay: durability, fatigue resistance, strength.

4.8.2 Corrosion Protection

For corrosion protection the following items are very highly rated in the All category of respondents:

- Parallel wire or parallel strand.
- Greased and plastic sheathed galvanized tension element.
- Epoxy coated and filled tension element.
- Some type of blocking system (numerous with about the same rating).
- HDPE external sheath.
- System: greased and individually sheathed galvanized tension element, with wax or cement grout and external HDPE.
- Portland cement grout is felt to be an adequate corrosion protective system and the grout is believed to completely encase the tension elements, although European respondents doubt the adequacy of the grout.
- Galvanizing, epoxy coating or greased and sheathed monostrand are preferred.

4.8.3 Inspectability/Durability

For inspection and durability the following items are very highly rated in the All category of respondents:

- Multiple protection and limited visual inspection but other monitoring options (electrical/magnetic).
- The entire stay should be replaceable as opposed to individual elements of the stay.
- Stay life expectancy is bimodal with a large group favoring 26-50 years and another favoring 76-100 years. Average stay life expectancy is 60 years.

4.8.4 Installation

For installation of the stay, the following items are very highly rated in the All category of respondents:

- Fully shop fabricated stay including blocking compound.
- Stress entire stay as a unit as opposed to stressing individual elements.
- Blocking compound should be installed after stay has been erected is slightly preferred over blocking installation before stay installation.
- Main contractor should install stay cables with supervision of stay supplier or the stay supplier should install the cables.

4.8.5 Aesthetics

For aesthetics, the following items are rated very highly in the All category of respondents:

- It is important to be able to chose the color of the stay.
- There is much varying opinion on whether it is important to have the smallest possible stay diameter.

4.8.6 Marketing

For marketing, the following items are very highly rated in the All category of respondents:

- Require technical documentation on system and design installation and provide design/installation support.
- There is a very strong interest in regular meetings concerning stay cables.

Chapter Five
Portland Cement Grout Series

Introduction

There are a number of materials available for use as blocking agents in the stay cable corrosion protection system. By far, the most popular system has been portland cement grout. In addition to providing a barrier to moisture and other contaminants the grout provides the high alkaline environment necessary to passivate the steel in the main tension element. Portland cement grout (in this chapter referred to as grout) is essentially a mixture of portland cement and water. Admixtures are generally used to increase the fluidity the mixture to facilitate injection. Sometimes expansive admixtures are used in an attempt to eliminate voids.

Grout has been used successfully for many years in post-tensioned concrete to provide bond between the tendon and surrounding concrete as well as corrosion protection. The methods and materials for injecting grout into post-tensioned ducts are very similar to the injection of stay cables. However, there is one significant difference which can make the use of the usual materials for post-tensioning duct injection inappropriate for use in injecting a stay cable

In grouting post-tensioning ducts or stay cables which have large changes in elevation, significant hydrostatic pressure can develop in the grout column. Schupack found that this pressure can cause segregation of the water and cement, also known as "bleeding."[101, 103, 104] In addition, he found that this bleeding is promoted by the presence of a bundle of prestressing strand or wire.

When the strand or wire bundle is present it draws the water into the interstices while leaving the cement particles outside the bundle. This, in essence, filters the cement out of the water. Because the density of the water is less than that of the grout, the water rises to the top of the column and forms a layer of bleed water at the top of the column. This behavior, in itself, is not detrimental to the protective layer of grout. The problem occurs when the bleed water does not rise all the way to the top of the grout column. Instead, lenses of bleed water can form at random locations along the length of the column.[101, 103, 104] The lens bleed water is subsequently drawn back into the grout leaving a void which results in a length of the strand or wire bundle unprotected by grout. Even without the introduction of corrosive elements into the duct, this area of unprotected strand is susceptible to corrosion because of the availability of moisture and oxygen and the lack of protection provided by the alkaline grout environment. One additional adverse effect of this phenomenon is

that the bleed water which filters into the interstices between the wires in the prestressing strand can remain even after the grout has set. This has been blamed for corrosion which accelerated the specimen failures in several fatigue acceptance tests conducted recently (see discussion of fatigue acceptance tests in Chapter One).

Objectives

It is reasonable to suggest that if a portland cement grout based system is selected for the stay cable corrosion protection system then, as a minimum, the full length of the stay should be surrounded by the alkaline protection of the grout with no potential for lenses to form. In order to satisfy this criterion the Portland Cement Grout Series was conducted with the following objectives:

- Develop a basic grout mix using anti-bleed admixtures which had a minimum of bleed and retained a reasonable fluidity for injection. This grout mix is denoted as Optimum Anti-bleed Grout Mix (OAG).
- Add corrosion inhibitors to the grout mix above to determine how the fresh properties were affected.
- Develop a silica fume modified grout which had a minimum of bleed and retained a reasonable fluidity for injection.

These grout mix designs then underwent further testing for corrosion protection properties in the Modified Accelerated Corrosion Test Method (ACTM) and Large Scale Durability Tests which are described in later chapters.

To satisfy the objectives, the fresh and hardened properties of the selected grout mixes were examined using the following tests:

- **Bleed Under Pressure:** Pressure test described in this chapter.
- **Standard Bleed:** ASTM C940-87 *Expansion and Bleeding of Freshly Mixed Grouts for Preplaced-Aggregate Concrete in the Laboratory*.[13]
- **Fluidity:** ASTM C939-87 *Flow of Grout for Preplaced-Aggregate Concrete (Flow Cone Method).*[12]
- **Initial Set Time:** ASTM C953-87 *Time of Set of Grouts for Preplaced-Aggregate Concrete in the Laboratory*.[14]
- **Cube Strength:** ASTM C109-90 *Compressive Strength of Hydraulic Cement Mortars (Using 2-in. or 50-mm Cube Specimens).*[10]

- **Alkalinity:** pH of wet grout using pH paper.

The **bleed under pressure** test simulates the pressure at the bottom of a column of grout in a stay. The desired property of the grout under these circumstances is the retention of water under the "filtering" action of the strands or wires. This prevents the transmission of bleed water up the column, thus preventing the formation of lenses.

The **standard bleed** test does not test the grout under pressure. The grout is placed in a graduated cylinder and allowed to bleed under gravity. This method does not test the grout adequately for applications in which there is a large change in elevation. However, the test was conducted because is it similar to the bleed test suggested by PTI *Recommendations for Stay Cable Design, Testing, and Installation*.[28]

The test for **fluidity** provides an indication of the pumpability of the grout. Anti-bleed admixtures tend to thicken grout which can make pumping difficult. This test was used to select grout mixes that would remain reasonably fluid after the addition of the anti-bleed admixtures. The test method used is a standard test method for fluid consistency of grout and is referenced in the PTI *Recommendations for Stay Cable Design, Testing, and Installation*. An ideal grout would have a very fluid consistency. A fluid grout can be pumped with a minimum of driving pressure and is able to flow into and completely fill the spaces.

The test for **initial set time** is used to determine the time from mixing until the initial set. Anti-bleed admixtures can retard the set of the grout significantly and some corrosion inhibitors can accelerate set time. As a result, it was necessary to monitor the set time of the various grout mixes to ensure that the set time was not changed drastically from the standard mix. PTI *Recommendations for Stay Cable Design, Testing, and Installation* require that the initial set time be no less than 90 minutes. There is no maximum limit.

PTI *Recommendations for Stay Cable Design, Testing, and Installation* require a minimum **cube strength** of 34.5 MPa at 28 days.

The test for **alkalinity** was conducted on selected grout mixes using pH paper. This test determined the pH level of the grout which should ideally be over 12.5 to be effective in passivating the steel.

The next part of this chapter describes the materials and equipment used in this test series. The selection criteria are developed and along with the test results are used to select the basic OAG mix. Corrosion inhibitors were then added to the OAG mix to determine the effect of the inhibitors on the fresh properties of the grout. Finally, development of a silica fume grout mix which has good

anti-bleed properties is described. It was selected for used in the further large scale corrosion study. The individual grout tests are described in detail in Appendix B along with modifications made to standard procedures or specimen configurations.

Materials and Equipment

Cement

Cement was obtained in bulk from the Balcones Plant of the Lafarge Corporation located in New Braunfels, Texas. The cement was transported in 55 gal barrels to the testing facility. The cement complied with the ASTM C109 Type I classification. The mill certificates are included in Appendix B.

Water

Distilled water was used in mixing the grout.

Admixtures

Admixtures used in the grout tests were obtained in sample quantities from the various manufacturers.

Anti-Bleed

There were two commercially available anti-bleed admixtures which were tested in this series: Sikament 300SC manufactured by Sika Corporation and Celbex 208 manufactured by Fosroc, Inc., Celtite Mining and Tunneling Division. Sikament 300SC comes in a brown liquid form and is described in the manufacturer's data sheet as a "product which will produce a grout with a relatively thick to stiff consistency, but will thin to a fluid, self-leveling consistency when mixed vigorously or pumped under moderate pressure. Celbex 208 is described in the manufacturer's data sheet as an "off-white free-flowing powder consisting of a balanced blend of organic polymers." It goes on to say that the admixture acts as a "... powerful dispersant and thixotropic agent when added to cement/water mixes, virtually eliminating bleed and the formation of water lenses in the cementitious grouting of long vertical and horizontal ducts." The data sheet for Celbex 208 recommends using a high shear mixer such as a disc mixer at a minimum speed of 1750 rpm.

Superplasticizer

The superplasticizer selected for use in these tests was WRDA-19 as manufactured by W. R. Grace, Inc. The manufacturer's data sheet describes WRDA-19 as a high-range water-reducer, commonly referred to as a superplasticizer. It is an aqueous solution of a modified naphthalene sulfonate and conforms to ASTM C494 - *Chemical Admixtures for Concrete* as a Type A or Type F admixture. Although superplasticizers are most commonly used in concrete, they are beneficial in

grouts as well, because the admixture acts as a dispersant for the cement particles suspended in the water-cement mix which provides a more fluid grout for the same w/c ratio.

In addition to WRDA-19 another plasticizer was tested in the first group of mixes. Tricosol 181(EH) is a German product manufactured by Chemische Fabrik Grünau, GmbH. The material was originally believed to be an anti-bleed admixture. However, preliminary tests indicated that it performed in a similar manner to the superplasticizer so it was not used in any further tests.

Corrosion Inhibitors

There were two corrosion inhibitors selected for use in the Modified ACTM (Chapter Six). Their effect on the fresh properties of the OAG mix developed in this series was evaluated. The first was a calcium nitrite formulation, DCI as manufactured by W. R. Grace. It is described as liquid which is added during the mixing process that chemically inhibits corrosive action of chlorides on reinforcing steel and prestressing strands. The admixture tested was guaranteed to contain a minimum of 30% calcium nitrite and meet the requirements of ASTM C494 for a type C admixture. The second corrosion inhibitor was Rheocrete 222 as manufactured by Master Builders. The product is described as a water-based, organic material formulated to inhibit the corrosion of steel in reinforced concrete by delaying the onset of corrosion activity in reinforced concrete, both in cracked and uncracked concrete.

Silica Fume

The silica fume selected for use in these tests was Sikacrete 950DP as manufactured by Sika Corporation. The product is described as a densified dry powder silica fume admixture for portland cement mortar and concrete. It is normally added at a rate of 5% to 15% by weight of cement.

Mixing Equipment

Mixing equipment consisted of a drill press with a spindle speed of 1700 rpm mounted on a floor stand and a "high shear" type mixing blade. The mixing blade was made from type 304 stainless steel and was manufactured by Jiffy Mixer Company, Irving, California. The size of the mixing blade used depended on the amount of grout that was prepared. Smaller batches were mixed in a 6 x 12 (152 mm x 305 mm) concrete cylinder mold using the type model LM mixing blade while large batches were mixed in 5-gallon (18.9-liter) buckets using the model PS mixing blade. Both the Type HS and PS mixers were used to mix the grout depending on the amount needed.

Test Format

Table 0.1 shows the complete list of mixes used in the grout series along with the water/cement ratio and type and quantity of admixtures added. The amount of grout mixed for

testing varied depending on which tests were being performed. Each mix number represents a unique combination of materials so that no two different mix numbers have exactly the same type and/or quantity of constituents.

The series can be divided into four groups. In the first group, several mixes of only water and cement were prepared with varying w/c ratios (mix nos. 1-3). This gave a baseline of results for plain water-cement mixtures of varying w/c ratios to compare with the subsequent tests. The complete set of tests was run on these mix designs. In addition, selected mixes of varying w/c ratios and quantities of anti-bleed or fluidifying admixtures (mix nos. 4 through 9) were tested. The purpose of these initial tests was to gain some experience with the effect that the admixtures had on the various fresh properties of the grout. Again, the full bank of tests was run on each of these mixes.

Development of the basic OAG mix design was the objective in the second group of the test series. The goal of this group of tests was to develop a grout mix which had minimum bleed under pressure, but still retained sufficient fluidity. The criterion used to rate the bleed properties was that the total bleed water must be less than or equal to 2% of the sample volume of grout at the end of the 3-minute hold period at 345 kPa in the bleed under pressure test. The development of this criterion is discussed in Appendix B.

There were two commercially available anti-bleed admixtures which could be used to provide the desired anti-bleed property. Maintaining a w/c ratio of 0.40, two separate grout mix designs were developed using the two anti-bleed admixtures. The amount of admixture in each mix

Table 0.1 - Portland Cement Grout Mixes.

Group	Mix No.	Water/Cement	Admixtures
1	1	0.35	None
	2	0.40	None
	3	0.45	None
	4	0.45	1.2% cwt* Celbex 208
	5	0.45	0.8% cwt Celbex 208
	6	0.40	0.8% cwt Celbex 208
	7	0.45	1.0% cwt Tricosal 181
	8	0.42	1.5% cwt Sikament 300SC
	9	0.35	1.0% cwt Tricosal 181
	10	0.45	1.5% cwt Sikament 300SC
2	11	0.40	1.7% cwt Sikament 300SC
	12	0.40	2.0% cwt Sikament 300SC
	13	0.40	1.5% cwt Sikament 300SC
	14	0.35	1.5% cwt Sikament 300SC
	15	0.35	1.7% cwt Sikament 300SC
	16	0.40	0.6% cwt Celbex 208
	17	0.40	0.8% cwt Celbex 208
	18	0.40	1.0% cwt Celbex 208
	19	0.40	2.2% cwt Sikament 300SC
	20	0.40	2.4% cwt Sikament 300SC
	21	0.40	1.2% cwt Celbex 208
	22	0.40	3.0% cwt Sikament 300SC
	23	0.40	2.2% cwt Sikament 300SC + 9.1 ml/kg cwt WRDA-19
	24	0.40	1.0% cwt Celbex + 9.1 ml/kg cwt WRDA-19
3	25	0.40	2.2% cwt Sikament 300SC + 19.8 l/m^3 DCI-S
	26	0.40	2.2% cwt Sikament 300SC + 19.8 l/m^3 DCI
	27	0.40	2.2% cwt Sikament 300SC + 5.0 l/m^3 Rheocrete 222
4	28	0.47	15% cement replacement with Sikacrete 950DP (by weight) + 9.1 ml/kg (c+sf)wt** WRDA-19
	29	0.47	15% replacement Sikacrete 950DP + 2.5 ml/kg (c+sf)wt WRDA-19
	30	0.38	15% replacement 950DP (by weight) + 7.8 ml/kg (c+sf)wt WRDA-19
	31	0.47	15% replacement Sikacrete 950DP
	32	0.47	2.2% cwt Sikament 300SC + 15% replacement Sikacrete 950DP
	33	0.40	2.2% cwt Sikament 300SC + 5% cwt Sikacrete 950DP (addition)

*cwt - cement weight

**(c+sf)wt cement + silica fume weight

was incrementally increased until the grout mix had a bleed under pressure of less than 2 percent at 345 kPa (mix nos. 11 through 24 in Table 0.1). The full set of tests was then conducted on these two optimized mix designs.

Of the other fresh properties tested, initial set time, compressive strength, and fluidity, fluidity is by far the most important. While it is necessary that a grout have sufficient strength, the degree of strength is not as important. Similarly, it is necessary that the grout set time be within a reasonable range but the degree, again, is not as important. Conversely, the degree of fluidity is very important. The more fluid the grout is, the less pressure is required for injection. This reduces wear and tear on the equipment and saves energy costs. But probably the most important reason is the reduction in pressure experienced by the grout. As has already been discussed, the higher the pressure on the grout the greater the tendency to bleed. Therefore, the next logical parameter to use to compare the two optimized grout mixes was the fluidity of the grout as characterized by the flow cone test.

The two optimized grout mixes which met the bleed criterion were then compared and ranked based on the results from the flow cone tests. In addition, the other parameters were checked against the minimum requirements set forth in PTI *Recommendations for Stay Cable Design, Testing and Installation*:[28]

- Flow Cone: 11 seconds minimum.
- Compressive Strength: 34.5 MPa minimum.
- Initial Set: 90 minutes minimum.

The objective of the third group of tests was to determine the effect of the corrosion inhibitors on their use in the OAG mix (mix nos. 25-27 in Table 0.1). The full group of tests was conducted for each mix. The results of the grout pressure tests for these new mixes were compared to the basic grout mix to ensure that the admixture did not affect bleed and flow adversely. The other test results were compared to the minimum requirements listed above.

The fourth and final group of grout tests consisted of the development of a grout mix containing silica fume which met the criterion for bleed under pressure (mix nos. 28-33 in Table 0.1). As with the group 2 tests, it was the objective to develop a mix which satisfied the bleed criterion but also maintain a reasonable fluidity. Therefore, only the grout pressure test and the flow cone test were performed initially. Previous studies have indicated that silica fume can provide a reduced-bleed grout even without the use of an anti-bleed admixture when used as a replacement for

cement in the range of 5-20% of cement weight (cwt).[39] The use of a superplasticizer is usually necessary to maintain fluidity when silica fume is used. Mix numbers 28-31 (Table 0.1) were developed using cement, water, silica fume, and superplasticizer. Fifteen percent replacement was selected for use in the initial mix designs. However, the initial tests in this group indicated that the silica fume, when used with a superplasticizer, tended to increase the bleed (mix nos. 25 through 31). As a result, the silica fume was tested in conjunction with the anti-bleed admixture used in the OAG mix to improve the bleed properties of the silica fume grout mix (mix nos. 32 and 33).

Summary and Analysis of Results

Each grout test was given a discrete test number which corresponded to the mix number being tested. If there was more than one test conducted for each mix design then a letter was added to the mix number to give the subsequent test number. For example, mix 19 (listed in Table 0.1) was tested several times which is indicated in the tabulated results by the test numbers 19, 19a, 19b, etc.

Group One

The results for grout mixes 1-10 are presented in Table 0.2. As expected, initial set times were increased and bleed was reduced in the grout mixes which contained the anti-bleed admixtures. It was also established here that Tricosal 181 was not effective as an anti-bleed admixture by examining the results of tests 7 and 9 in which pressure was lost in both tests at less than 207 kPa.

Group Two

The second group of tests were conducted to develop two optimal reduced-bleed mix designs using Celbex 208 and Sikament 300SC (see Table 0.2). The w/c ratio was held constant at 0.40 while the amount of anti-bleed admixture was varied. Since addition of the anti-bleed admixtures eliminated the bleed in the ASTM bleed test, only the grout pressure test was used in testing these mixes for bleed.

The results of the bleed tests on grouts using the two anti-bleed admixtures are shown in Figure 0.1 plotted as cumulative bleed volume as a function of applied air pressure. Each curve represents a different addition rate for the admixture considered. Each curve has two discontinuities. The first discontinuity occurs near the pressure of first bleed. This discontinuity

Table 0.2 (a) - Results of Grout Tests for Group 1 Through 3.

Group	Test No.	Standard Bleed**		Grout Pressure Test			
		% Bleed	% Expansion	First Bleed (kPa)	Loss of Pressure (kPa)	Amount of Bleed (% of sample volume)	
						345 kPa	552 kPa
1	1	2.88	0	0	276	n/a	n/a

	2	3.80	0	0	138	n/a	n/a
	3	8.22	0	0	138	n/a	n/a
	4	0	0	552	no loss	0	1.5
	5	0	0	138	no loss	2.3	8.5
	6	0	0	207	no loss	<1.5	5.3
	7	11.2	1.3	0	138	n/a	n/a
	8	0	0	70	no loss	2.3	4.0
	9	2.6	1.3	0	210	n/a	n/a
	10	0	0	0	552	7.5	21.5
2	4a	n/r	n/r	276	no loss	<1.5	3.3
	11	n/r	n/r	69	no loss	4.3	1.3
	12	n/r	n/r	138	no loss	2.5	8.0
	13	n/r	n/r	138	no loss	3.3	9.8
	13a	n/r	n/r	138	no loss	4.3	9.8
	14	n/r	n/r	138	no loss	4.3	11.0
	15	n/r	n/r	207	no loss	2.3	6.8
	15a	n/r	n/r	69	no loss	3.0	9.8
	16	n/r	n/r	138	no loss	4.8	15.0
	17	n/r	n/r	138	no loss	2.8	9.8
	18	n/r	n/r	0	no loss	1.5	5.0
	19	n/r	n/r	207	no loss	1.5	5.5
	20	n/r	n/r	138	no loss	1.5	5.3
	21	n/r	n/r	345	no loss	<1.5	2.3
	22	n/r	n/r	207	no loss	<1.5	4.3
	19a	n/r	n/r	n/r	n/r	n/r	n/r
	19b	0	0	207	no loss	<1.5	2.6*
	18b	0	0	276	no loss	<1.5	2.6*
	19c	0	0	138	no loss	2.3	1.8*
	19d	0	0	207	no loss	<1.5	3*
3	25	0	0	138	no loss	2.5	5.9*
	26	0	0	207	no loss	<1.5	3.3*
	27	0	0	207	no loss	<1.5	2.8*

* Percent bleed at indicated pressure after 3 minutes.

** Percentage of sample volume.

Table 0.2 (b) - Results of Grout Tests for Group 1 Through 3.

Group	Test No.	Initial Set (hr)	Flow Cone-Time to Exit (sec)	Cube Strength (MPa)		
				1 Day	7 Day	28 Day
1	1	<3.00	invalid	25.4	40.4	47.0
	2	3.69	163.	22.0	39.3	39.8
	3	4.45	n/r	15.0	33.9	37.4

	4	11.9	invalid	12.4	30.0	39.0
	5	12.7	82.5	5.4	25.9	34.9
	6	9.95	103.	12.3	32.6	37.6
	7	7.83	12.5	11.8	34.3	41.7
	8	5.19	invalid	15.3	38.8	32.2
	9	6.87	56.0	24.2	39.0	32.0
	10	5.48	31.5	12.5	n/r	n/r
2	4a	n/r	n/r	n/r	n/r	n/r
	11	n/r	n/r	n/r	n/r	n/r
	12	n/r	n/r	n/r	n/r	n/r
	13	n/r	n/r	n/r	n/r	n/r
	13a	n/r	n/r	n/r	n/r	n/r
	14	n/r	n/r	n/r	n/r	n/r
	15	n/r	n/r	n/r	n/r	n/r
	15a	n/r	n/r	n/r	n/r	n/r
	16	n/r	n/r	n/r	n/r	n/r
	17	n/r	n/r	n/r	n/r	n/r
	18	n/r	n/r	n/r	n/r	n/r
	19	n/r	n/r	n/r	n/r	n/r
	20	n/r	n/r	n/r	n/r	n/r
	21	n/r	n/r	n/r	n/r	n/r
	22	n/r	n/r	n/r	n/r	n/r
	19a	n/r	44.5	n/r	n/r	n/r
	18a	n/r	>120	n/r	n/r	n/r
	19b	7.53	39	19.9	36.5	42.7
	18b	8.52	103	16.9	29.9	37.2
	19c	9.97	34.8	21.2	27.2	38.5
	19d	6.17	31.8	n/r	n/r	n/r
3	25	>>10	31.6	2.7	25.0	35.2
	26	5.38	22.5	19.7	24.3	39.4
	27	6.13	24.5	22.1	39.3	n/r

occurs because the 25 ml graduated cylinder used to collect the bleed water did not allow an accurate reading of bleed volume below 3 ml. When the bleed amount was under 3 ml the reading was recorded as <3 ml. The plot shows the readings of <3 ml as zero. In subsequent pressure bleed tests a 10 ml graduated cylinder was used which allowed the volume to be read to the nearest 0.5 ml.

The second discontinuity occurs at the 483 kPa level. The bleed at each pressure increment was taken after 3 minutes except for the 552 kPa increment. The reading at 552 kPa was taken after

a hold period of 30 minutes. Since the final reading was taken at 30 minutes, rather than 3 minutes, a much larger volume of bleed was recorded than the other increments. In all tests subsequent to test 19a a reading was taken after 3 minutes at the 552 kPa level.

If these two discontinuities are discounted and the remainder of the curve is examined the result is very interesting. Consistently, the data plot linearly. As the dosage of admixture is increased, the slope of the line decreases. This is reasonable when the limits of the problem are examined. For a given w/c ratio, in this case 0.4, and no other admixtures there will be some limit of the slope as is shown. As admixture is increased, the slope tends to approach zero. Ideally, this is the point where the volume of bleed would be negligible for any applied pressure.

Selection of the optimum reduced-bleed grout mixes can be made from the graph of cumulative bleed. The maximum volume of bleed allowed at the end of the 3 minute period at 345 kPa is 2% of the sample volume. Mix number 18 (1.0% Celbex 208) and mix number 19 (2.2% Sikament 300SC) satisfied this requirement with the least amount of admixture. Additional tests were conducted on these mix designs and the averages of the pertinent results are summarized in Table 0.3. Although test 19c gave a bleed volume of 2.3% the average of the test results for all of the tests conducted on mix number 19 give a bleed volume of 1.7% which meets the stated criterion. The initial set of both mixes were relatively close in value and both satisfied the PTI minimum time of initial set of 90 minutes. Both mixes also satisfied the requirements for compressive strength (34.7 MPa minimum) and time to exit (11 seconds minimum). However, there was a wide difference in the time-to-exit of the flow cone. Mix 19 exhibited much more fluidity with a time-to-exit of 37.5 sec. compared to 112 sec. for mix eighteen. This made mix 19 the clear choice for OAG mix.

In mix number 23 and 24, the superplasticizer was added to the OAG grout mix design for each anti-bleed admixture. This was an attempt to improve the fluidity of the admixture. However, in both cases, when the grout was mixed with the superplasticizer and placed in the filter for the grout pressure test, bleed occurred before the application of pressure. As a result, there was no further testing conducted on these mixes.

Alkalinity was tested in mix number 19 and compared to that of mix number 2. If there was a reduction in pH then this would indicate that the admixture had reduced the pH. The test was conducted using 12.5-14 range pH paper. The pH was found to be 13 in both mix number 19 and mix number 2.

Table 0.3 - Average of Grout Test Results for Optimum Grouts Using Anti-Bleed Admixtures.

Mix	Grout Pressure Test			Initial	Flow Cone	Cube Strength (MPa)
	First	Loss of	Bleed at			

No.	Bleed (kPa)	Pressure (kPa)	345 kPa	Set (hr)	Time to Exit (sec)			
						1 Day	7 Day	28 Day
18	207	no loss	1.5%	8.52	112	16.9	29.9	37.2
19	190	no loss	1.7%	7.89	37.5	20.5	31.9	40.6

Group Three

The purpose of this group of tests was to determine the effect of the selected corrosion inhibitors on the fresh properties of the OAG mix. Mix number 25 included admixture DCI-S in the mix formulation (see Table 0.2). DCI-S is a calcium nitrite formulation with a retardant added to offset the accelerating effect of the calcium nitrite. The anti-bleed admixture also provides a retarding effect. This is clear when the initial set times of the grouts with and without the anti-bleed admixtures are compared. The grout mix using 0.4 w/c ratio with no admixtures (mix no. 2) had an initial set of 3.69 hours while grout mix (using the anti-bleed admixtures) number 18 and 19 had initial set times of 8.52 and 7.53 hours, respectively. Because of the combined retardant action of the DCI-S and anti-bleed admixture the initial set time was very high. The one-day cube strength of 2.7 MPa indicates that the set time of the grout was greatly lengthened from the combined effect of the retardants.

The average values of mix 19 shown in Table 0.3 can be compared to the results of tests 26 and 27 (Table 0.2) to illustrate the effect of the corrosion inhibitors on the fresh properties of the grout. When DCI (mix 26) was used as the corrosion inhibiting admixture the accelerating effect of the calcium nitrite actually offset the retarding effect of the anti-bleed admixture. This can be seen when the initial set time of 5.38 hours for DCI is compared to the average for the OAG mix of 7.89 hours. Rheocrete 222 (mix 27) also acted as an accelerator with an initial set time of 6.13 hours.

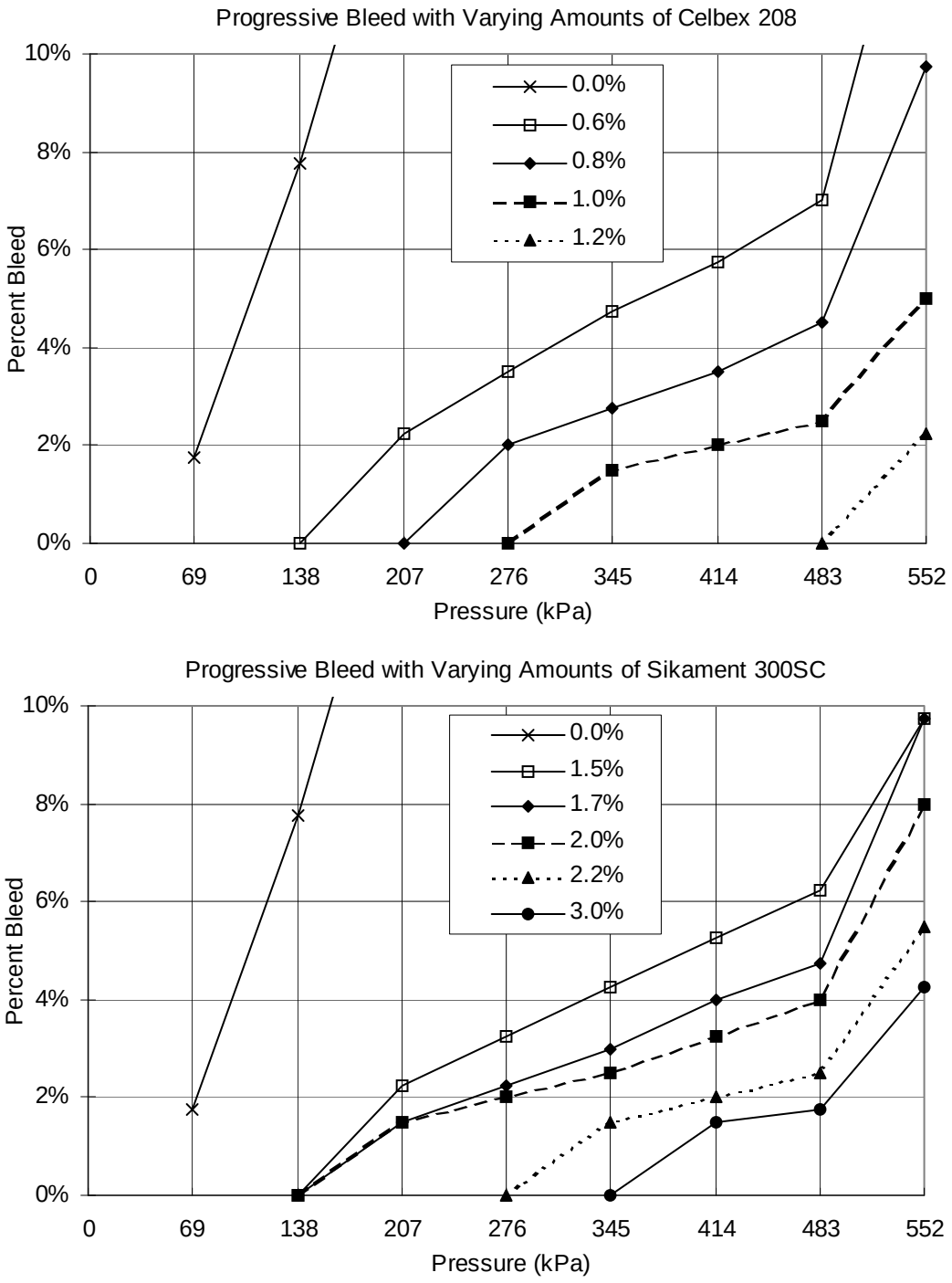

Figure 0.1 - Comparison of Progressive Bleed with Anti-bleed Admixtures.

The flow cone test indicated that both corrosion inhibitors improve the fluidity of the grout as the time-to-exit is 40% less with DCI and 35% less with Rheocrete 222. Cube strength is slightly less but the difference is so small as to be negligible. The bleed properties were not adversely affect by the addition of the corrosion inhibitors with both admixtures bleeding less than 1.5% at 345 kPa.

Group Four

The final group of grout tests were used to develop a grout mix with silica fume. As with the group 2 tests, it was the objective to develop a mix which satisfied the bleed criterion but also maintain a reasonable fluidity. The results for the initial tests using silica fume and superplasticizer are presented in Table 0.4.

In mix numbers 28-31 the amount of superplasticizer as well as w/c ratio was varied in an attempt to find a mix which would meet the bleed criterion. The results of the pressure bleed tests indicated that all mixes bled immediately when placed in the filter funnel and that all had lost pressure at or before reaching 207 kPa. This indicated that the silica fume used with a superplasticizer did not produce the desired bleed properties. As a result, mix 32 and 33 were developed contained silica fume and Sikament 300SC. The results for these tests are also shown in Table 0.4 (a) and (b).

Difficulties with Anti-Bleed Admixture

It was suspicious that the results from test 32 and 33 gave a much higher bleed than the previous tests on mix nineteen. Mix number 32 had the same constituents as 19 except that silica fume had been used in the amount of 15% replacement of cement. The large increase in bleed from mix 19 to this mix (1.7% to 3.8%) might be explained by the effective increase in w/c ratio for this mix. However, the results for test 33 should have given better bleed properties than for mix 19 because silica fume was added which left the effective w/c ratio is unchanged. To eliminate the silica fume as a possible cause for the discrepancy, another test was run using the OAG mix (test 19f). The results of this pressure bleed test varied markedly from the previous tests on the same mix design with an increase in bleed at 345 kPa of over 130 percent.

This indicated that there was a problem with one of the constituents. Water was eliminated because distilled water of reliable consistency was being used for mixing. The cement was obtained in bulk and was the same cement for all the tests. In addition, the cement was kept in closed containers to prevent contamination with moisture. The admixture Sikament 300SC seemed to be the only likely candidate for causing the bleed problem.

Table 0.4 - Partial Results of Grout Tests for Group 4.

Group	Test No.	Standard Bleed**		Grout Pressure Test			
		% Bleed	% Expansion	First Bleed (kPa)	Loss of Pressure (kPa)	Amount of Bleed (% of sample volume)	
						345 kPa	552 kPa
4	28	2.4	0	0	138	n/a	n/a
	29	4.2	0	0	207	n/a	n/a
	30	1.6	0	0	207	n/a	n/a
	30a	n/r	n/r	n/r	n/r	n/r	n/r
	31	2.4	0	0	138	n/a	n/a
	32	n/r	n/r	69	no loss	3.8	6.8*
	33	n/r	n/r	69	no loss	3.5	6.0*
	19e	n/r	n/r	69	no loss	4.0	6.8*
♦	19f	n/r	n/r	138	no loss	2.5	4.5*
♦	32a	n/r	n/r	138	no loss	3.7	6.7*
♦	19g	n/r	n/r	138	no loss	2.5	4.6*
♦	33a	n/r	n/r	138	no loss	2.5	4.5*
	19h	n/r	n/r	138	no loss	4.3	7.5*
♦	33b	n/r	n/r	207	no loss	1.8	3.8*

* Percent bleed at indicated pressure after 3 minutes.

** Percentage of sample volume.

♦Fresh Sikament 300SC used in these tests.

Table 0.4 (b) - Results of Grout Tests for Group 4.

Group	Test No.	Initial Set (hr)	Flow Cone-Time to Exit (sec)	Cube Strength (MPa)		
				1 Day	7 Day	28 Day
4	28	n/r	31.5	n/r	n/r	n/r
	29	n/r	13.8	n/r	n/r	n/r
	30	n/r	27.2	n/r	n/r	n/r
	30a	n/r	n/r	27.6	49.1	n/r
	31	n/r	31.5	n/r	n/r	n/r
	32	n/r	39.0	n/r	n/r	n/r
	33	n/r	n/r	n/r	n/r	n/r
	19e	n/r	n/r	n/r	n/r	n/r
♦	19f	n/r	n/r	n/r	n/r	n/r
♦	32a	n/r	n/r	n/r	n/r	n/r
♦	19g	n/r	n/r	n/r	n/r	n/r
♦	33a	n/r	n/r	n/r	n/r	n/r
	19h	n/r	n/r	n/r	n/r	n/r
♦	33b	9.5	40.0	18.9	25.6	43.0

♦Fresh Sikament 300SC used in these tests.

Grout tests 1-30a were completed in the time period from March through August of 1993, while the remainder of the tests were completed in October, 1994, approximately one year later. The admixture was originally obtained in two 3.8 liter containers. When that was finished, additional admixture (from a different batch) was obtained in the quantity of 18.9 liters. This change was made during the testing time period of March-August 1993 during which there were no distinguishable differences noted in the test results. This seemed to indicate that there was good consistency in the admixture from batch to batch. In addition, there was no shelf life given for the admixture.

To determine if there had been some change in the admixture in the time between tests, an additional 18.9 l batch was ordered from the manufacturer and tested. Test 19e and 19h were conducted with the old admixture and 19f and 19g were conducted with the fresh admixture and are compared in Table 0.5. It can be seen that the test results for both the old and new admixture were repeatable, which ruled out the possibility of error in the test procedures causing the discrepancy. Two peculiarities were also noted in the results of these tests. The first was that the mix with the old admixture bled much more than the mix with the fresh admixture (for example a 60% increase at 345 kPa level). The second was that even with the fresh admixture the grout did not match the performance of previous tests. In fact, the bleed at 345 kPa of 2.5% was greater than the criterion of 2.0% established previously in this chapter for the selection of the best grout mix.

Table 0.5 - Summary of Grout Pressure Test Results with Fresh and Old Sikament 300SC.

Admixture	Mix No.	First Bleed kPa	Loss of Pressure kPa	Amount of Bleed (% of sample volume)	
				345 kPa	552 kPa
Previous**	19	27.5	no loss	<1.5	3.2
Old	19e	10	no loss	4.0	6.8*
Old	19h	20	no loss	4.3	7.5*
Fresh	19f	20	no loss	2.5	4.5*
Fresh	19g	20	no loss	2.5	4.6*

*Percent bleed at indicated pressure after 3 minutes.
**Average of tests 19 through 19d

This suggested an inconsistency among the different batches of Sikament 300SC tested. It is suspected that the bleed performance of the admixture is directly tied to the level of agitation just prior to use. This became apparent during the grouting of the first lift of specimen LS-2 of the large-scale test series (Chapters Eight and Nine). While it was normal procedure to stir the admixture prior to use, on this particular lift the admixture was inadvertently used without mixing. As a result a

large amount of bleed water was noted at the top of the lift. There was no bleed water noted at any location in the second lift of this specimen nor in any of the other large scale specimens. The manufacturer's directions did not indicate that the admixture should be stirred prior to use. It is possible that the organic polymer and superplasticizer segregate when left undisturbed. If the polymer sinks to the bottom then samples taken would be primarily superplasticizer. This would explain the excessive bleed which occurred on LS-2.

Unfortunately, much of the other testing which made use of the OAG mix had been completed by the time this problem became apparent. In order to maintain consistency in the other test series, it was decided that the originally selected OAG mix design would be used to complete the testing program.

Mix number 32 had a water to cement+silica fume ratio of 0.40. It was anticipated that this combination when used with the 2.2% Sikament 300SC would provide essentially the same bleed properties as the OAG mix design which used all cement. The results indicated that this mix had a higher bleed than the OAG mix even with the new admixture. One explanation is that the size of the silica fume particles affect the bleed properties. Bleeding can be looked at as consolidation of the cement particles with the water rising to the top to form the "bleed." Silica fume particles are on the order of 100 times smaller than cement particles. This, in combination with the superplasticizer, may allow the particles to consolidate easier. An analogy would be the consolidation of well-graded aggregate where the smaller sizes fill the spaces between the larger sizes to produce less total void space.

To remedy the problem the w/c ratio was lowered to 0.40 and 5% silica fume (by weight) was added (mix number 33). The low addition rate of silica fume helped to maintain the fluidity of the grout. This mix design performed well in tests 33a and 33b using the fresh admixture. Therefore, mix number 33 was selected as the optimum mix design with silica fume for use in further corrosion testing.

Conclusions

The portland cement grout series measured the fresh and hardened properties of portland cement grout with various admixtures and water/cement ratios. Tests included fluidity, bleed, bleed under pressure, initial set time, cube strength and pH. The primary goal of the test series was to develop a grout mix which had minimum bleed and still remained fluid. The following findings were made:

- An optimum mix design was developed which met the designated criterion for bleed under pressure. The mix consisted of 0.40 water/cement ratio with 2.2% Sikament

300SC (by cement weight). This mix design was used in all of the large scale test specimens except LS-5 (see Chapters 7-9).

- DCI, manufactured by W. R. Grace, is a 30% calcium nitrite solution. This corrosion inhibitor was added to the optimum grout mix to determine the effect on the properties of the grout. The only significant effect was the reduction of the set time. This had the beneficial effect of offsetting the delay in set time caused by the Sikament 300SC. This mix was tested in the Modified ACTM reported in Chapter Six.
- Rheocrete 222, manufactured by Master Builders, is an organic-based inhibitor added to the optimum grout mix to determine the effect on the properties of the grout. No significant effects were noted. This mix was also tested in the Modified ACTM reported in Chapter Six.
- Sikacrete 950DP, a densified silica fume manufactured by Sika, was used in conjunction with Sikament 300SC to produce a reduced-bleed silica fume grout. This mix was tested in the Modified ACTM and was also used in LS-5 in the large scale test series.
- Some inconsistency was noted in the performance of the anti-bleed admixture Sikament 300SC. There was an indication that the admixture was not mixed thoroughly prior to use and that this may have caused the inconsistencies. However, the manufacturer does not specifically recommend that the admixture be mixed prior to use.
- Bleed under pressure tests indicated that the cumulative volume of bleed water collected at each pressure level is linear with increasing pressure. Further testing of anti-bleed grouts may indicate that the slope of the bleed curve can be used to characterize a grout with respect to bleed. In addition, further work is needed to determine a maximum allowable bleed for anti-bleed grouts.

Chapter Six
Modified Accelerated Corrosion Test Method

Introduction

The use of portland cement grout as a blocking agent in the stay cable corrosion protection system has become popular in the last twenty years. While the performance of portland cement grout in post-tensioning ducts (when proper methods and materials are used) has generally been good, there has been little field evaluation of the performance of portland cement grout in stay cables. In addition, there are no laboratory evaluation methods for testing the corrosion protection provided by portland cement grouts.

In an effort to address this issue Thompson, Lankard, and Sprinkel developed the Accelerated Corrosion Test Method (ACTM).[120] This test method was devised to give a simple and efficient evaluation of the corrosion protection properties of portland cement grout (in this chapter referred to as grout).

Several modifications were made to the specimen configuration and test procedures of the original ACTM in order to improve the ability of the test to evaluate precracked grout. The modified test method will be referred to subsequently as the "Modified ACTM." The overall test setup is shown in Figure 0.1. It should be noted that all tests performed in this series were on precracked specimens.

The grout mix designs tested in this series were developed in the grout development test series reported in Chapter Five. The grout mix designs incorporated admixtures which were intended to improve the corrosion protection performance of the grout. The results of the Modified ACTM on these grout mix designs are reported in this chapter. In addition, the grout mix which provided the best performance in these tests was selected for use in the large-scale tests which are reported in Chapter Eight and Nine.

Several potentiodynamic tests were also conducted to determine if the differences in the IR drop caused by the grout would substantially effect the results of the tests.

Thermodynamic and mixed-potential principles are the foundation for this test method. A discussion of background and development of these principles is included in Chapter Two.

Figure 0.1 - Modified Accelerated Corrosion Test Method Setup.

Original ACTM[120]

The original ACTM was developed to test the effectiveness of portland cement based grouts for corrosion protection of tendons in post-tensioning applications. The goal was to develop an accelerated test method which tested grout design mixtures in a very short time period and predicted the effectiveness of the grout in preventing corrosion of prestressing steel over a 50-year life. It was found that the test times could be as long as 40 days but were usually within 20 days. In addition, the test was designed so that it could be used routinely by civil engineering technicians.

Accelerated corrosion test methods are difficult to design. The primary difficulty is in providing an accelerated corrosion process without altering the corrosion mechanism. Anodic polarization was selected as the method because it would:

- Tend to drive the chlorides toward the specimen by providing a potential gradient
- Tend to increase the rate of corrosion following breakdown of the passive layer when and if breakdown occurs
- Likely decrease the incubation time for passive film breakdown at a given chloride concentration

The test series included specimens which were cracked and uncracked prior to the accelerated corrosion test, although the majority of specimens actually tested were uncracked.

Various mix designs were developed as a part of the test program for testing. The grout additives used included superplasticizer, silica fume, fly ash, polymer modifier, corrosion inhibitor, expansion agent, anti-bleed agent, and sand.

Original Test Procedures and Results[120]

The original ACTM specimen was constructed by placing a 267-mm long by 12.7-mm diameter seven-wire prestressing strand inside a 19-mm diameter PVC pipe. The strand was masked with epoxy in those areas outside the section of pipe to be removed for testing. Washers were used to keep the strand centered in the pipe. The pipe was then filled with grout and "vibrated" for two minutes or until no bubbles appeared. After the grout was cured for twenty-eight days the specimen was placed in a lathe and a 114-mm section of the pipe was removed to expose the grout. After the pipe had been removed the surface of the grout was visually inspected for cracks. Any visible cracks were cause for rejection of the specimen.

Eight specimens were required for each test with four of these being precracked. The specimens were precracked by placing them in a loading frame and applying a load at the midspan of the specimen while the midspan deflection was measured with a micrometer. The load was increased in 508 μm deflection increments and the surface of the grout was examined. At the first sign of visible cracking the specimen was unloaded and was ready for testing.

The specimens were then anodically polarized using 5% (by weight) salt solution as the electrolyte. The polarization level was held at a constant +600 mV_{SCE}. Anodic current was monitored until a sharp rise indicates that the chlorides had permeated through the grout (or crack) and reached the surface of the strand. The time from initiating the polarization to the sharp rise in corrosion current was denoted "time-to-corrosion."

The time-to-corrosion results from the ACTM were not intended to be extrapolated to an expected life in the field. Instead, the test is best used as a relative comparison. A proven grout mix design is tested using the ACTM. The results of this test are then compared to subsequent tests conducted on grouts with other variables such as water/cement ratio or admixtures. Further details of the test procedures and specimen configuration can be found in Reference 120

A summary of results for the original ACTM is given in Table 0.1. Table 0.2 gives the grout mix designs used in each of these tests. Note that several of the anodic polarization tests were run at both +600 and 0 mV_{SCE}. Comparing the results obtained in test P1a (no additives) and P7a (calcium nitrite) indicates that the addition of calcium nitrite impaired the performance of the grout in this test. Based on this finding the researchers conducted an additional test on the same mix designs except that the polarizing potential was set to 0 mV_{SCE}. They felt that the high polarizing

potential of +600 mV_{SCE} was "above the breakdown potential for the inhibitor" and that a more equitable test should be conducted at the lower potential. The results indicated that the calcium nitrite provided a significant increased protection when tested at this level of potential. However, it should be noted that the data are limited in that there were only two specimens prepared for test P1b for comparison.

Table 0.1 - Summary of Times to Corrosion from Original ACTM Tests[120]

Test	Potential mV_{SCE}	Time-to-corrosion (hours)			
		Uncracked	Ave.	Precracked	Ave.
P1a	600	140, 205, 170, 180	174	50, 150, 25, 130	89
P1b	0	290, 65	178	none	-
P2	0	50, 25, 27, 20	31	none	-
P3	600	335, 535, 350, 450	418	25, 0, 0	25
P4	600	245, 150, 650, 135	295	25, 0	25
P5	600	335, 125, 150, 200, 220, 390	237	90, 0, 0, 0	90
P6	0	190, 140, 200, 140	227	10, 2, 0, 20	8
P7a	600	70, 105, 160, 180	129	55, 40	48
P7b	0	546, 430, 875, 1000	713	none	-

Table 0.2 - Grout Mix Designs in Original ACTM Tests[120]

Test	Water/Cement	Admixtures
P1	0.44	None
P2	0.65	None
P3	0.32*	33% cwt** Fly Ash + 52% cwt Silica Sand + 0.05% cwt Polysaccharide Gum + 26 ml/kg cwt HRWR‡
P4	0.365†	11% cwt Silica Fume (addition) + 10-36 ml/kg cwt HRWR‡
P5	0.29	31.5% Latex Polymer Modifier + 10 ml/kg cwt HRWR‡
P6	0.365	0.75% cwt Aluminum Powder + 0.01% cwt Polysaccharide Gum + 21ml/kg cwt
P7	0.44	29 l/m^3 Calcium Nitrite (DCI-W. R. Grace)

*water/(cement + fly ash)
**cement weight
† water/(cement + silica fume)
‡ High-range water reducer

Test Method Modifications

One of the primary goals of this series was to test the performance of various grouts in the cracked condition. Due to the high variability in the data gathered in the original tests the uniformity

of specimen preparation is a very important issue. In the series reported herein, there were several changes made to improve the uniformity of specimen preparation:

- The form system was designed so that the specimen disturbance was minimized during removal of the pipe section.
- The grout was precracked and the largest crack was then isolated. The selected crack was then opened to a uniform crack width prior to testing.
- Only the selected crack was exposed to the solution during anodic polarization.

Four trial configurations were constructed and tested to determine the best method for precracking the specimen. All of the trial specimens were intended to force a single crack to occur at the midpoint of the specimens. As shown in Figure 0.2 these attempts were met with varying degrees of success.

The first and second trial specimens had notches at the load point. These notches were made by a plastic strip attached to the inside face of the removable portion of the mold. There were two problems with these specimens. The grout form was oriented vertically when the grout was placed. The grout was poured into the top of the form. After the grout was poured into the form, the bleed water and/or air bubbles would be trapped under the plastic strip causing voids in the notch area. The second problem was that a single crack would not consistently form in the notch but adjacent to the notch.

The plastic strip was eliminated in the third trial specimen to eliminate the void problem. However, when the grout was precracked the cracks would form adjacent to the end of the pipe. This made isolation and measurement difficult.

The fourth and final configuration solved both problems. A transparent PVC pipe was used as a form and the grout was precracked prior to exposing the grout. The transparent pipe allowed the isolation and measurement of the largest crack prior to removal of the sheathing. The sheathing was then gently removed only in the area of the selected crack using the wire brush on a pedestal grinder. This method also minimized the time that the surface of the grout was exposed to air.

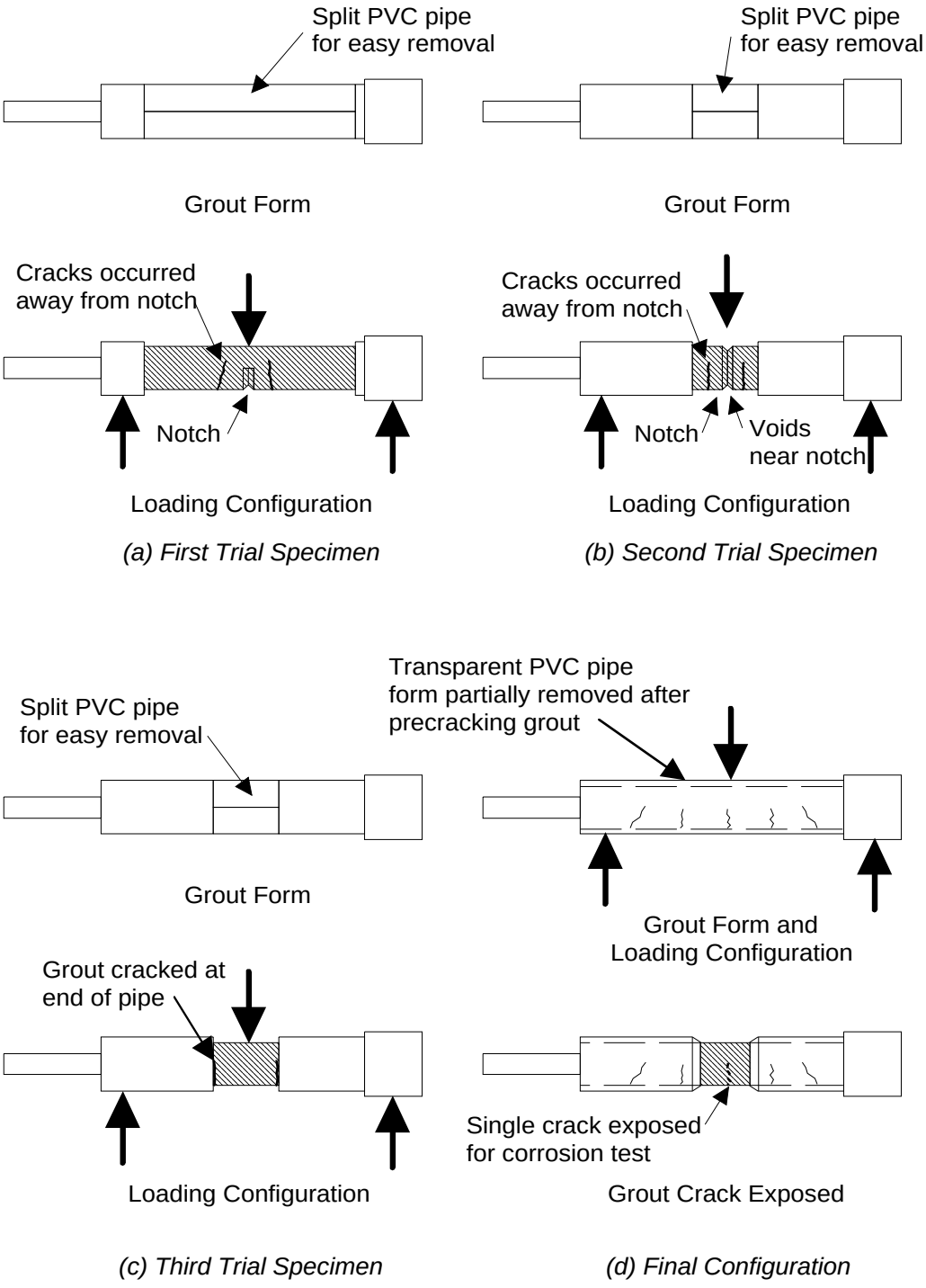

Figure 0.2 - Trial Configurations for Modified ACTM Tests.

IR Drop in Grout

Because grout is a poor conducting electrolyte, one of the major problems in the measurement of the corrosion rate is the ohmic resistance or "IR drop" caused by the grout. This IR drop can cause problems in anodic polarization tests as well. Ideally, the measurement of the set potential in the anodic polarization test would be made near the steel/concrete interface. This would eliminate the possible differences in polarization level at the steel surface due to differences in the ohmic resistance of the grout. However, this is not practical from an experimental perspective. The level of polarization maintained by the potentiostat is actually read at the tip of the reference electrode. So any significant differences in the ohmic resistance of the electrolyte or grout would affect the actual polarization potential at the level of the steel.

This difference in ohmic resistance in concrete has been measured in previous work and has been found to be quite variable between concretes with different types of admixtures.[18] It was found that the addition of calcium nitrite can reduce the ohmic resistance of the concrete while the use of silica fume can increase the ohmic resistance significantly. This would result in a larger IR drop for the silica fume than for the calcium nitrite.

Other experimental work has found that the addition of silica fume to a portland cement based grout increases the ohmic resistance when compared to a grout without silica fume.[61] The study also indicated that the ohmic resistivity of the silica fume grout increased with age while that of the control grout remained constant.

If all of the grouts to be tested with ACTM had the same ohmic resistance, then the IR drop would be the same for each specimen and would influence the time-to-corrosion of all the tests to the same extent. The relative performance of different grout mixes would remain unchanged. However, as mentioned previously, all grouts do not have the same ohmic resistance. There are several methods available to measure the ohmic resistance of an electrolyte in a test cell.[56] However, these methods require equipment which was not available for the Modified ACTM.

Lacking the sophisticated equipment necessary to quantitatively determine the ohmic resistances of the various grouts it was decided that several crude potentiodynamic tests would be conducted to give a qualitative indication of the differences in ohmic resistance of the grout and if this difference may affect the outcome of the test.

Grout Mix Designs

In the grout development series the fresh properties of several grout mix designs were examined. Six grout mixes were selected for use in the Modified ACTM tests and are presented in

Table 0.3. In addition, one trial mix is listed which was used in testing the various specimen designs. Admixture descriptions and manufacturers' data are presented in Chapter Five.

Table 0.3 - Grout Mixes Tested with Modified ACTM.

Mix No.*	Water/Cement	Admixtures
trial 1	0.40	1.90 ml/kg cwt WRDA-19
2	0.40	None
19	0.40	2.2% cwt** (of cement weight) Sikament 300SC
26	0.40	2.2% cwt Sikament 300SC + 19.8 l/m^3 DCI
27	0.40	2.2% cwt Sikament 300SC + 5.0 l/m^3 Rheocrete 222
30	0.47	15% cement replacement with Sikacrete 950DP (by weight) + 3.0 ml/kg cwt WRDA-19
33	0.40	2.2% cwt Sikament 300SC + 5% cwt Sikacrete 950DP (addition)

*Mix designs and numbers are taken from the list in Chapter 6.
**cement weight

Equipment and Materials

Strand

The strand used in these tests was obtained from Florida Wire & Cable, Inc. The chemical analyses and mill certificate data are included in Appendix C. The strand was 12.7-mm diameter low-relaxation seven-wire prestressing strand, grade 270, and was taken from two different reels.

Cement

Description of the cement is included in Chapter Five.

Admixtures

Descriptions of the admixtures are included in Chapter Five.

Water

Distilled water was used for mixing the grout and for mixing the 5% NaCl test cell solution.

Sodium Chloride

A reagent grade NaCl was used to mix the salt solution.

Specimen Mold

Figure 0.3 shows the form used for grouting and testing. Each specimen was constructed using prestressing strand, transparent PVC pipe and endcap, and plastic reinforcing bar supports which held the strand centered in the pipe.

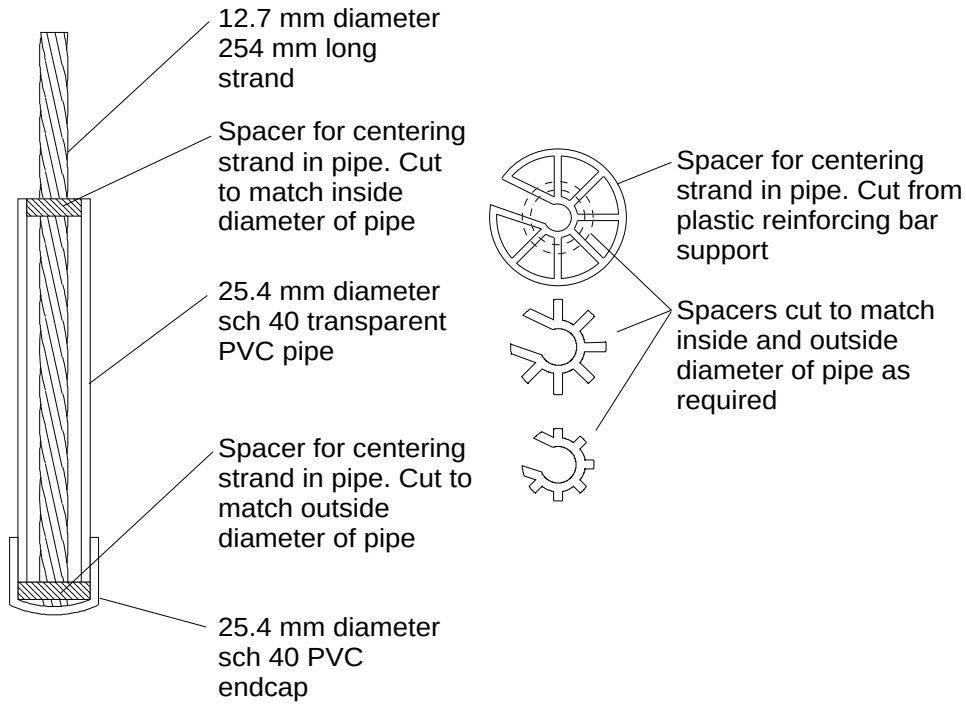

Figure 0.3 - Details of Modified ACTM Specimen

Mixing Equipment

See Chapter Five for mixing equipment details.

Corrosion Test Equipment

Potentiostat

The anodic polarization was accomplished with a model 125 six-channel potentiostat manufactured by Cortest, Inc., Willoughby, Ohio. The specifications are as follows (per channel):

- Max output: ± 12 Volts/0.5 Amps
- Internal potential control: ± 2.0 Volts
- Reference electrode current: 0.1 picoamp
- Response time: < 5 microvolts/deg. C
- Power: 110/220 VAC, 50/60 Hz

Reference Electrodes

Calomel Reference Electrodes were manufactured by Fisher Scientific and were of the gel-filled, polymer-body type. The design consisted of mercury/mercury chloride reference element surrounded by an electrolyte (gelled saturated KCl solution). When the electrode is immersed in a

solution, contact is made between the solution and the reference electrolyte through an opening at the end of the polymer body. The reference electrode opening has a porous polymer junction to allow a slow electrolyte flow.

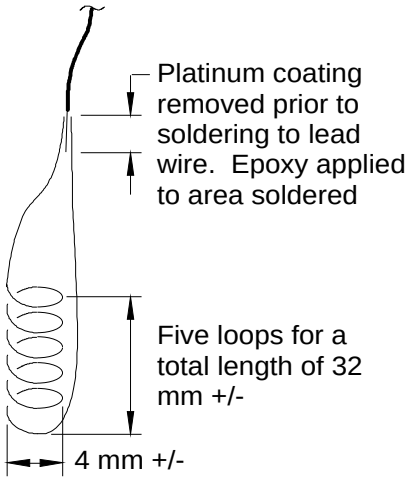

Figure 0.4 - Details of Platinum Auxiliary Electrode.

Auxiliary Electrodes

The auxiliary electrodes were fabricated from platinum-clad wire with a niobium/copper core (40% niobium by area). The wire was 1.14 mm diameter, had a platinum coating thickness of 1.02 μm, and was manufactured by IGC Advanced Superconductor, Inc., Waterbury, Connecticut. The wire was deformed as shown in Figure 0.4, the platinum was removed near the tip, and the exposed niobium/copper core was soldered to the lead wire. The soldered area was then protected with a thin coating of epoxy.

Cracking Frame

The grout in each specimen, just prior to corrosion testing, was precracked. This was accomplished with the steel frame shown in Figure 0.5. The frame was constructed from structural steel angle and was shaped to allow the use of a portable microscope to measure crack widths during loading.

Portable Microscope

The portable microscope used to measure crack widths during precracking measured to the

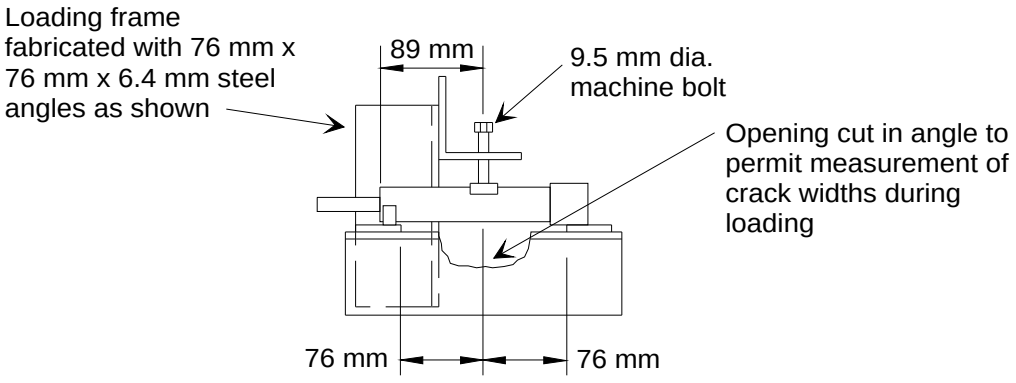

Figure 0.5 - Details of Frame to Precrack Grout

nearest 0.0254 mm.

Instrumentation

There were six corrosion cells which corresponded to the six channels available on the potentiostat. Each corrosion cell had the configuration shown in Figure 0.6. The grout and strand specimen, auxiliary electrode, and reference electrode were immersed in a 5% NaCl solution. The solution was contained in a 3-l beaker and the electrodes were held in position with a 12.7-mm thick acrylic plate cut to a diameter slightly large than the diameter of the beaker. A 100-Ω resistor was placed in the wiring between the auxiliary electrode and the potentiostat in order to make corrosion current measurements.

The data was recorded with a 21X Micrologger portable data acquisition system manufactured by Campbell Scientific, Inc., Logan, Utah. The micrologger had an 8-digit LCD display and a 16 character keyboard. There was a 9 pin I/O port for connection to peripherals. Connection to a personal computer required the use of a SC32A interface (also manufactured by Campbell). Analog inputs, switched excitation outputs, continuous analog outputs and digital control ports were all available on the micrologger. The analog input range used in these tests was ± 5 V which had a resolution of 333 μV and an input impedance of 200 gigohms.

Voltage was also monitored with a Fluke 8800A benchtop multimeter. The multimeter ranges used and associated input impedance were as follows:

- Range: 0-200 mV Impedance: 1000 megohms
- Range: 0-2 V Impedance: 100 megohms

Experimental Procedures

Specimen Assembly

A total of six specimens were prepared for each test. In selected tests additional specimens were prepared for use in potentiodynamic polarization tests. The following procedures were used for form preparation:

1. The PVC pipe and prestressing strand were cut to the specified length (Figure 0.3).
2. The strand spacer, which keeps the strand centered during grouting, was cut to the required diameter from a plastic reinforcing bar support. The two spacers were cut to fit snugly the inside diameter of the endcap and the inside diameter of the pipe, respectively.

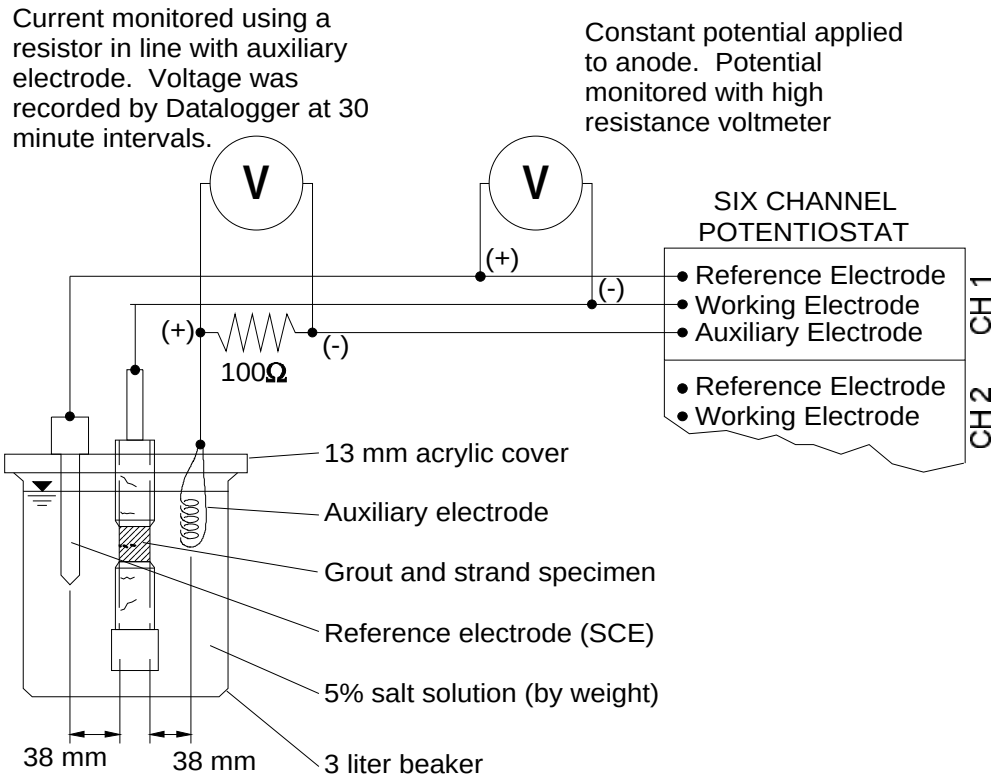

Figure 0.6 -Instrumentation for Anodic Polarization Test

3. Assembly consisted of inserting the spacer into the endcap and placing PVC solvent glue at the end of the pipe on the outside surface. Immediately after the glue was applied, the end of the pipe was inserted into the endcap and pushed tightly against the spacer at the bottom of the endcap.
4. The strand was then inserted in the form and pushed into the spacer in the endcap. To ease the installation, the ends of the strand were rounded slightly and the strand was twisted as it was pushed into the spacer.

Grouting

All specimens in a test were grouted at the same time from the same grout mix using the following procedures:

1. Water, cement and admixture quantities were measured by weight prior to initiation of mixing.
2. Approximately 1.9 l of grout was mixed in a 152-mm diameter x 305-mm long concrete cylinder mold using a high-shear mixing blade turning at approximately 1200 rpm.

3. The water was placed in the mixing container and the Sikament 300SC admixture was added. The mixer was started and the addition of the cement was started immediately thereafter. The cement was added slowly enough to allow thorough mixing to occur. Silica fume, when used, was blended with the cement prior to adding to the mixing water.
4. Following addition of the cement, any other admixtures to be used were added. Total mixing time was 2-3 minutes.
5. Following mixing the grout was then poured into the molds in three lifts. After pouring each lift, the exposed portion of the strand was moved briskly from side to side of the mold in order to remove as much air as possible from the grout.
6. Proportions, mixing time, and date were recorded. The specimens were then allowed to cure for 72 hours prior to the initiation of the corrosion test.

Precracking Grout

After the 72 hour curing period the grout in each specimen was flexurally precracked as is shown in Figure 0.7. The following procedures were used in precracking:

1. The specimen was placed in the frame and the bolt was tightened until cracks appeared. Cracks were visible under the transparent PVC.
2. The crack closest to the midspan of the specimen was “selected” and monitored with the portable microscope until a crack width of 0.13 mm was reached.
3. The load was held at that point while crack locations were marked on the surface of the pipe for future reference. The crack selected for exposure was marked so that the pipe was removed only in the area around it.
4. The crack locations were recorded relative to the end of the pipe for reference when the specimens were disassembled.
5. The bolt was loosened and the specimen removed from the frame. All of the six specimens were precracked within approximately thirty minutes.

Anodic Polarization

Immediately after precracking the following procedures were used to apply the anodic polarization:

1. A portion of the pipe in the area around the selected crack was carefully removed using the wire wheel attachment on a pedestal grinder. Care was taken to avoid damaging the surface of the grout after the wire wheel had cut through the pipe. Figure 0.8 shows a specimen after removal of the pipe section.

2. Immediately following removal of the pipe section, the exposed grout surface was covered tightly with a moist cloth to prevent drying shrinkage of the grout. The anodic polarization was initiated as soon as possible after the pipe had been removed.
3. Each specimen was immersed in the test cell as shown in Figure 0.6. The time of immersion and free corrosion potential were recorded.
4. The potentiostat was set to apply a potential of +600 mV_{SCE} to the working electrode. The potentiostat was then switched from "isolate" to "run" to initiate the anodic polarization immediately after the second free corrosion potential had been taken.
5. The potential between the reference electrode and the specimen was adjusted and monitored periodically with the bench multimeter. The leads were connected as shown in Figure 0.6. This minimized the possibility of ground loops harming the reference electrode. With this However, when the potentiostat was set to +600 mV_{SCE}, the multimeter read -600 mV.
6. The voltage across a 100 Ω resistor connected in line between the potentiostat and the auxiliary electrode was measured with the Datalogger. The corrosion current was then equal to the voltage divided by the resistance in accordance with Ohm's Law.
7. The anodic polarization was continued until a large increase in current was detected which indicated that the chloride ions had reached the surface of the strand.
8. The anodic polarization was terminated as soon as possible after the corrosion current reached the 300 to 500 mA range. This prevented severe corrosion from destroying the specimen.
9. The specimens were disassembled and visually examined to ensure that the corrosion only occurred at the base of the crack which was selected during precracking.

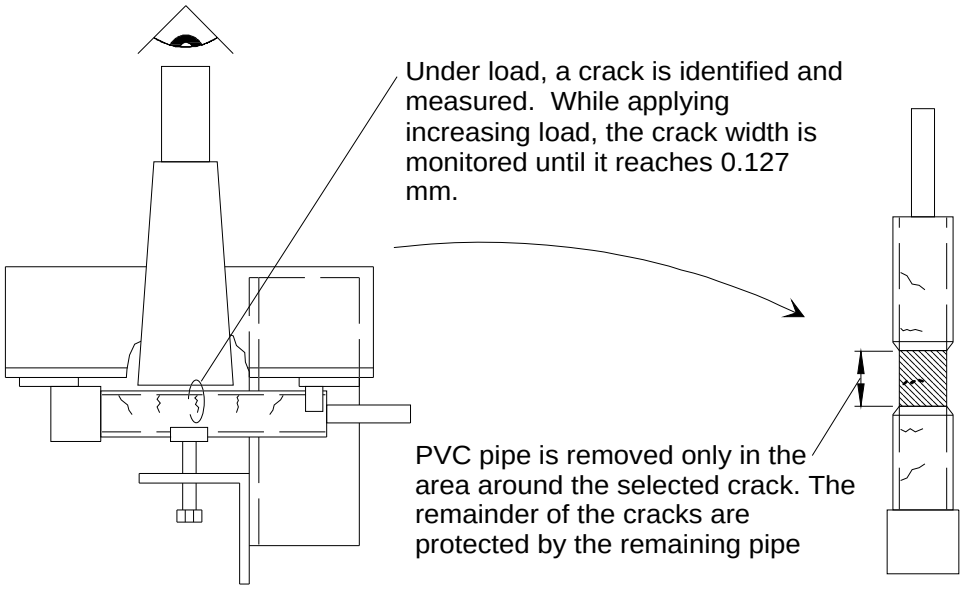

Picture of Cracking Grout

Figure 0.7 - Precracking of Grout and Removal of Pipe Prior to Initiation of Corrosion Test.

Specimens which had corrosion occur in air voids rather than in the selected crack were considered invalid.

10. The parameter used to compare the different grout mixes was the time-to-corrosion. This was defined as the time from initiation of the anodic polarization to the time when a large increase in corrosion current was noted.

Figure 0.8 - Specimen After Removal of Pipe, Ready for Corrosion Testing.

The anodic polarization tests were performed in a climate controlled room where the yearly average temperature was 23°C. About 90% of the time the temperature remained within 3°C of this average. Because the fluctuations were small, the effect of temperature change on the tests was neglected.

Potentiodynamic Tests

Potentiodynamic tests were conducted on selected mix designs which were also to be tested by the Modified ACTM. Table 0.4 shows the Modified ACTM tests in which the potentiodynamic test was also conducted. In these tests additional specimens were made beyond the 6 required to run the Modified ACTM. The additional specimens were made from the same grout that was used for the six specimens. The same equipment used in the Modified ACTM was used in the potentiodynamic tests with the following procedures:

1. Specimen construction and grouting were identical to the Modified ACTM.
2. The specimen was precracked (if required) and the sheathing was removed as in the Modified ACTM.
3. Thirty minutes after the specimen was placed in the test cell the free corrosion potential was taken and the potentiodynamic test was initiated.

4. The potentiostat was initially set at -250 mV_{SCE} to start the test and the potential was increased 50 mV_{SCE} every 15 minutes. The corrosion current was read at the end of the potential hold period for each increment of potential. The test was continued until a potential of +800 mV_{SCE} was reached at which time the test was terminated.
5. The specimen was then broken open and examined for traces of corrosion.

Specimen Variables

There were several variables present in the test series. Tests A through D used the specimen configuration shown in Figure 0.2(c) and the remainder of the specimens were tested with the final configuration (Figure 0.2(d)). Tests A through E used strand from Reel 1 while the remainder of the specimens were tested with strand from Reel 2. Test C was conducted on specimens in which a temporary corrosion protection (TCP) had been applied to the strand prior to grouting. The TCP was Dromus B, an emulsifiable oil manufactured by Shell Oil Company. In test G, a crack width of 0.076 mm was used to determine if a smaller crack width would reduce the scatter of the test results.

Table 0.4 - Summary of Variables in Test Series.

Test	Grout Mix Design	Specimen Configuration	Temporary Corrosion Protection	Crack Size (mm)	Strand*	Potentio-dynamic Test Conducted?
A	trial 1	3rd trial	none	0.13	Reel 1	no
B	26	3rd trial	none	0.13	Reel 1	no
C	27	3rd trial	Dromus B	0.13	Reel 1	no
D	19	3rd trial	none	0.13	Reel 1	yes
E	19	final	none	0.13	Reel 1	yes
F	26	final	none	0.13	Reel 2	yes
G	19	final	none	0.076	Reel 2	no
H	27	final	none	0.13	Reel 2	no
I	30	final	none	0.13	Reel 2	no
J	33	final	none	0.13	Reel 2	yes
K	19	final	none	0.13	Reel 2	no
L	2	final	none	0.13	Reel 2	no

* See Appendix D for strand chemical analysis

Data Presentation

Time-to-corrosion Plots

Results of each test consisted of the corrosion rate for each specimen, in terms of corrosion current, taken every 30 minutes. Each test produced six sets of data which were initially plotted in the form of corrosion current vs. time as shown in Figure 0.9 through Figure 0.12.

Ideally, every plot would contain six curves, one for each of the six specimens, with each curve being composed of two segments. The first segment would be the constant (and relatively low) corrosion rate of the strand in the alkaline environment of the grout prior to the chloride ions reaching the surface of the strand. Once the chloride ions reached the surface of the strand there would be a dramatic increase in the corrosion current which is defined as the "time-to-corrosion" and given the designation t_c. Time-to-corrosion is misleading because the strand is corroding throughout the duration of the test as evidenced by the small amount of corrosion current prior to initiation. The parameter being measured is actually the "time to a rapid increase in corrosion rate." However, for convenience this point will be referred to as time-to-corrosion.

The graphical format provided a convenient visual presentation of the data in which t_c can easily be interpreted as well as giving a visual indication of the degree of scatter for each test.

Tabulated Data

Three parameters which were deemed useful in the analysis were extracted from the test results: Time-to-Corrosion (t_c), Free Corrosion Potential (E_{corr}), and Average Current Density (i_{corr}).

Time-to-corrosion (t_c) is the time, measured in hours, required for a rapid increase in corrosion current to occur under anodic polarization. Corrosion current was taken at half-hour increments throughout the anodic polarization. Because the increase in corrosion current was so rapid it was possible to determine t_c to within the half-hour. These values are tabulated in Table 0.5. Also tabulated are average t_c values for all stations and for those stations having non-zero t_c values. Stations which had a t_c greater than 24 hours were defined as non-zero. Stations which had invalid tests were not included in either of the averages.

The free corrosion potential E_{corr} was read immediately after the specimen had been immersed in the test cell. E_{corr} readings are presented in Table 0.6 along with the averages of the stations which correspond to the stations used for averaging in Table 0.5

Figure 0.9 - Modified ACTM Results for Tests A, B, D.

Figure 0.10 - Modified ACTM Results for Tests E, F, G.

Figure 0.11 - Modified ACTM Results for Tests H, I, J.

Figure 0.12 - Modified ACTM Results for Tests K, L.

Table 0.5 - Summary of Times to Corrosion from Modified ACTM Tests.

Test	Time-to-corrosion (hours)*							
	Station						Average	Average
	1	2	3	4	5	6	All	Nonzero
A	248	329	216	255	313	n/v	262	262
B	0	0	0	193	151	156	129	143
C	0	0	0	0	0	0	0	0
D	3	95	91	0	128	136	86	72
E	129	4	107	159	101	0	88	74
F	102	2	45	99	126	89	89	87
G	0	99	159	9	201	4	95	102
H	176	170	71	88	n/v	156	105	105
I	197	188	150	206	90	213	165	165
J	189	0	123	190	0	233	133	119
K	107	0	138	144	n/v	188	158	163
L	144	316	30	320	4	116	118	118

n/v - not valid

*Nonzero stations are those with $t_c > 24$ hours.

Another parameter which proved to be useful in analyzing the data was gathered by taking an average of the corrosion current readings between the initiation of anodic polarization and time-to-corrosion, when the corrosion current is relatively steady. The current density was calculated by dividing the current by the exposed surface area of the outer six wires of the strand for the length of strand in contact with grout. These values are summarized in Table 0.7.

Potentiodynamic Plots

A total of six potentiodynamic tests were conducted. The results are presented in Figure 0.13 and are plotted in the form of potentiodynamic anodic polarization curves. Each curve is designated with a letter which corresponds to the Modified ACTM that the specimens came from. E and J are followed by numbers which indicates that there were two potentiodynamic tests conducted for those specimens. Corrosion current densities recorded at +600 mV_{SCE} are shown in Table 0.8. Variables for the potentiodynamic tests are also presented.

Analysis and Discussion

The first part of the discussion will focus on the effectiveness of the test method in evaluating corrosion protection properties of cracked grout. The second part of the discussion will focus on the selection of the grout mix which was used in the Large-Scale test series.

Table 0.6 - Summary of Free Corrosion Potentials from Modified ACTM Tests.

Test	Free Corrosion Potential (-mV_{SCE})							
	Station						Average	Average *
	1	2	3	4	5	6	All	Nonzero
A	173	193	200	193	179	n/v	191	191
B	206	200	229	195	209	207	210	208
C	256	220	258	202	213	215	221	218
D	206	209	227	209	209	214	214	211
E	199	205	216	199	205	199	205	206
F	217	225	236	208	218	210	218	220
G	202	219	233	205	209	211	214	209
H	200	215	223	234	n/v	212	223	223
I	197	231	274	201	253	212	235	235
J	188	203	211	191	201	207	203	206
K	203	199	200	204	n/v	203	203	202
L	202	217	220	197	204	211	208	208

n/v - not valid

* Non-zero stations are those with t_c > 24 hours.

Table 0.7 - Summary of Corrosion Currents from Modified ACTM Tests.

Test	Average Current Density ($\mu A/cm^2$)**							
	Station						Average	Average *
	1	2	3	4	5	6	All	Nonzero
A	2.90	5.37	4.48	2.91	2.69	n/v	3.36	3.36
B	0	0	0	5.27	6.60	6.13	4.68	5.41
C	0	0	0	0	0	0	6	5
D	0	7.03	8.84	0	6.50	6.35	5.11	3.87
E	4.60	0	8.57	5.35	4.94	0	4.68	4.55
F	2.07	0	9.28	5.01	5.59	5.99	6.54	6.85
G	0	4.00	4.51	0	2.66	0	1.73	1.46
H	3.76	5.19	8.32	5.26	n/v	4.02	5.87	5.87
I	1.81	4.62	5.12	1.51	2.93	2.32	2.97	2.97
J	2.30	10.6	4.95	2.26	0	2.59	2.47	2.52
K	2.92	0	3.26	2.70	n/v	2.18	2.72	2.72
L	2.25	2.24	5.83	1.93	0	3.19	2.74	2.74

n/v - not valid

* Non-zero stations are those with t_c > 24 hours.

** Average current density prior to t_c.

Data Scatter

Theoretically, all the specimens in a single test should have the same time-to-corrosion. However, when examining the results in Table 0.5, it can be seen that the there was a large variability in the time-to-corrosion. For example, test J had a minimum t_c of 0 and a maximum of 233 hours with an average of 123 hours. To minimize the variability, all specimens in a given test were prepared from the same grout mix, used strand from the same reel, were cured for the same time period, and were anodically polarized at the same time. There was probably some variability introduced by the testing and data acquisition equipment. However, it is not expected that these would contribute substantially.

Table 0.8 - Potentiodynamic Tests Conditions

Test	Grout Mix Design	Specimen Configuration	Pre-cracked?	Age** (days)	Time After Immersion* (days)	i_{corr} at 600 mV_{SCE} ($\mu A/cm^2$)
D1	19	3rd trial	No	7	0	4.57
E1	19	final	Yes	3	0	7.50
E2	19	final	Yes	10	7	3.76
F1	26	final	Yes	?	0	4.85
J1	33	final	Yes	4	0	4.05
J2	33	final	Yes	4	0	2.27

* Time between immersion in test cell and initiation of test.
** Age of grout at time of test..

One probable contributor to the data scatter was the surface condition of the strand. Variations in the surface condition of the strands may cause differences in how tightly the crack is closed after precracking. This theory is supported by the results of test C in which the strands were coated with an oil prior to grouting. In that test, all of the specimens had a rapid increase in the corrosion rate immediately after anodic polarization was initiated (that is tc ≈ 0). There were no other tests which had $t_c \approx 0$ on all six stations and in none of the other tests was oil used on the strands prior to grouting. It appears that the oil was responsible for drastically reduced the protective properties of the grout in the cracked condition. After the specimens were flexurally precracked and the load was removed, the flexural stiffness of the strand should return the specimen to its original shape and thus close any grout cracks which may be present Under these conditions, how tightly the cracks close is directly related to the measure of adhesion between the strand and grout. If the adhesion is reduced or eliminated, then the crack may not close as tightly; thus, allowing chlorides to penetrate to the surface of the strand almost immediately.

This behavior can be taken a step further to explain the scatter in the other test results. The production of prestressing strand generally requires the use of a lubricant to facilitate the pulling and stranding operations. It is possible that a variation in the amount of lubricant along the length of strand on a particular reel is enough to cause significant differences in the adhesion between specimens in the same test. This would explain the large differences in t_c between specimens in the same test. However, this is contradicted by the results of the original ACTM tests on uncracked specimens shown in Table 0.1. These results have a wide scatter among specimens in the same test even in the uncracked condition which indicates that there may be other factors causing the variability.

Rating of Grout Mixes

Table 0.5 presents two sets of averages for each test. The first average is for the stations which are valid. The second average is for stations which are non-zero. Non-zero stations are defined as stations which have a t_c greater than 24 hours. Based on the results of test C it was

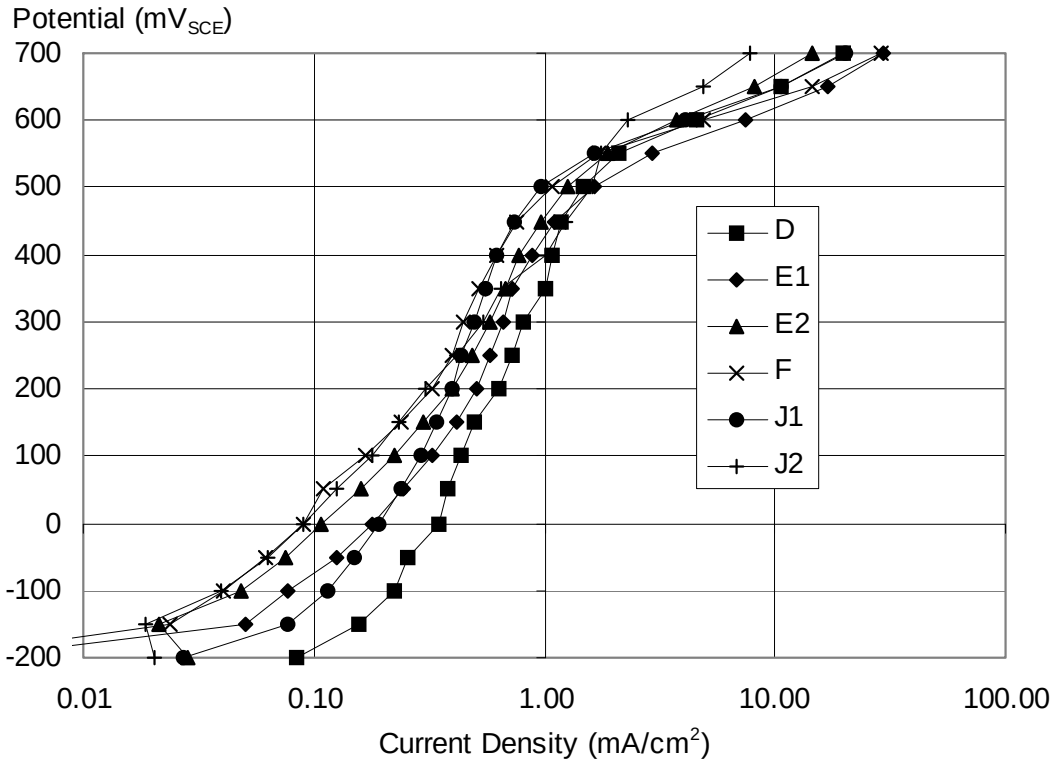

Figure 0.13 - Potentiodynamic Anodic Polarization Curves for Selected Specimens from Modified ACTM Tests.

decided that a t_c close to zero indicated that the crack was probably not fully closed and should be considered an invalid station. As a result, each grout mix was rated on the basis of the average of the non-zero t_c value.

One of the major objectives of this test series was to determine which of the grout mixes 26, 27 or 33 (Table 0.3) gave the best improvement in corrosion protection in the Modified ACTM test. Using the average time-to-corrosion of the non-zero stations the following summarizes the relative level of performance of each of the grout mixes:

(1) No additives (Modified ACTM Test L/Grout mix 2)
t_c = 185 hours.
(2) 300SC (Average of Modified ACTM Tests D, E, K/Grout mix 19)
t_c = 127 hours.
(3) 300SC + Calcium Nitrite (Modified ACTM Test F/Grout mix 26)
t_c = 92 hours.
(4) 300SC + Rheocrete 222 (Modified ACTM Test H/Grout mix 27)
t_c = 132 hours.
(5) 300SC + Silica Fume (Modified ACTM Test J/Grout mix 33)
t_c = 184 hours.

When comparing (1) and (2) it is apparent that the addition of the thixotropic admixture to the grout reduces the ability of the grout to provide corrosion protection in the cracked condition by approximately 30%. It would seem prudent to eliminate the use of the anti-bleed admixture. However, as was discussed in Chapter Five, the use of the anti-bleed admixture was deemed necessary for the proper placement of the grout. Specifically, to reduce the probability that bleed lenses will form. The water/cement ratio of concrete provides a convenient analogy to illustrate this point. It has been shown that as the water/cement ratio is decreased the chloride permeability is decreased. Therefore, for bridge decks where deicing salts will be applied, the amount of water used in the mix should be at the minimum required for complete hydration of the cement. However, additional water must be added to allow proper placement of the concrete. Thus, some sacrifice is made in the permeability of the concrete to allow proper placement. The same can be said for the grout mix design incorporating the anti-bleed admixture (2).

Additives were then used to improve the performance of the grouts relative to the corrosion protection provided by the basic grout mix with anti-bleed admixture (2). Calcium nitrite (3) actually decreased the time-to-corrosion of the grout by 27% when compared to the basic grout mix

(2). Both Rheocrete 222 (4) and Silica Fume (5) improved the performance of the grout in these tests by 4% and 45% respectively when compared to the performance of the basic grout mix (2). Clearly, the silica fume mix provided the best performance in these tests and was the mix selected for use in the large-scale test specimen LS-5.

Trends

There were no significant trends noted in the free corrosion potential readings. The high and low average readings were -188 and -228 mV_{SCE}, respectively, while the range was generally between -199 and -220 mV_{SCE}. The corrosion potential of passivated steel in sound concrete may vary over a wide range from +200 mV to -700 mV_{SCE}. However, typically this range is between +100 mV and -200 mV_{SCE}.[99] The free corrosion potentials of the Modified ACTM were at the lower end of this range

The average corrosion rates varied significantly from test to test with a range of 3.67 to 7.18 $\mu A/cm^2$. There is some degree of correlation between the corrosion current and time-to-corrosion when the data from tests E through L are compared in Figure 0.14. Note that the test results are placed in order of increasing t_c from left to right of the chart. Figure 0.14(a) shows no distinguishable trend in free corrosion potential relative to the time-to-corrosion. However, there is a rough downward trend in the average corrosion rate as the time-to-corrosion is increasing (Figure 0.14 (b)).

This may be an indication of the effect of IR drop. The low ohmic resistance calcium nitrite grout (test F) is located to the left of the chart indicating a lower time-to-corrosion. The higher ohmic resistance grouts (those with no admixtures and those with silica fume) are located to the right of the chart indicating a higher time-to-corrosion. The chart indicates that the lower ohmic resistance grouts had a higher corrosion current prior to tc while the grouts with higher ohmic resistance had a lower corrosion current. This can be explained by the higher effective polarization at the surface of the strand (due to the low ohmic resistance of the grout).

Crack Width Adjustment

The crack width was reduced to 0.0762 mm in test G to determine if the scatter could be reduced. As can be seen in Table 0.5 there was no apparent reduction in scatter. In fact, the data

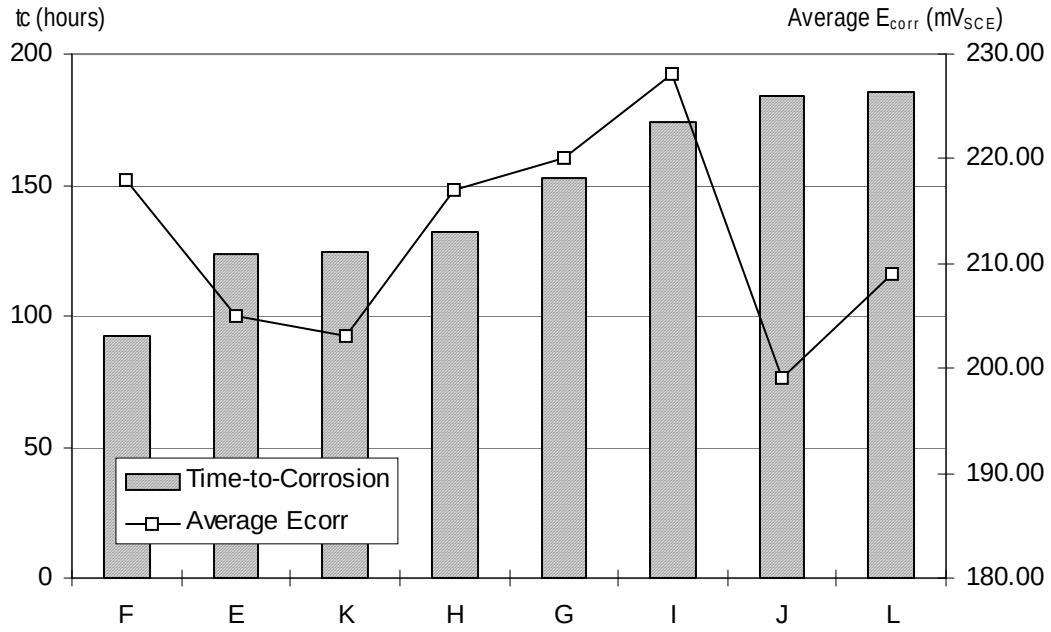

(a) Comparison with Average Free Corrosion Potential

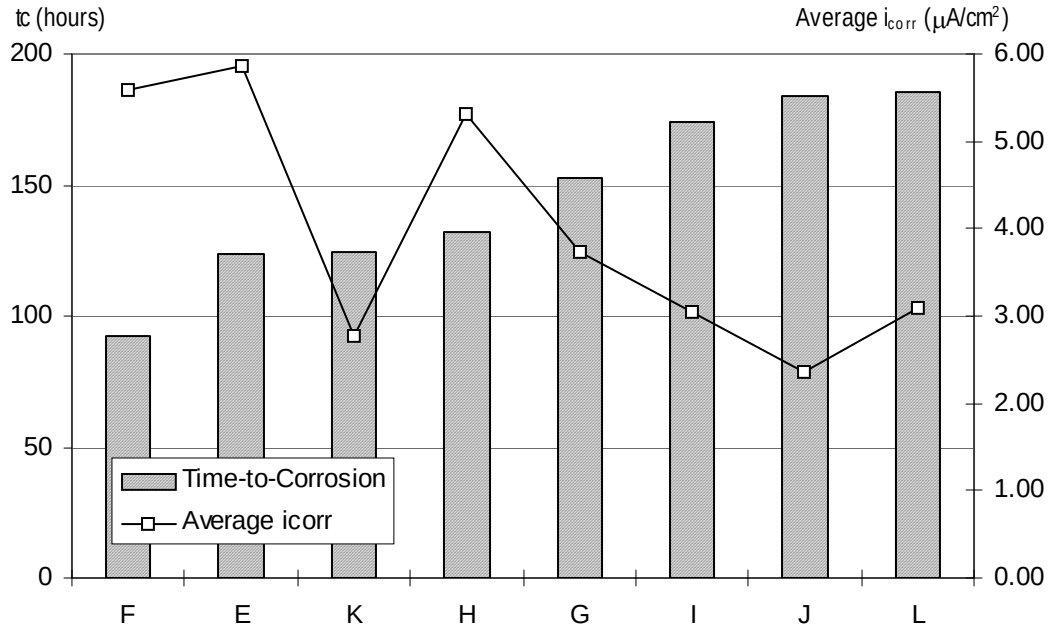

(b) Comparison with Average Corrosion Current

Figure 0.14 - Correlation of Time-to-Corrosion with Free Corrosion Potential and Corrosion Current.

appears to have an increased scatter. The t_c minimum is 0 and maximum is 201 hours with an average of 79 hours.

Potentiodynamic Tests

Theoretically, if there were significant differences in the ohmic resistances of the grouts used in the potentiodynamic test, then the polarized potential at the steel/grout interface would be proportionately different between each grout. If a potentiodynamic test was conducted on a high ohmic resistance grout, the polarization curve would be shifted to the left as shown in Figure 0.15. Conversely, if the same test was conducted on a low ohmic resistance grout then the curve would be shifted to the right. This is assuming that all other test conditions are identical.

The reason is that the potential plotted on the y-axis is the set potential of the potentiostat (E_{set}) which is controlled by the potential sensed at the reference electrode. The actual polarization level at the surface of strand is a function of the grout ohmic resistivity. This results in a high resistance grout ($i_{H\text{-}\Omega}$) having a lower corrosion current than a low resistance grout ($i_{L\text{-}\Omega}$) for a particular E_{set}.

However, this behavior is not reflected in the experimental polarization curves shown in Figure 0.13. In fact, the corrosion currents in the experimental curves are grouped reasonably closely together in the region of potential used in the anodic polarization tests (+600 mV_{SCE}). The corrosion currents for the different grouts at the set potential of +600 mV_{SCE} are shown in Table 0.8. The two values for the silica fume grout (J1 and J2) are 4.05 and 2.27 $\mu A/cm^2$ while the value for the calcium nitrite grout (F1) is 4.85 $\mu A/cm^2$. The calcium nitrite corrosion current is higher than both of the silica fume grouts as would be expected. However, corrosion currents for D1, E1, and E2 are 4.57, 7.50, and 3.76 $\mu A/cm^2$, respectively. Corrosion current of E1 is much higher than that of the calcium nitrite grout, which contradicts the above hypothesis; while the corrosion currents for D1 and E1 are less than that of the calcium nitrite which agrees with the theory.

Conclusions

The Modified Accelerated Corrosion Test Method was used to test the durability of several grout mix designs. The grout was placed around a seven-wire prestressing strand using a PVC mold. After curing the grout was flexurally precracked and a section of the pipe was removed, exposing the resulting crack. The specimen was then immersed in a 5% salt solution and anodically polarized at +600 mV_{SCE}. This accelerated the migration of the chlorides through the exposed crack in the grout to the surface of the steel to initiate corrosion. The time necessary for the chlorides to penetrate the grout was deemed time-to-corrosion. The times-to-corrosion of grouts with various admixtures were compared and ranked. The following findings were made:

- The optimum anti-bleed grout developed in Chapter Five (w/c = 0.40 and 2.2% Sikament 300SC) had a time-to-corrosion 30% less than that of a standard grout (w/c = 0.40 and no admixtures). Based on these results it can be concluded that the use of Sikament 300SC can reduce the effectiveness of cracked grout in providing corrosion protection.
- The use of calcium nitrite reduced the effectiveness of cracked grout in providing corrosion protection. The reduction in time-to-corrosion was 27 percent.
- The use of Rheocrete 222 improved the effectiveness of cracked grout in providing corrosion protection. The increase in time-to-corrosion was 4 %, which is not significant considering the scatter of the data.
- The use of silica fume improved the effectiveness of cracked grout in providing corrosion protection. The increase in time-to-corrosion was 45 percent. The silica fume mix was selected and used in the "improved grout" specimen (LS-5) in the large-scale tests reported in Chapters 8 and 9.
- Other researchers have documented that the ohmic resistance of concrete can vary widely depending on the types of admixtures used. Calcium nitrite can cause a reduction in ohmic resistance while silica fume can cause a large increase in ohmic resistance. It has been shown here that, theoretically, this should cause the anodic polarization tests to give

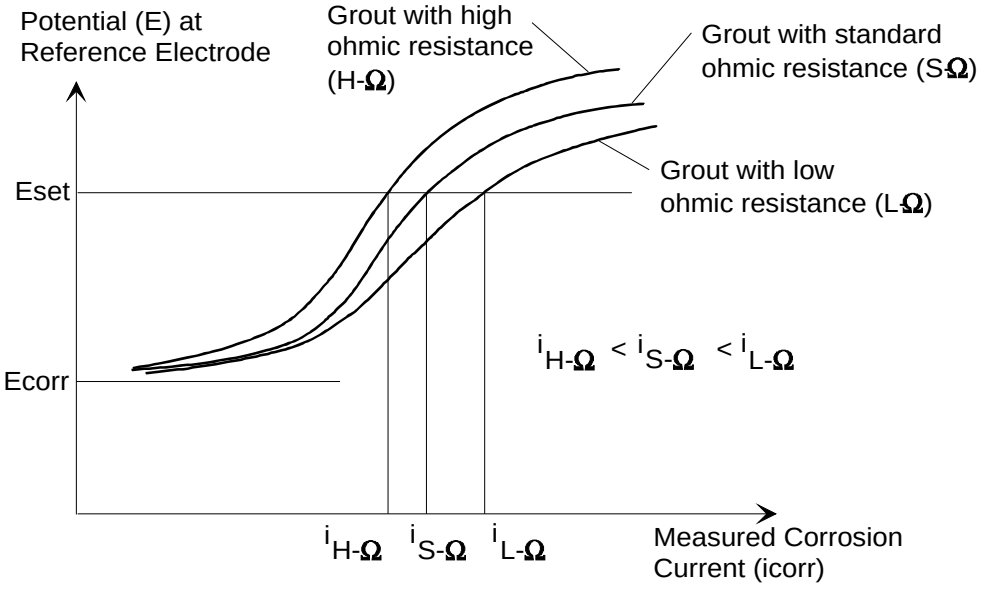

Figure 0.15 - Hypothetical Polarization of Grouts with Significant Differences in Ohmic Resistances.

skewed results. To investigate this possibility, several potentiodynamic tests were conducted. There was no strong indication from these tests that would indicate an effect from grout ohmic resistance. However, average corrosion currents recorded prior to the time-to-corrosion indicated that there may be some effect from the difference in polarization. No conclusion can be drawn at this point. Further investigation with more sophisticated equipment is required.

Chapter Seven
Large-Scale Test Series:
Assembly, Grout Injection, and Load Tests

7.1 Test Concept and Objectives

In the survey presented in Chapter Four, it was found that the average life which the surveyed bridge owners expected from the stay cables on their bridges was approximately 75 years. This presents a dilemma when designing a relatively short-time experimental program which is intended to test the durability of a bridge stay cable. Static and fatigue loading can be simulated in the laboratory in such a way as to mimic, reasonably well, the critical load effects which the structure might experience in its lifetime. However, durability is very much a time related and site specific characteristic. Ambient temperature, thermal heating, precipitation, humidity and pollutants all combine to "load" the structure in a very complex and little understood manner. To develop a test which directly addresses all of these areas is not economically feasible or, considering the extremely long time duration, not even technologically desirable.

Accelerated corrosion tests have been developed which can provide a basis with which to select corrosion resistant materials for long term use without having tested them for the expected life of the structure. One example of this is the macrocell test which is designed to represent corrosion of reinforcement in a concrete bridge deck. The macrocell specimen is constructed to represent a small section of bridge deck and is then ponded with salt water in wet/dry cycles to represent the application of deicing salts, but in a much accelerated manner.

The objective in designing the accelerated stay cable corrosion test was to identify a realistic but severe corrosion mechanism, somewhat similar to the macrocell test, by which the cable could be tested in a reasonable amount of time. Another objective was to have a test which included the entire stay system and not just one single aspect or element of the stay. The final objective was to have the test conditions in the laboratory simulate the actual field conditions as closely as possible.

The test program was divided into two groups of tests. The first group of tests focused on the performance of the "two-barrier system." This is the configuration which provides essentially two layers of protection: the PE sheathing and the portland cement (pc) grout. PE pipe, when intact, provides an excellent barrier to moisture. However, it has been documented that some bridges in service have developed cracks or breaks in the PE sheathing. Consequently, it was decided that the

protection provided by the pc grout after a local break in the PE sheath would be the focus of the accelerated corrosion tests. Small local openings were made in the sheathing (to simulate accidental breaks) of each specimen and salt solution was ponded on the exposed grout surface in wet/dry cycles. Application of the salt solution represents an accelerated version of the intrusion of airborne chlorides which would occur on a bridge near the seacoast or in a region where heavy applications of deicing salts are used.

The second group of tests focused on improving the corrosion protection system tested in the first group. Individual barriers were added to the strands in several of the specimens. In addition, a silica fume grout was used in one of the specimens in an attempt to improve the performance of the grout.

7.2 Selection of Specimens

As discussed previously, the large scale tests were divided into two groups. The first group was composed of four specimens. All of the specimens were constructed using bare prestressing strand and using the basic anti-bleed grout mix reported in Chapter Five. The second set of tests was also composed of four specimens. The first specimen of the group had bare strand and used the anti-bleed silica fume grout reported in Chapters Five and Six. The remainder of the specimens had individual protection applied to each of the strands. The eight test specimens were as follows:

- LS-1: Bare strand. No additional load applied during corrosion test
- LS-2: Bare strand
- LS-3: Bare strand coated with temporary corrosion protection (TCP) prior to grouting. No additional load applied during corrosion test
- LS-4: Bare strand coated with TCP prior to grouting
- LS-5: Bare strand coated with TCP prior to grouting. Grout improved through the addition of silica fume.
- LS-6: Epoxy-coated strand.
- LS-7: Galvanized strand.
- LS-8: Greased and sheathed strand.

7.3 Test Procedure

A graphical summary of the test program is shown in Figure 7.1. Note that the test program can be divided into five major steps:

1. Assembly and Stressing

2. Grout Injection
3. Lateral and Axial Load Testing (not performed on LS-1 and 3)
4. Accelerated Corrosion Test
5. Post-mortem Examination

Because of the complexity of the tests and the large volume of data generated, the presentation of the large scale tests is divided into three chapters. This chapter covers the construction details and procedures for steps 1 through 3. Problems that were encountered during these steps are discussed in the related sections. The results for each step are presented in the associated section along with any discussion. Preliminary analytical estimates made for the load tests are presented in the section which covers step 3. Conclusions for steps 1 through 3 are made at the end of this chapter.

Chapter Eight covers the remainder of the experimental work including the procedures, problems and results associated with the accelerated corrosion tests and post-mortem examinations. Chapter Nine is composed of the analysis, discussion and conclusions associated with the accelerated corrosion portion of the test.

7.4 Specimen Design

7.4.1 Configuration

Each stay specimen was constructed with twelve 12.7-mm diameter seven-wire strands, each with a guaranteed ultimate tensile strength of 1860 MPa. The strand bundle was placed inside transparent sheathing to aid in visual observation of grouting and corrosion tests. The stay specimen configuration is shown in Figure 7.2. Transparent extruded acrylic tube was used in the transition lengths while transparent PVC was used for the free length.

7.4.2 Initial Stress

Cable-stayed structures are by necessity constructed in stages. These stages usually require that the complete bridge be constructed and the alignment set before the blocking agent can be injected into the stay sheathing. This results in a configuration, in the absence of live load, in which the stress in the main tension elements is equal to the permanent loads and stresses locked

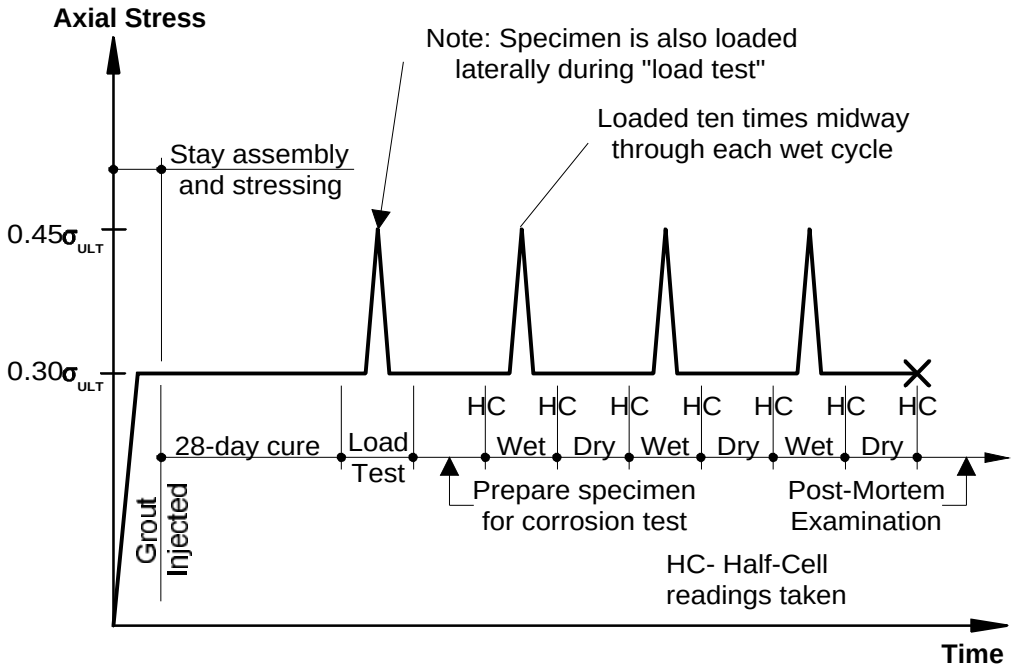

Test History for Specimens LS-2, 4, 5, 6, 7, and 8.

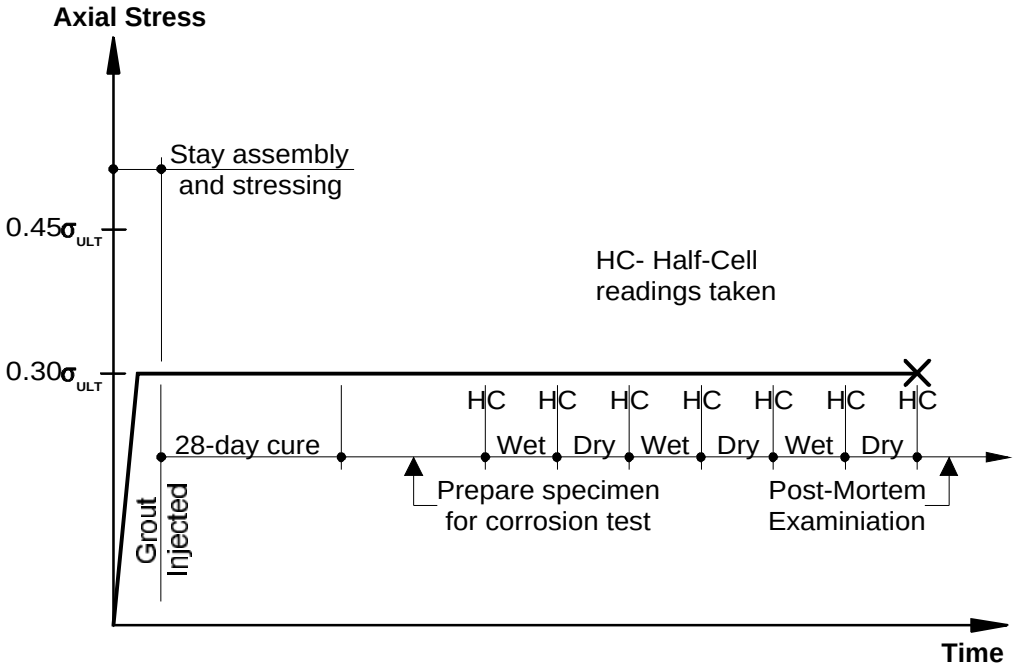

Test History for Specimens LS-1 and 3.

Figure 7.1 - Summary of Test History of Large Scale Specimens.

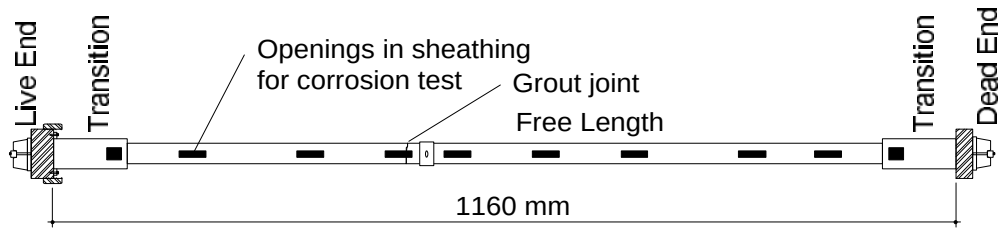

Figure 7.2 - Stay Specimen Schematic.

into the structure prior to injection. The blocking agent does not experience this stress because it is injected after the bridge is in its final form. Live load and other applied load stresses induced after completion of the construction of the bridge are then applied to both the main tension element and the blocking agent. As a result, it was necessary to develop a reasonable minimum or "dead load" stress to which the stay cable specimens would be subjected during the test procedures. Dead load stresses in actual bridges can vary widely depending on the intensity of the live load. This can also be examined from a live load/dead load perspective. Walther et al.[125] suggest:

$$\eta = \frac{q}{g}$$

q = *Distributed live load*

g = *Self-weight and permanent loads*

Where:

η =*0.2 - 0.3 for concrete highway bridge*

1.0 - 2.0 for steel railway bridge

These are essentially the extreme limits for live load to dead load ratios that might be found in practice for this type of construction. Looking at the lower and upper values of η, g would range from $0.37\sigma_{ULT}$ to $0.15\sigma_{ULT}$. Somewhat arbitrarily, a value of η= 0.5 was selected so as to give a value of g about 2/3 of the way towards the upper part of the stress range. Post-Tensioning Institute *Recommendations for Stay Cable Design, Testing and Installation* suggests that the dead load plus live load allowable axial stress in the stay be limited to 45% of the guaranteed ultimate tensile strength.[28] Therefore:

$$g + q = 0.45\sigma_{ULT}$$

Substitute $g\eta = q$

$$g + g\eta = 0.45\sigma_{ULT}$$

$$g = \left(\frac{0.45}{\eta + 1}\right)\sigma_{ULT}$$

For $\eta = 0.5$

$$g = 0.30\sigma_{ULT}$$

This procedure gives the "dead load" stress minimum level for the specimens during the testing period. For a twelve strand stay this results in the following loads:

$$F_{ULT} = \sigma_{ULT} A_S = (12)(98.7\ mm^2)(1860\ MPa)\left(\frac{kN/10^3\ mm^2}{MPa}\right) = 2200\ kN$$

$$Dead + Live\ Load: g + q = 0.45\left(F_{ULT}\right) = 990\ kN$$

$$g + 0.5g = 1.5g = 990\ kN$$

$$Dead\ Load: g = 660\ kN = 0.30\left(F_{ULT}\right)$$

7.4.3 Prestressing Strand

7.4.3.1 Bare Strand (LS-1 through LS-5)

Prestressing strand used for specimens LS-1 through LS-5 was 12.7-mm diameter seven-wire low-relaxation strand with a guaranteed ultimate tensile strength of 1860 MPa and met ASTM A416-90A (reel 1) and A416-93 (reel 2). Mill certificates and chemical analyses for the strand are included in Appendix B. The strand from reel 1 was used in specimens LS-1 through LS-4 and the strand from reel 2 was used in specimen LS-5.

7.4.3.2 Epoxy-Coated Strand (LS-6)

Epoxy-coated strand was obtained from Florida Wire and Cable, Inc. for use in specimen LS-6. The strand was 12.7-mm diameter seven-wire low-relaxation strand with a guaranteed ultimate tensile strength of 1860 MPa and met the requirements of ASTM A416-90A. Two types of epoxy-coated strand were used in the specimen. *Flo-Gard* and *Flo-Fil Gard* are trade names for the strand used in the specimens. As discussed in Section 3.7.2, Flo-Gard strand only has coating applied to the external periphery of the strands. In the Flo-Fil Gard the interstitial spaces between the wires are filled with epoxy in addition to the external periphery coating.

7.4.3.3 Galvanized Strand (LS-7)

While the Federal Highway Administration does not currently allow the use of galvanized strand in the United States, it has been successfully used in Europe.[96] As discussed in Chapter Two there has been concern about the use of galvanized strand in contact with concrete or portland cement-based grouts because of the potential for hydrogen embrittlement. However, it was felt that there is not enough evidence available to preclude the use of galvanized strand in concrete or grout so it was selected as one of the variables.

Because of the lack of demand for galvanized strand in the US there is no strand available for structural applications. Florida Wire and Cable, Inc. produces a 1860 MPa galvanized strand (see Figure 7.3) which is generally used as barrier cable in parking garages and other miscellaneous applications. The wire is originally drawn to approximately 2070 MPa, cleaned chemically and then hot-dip galvanized. The heat from the molten zinc reduces the strength of the wire to 1860 MPa. The galvanized wire is then stranded to the final configuration. It should be noted that the strand is stress-relieved but is not low-relaxation. The strand will relax under load because there is a layer of soft zinc between the outer wires and the center wire. This zinc will yield when the strands are tensioned causing a net elongation under constant load. It is not intended or recommended that this particular manufacturing process be used to manufacture galvanized strand for use in stay cables. The intent in these tests was to test the performance of the zinc coating for providing protection to the strands under accelerated corrosion conditions. Due to the lack of availability of appropriate galvanized strand for use in these tests, this product was selected. Fatigue resistance of this strand was not tested nor was its susceptibility to hydrogen embrittlement or stress corrosion cracking examined.

7.4.3.4 Greased and Sheathed Strand (LS-8)

Greased and sheathed strand over the years has been used almost exclusively in parking and office structures. However, in recent years VSL and Freyssinet have been marketing a greased and sheathed strand system for their stay cables. VSL uses a system which incorporates a bare strand coated with a lubricating grease with "wire cable rust and corrosion inhibition additives." A tightly fitting high-density polyethylene sheath is then extruded over the strand. Freyssinet uses a strand which is similar except that a petroleum wax is used instead of a grease and the strand is galvanized before the wax and sheathing are applied. These systems are discussed in more detail in Chapter Three.

Although greased (or waxed) and sheathed strands have not been used in any cable-stayed bridges constructed to date in the United States, their use has become popular in other countries in recent years.

The greased and sheathed strand used in these tests was provided by VSL Corporation (see Figure 7.4). The greased and sheathed strand is discussed in more detail in Chapter Three.

Figure 7.3 - Galvanized Strand.

Figure 7.4 - Greased and Sheathed Strand Used in Specimen LS-8.

7.4.4 Anchorages

Because of the special requirements of the test program, the anchorages needed for testing were not available as standard prestressing items and had to be specially fabricated. Some mechanism was required so that the stay stress could be adjusted to the correct level prior to grout injection. While this could have been accomplished by stressing individual strands, the application of additional axial stress was also necessary after the grout was injected and cured. This precluded the stressing of individual strands. As a result, an anchorage system had to be devised which allowed the stay specimen to be stressed as a unit. The resulting anchorage system was composed of two different style anchor heads designated as *Live End* and *Dead End*.

7.4.4.1 Live End

The live end anchor head was 203-mm diameter x 102-mm thick and was provided with ACME threads for the full thickness (Figure 7.5). Additional thickness over the standard anchor head size was required so that there was sufficient space for the ring nut and the threaded coupling used for stressing the stay. The ring nut was provided in the place of shims to allow better control over the stress in the specimen. It also allowed the additional stress to be added without having to secure the shims in place. A standard off-the-shelf grout cap was used to cover the exposed ends of the strands and to aid in the grout injection. The grout cap was provided with rubber gaskets and holes tapped for NPT piping.

The strands were secured to the anchor head with standard two piece wedges which were drawn into the beveled holes machined into the anchor head. The strand pattern is shown in Figure 7.6. Specimen LS-6 (epoxy-coated strand) required the use of special wedges. To preserve the effectiveness of the epoxy, special wedges are used so that the epoxy does not have to be removed in the anchor head region. The special wedges are manufactured with deeper teeth than standard wedges (Figure 7.7) which allows the teeth to penetrate the epoxy and grip the underlying strand. The standard teeth only grip the surface of the epoxy and do not provide an effective connection.

The acrylic sheathing shown in Figure 7.5 was attached to the anchor head using 12.7-mm acrylic flat stock fabricated into a flange. The flange was machined to fit snugly on the outside diameter of the transition sheathing and was attached with solvent glue. The flange was then bolted directly to the anchor head during assembly of the stay. Silicone sealant was placed in the flange-anchor head interface to prevent grout leakage.

The anchor plate provided the bearing surface for the ring nut and also transferred the anchor head load to the heavy channels at the end of the reaction frame. The anchor plate used with reaction frame F1 had a thickness of 102 mm while the anchor plates for the remainder of the reaction frames had a thickness of 76 mm.

Specimen LS-8 (Greased and sheathed) required special fittings for the anchor head. The sheathing was not continued through the anchor head to the wedges, but was terminated just prior to the anchor head. The sheathing was then sealed against the anchor head to prevent the grout from entering the anchorage region. For each strand a 12.7-mm diameter (nominal) schedule 40 PVC pipe was inserted into the anchor head as shown in Figure 7.8. The anchor head was drilled

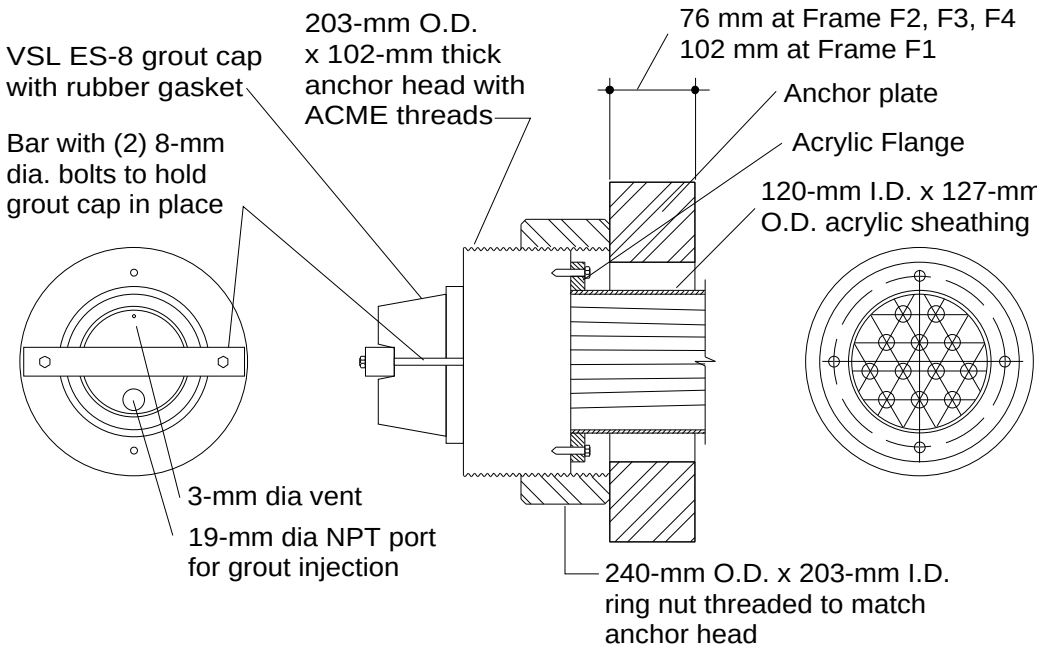

(a) Live End Anchorage Schematic.

(a) Live End Anchor Head and Transition Sheathing.

Figure 7.5 - Detail of Live End Anchorage.

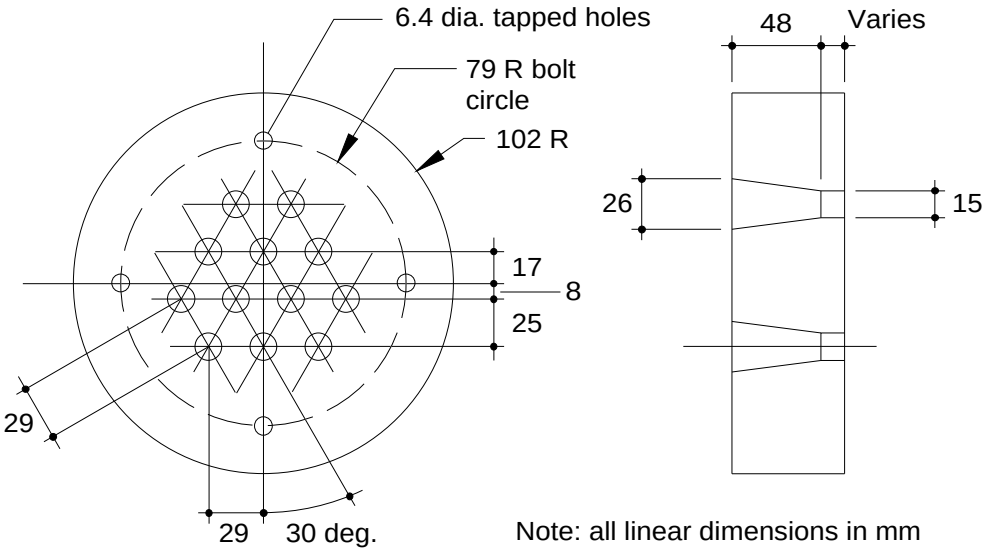

Figure 7.6 - Detail of Strand Pattern in Dead and Live Anchor Heads.

Figure 7.7 - Special Wedges for Epoxy-Coated Strand.

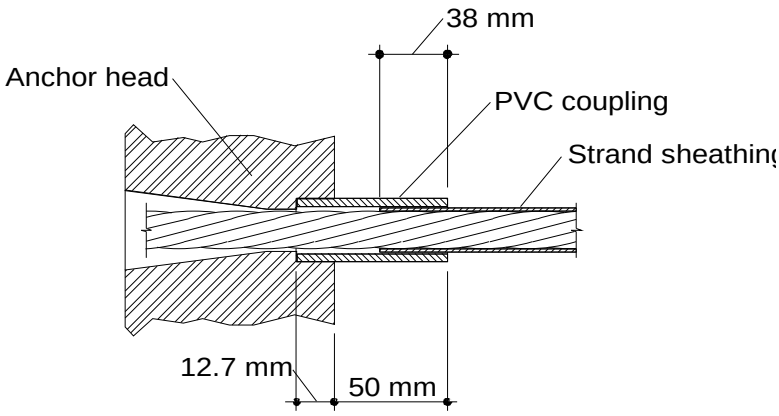

(a) Detail of Sheathing to Anchor Head Coupling.

(b) Installation of LS-8 Anchor Head.

Figure 7.8 - Detail of Anchor Seal for LS-8 (Greased and Sheathed).

and tapped to accept the threaded PVC pipe. Sealant was then applied to the sheathing during assembly to provide the seal between the sheath and the pipe insert.

7.4.4.2 Dead End

The dead end anchorage shown in Figure 7.9 utilized a 203-mm diameter by 60-mm thick anchor head. Drilled and tapped holes were provided to attach the grout cap to the anchor head.

Special wedges were also used for the epoxy-coated strand. In addition, provisions similar to those used at the live end were used for sealing the sheathing of the greased and sheathed strand against the anchor head.

Anchor plates under the dead end were the same thickness as provided for live end. The anchor plates were fabricated as shown in Figure 7.9 to hold the transition sheathing against the anchor head. A 25-mm long slice of acrylic tube was solvent welded onto the outside diameter of the transition sheathing flush with the end. The anchor plate was fabricated in two pieces. The 25-mm thick segment was fabricated to match the retainer ring while the second segment was fabricated to match the outside diameter of the transition sheathing. The anchor plate with the smaller diameter clenched the retainer ring against the backside of the anchor head. Sealant was applied to the interface between the anchor head and sheathing to provide a leak proof seal.

7.4.5 Deviator Rings

The deviator ring gathered the strands into a tight bundle for the free length and also adjusted the sheathing diameter (Figure 7.10). The deviator rings were fabricated from 25 mm flat-stock ASTM A36 grade 50 steel plate. The deviator ring was held in place by a fabricated PVC pipe flange and was connected with four bolts. The PVC flange was connected to the free length sheathing with PVC solvent glue. The deviator/flange assembly was fabricated to fit snugly inside the transition sheathing. An O-ring was placed in the chamfers between the deviator ring and flange to provide a leak proof joint.

7.4.6 Sheathing

In practice the sheathing provides two functions for the stay cable. It provides a continuous external barrier to the corrosive elements. In addition, the sheathing acts as a conduit which retains the grout as it is injected. In these tests, the sheathing is only acting as a conduit for the grout. It is necessary that the sheathing be sufficiently leak proof from end to end of the stay to retain the grout until it has set. Figure 7.11 shows the layout of the specimen sheathing. The transition length was composed of 120-mm inside diameter extruded transparent acrylic tube while the free length sheathing was composed of 76-mm inside diameter, transparent PVC pipe. Because

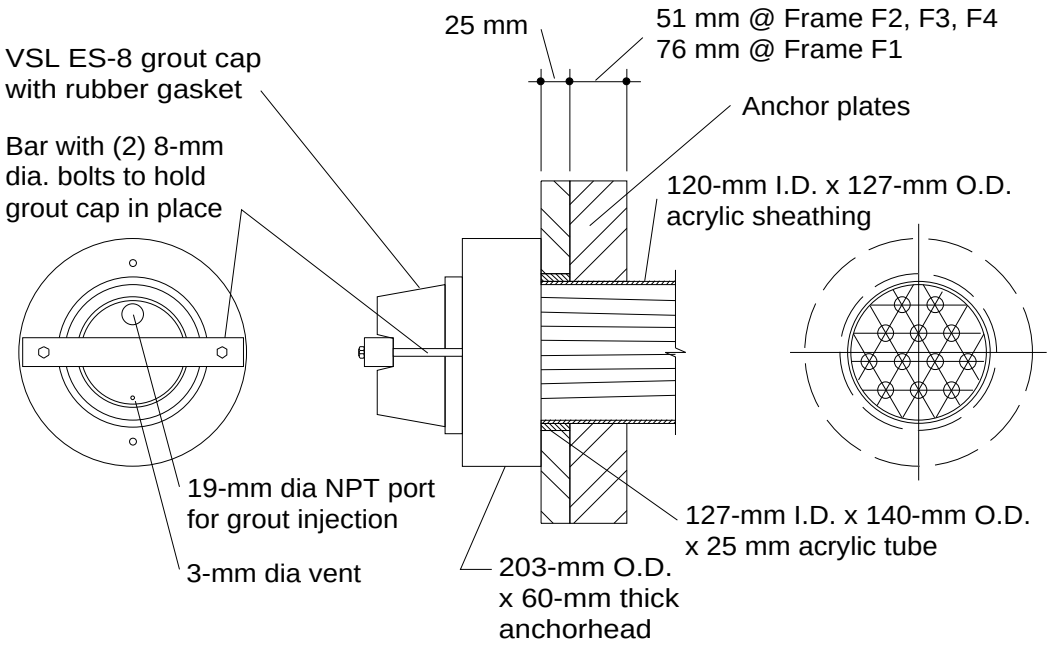

(a) Dead End Anchorage Schematic.

(a) Dead End Anchor Head and Transition Sheathing.

Figure 7.9 - Detail of Dead End Anchorage.

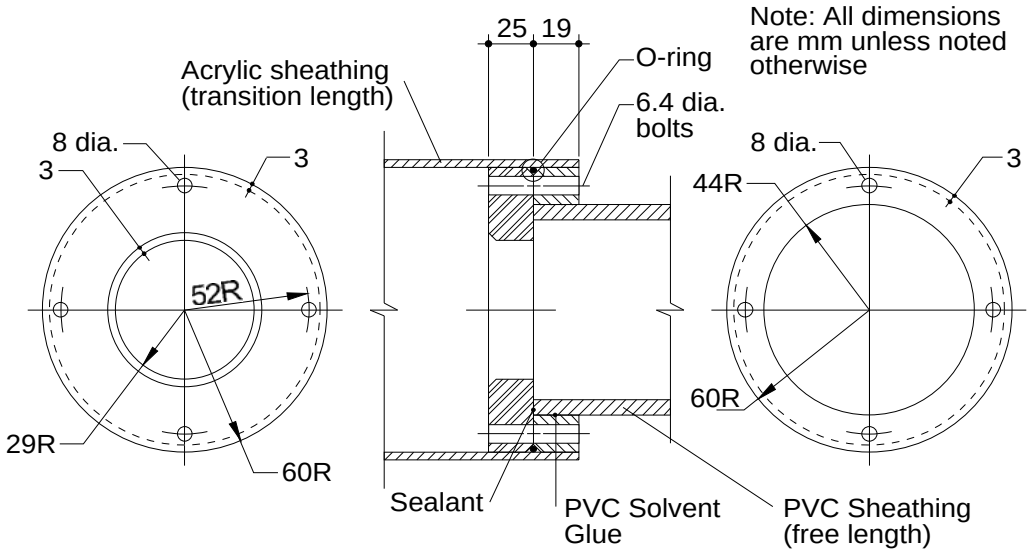

Figure 7.10 - Deviator Ring Details.

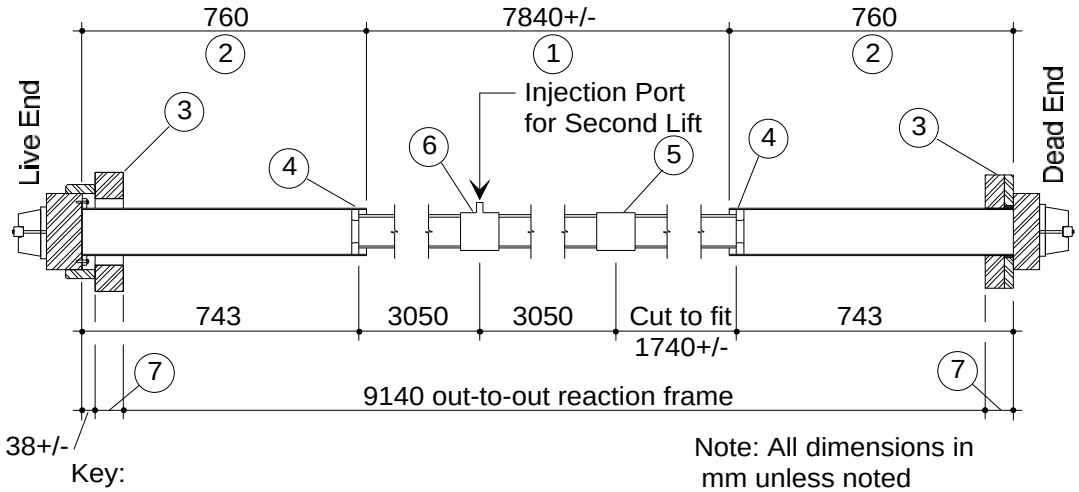

Key:

1 Free length - 76 ID transparent PVC pipe
2 Transition length - 120 ID transparent acrylic tube
3 Anchor plate
4 Deviator ring
5 PVC coupling
6 PVC tee
7 102 mm for frame F1 (LS-2 and LS-6)
76 mm for frame F2, F3, F4 (all other specimens)

Figure 7.11 - Sheathing Details.

the PVC pipe was only manufactured in 3-m lengths it was necessary to provide two couplings in the free length. The first coupling was a tee which served as the injection port for the second lift of grout. The second coupling was a standard PVC coupling.

7.4.7 Helical Spacer

In order to provide a minimum annular space of grout around the strand bundle, it is necessary to install a spacer between the bundle and sheathing. This is generally accomplished with a 6.4- to 9.5-mm diameter wire wrapped helically around the bundle. In many cases this wire is epoxy-coated for corrosion protection and to prevent fretting fatigue in the contact area with the strand bundle. The wire used in these tests was a 6.4-mm diameter prestressing wire which is the minimum diameter prescribed by the PTI Recommendations. The wire was polyester coated and formed a pitch of approximately 1000 mm when placed on the bundle. While this pitch was greater than that allowed by the PTI *Recommendations for Stay Cable Design, Testing and Installation*, it was necessary to limit the pitch so that the wire would not be exposed in all of the sheathing openings when later made for the corrosion tests. A chemical analysis was conducted on the wire and is included in Appendix B.

7.5 Reaction Frame and Supporting Elements

Four reaction frames as shown in Figure 7.12 were constructed. Two specimens were assembled and tested sequentially in each frame for a total of eight specimens. The complete process of assembly and testing generally took six to seven months per specimen. Since the grout was injected with the specimen in the inclined position it was necessary to construct the frames so that they could be moved while the specimen was still stressed. This would allow assembly, stressing, and later load and exposure testing to be performed while the frame was in the prone position. The frame was designed so that the dead load stress in the stay specimen could be maintained while the frame was lifted at the center point by the crane.

7.5.1 Specimen Frame

The reaction frames were constructed with two main struts (structural steel wide-flange sections) that were spaced 305-mm apart (Figure 7.12). Each strut terminated with a steel base plate at each end. Mounted on the steel base plates at each end were two heavy channel sections which acted as transfer beams, transferring the load from the stay anchorage to the strut base plates. Frame F1 was constructed with a 229-mm clear space between the channels while frames F2, F3, and F4 were constructed with a 178-mm clear space.

The struts were braced at the ends and at the midpoint with light steel channels top and bottom. At the midpoint of the reaction frame a lifting frame was mounted on the struts which

allowed the frame to be lifted by the crane at a single point. This single point lifting eye allowed the reaction frame to rotate about the lift point so that it could readily be "leaned" against the reaction walls in Ferguson Laboratory.

To facilitate the assembly/disassembly of the specimen, all channels on the top side of the frame, including the transfer beams at the end and the lifting eye frame, used bolted connections. This allowed clear access to the unstressed stay specimen for the full length of the frame. Although all stay specimens were fabricated in place for this series of tests, the removable channels would also allow testing of prefabricated stay specimens. Specimens could be fabricated off-site, shipped in on reels and placed in the frame as a unit. The channels could then be reattached and the specimen stressed as a unit.

The frame was designed to resist an axial load of 1000 kN while resting on the floor and an axial load of 700 kN while being lifted by the crane. This included the weight of the frame plus the weight of the specimen.

7.5.2 Placement of the Frame in Grouting Position

For assembly of the specimen, the reaction frame was placed prone on the floor adjacent to the grout injection position (Figure 7.13). Following assembly and stressing, the reaction frame was lifted by the crane and placed in the sloped position for grout injection (Figure 7.13 and Figure 7.14). The low end of the frame was supported by a cast concrete pedestal which was attached to the strong floor with bolts. The upper end of the frame was supported by structural steel tubes which were bolted to the top level of holes in the reaction wall. A platform was constructed around the upper supports at the reaction wall so that safe access was provided to the upper end of the frame during grout injection (Figure 7.15).

7.6 Stay Assembly

With the reaction frames placed flat on the floor the stays were assembled directly in the reaction frames. However, prior to starting the assembly several items needed to be completed. The deviator rings and PVC flanges were preassembled. In addition, the flanges were glued to their respective transition pipes. The bolts on the reaction frame were tightened. Support blocks were installed as well as the temporary corrosion protection oil catch trough (if required). The strand bundle was then installed by inserting one strand at a time through a comb mounted at each end. This held the strands parallel from end to end. When a specimen was being assembled in frame F1

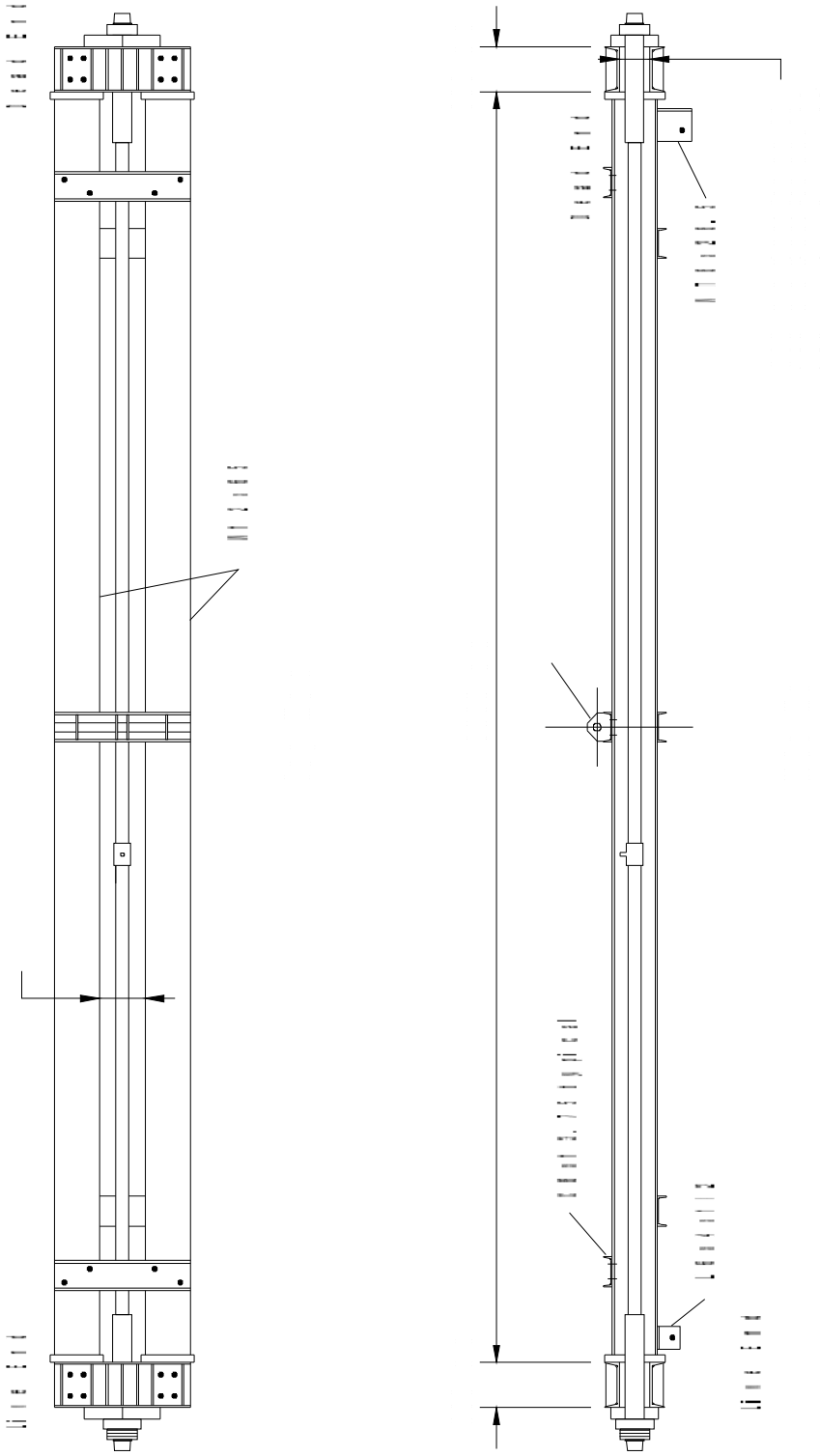

Figure 7.12 - Layout of Reaction Frame.

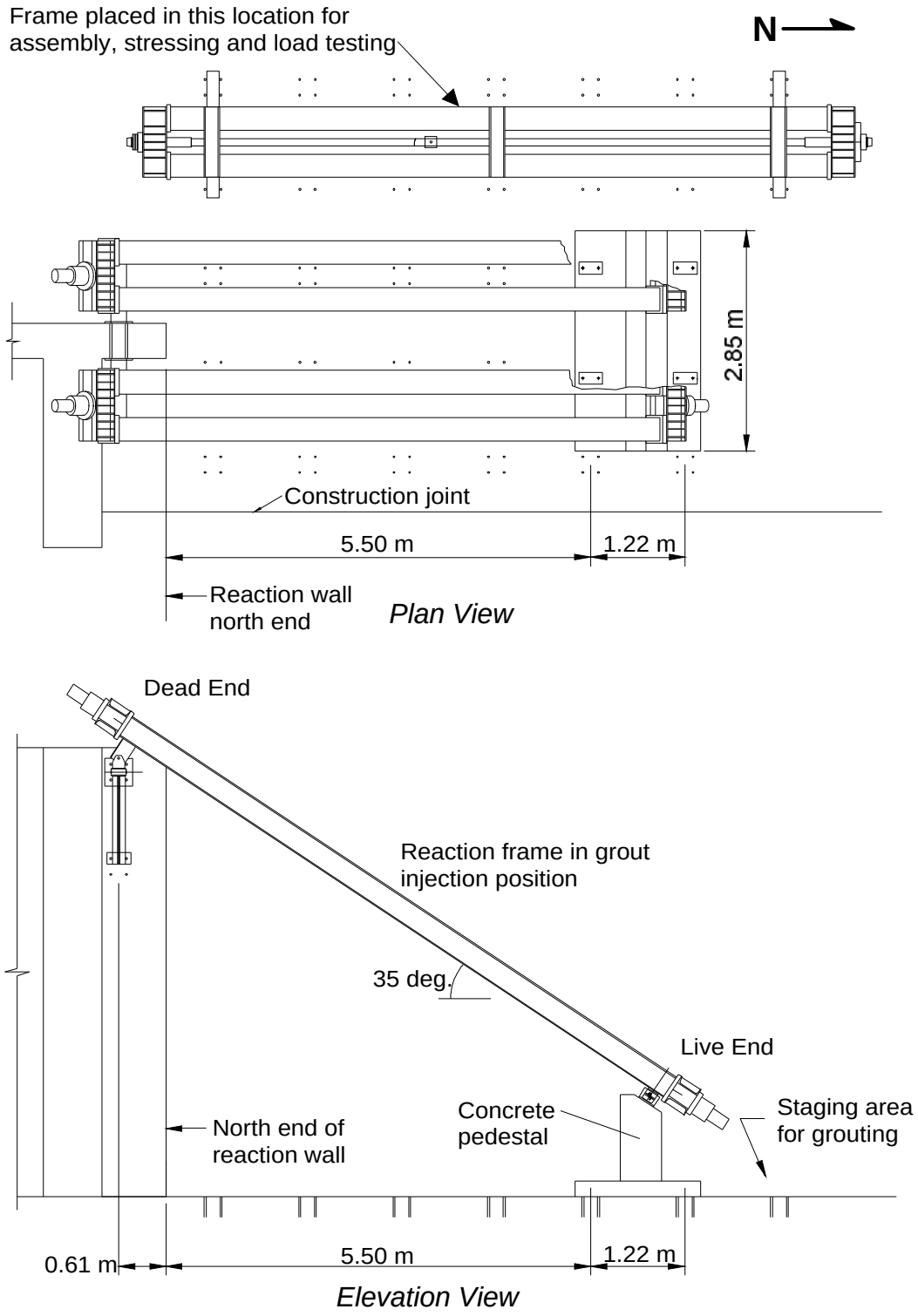

Figure 7.13 - Schematic of Assembly and Grout Injection Position.

Figure 7.14 - Reaction Frames with One Frame in Grout Injection Position.

Figure 7.15 - Platform at Top of Reaction Wall.

it was necessary to install the anchor plates at this point because the anchor plates were not split as was the case with the other anchor plates. The strands were then clamped into a bundle with hose clamps and an emulsifiable oil (Dromus B manufactured by Shell Oil) was applied liberally to specimens LS-3, 4, and 5 using a spray bottle. The bundle was allowed to drain at least overnight. The helical wrap was installed and the oil trough, if used, was drained and removed. Installation of the components started at the live end with the deviator ring, transition pipe, and anchor head. On frames F2, F3, and F4, the anchor plates were installed under the anchor head and clamped in place.

Installation of the free length sheathing was done from the dead end. One section of 3-m PVC sheathing was threaded onto the bundle and glued into the PVC flange in the live end deviator ring. This was followed by the PVC tee, another 3-m section of PVC and a coupling. The final section of PVC was cut to length after measurements were taken. All connections were made with solvent glue. The dead end deviator assembly was then installed and glued to the exposed end of the PVC sheath. The transition pipe was slipped onto the deviator ring assembly, followed by the dead end anchor head and anchor plates. Silicone sealant was applied to the end of the transition piping. The detailed assembly procedure is presented in Appendix C.

7.7 Stay Stressing

Initial stressing of the specimen was conducted from the dead end using a monostrand jack. Each strand was stressed twice so that each strand had nearly the same stress close to $0.30F_{ULT}$. The load in the stay was then adjusted to $0.30F_{ULT}$ from the live end. At the same time, the load was taken to $0.45F_{ULT}$ to set the wedges and to determine the stiffness of the stay without grout.

7.7.1 Single Strand Stressing

After the stay was assembled, the strands were individually stressed to a load target load of $0.30F_{ULT}$ using a monostrand jack. This load was never quite reached because of the seating losses at release. This portion of the stressing operation was accomplished from the dead end (see Figure 7.16). The stress was monitored visually using a pressure gage and electronically using a pressure transducer. Hydraulic pressure was supplied to the jack with a hand pump. The hydraulic jack was a single strand jack typically used for stressing monostrand tendons. The strands were stressed to a nominal level initially to lock the anchor heads in place (see first round Figure 7.17). In the second and third round the strands were stressed to $0.30\sigma_{ULT}$ (second and third round Figure 7.17). The

Figure 7.16 - Dead End Stressing Equipment.

strands were stressed a third time in order to reduce the elastic losses which resulted from the shortening of the frame.

Stay LS-6, which had epoxy-coated strand, required the use of special wedges that had deep teeth capable of penetrating the epoxy and biting into the strand. When using epoxy-coated strand it is not advisable to re-stress because epoxy may be caught in the wedges and cause the strand to slip on a subsequent release. To offset the elastic losses, the shortening of the reaction frame was calculated and the release stress (assuming identical seating losses) for each strand was adjusted so that the stress in each of the strands would be equal at the end of the stressing operation. The total final stress was somewhat lower than the target stress because of seating losses at release. However, this was adjusted for when the specimen was stressed from the live end.

7.7.2 Multiple Strand Stressing

Following completion of the dead end stressing operation, the specimen was stressed from the live end for the following purposes:

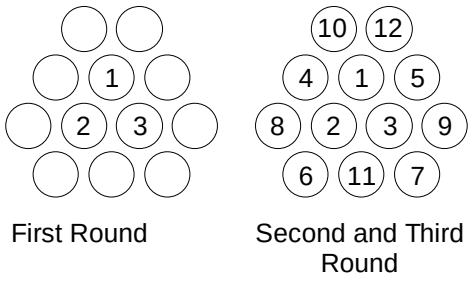

Figure 7.17 - Dead End Stressing Sequence.

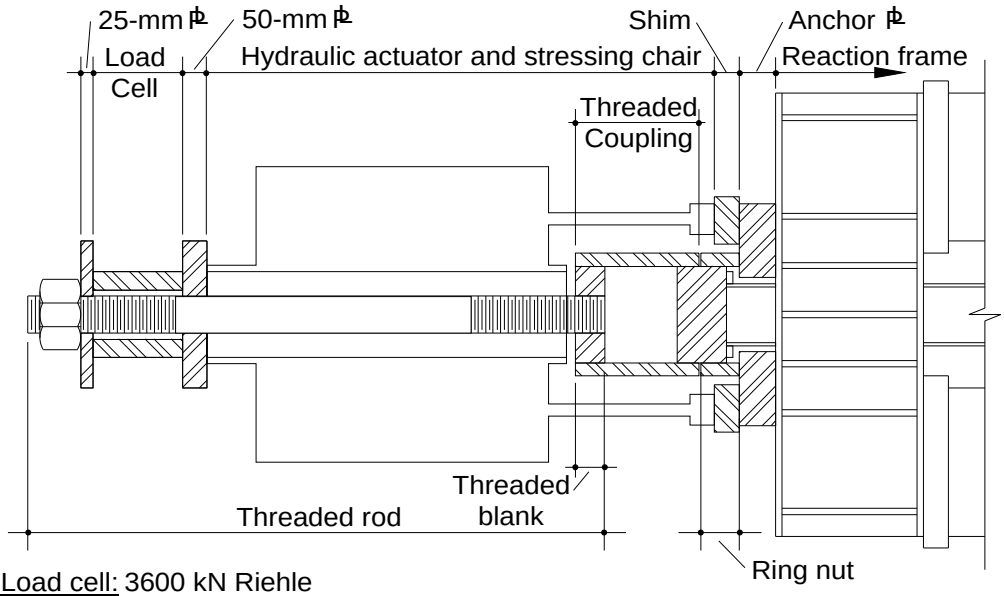

Load cell: 3600 kN Riehle
Threaded blank: 200-mm O.D. x 76-mm I.D. x 60-mm thick, threads inside and outs
Threaded coupling: 240-mm O.D. x 200-mm I.D. x 250-mm long, threaded inside to match blank and live end anchor head
Threaded rod: 76-mm dia. x 1220-mm long

Figure 7.18 - Live End Stressing Assembly.

Figure 7.19 - Live End Stressing Setup.

- Increase load to $0.45F_{ULT}$ to seat wedges
- Adjust load in the specimen to $0.30F_{ULT}$ for grouting
- Determine effective modulus of elasticity

The stressing operation was conducted with a 4500 kN capacity center-hole hydraulic ram (Figure 7.18 and Figure 7.19). A 3600 kN load cell was used to monitor load and a pressure gage was used to monitor hydraulic pressure as a backup. The threaded coupling was turned onto the live end anchor head. A threaded blank was then inserted in the coupling and the rod was inserted in the blank. The rod was then passed through the ram, load cell and two plates. The assembly was held together with a nut on the end of the rod. The hydraulic ram was fitted with a stressing chair. However, the chair was short by a few inches so that shims were inserted between the chair and the anchor plates. During stressing the chair reacted against the reaction frame as the ram piston pushed against the nut on the rod.

Stress in the stay was measured using lift-off tests. This involved measuring the relative displacement between the anchor head and reaction frame as the pressure in the ram was increased. The load at which the anchor head first moved relative to the reaction frame gave the stress in the stay.

The stressing operation generally involved the following steps:

- Assemble stressing equipment and adjust alignment of ram.
- Install linear potentiometer on ring nut to measure displacement of anchor head relative to reaction frame.
- Install device to measure reaction frame shortening. This was done with specimens LS-1, 2, and 4.
- Set-up XY plotter to plot stay load vs. anchor head displacement. This was necessary for visual reference during lift-off tests.
- Use voltmeter to take displacement and load readings.
- Increase ram hydraulic pressure until lift-off. Note lift-off load.
- Continue increasing load until $0.45F_{ULT}$ is reached. Take readings of load and displacement.
- Reduce load back down to $0.30F_{ULT}$ and increase load incrementally back up to $0.45F_{ULT}$ again taking readings of load and displacement. The second pull gives a higher modulus of elasticity because the wedges have been seated during the first pull.

- Reduce load back to just above $0.30F_{ULT}$ and adjust ring nut to be tight against anchor plate.
- Perform lift-off tests and adjust ring nut as necessary to lock stay stress at $0.30F_{ULT}$.

Because of the positioning of the linear potentiometer, the measured stay anchor head displacement under axial load included both the stay elongation and reaction frame shortening. Therefore, it was necessary to take measurements of the reaction frame shortening. Frame shortening measurements were taken with a device which consisted of a 12-mm diameter steel pipe cut to a length of 8.3 m and placed on the bottom flange of the W12x65 strut in the reaction frame. The pipe was supported along the length by wood blocks cut to fit the outside diameter of the pipe and coated with grease. The greased support blocks allowed the pipe to slide easily along its length. One end of the pipe was anchored to the base plate at the end of the strut. At the other end of the pipe a linear potentiometer or dial gage was used to measure the change in distance between the end of the pipe and the base plate of the reaction frame or the frame shortening. The frame shortening was subtracted from the total measured displacement to give the stay displacement and thus the stay stiffness.

It was desirable to eliminate the need to measure the frame stiffness during each test. Instead, an average value could be used for the frame stiffness to reduce the stay displacement to the proper level. The concern with using an average frame stiffness value for all of the frames is that this may adversely effect the accuracy of the stay stiffnesses. To examine this possibility, the measured reaction frame stiffness was compared to the stay stiffness.

The measured axial stiffnesses for frames F1, F2, and F4 were 664, 646, and 632 kN/mm, respectively. The difference between the high and low measured stiffnesses is 5%. However, compared to the axial stiffness of the stay specimens (24.4 kN/mm for LS-1) this difference becomes insignificant when considering the accuracy of the displacement measurements. For example, a 10% error in the reaction frame stiffness would give an error of only 1% in the stay stiffness. This was sufficient justification for using an average frame stiffness value of 647 kN/mm for calculating the stiffness of the stays from the measured data.

The resulting stay stiffnesses and comparisons to the effective modulus of elasticity are presented in Table 7.1. Note that the measured stiffnesses are slightly below the stiffnesses that are calculated from the modulus of elasticity given on the mill certificate. The stiffness measurement was made on the second pull made from the live end. Thus, most of the seating losses were removed. However, there were probably some additional losses which occurred on the second pull

Table 7.1 - Stay Specimen Axial Stiffness Prior to Grouting (GPa).

Specimen	Measured	Reported on Mill Certificate
LS-1	*	194.4
LS-2	188.8	194.4
LS-3	186.8	194.4
LS-4	193.6	194.4
LS-5	193.7	197.2
LS-6	184.5	197.2
LS-7	186.6	198.6
LS-8	177.1	197.9

* instrumentation malfunction

giving a slightly low stiffness. Another explanation is that the loading rate used to test the strand for the mill certificate was higher than the loading rate used in large-scale specimens.

7.7.3 Monitoring Stress

The time required to test a single specimen was approximately six to seven months in length. For a large percentage of this time the specimens were at the dead load stress level. Hence, there was some concern that the frames and/or specimens would relax and transfer stress to the grout.

Originally, the reaction frames were instrumented with strain gages to allow continuous monitoring of the stress in the frame. This method of monitoring the stress was tested on the first specimen constructed (LS-1). The specimen was assembled, stressed, and monitored over a period of approximately two weeks. Prior to stressing, strain gages were attached to the top and bottom of each flange near the flange tip on both struts for a total of sixteen strain gages per reaction frame. Three dummy strain gages were attached to an unstressed section of plate steel to account for strain due to temperature fluctuations. It was found that the strain readings over the two week period were greatly affected by temperature fluctuations and were erratic and difficult to interpret. This was probably due to the low nominal stress in the reaction frame with the stay specimen at “dead load” (27 MPa).

At the end of the two week period a lift-off test was conducted which indicated that no discernible change in stress had occurred since the initial strain reading had been taken when the specimen was stressed. This indicated that there would be no significant loss in stress which might occur over the test period. Thus, testing on LS-1 and 3 continued without monitoring the strain in the reaction frames. Note that these specimens were to have no additional axial or lateral loads applied after they were injected with grout.

In specimens LS-2, 4, and 5 through 8, lift-off tests were performed when the additional axial load was applied to the specimens. This was five to six weeks after the specimens had been assembled and stressed. Again, there was no significant change in the stress in the specimens over this time period (no more than 3% - 4%). As a final confirmation of the stability of the load level, a lift-off test was performed on LS-2 during post-mortem examination. The test was conducted after the sheathing and grout had been removed. The results indicated that the stress in the specimen had not changed significantly (3% increase).

7.7.4 Difficulties

The assembly of the specimen was complicated by the fact that the components had to be installed in the correct order from the end of the strand bundle. This precluded the use of a strand "comb" which keeps the strand parallel. Great care had to be taken to ensure that the correct strand was placed in the correct hole in the anchor heads at each end. Unfortunately, it is difficult at best to determine if strands have been twisted once the assembly is complete. Despite the care taken during assembly, LS-3 had strands 1 and 4 twisted one complete turn between the anchor heads. This was not discovered until the post-mortem examination.

The acrylic pipe used for the transition sheathing was very brittle. Great care was required when installing the live end anchorage to prevent fracturing the pipe or the flange. This brittleness also presented a problem during stressing. The alignment of the ram prior to stressing was crucial because there was no lateral restraint on the stay during stressing. Misalignment of the ram and stay centerlines would cause the live end anchor head to move laterally at lift-off. This movement would force the sheathing against the anchor plate and cause damage to the sheathing.

Another problem noted during the stressing operations was that the glued joint between the PVC free length sheathing and the deviator ring assembly could break during the application of addition load. This only occurred when the specimen was loaded prior to the injection of grout.

During the live end stressing on the first test the stay was observed to rotate relative to its centerline as the load was being released from 0.45 to $0.30F_{ULT}$. Each time the specimen was unloaded it would rotate a little more. It was discovered that the hydraulic ram piston was rotating as well. There was no restraint other than the friction between the piston and the cylinder to prevent the specimen and piston from rotating. Because the wires on each of the strands are wound in the same direction, there is a net torsional force when the specimen is loaded. In essence, the strands are trying to unwind. The rotation was prevented by restraining the rotation of the stressing rod.

7.8 Grout Injection

When polyethylene pipe is specified for use as the sheathing in a stay cable, PTI *Recommendations for Stay Cable Design, Testing and Installation* restricts the maximum vertical height of the first grout lift to 6.1 m and subsequent lifts to 38 m.[28] This prevents the pipe from being overpressurized during the injection of the grout. For the typical cable-stayed bridge, this requires that the grout be injected in several lifts, leaving a grout joint at regular intervals along the length. To simulate this method of grout placement, the grout was injected into the specimens in two lifts. This provided a simulation of the actual field installation procedures as well as the opportunity to test the effectiveness of the grout joint area in providing corrosion protection to the strand bundle.

Following completion of the assembly and stressing of the strands, the reaction frame with the stay specimen in place was lifted into the grouting position (Figure 7.13) and the grout was injected into the specimens. The first lift was injected to approximately halfway up the length of the stay and allowed to cure overnight. The second lift was then injected into a port just above the top of the first lift (see Figure 7.11) to complete the process. The grout was allowed to cure a minimum of 28 days prior to the load tests.

7.8.1 Grout

The grout mix used to inject all specimens excluding LS-5 was a water and portland cement mixture (water/cement = 0.40 by weight) with addition of the anti-bleed admixture Sikament 300SC at the rate of 2.2% by cement weight. The grout mix for LS-5 used the same constituents but also had silica fume added at the rate of 5% by cement weight. Development of these mix designs is discussed in detail in Chapter Five.

7.8.2 Grouting Procedure

A detailed listing of the grouting procedure is included in Appendix C. Only a short descriptive version of the grouting procedure is given here.

Following completion of assembly and stressing, the necessary plumbing fixtures were installed on the specimen to allow an air pressure test for leaks. The specimen was pressurized up to 69 kPa of air pressure. The air pressure was monitored to determine how quickly the specimen lost pressure. If the pressure dropped too quickly (qualitatively) then the leak was located and repaired (if possible). In a few cases the air leaks were between the base of the transition sheathing and the anchor head. This area was impossible to repair without complete disassembly.

The reaction frame was placed on the slope to prepare for grout injection. Scaffolding was then placed under the frame to allow access to the area where the second lift would be injected. A

16-mm diameter hole was drilled through the underside of the sheathing to act as a discharge port for the first lift.

A single batch of 14 liters was mixed in a 5-gallon bucket (18.9 l) using a drill press with a spindle speed of 1700 rpm and a type PS mixing paddle as manufactured by Jiffy Mixing Company, Irving, California. Each batch contained the following constituents:

- 19.7 kg Type I portland cement
- 7.89 kg distilled water
- 0.434 kg Sikament 300SC
- 0.986 kg Silica Fume (LS-5 only)

Two batches were mixed for the first lift and three for the second lift.

The grout was injected with a positive displacement screw type pump designed for the purpose of injecting grout (Figure 7.20). The pump was mounted on a frame along with an inoperative mixer. The grout was mixed using a floor stand mounted drill press. Prior to initiating grout mixing the pump was tested by filling the inlet hopper with water and starting the pump. The pump was run several minutes allowing the water to discharge back into the inlet hopper to clear any obstructions from the pump and lines.

Each batch was mixed for approximately 3 minutes. Water was added first, followed by the admixture and finally the cement. In LS-5 the silica fume was blended with the cement prior to initiating the mixing. After each batch was mixed a hand drill with a mixer attachment was used to gently agitate the grout to prevent segregation while the other batches were being mixed.

Figure 7.20 - Pump for Injecting Grout in Large Scale Specimens.

When the mixing had been completed the first batch that had been mixed was poured into the hopper through a wire mesh to strain any possible lumps or other foreign matter which might clog the pump. The pump was started and the grout was discharged into a waste bucket until the water had been removed and the grout looked uniform. Then the discharge was redirected to the inlet hopper and allowed to run until the air had been removed from grout in the pump. The discharge hose was then connected to the inlet on the specimen and the pump was started. During injection operations the grout in the hopper was stirred with a trowel to prevent segregation and to prevent air from being drawn into the pump suction. In general, the grout was injected at a rate of 10 to 14 meters/minute until the grout front reached the discharge point. This was adjusted on some of the specimens to determine if reducing the rate would eliminate the problem with air pockets which was encountered. On the first lift the pump was cycled on and off to prevent the grout from overrunning the discharge port. This would leave a thin film of grout on the sheathing and strand just upstream of the discharge port. On the second lift the same procedure was followed to prevent the pump from overpressuring the stay and initiating a leak.

Injection continued until the discharge grout looked uniform. The amount of grout discharged from the stay varied from 20% to 63% of the total volume injected.

Nine grout cubes were made from each lift. The cubes were made from the grout discharged from the stay and were cured in a moist room at 100% humidity, uncovered. Three were tested at 1 day and six were tested at 28 days. The resulting cube strengths are presented in Table 7.2. The 28-day strengths generally range from 38 to 44 MPa and all except LS-1 were above the minimum of 34.5 prescribed by PTI *Recommendations for Stay Cable Design, Testing and Installation*.[28] There were some difficulties experienced in the 28-day compression tests on LS-1 which explains the low compressive strength shown in the table.

Table 7.2 - Grout Cube Strengths (MPa).

Specimen	1-day		28-day	
	1st lift	2nd Lift	1st lift	2nd Lift
LS-1	20.5	18.9	n/r	28.2
LS-2	14.6	16.0	42.6	45.9
LS-3	14.8	17.9	48.2	38.8
LS-4	15.8	14.5	39.0	45.6

LS-5	18.8	17.6	45.6	47.4
LS-6	26.6	27.4	38.1	43.2
LS-7	20.4	20.5	37.5	42.5
LS-8	21.8	19.5	44.8	44.0

n/r - not run.

Immediately after the completion of the injection of the first lift, the valve in the plumbing at the live end grout cap was closed and the grout line was removed. The discharge port was left open until the following day when it was sealed so that the second lift could be injected.

The injection procedures were essentially the same for the second lift with a few exceptions. The discharge hole at the top of the second lift was sealed and a hose clamp was placed around the sheathing just below the top of the first lift (Figure 7.21) to prevent the grout from the second lift from running down the annular space between the grout and sheathing. The grout line was connected to the plumbing at the PVC Tee just ahead of the top of the first lift. In addition, prior to injecting the second lift, a 5-mm diameter hole was drilled in the top of the sheathing just ahead of the first grout lift. This hole allowed air that might otherwise be trapped between the lifts to escape so that the grout joint was solid. At the completion of the second lift the valve in the plumbing at the PVC Tee was closed and the grout port at the discharge was sealed.

Figure 7.21 - Top of First Grout Lift.

Following the completion of the injection of each lift, the grout was visually monitored during the time up to the initial set of the grout. It had been determined in previous tests that the initial set time of this particular mix was in the range of seven to nine hours. The visual monitoring was necessary because of the unexpected appearance of air pockets in the grout well after the grout had been injected.

7.8.3 Air Pockets in Grout

The methods and materials used to inject the large scale specimens with grout have been discussed in detail in the previous sections. Every reasonable precaution was taken to ensure that the grout was injected properly into the stay specimens. These precautions included:

- Use of an anti-bleed grout with reasonably fluid characteristics developed to prevent lens formation
- Use of a high-shear mixer turning at 1700 rpm to ensure complete mixing without overmixing
- Use of adequate grout line size to prevent blockages or overpressuring the grout
- Sieving the grout just prior to pumping to prevent lumps and foreign matter from entering pump.
- Agitating the grout from completion of mixing until it was drawn into pump suction for delivery.
- Use of a positive displacement pump specifically designed for grout injection
- Recirculating the grout through pump to remove air from pump system
- Test of the pump to determine if air was being drawn into the grout as it was being injected.
- Discharging at least 20% (usually 50%) of the filled volume of grout from stay.

Even taking these precautions and considering the ideal laboratory conditions, there was a significant problem with air pockets forming in the specimens. Figure 7.22 shows the orientation of the specimens when the grout was injected. As the figure indicates, all of the air pockets formed in the top side of the stay. In addition, air pockets formed in the unvented corners of the specimen such as at the top end of the live end transition length and the underside of the dead end anchor head. Generally, the shape of the air pockets along the free length of the stay shown in Figure 7.23 and Figure 7.24 could be described as very wide cracks in the grout. They were not actual grout cracks because they formed prior to the grout setting.

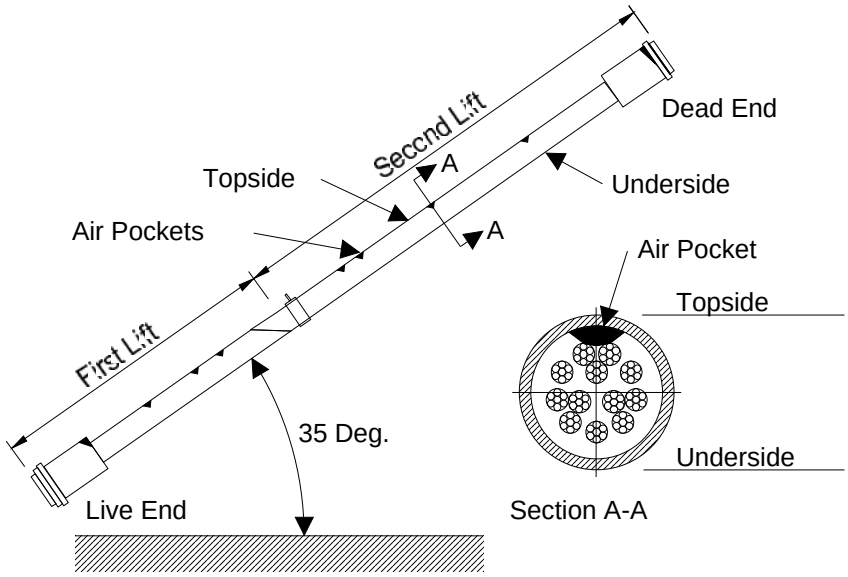

Figure 7.22 - Orientation of Stay Specimen for Grouting and Air Pocket Locations.

Figure 7.23 - Typical Air Pocket.

Figure 7.24 - Typical Air Pocket.

The air pockets generally formed in the following manner. Usually within 30 minutes after the completion of the grout injection the air pocket would make its way to the top side of the stay so that is was visible through the transparent sheathing. Depending on the size and location of the air pocket, it would migrate slowly towards the top of the grout lift sometimes increasing in size as it moved upward. The air pocket would then stop moving when the grout reached initial set.

Air pockets also formed adjacent to the helical spacer on the top side of the sheathing (see Figure 7.25). Air rising to the top of the lift would be stopped against the spacer on the low side.

Figure 7.25 - Air Trapped Adjacent to Helical Spacer.

Engelke [42] suggests that when a post-tensioning duct is being injected the grout front travels faster in the open space around the bundle and consequently air pockets are trapped between the wires or strands (see Figure 7.26). Assuming that the grout is sufficiently fluid, these air pockets would rise out of the wire or strand bundle and be taken (by grout flow) or migrate (if grout injection has ceased) to the nearest vent. This theory can readily be applied to injection of the large scale specimens. The grout front travels faster in the annular space around the bundle because of the clear space and reduced friction. This allows air to be trapped in the area between the strands as well as the area between the wires of the individual strands. If the grout used to inject the stays had a low viscosity then it is likely that the trapped air would travel almost immediately to the top side of the sheathing and on up to the top of the lift. However, an anti-bleed admixture was used which makes the grout thixotropic. This implies that the grout is fluid while being pumped, but that the grout thickens when the injection is stopped. If this is the case, then the air that might be trapped between the strands would probably not rise immediately to the top of the lift, but would move slowly depending on the viscosity of the grout. This is consistent with the observations made after the completion of the injection where the air slowly moved to the top side of the stay and then made its way to the top of the lift.

Air pockets are not desirable at any location in the stay. However, the air pockets in these tests were consistently in the top side of the specimen. This is the worst possible place for them to occur because the grout thickness is at a minimum over the strand. This improves the probability, depending on the volume of trapped air, that the air pocket will leave the strand unprotected.

In an effort to determine the cause, or at least to identify factors contributing to the air pockets, the occurrence of air pockets was quantified. The ideal condition would be to determine the total volume of trapped air as a function of the length of the stay. However, measuring the volume was not practical.

The configuration of the trapped air on all of the specimens was very similar. The air pockets only occurred at the top side of the sheathing with the largest portion of the void against the sheathing. As an alternative to volume, the area (mm^2) of the void, where it intersected the sheathing, was used as an index of the quantity of air trapped. During the post-mortem examination, an estimate was made of the area of grout missing at each of the air pockets. The results of this survey are presented in Table 7.3 and Figure 7.27.

Table 7.3 presents a summary of the areas measured for each specimen. The summary is divided into the free length and transition portion of the first and second lifts. Totals for each lift as well as the total for the specimen are also presented.

Table 7.3 - Summary of Air Pocket Areas (mm^2).

Specimen	First Lift			Second Lift			Total Both Lifts
	Live End Transition	Free Length	Total	Dead End Transition	Free Length	Total	
LS-1	0	131	131	181	0	181	312
LS-2	645	477	1122	36	1290	1326	2448
LS-3	0	408	408	1400	257	1657	2065
LS-4	0	1170	1170	1760	0	1760	2930
LS-5	645	112	757	1890	1330	3220	3977
LS-6	0	0	0	760	0	760	760
LS-7	1330	0	1330	0	0	0	1330
LS-8	0	0	0	0	0	0	0

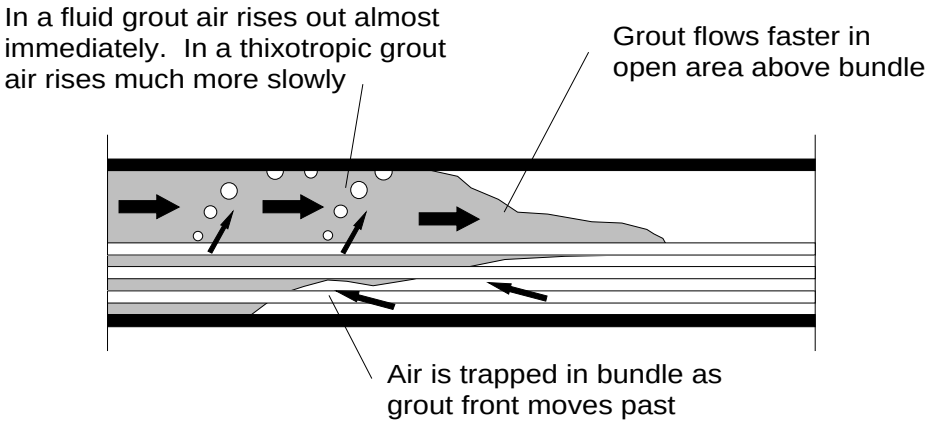

Figure 7.26 - Trapping of Air in a Post-Tensioning Duct (adapted from42).

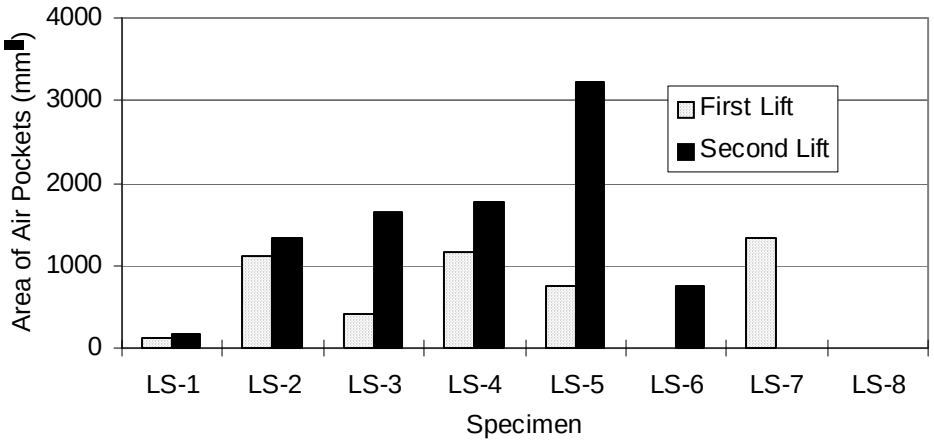

Figure 7.27 - Comparison of Air Pockets for Different Stay Specimens.

Trends are more easily identified in the bar graph which compares the first and second lift areas for each specimen (Figure 7.27). If LS-1 is ignored, then the stay specimens which used a smooth continuous sheathing (LS-6 and 8) had less voids than those that did not (LS-2 through 5). The larger quantity of air pockets in the uncoated strand specimens may be due to the slow release of air from the interstitial spaces in the strand. Post-mortem examination of the stay specimens with uncoated strands indicated that much of the interstitial space was filled with grout. This may explain why the strands in LS-7 behave like the strands which had a continuous coating. The soft zinc layer on the wires provided a continuous seal between the outer wires. This prevented grout from seeping into the interstices.

Specimen LS-8 used greased and sheathed strand where the strand sheathing was terminated at the anchor head and sealed as shown in Figure 7.8. Consequently, the grout was injected through the anchor head to the interior of the stay without the use of a grout cap. This made performance of the strand sheath/anchor head seal crucial. The seal was intended to prevent grout from penetrating the anchor head area where the strand was exposed. Figure 7.28 shows the outside face of the anchor head after grout injection. Note that several of the seals failed where the grout leaked into the anchor head region.

The design of the seals could use improvement such as a tighter fit between the coupling and the strand sheath and a longer length of coupling to provide a greater seal area. However, there is one basic problem with the system which would be difficult to change. Once the anchor head has been placed against the bearing, the strand sheath/coupling is completely covered by the transition sheathing which makes visual inspection impossible. So if the coupling installation was not done properly, the result will be the leakage of bleed water and/or grout into the anchor head area.

7.8.4 Difficulties with Anti-Bleed Admixture

After injecting the first lift into specimen LS-2 (bare strand with temporary corrosion protection) an unprecedented amount of bleed water gathered at the top of the lift (see Figure 7.29). In no other instance of grout injection (prior to or following this instance) had any perceptible bleed water collected at the top of the lift. In fact, the first lift of specimen LS-4 was injected just prior to LS-2 without any bleed problems. The procedures used for grouting LS-2 and 4 were the same as for a single specimen except that the quantities were doubled. Thus the constituents for the grout for both specimens were measured at the same time from the same materials. This indicated some type of inconsistency in one or more of the constituents.

The grout mix design used in the large scale test specimens had been developed (in small scale tests reported in Chapter Five) to eliminate bleed. However, there were some difficulties encountered with the anti-bleed admixture as discussed in detail in Chapter Five. The essence of the discussion was that the anti-bleed admixture used in the grout mix was a blend of organic polymer and superplasticizer and while the manufacturers instructions did not specifically call for mixing, it was standard procedure to mix the admixture just prior to use. It is believed that

Figure 7.28 - Specimen LS-8 Grout Leak Through Anchor Head.

Figure 7.29 - Bleed Water Collected at the Top of the First Lift in LS-2.

somehow when the admixture for LS-2 was measured it was not mixed, but that when the admixture for LS-4 was measured the admixture had been agitated sufficiently.

7.9 Load Tests

When cement grout is used for corrosion protection in stay cable construction, usually the entire bridge is erected and the alignment is adjusted prior to injection of the grout. After the grout is injected and has cured, any subsequent change in strain is transferred to the grout from the main tension element via bond. Since the grout is injected after the bridge is erected and all of the dead load strain has been taken by the main tension element, the grout is subjected only to the subsequent strains in the main tension elements caused by live, wind, and earthquake loads as well as thermal expansion and contraction. If these strains are in tension and of sufficient magnitude the grout will crack. This cracking can impair the corrosion protection provided by the grout.

Another source of tensile strain in the grout is from shrinkage. There are three different types of shrinkage which can occur after the grout has set:[83]

- **Drying shrinkage**: Reduction in volume caused by the withdrawal of moisture from concrete stored in unsaturated air.
- **Carbonation shrinkage:** CO_2 reacts, in the presence of moisture, with the hydrated cement materials causing a net reduction in area.

- **Autogenous shrinkage:** When no moisture movement to or from the cement paste is allowed during continued hydration shrinkage will occur.

Because the stay sheath provides a moisture-proof barrier, it is likely that only the autogenous shrinkage could occur. This type of shrinkage can cause strains of 40 με after 28-days of curing to 100 με after five years. Saul and Svensson indicate that the ultimate strain of ordinary cement grout is on the order of 100 με.[98] Thus, at 28 days after injection the strain level in the grout could be at 40% of cracking strain and at 5 years the strain could reach the level required to initiate cracking. This is with no additional loads applied!

Two load tests were developed to simulate the application of axial and lateral loads. The objectives of the load tests were twofold. The first objective was to determine what change in stiffness, if any, occurred when the grout cracked. The second objective was to characterize the progression of cracking during the of the application of the loads.

As noted previously, the specimens were assembled and stressed to the dead load stress load level of $0.30F_{ULT}$ after which the grout was injected and allowed to cure for 28 days minimum. Following the curing period, the lateral load test was first conducted followed by the axial load test.

The most important data collected during the load test was the occurrence of cracking. The use of transparent sheathing in constructing the specimens allowed visual monitoring of the surface of the grout during the application of additional load. In addition to locating cracks during the axial load test, it was possible to measure crack widths at selected load steps. Crack locations were marked on the sheathing for reference. Crack widths were then measured using a portable microscope at regular intervals throughout the loading sequence. Some portions of the specimen such as the anchorage region and load points were hidden from view by the frame or loading devices. This prevented the search for cracks in these areas during the application of additional load. Crack formation was accompanied by a sharp audible “pop” which allowed a recording of crack initiation relative to load level.

7.9.1 Lateral Load Test

Stay cables are uniaxial elements which are intended to carry load parallel to their axis. Some other types of cables are intended to carry loads inclined to their axis such as the main cable in suspension bridges. The stay cable is drawn taut and all intended loads are applied at the anchorage in a uniaxial fashion. However, the typical stay experiences incidental loads perpendicular to their axis from wind, earthquake or vibrations caused by live loads. The stay element is usually considered a truss type element which has only axial stiffness. However, because of the flexural

slenderness of the stay (very low moment of inertia relative to length) and the typical partial fixity condition at the end anchorages, flexural tensile stresses from lateral loads can be very high near the anchorage.

The objective of the lateral load test was to determine the amount and location of cracking that might occur when the specimens were subjected to a concentrated lateral load at the midspan. This method of applying the lateral load did not mimic actual field conditions. In the field, the load condition would likely be some form of distributed load. Based on the additional time and effort involved in applying a distributed lateral load to the specimen contrasted to the limited benefits of such a procedure, it was decided that a single concentrated load would be used. This would give the desired high stresses at the anchorage similar to those from a distributed load, but would require considerably less time and effort. The specimens were loaded while they remained in the reaction frame at the load level of $0.30F_{ULT}$. During the lateral load test, supports were installed at the interface between the transition length and the free length. These supports simulated dampers which are typically installed on stays to reduce vibrations (see Figure 7.30). They also alter the pattern of bending stresses in the stay when it is subjected to lateral loads.

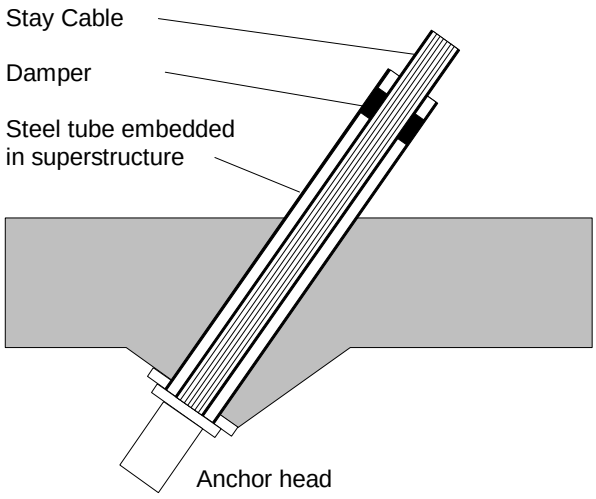

Figure 7.30 - Schematic of Stay Damper.

7.9.1.1 Analytical Estimate

An analytical model was developed to predict the behavior of the specimen under lateral load. The analysis was run on ANSYS version 5.0a, a comprehensive commercially available structural analysis program. The analysis included the effects of geometric nonlinearities and large displacements and was able to apply the loadings incrementally with the use of intermediate equilibrium iterations. An analytical model was developed (Figure 7.31) which consisted of 128 "BEAM3" elements. BEAM3 elements are two-dimensional uniaxial elements with nodes at each end. Each node has three degrees of freedom. The model was essentially analyzed as it would be loaded during the lateral load test. Initial strains were specified for each element to bring the load in the model to $0.30F_{ULT}$ prior to the application of any external loads. A distributed load was then

applied to each element to simulate the gravity loads. Finally, a series of concentrated loads were applied to the midpoint of the stay in the upward direction (opposite of gravity) as was done in the test.

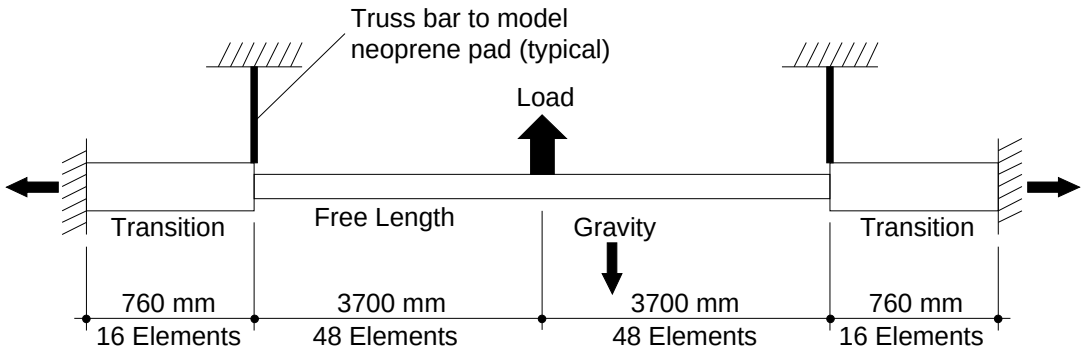

Figure 7.31 - Schematic of Analytical Model.

Calculation of the section properties for the analysis required an estimate of the modulus of elasticity for the grout. The ACI *Building Code Requirements for Reinforced Concrete* equation was used to estimate the modulus substituting an assumed cube strength for f'c:[3]

$$E_c = w^{1.5} 0.043 \sqrt{f_c'}$$

There were no formulas found in the literature that gave the modulus for grout. So, even though this equation is not necessarily appropriate for grout, it was used to estimate the grout modulus. The analysis was performed prior to the construction of any of the stay specimens. A cube strength of 41.4 MPa was assumed based on strength results obtained from the tests conducted in Chapter Five. However, it was found that this strength was in the range of the cube test results for the large scale specimens (see Table 7.2). Therefore, the analysis remained valid using this cube strength. Substituting the cube strength for the concrete strength and using the unit weight for a 0.40 water/cement ratio grout:

$$f_c' = 41.4\ MPa$$
$$w = 2150\ kg / m^3$$

Then:

$$E_{grout} = 27{,}600\ MPa$$

An estimate of the strand bundle modulus (E_{strand}) was used to calculate the modular ratio (n):

$$E_{strand} = 190{,}000\ MPa$$
$$n = 6.88$$

The modular ratio was then used to transform the section properties of the strand to grout.

Because the maximum lateral load level was not known, the analysis was conducted using an incrementally increasing midpoint load. The deflections and stresses were calculated for each increment. This gave a range of bending stresses which were helpful in determining the maximum load level. A maximum load level of 7.3 kN was selected during the test on specimen LS-4 (see Section 7.9.1.3 for further discussion).

Figure 7.32 shows the bending moments from the analysis for a 7.3 kN midspan load. The cracking moment envelopes are also shown to indicate the areas where the stress is over the calculated tensile strength of the grout. The cracking moment was developed using the concrete tensile strength formula recommended by Committee 224:[2]

$$f_r = 0.0069\sqrt{w_c \cdot f_c'}$$

Substituting the grout unit weight and cube strength given previously for w_c and f'_c, respectively:

$$f_r = 0.0069\sqrt{2150 \cdot 41.4} = 2.06\ MPa$$

Compare this to the tensile strength derived from the ultimate elongation of 100 microstrain suggested by Saul and Svensson:

$$f_r = 27{,}600\ MPa \cdot 100\ \mu\varepsilon = 2.76\ MPa$$

The equivalent tensile strength given by the Committee 224 formula is somewhat lower than that suggested by Saul and Svensson. To develop the cracking moment envelope the lower value was used.

7.9.1.2 Loading Arrangement and Instrumentation

The lateral load test was conducted on the specimen while it remained in the reaction frame so that the minimum axial stress of $0.30F_{ULT}$ could be maintained. The lifting eye was removed from the reaction frame and the lateral loading frame attached as shown in Figure 7.33 and Figure 7.34. A center-hole hydraulic ram was placed on top of the loading frame. The load was measured with an Interface 111 kN load cell attached to the loading rod which passed through the center-hole ram. The opposite end of the load cell was attached to the specimen loading plates.

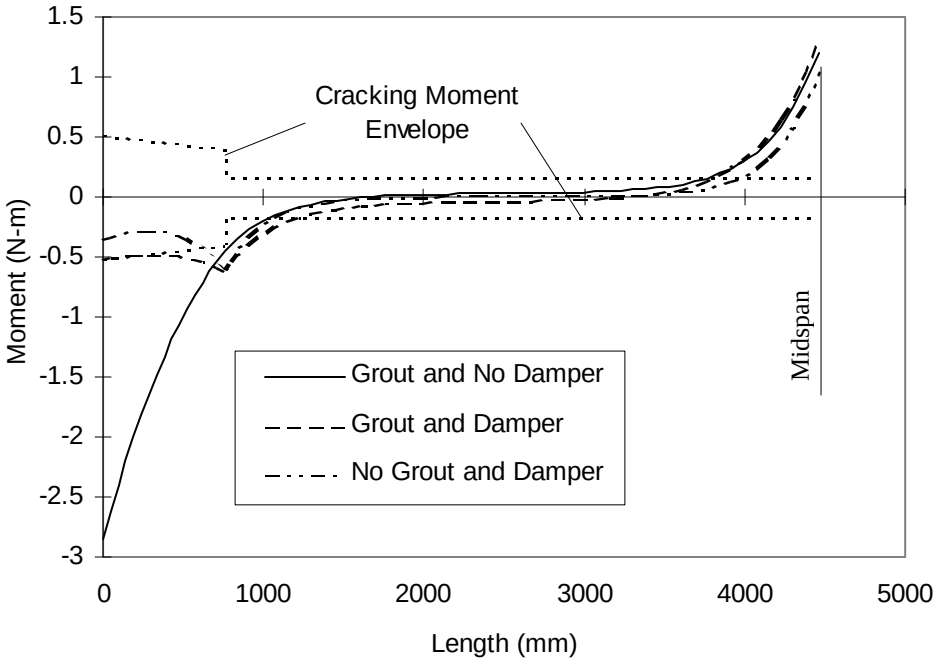

Figure 7.32 - Bending Moments from Analysis of Stay Cable Specimen.

Figure 7.33 - Lateral Load Test Frame.

A neoprene pad was placed between the specimen and the loading plate to prevent damage to the specimen. Specimen displacements were measured with dial gages in the locations noted in the figure. Midspan displacement was also measured with a 50-mm linear potentiometer. Excitation voltage for the linear potentiometer and load cell was set at 10 volts. At each load step signal voltage was read with a voltmeter and taken by hand along with readings from the dial gages.

7.9.1.3 Test Procedures and Observations

The first specimen to undergo the lateral load test was LS-4 (bare strand with temporary corrosion protection). Initially, the specimen was loaded to 2.0 kN twice to test the loading system and to work the bugs out of the testing procedure. During this loading one crack was heard to form but no cracking was visible. The load deflection remained linear throughout the application of load. Lift-off tests were then performed to determine the axial stress in the stay.

As discussed previously, the maximum load level for the test was not known. The plan was to load the specimen in small load steps and visually monitor for cracks until they became visible. In addition, the load vs. displacement was plotted and monitored for loss of stiffness due to cracking. When the cracks became visible the sizes and pattern would then be noted. At that point, a decision would have been made concerning the maximum load level.

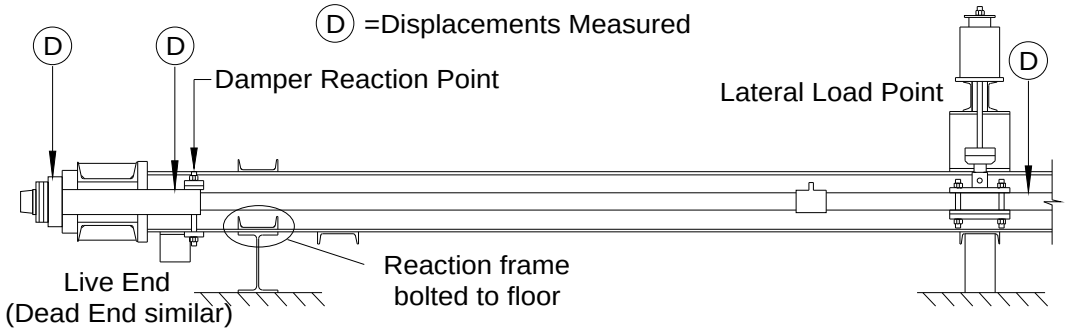

Partial Elevation View of Reaction Frame Ready for Lateral Load Test

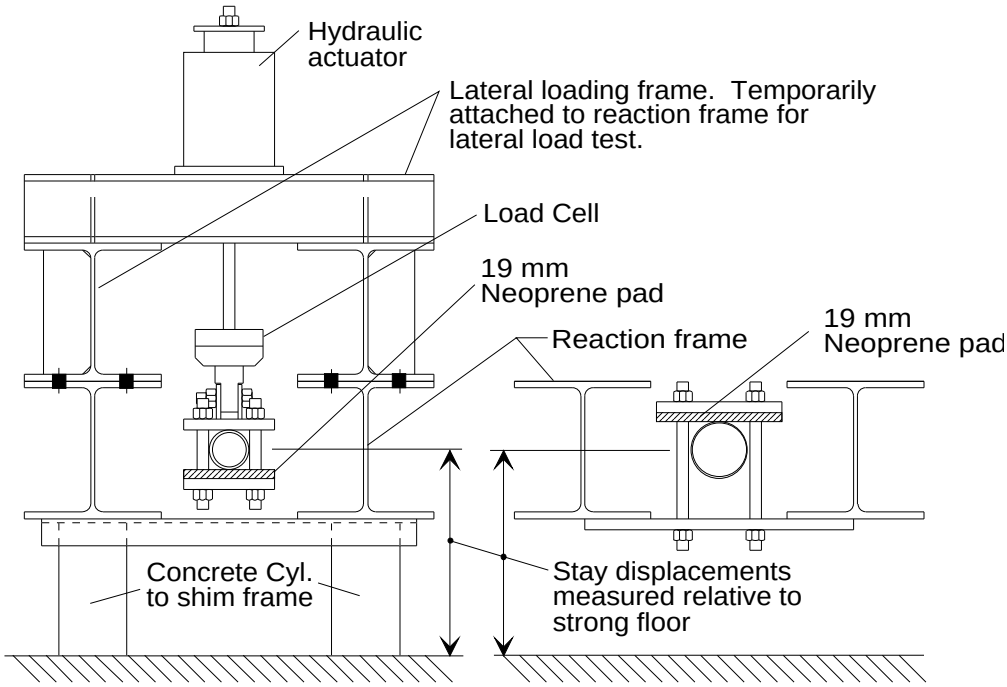

Detail of Lateral Load Point *Detail of Damper Reaction Point*

Figure 7.34 - Details and Layout of Lateral Load Test.

The first test was started on LS-4 and the load was increased in very small increments (2.2 kN) up to a level of 7.3 kN. However, there was no audible or visible cracking at any time during the load test. At this load level the stay midspan displacement was approximately 20 mm. There was concern that continued loading would damage the specimen, especially in the area of the load point, which would make subsequent accelerated corrosion testing difficult.

The lateral load test was terminated at this level and the axial load test was run as is described in a subsequent section. It was found during the axial load test that widespread cracking occurred over the full length of the specimen. The lateral load was then applied again to the specimen in order to allow a closer look for the presence of cracks. The results from the analytical model indicated that except for the inaccessible end regions, the next most highly stressed area was under the load point. If any cracks opened enough to be visible, then they should be visible in this area. However, the view of the specimen in this area was partially blocked by the loading plates. To alleviate this problem, the specimen was loaded to 6.2 kN and the stay was shimmed against the reaction frame to maintain the load while the loading plates were removed. The loading plate on the top side of the stay was removed so that the grout could be viewed from above. No cracks were visible even directly under the load point.

The conclusion subsequent to the axial load test was that it was much more severe than the lateral load test when considering the number and size of cracks caused by the tests. However, in order to maintain uniformity in the testing procedures it was decided that each specimen would be laterally loaded to the same level to which LS-4 was loaded.

On the remainder of the large scale specimens (LS-3, 5, 6, 7, and 8) the lateral load test was conducted prior to the axial load test and consisted of loading the specimen laterally to 7.3 kN (similar to LS-4). This was followed by the axial load test. This test order was selected so that the severe cracking caused by the axial load test would not affect the cracking that may result from the lateral load test.

7.9.1.4 Results and Discussion

The load-displacement at the midspan of the specimens was monitored to determine if there was any detectable change in the stiffness as cracking progressed. However, all of the load-displacement relationships were linear up to the maximum lateral load level. Figure 7.35 shows the load-displacement plot for the test run on LS-2. The degree of linearity for this test was typical for all of the lateral load tests. The stiffnesses measured during the lateral load tests along with those resulting from the analysis are compared in Table 7.4.

The following visual observations were made during each of the lateral load tests. Note that LS-1 and LS-3 were not loaded after grout injection.

Bare strand (LS-2). No audible or visible cracking occurred.

Bare strand with temporary corrosion protection (LS-4). No audible or visible cracking occurred.

Bare strand with temporary corrosion protection and improved grout (LS-5). Audible cracking was first heard at 2.7 kN load level. Cracking was heard at regular intervals of 1.0 kN up to the maximum lateral load of 7.3 kN. Generally, the cracking occurred during the application of load, although some cracking was audible during load hold periods. Cracks were not visible during the test.

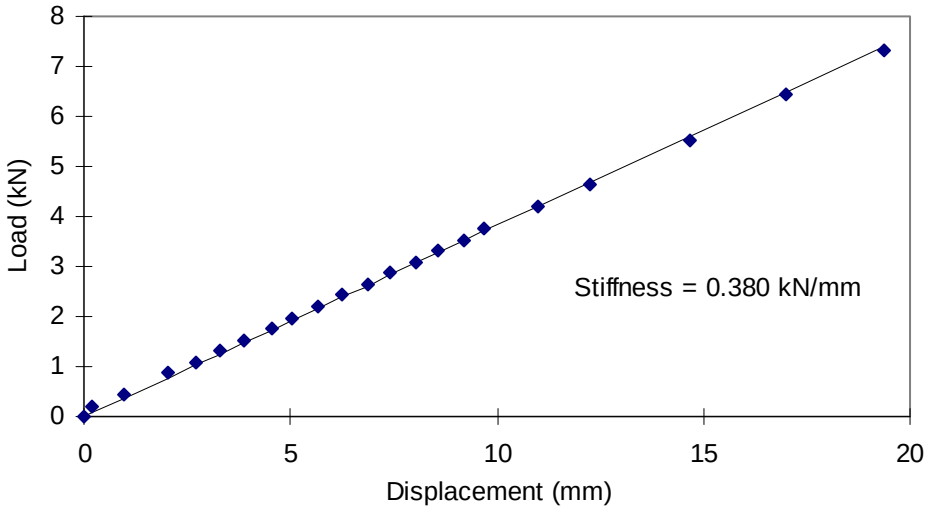

Figure 7.35 - Typical Load-Displacement Relationship from Lateral Load Test.

Table 7.4 - Stiffness of Stay Specimens Under Center Point Load.

Specimen	Stiffness (kN/mm)
Analysis (without grout)	0.402
Analysis (with grout)	0.436
LS-2	0.380
LS-4	0.369
LS-5	0.362
LS-6	0.368
LS-7	0.369
LS-8	0.369

Epoxy-coated strand (LS-6). Audible cracking occurred between 6.2 and 6.7 kN during the lateral load test. Cracks were not visible during the lateral load test.

Galvanized strand (LS-7). Audible cracking was first heard at 3.1 kN. Many cracks were audibly noted between 4.0 kN and 4.9 kN after which no more occurred. Cracks were not visible during the lateral load test.

Greased and Sheathed strand (LS-8). Audible cracking occurred only at the 3.1 kN load level. Two cracks were visible above the 4.2 kN load level under the loading plate at the midspan of the stay specimen.

7.9.2 Axial Load Test

The axial load test called for stressing the specimen from the "dead load" of $0.30F_{ULT}$ to the "live load" of $0.45F_{ULT}$. This simulated the change in grout strain caused by the application of full live load plus impact.

7.9.2.1 Analytical Estimate

The analytical modeling of the response of the specimens to axial load was much simpler than that of the lateral load. The transformed section properties were used to calculate the effective axial stiffness of the specimen which was 42.0 kN/mm. The load at which the stress in the grout would reach the estimated cracking stress was calculated as:

- Grout injected: $0.30F_{ULT}$
- Free length reaches cracking stress: $0.312F_{ULT}$
- Transition reaches cracking stress: $0.318F_{ULT}$

7.9.2.2 Loading Arrangement and Instrumentation

The axial load test was conducted with the same apparatus as was used to adjust the stress in the specimen during assembly (Figure 7.18).

7.9.2.3 Test Procedures and Observations

Immediately following the completion of the lateral load test, the axial load test was conducted. As with the lateral load test, the axial load test was conducted on specimens LS-2, 4, and 5 through 8. Although there was some variation in test method between specimens, the following procedure was generally used in the axial load test:

- Tension in the stay was increased in 4.45 kN increments up to $0.363F_{ULT}$ (800 kN) at which point load increments of 22.2 kN were used until the maximum load of $0.45F_{ULT}$ (990 kN) was reached.
- Visual monitoring for new cracks was made at each load step.
- When a new crack was found, it was assigned a crack number and the location was marked on the sheathing along with the crack number. The crack width was then measured with a portable microscope (0.0254-mm divisions) and noted along with the crack number and load level at which the crack was found.

- Generally, cracks did not become visible until the load reached approximately $0.322F_{ULT}$ (710 kN).
- After a new crack had been found and the initial width had been measured, the width was again measured at the following load steps: 0.333, 0.373, 0.413 and $0.45F_{ULT}$.
- Crack formations were accompanied by sharp pops which were clearly audible. Generally, most of the audible crack formations were heard near the beginning of the test when the stress in the grout was relatively low. However, this was not the case with all of the specimens so the number (if it was possible to count) and load step at which these sounds were heard were noted throughout the load test. The cracking was audible while the load was being increased. Once the load increment had been applied there were no more cracks heard until the load was increased to the next step.

In looking for new cracks, the surface of the grout was scanned while holding a flashlight nearly parallel with the surface of the sheathing. This illuminated the surface of the grout through the sheathing but left a shadow in the cracks giving a contrast that was easy to spot if the crack was sufficiently wide. It was found that the minimum width crack which could be detected with the naked eye using a reasonable visual scan rate was approximately 0.025 mm. These very narrow cracks were visible because the sheathing gave the grout a smooth surface finish. This smooth finish gave the crack edges a sharp corner which was easier to spot than the broken and rounded corners that would be found on the rough surface of hand-finished concrete.

7.9.2.4 Results and Discussion

During the axial load test the specimen was monitored both visually and audibly for cracking. The voltage output from the linear pot measuring anchor head displacement was monitored continuously with a voltmeter. If cracking was heard during the load hold period, it was generally accompanied by a slight increase in displacement. This indicated that the cracking was causing slight reductions in stay stiffness. This slight change in stiffness accompanying the cracking sound occurred on all of the specimens tested. In addition, all of the cracks which occurred during the load test closed and were not visible when the load was reduce to the dead load level. This was typical for all of the specimens. The observations for each specimen are summarized. Note that LS-1 and LS-3 were not load tested.

Bare strand (LS-2). Cracking was audible up to $0.339F_{ULT}$. No sound was heard above this load level.

Bare strand with temporary corrosion protection (LS-4). Cracking was audible during load test. However, the load levels at which the cracking was audible were not recorded.

Bare strand with temporary corrosion protection and silica fume grout (LS-5). Cracking was heard (10 or more sounds) just above $0.30F_{ULT}$ and continued somewhat regularly up to $0.330F_{ULT}$ where the regular audible cracking ceased.

Epoxy-coated strand (LS-6). Most of the intense audible cracking occurred between $0.30F_{ULT}$ and $0.325F_{ULT}$. A few cracks occurred between $0.325F_{ULT}$ and $0.341F_{ULT}$ where the audible cracking ceased.

Galvanized strand (LS-7). Cracking occurred mostly between $0.30F_{ULT}$ and $0.335F_{ULT}$. The cracking seemed to be more intense than in the other tests based on the number of cracks heard. Most cracking had ceased when the $0.335F_{ULT}$ level was reached although the cracking continued throughout the load test. A large quantity of grout had leaked into the area under the ring nut during injection of the first lift. This area is probably where the cracking was occurring at the higher load levels.

Greased and sheathed strand (LS-8). Cracking occurred in this specimen for the full range of loads at regular intervals. This was probably due to the lack of bond between the grout and strand. The strand sheathing allows the strand to elongate significantly before strain is transferred to the surrounding grout.

The grout crack width and spacing depend on the degree of mechanical bond and adhesion between the strand and the grout. Bare strand with no temporary corrosion protection (TCP) would be expected to have better bond than strand coated with TCP or encased in sheathing. The specimen with better bond would have *more* cracks with a *smaller* average crack width than the specimen with inferior bond. This criterion can be used to compare the stay specimens and determine how the various systems performed.

A summary of the crack data is presented in Table 7.5 including the number of cracks, and maximum and average crack widths for two load levels. The load level of $0.333F_{ULT}$ corresponds to the load level at which the first crack width readings were taken. The load level of $0.450F_{ULT}$ corresponds to the maximum load level applied in the test. The table presents the crack width data taken during the axial load test. Note that the number of cracks recorded in the table corresponds to the number of cracks which were detectable using the scanning method previously described. Therefore, it is probable that grout cracks were present which were not detected.

Another useful format for examining the cracking behavior of the specimens is shown in Figure 7.36. The y-axis gives the cumulative number of visible cracks (normalized to the total number of visible cracks at $0.450F_{ULT}$) recorded for the corresponding load level shown on the x-

axis. This gives an indication of the nature of the cracking and the bond characteristics between the strand and grout. Ideally the cumulative cracking should reflect the bond characteristics. For instance, in a specimen which has good bond, the cracking would be narrow and closely spaced. It would become visible later in the test than would cracks in a poorly bonded specimen.

LS-2 and LS-4 can be compared using this concept. It is expected that LS-2 would have better bond characteristics than LS-4 because LS-4 has temporary corrosion protection (TCP) applied to the strands. This is reflected in the figure as LS-2 has lower cumulative cracking than does LS-4 for most of the load steps. Another example is the bond of LS-7 compared to the other specimens. During post-mortem examination (discussed in Chapter Eight) of LS-7 it was noted that the grout had adhered to the surface of the strand very tightly. This was probably caused by the reaction between the wet grout and the zinc. The figure indicates that the galvanized strand had a significantly better bond than any of the other specimens. At the other extreme, LS-8 had much lower bond than the other specimens. This would be expected in a greased and sheathed system.

7.9.3 Previous Tests

Saul and Svensson presented the results of three stay cable tests which were conducted in Japan during 1975 through 1978.[98] The tests were conducted on stay cable specimens which were 1580-mm long and were constructed with (19) 7-mm diameter wires placed inside a PE sheath. The specimens were stressed to 530 MPa for pc grout injection. After the grout had reached a compressive strength of 20 MPa the sheathing was removed and the specimens were subjected to static and fatigue loads. While each specimen was being tested the grout was monitored for cracking. The results of the static tests are presented in Table 7.6. The stress levels shown in the table have been calculated from the data presented in Saul and Svensson's report using an assumed value of σ_{ULT} = 1860 MPa since it was not given. Note that the "first crack" was not defined in the reference. It is not known if this value is when the cracks formed or when they became visible.

7.10 Conclusions

7.10.1 Grout Injection

The grout injection was not an entirely successful operation in that the specimens were not filled completely with grout. Air pockets were present to some degree in all of the specimens except

Table 7.5 - Summary of Crack Data.

Specimen	at Load Level 0.333F_{ULT}			at Load Level 0.450F_{ULT}		
	Number of Cracks	Max Width (mm)	Ave Width (mm)	Number of Cracks	Max Width (mm)	Ave Width (mm)
LS-2	3	*	*	206	*	*

LS-4	0	*	*	123	*	*
LS-5	21	0.076	0.031	165	0.18	0.041
LS-6	8	0.13	0.038	132	0.31	0.047
LS-7	1	0.051	0.051	31	0.28	0.040
LS-8	12	0.17	0.14	21	0.61	0.29

* Crack widths not measured during these tests.

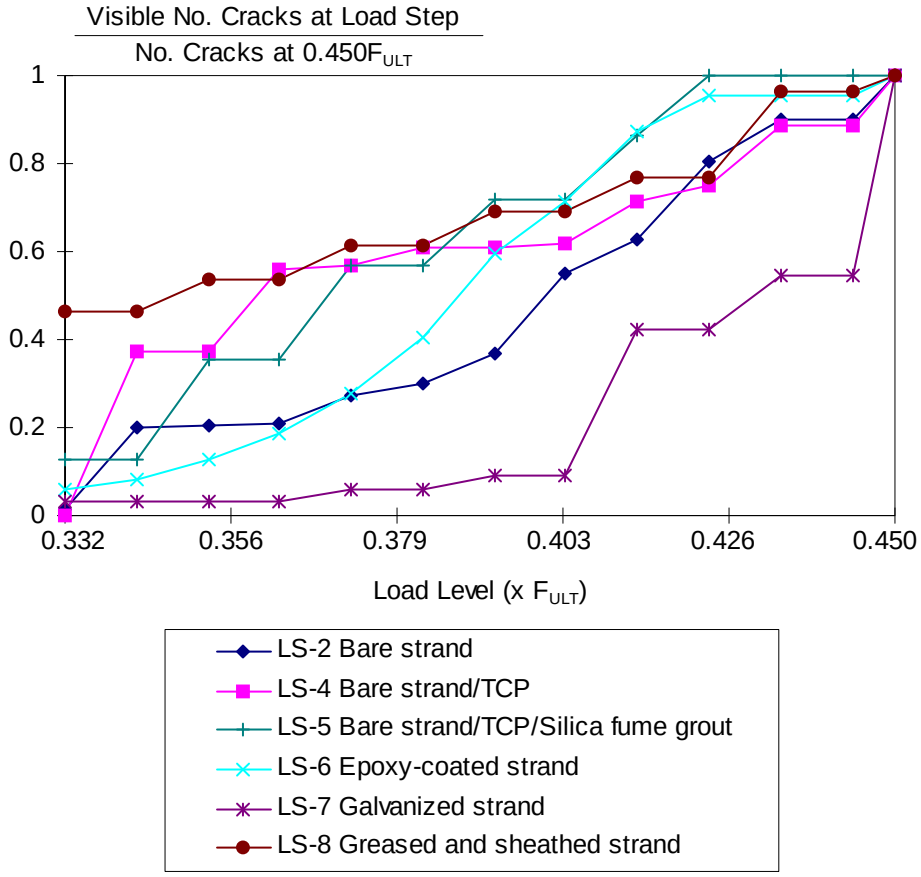

Figure 7.36 - Cumulative Cracking of Specimens.

one. It is speculated that the cause of the air pockets was related to the use of the anti-bleed admixture which thickens the grout. This slowed the escape of any air which may have been trapped in the strand bundle during the injection of the grout. In some cases the escape was slowed sufficiently so that the air did not reach the top of the lift before the grout set. The orientation of the

stay in the inclined position may have also contributed to the entrapment of air. If the stay had been oriented vertically as is frequently done in stay fatigue testing the air pockets probably would not have occurred. Air was also trapped in unvented corners and under the dead end anchor head.

Table 7.6 - Summary of Static Tests Reported in Reference 98.

	Grout A	Grout B	Grout C
water/cement admixture admixture/cement compressive strength	0.42 Pozzolith No. 8 0.25% 21 MPa	0.31 Icoment 35% 23 MPa	0.45 Conbex 208 1.2% 30 MPa
Stay stress at grout injection	$0.285\sigma_{ULT}$	$0.285\sigma_{ULT}$	$0.285\sigma_{ULT}$
Stay stress at first crack	$0.352\sigma_{ULT}$	$0.331\sigma_{ULT}$	$0.316\sigma_{ULT}$
Δ_{ST} at first crack	$0.067\sigma_{ULT}$	$0.046\sigma_{ULT}$	$0.031\sigma_{ULT}$
Crack width at $0.366\sigma_{ULT}$ ($\Delta_{ST} = 0.081\sigma_{ULT}$)	0.03 mm	0.03 mm	0.03-0.05 mm

Δ_{ST} = change in stay stress from stress at which the grout was injected.

A decrease in the number and size of air voids was noted in the specimens with individual protection systems. However, air pockets were not completely eliminated except for specimen LS-8 (greased and sheathed strand). In addition, it can be argued that the protection provided by the grout is irrelevant when individual protection systems are used. Thus, this improvement is somewhat trivial.

7.10.2 Lateral Load Tests

7.10.2.1 Preliminary Analysis

- Flexural stresses are significantly reduced at the anchor head when a damper is used.
- Moment was found to be rather insensitive to the presence of grout. This is because of the small cross sectional area of grout relative to the area of the strand bundle.

7.10.2.2 Load Tests

- Audible cracking occurred on four of the six specimens tested with no discernible effect on the stiffness. In addition, the measured midspan load-displacement relationship was linear. These results confirm the analysis which suggests very little contribution from the grout to flexural stiffness.
- The specimens were tested to a midpoint load of 7.3 kN for a displacement of approximately 20 mm. The preliminary analysis indicated that the flexural stresses in the

specimens at the load point and anchorage should have been well above the cracking limit. While cracking (audible) occurred on most of the specimens, midspan cracks became visible on only one specimen. LS-8 (greased and sheathed) had two cracks form at the load point under the loading plate. This lack of visible cracking indicates that the cracking caused by lateral loads is not significant when compared to the cracking caused by axial loads.

7.10.3 Axial Load Tests

- Cracking occurred almost immediately upon lift off in all of the specimens. It is suspected that the grout already had tensile shrinkage strains from autogenous shrinkage.
- Specimen LS-7 (galvanized strand) had narrow closely-spaced grout cracks during the application of additional axial load. This indicated that there was good bond between the galvanized strand and grout. This was probably due to the chemical reaction between the zinc and wet grout.
- Specimen LS-8 (greased and sheathed) had wide cracks at large spacings. This indicated poor bond between the strand and grout. While all of the other specimens had cracking occur only during the early stages of the load test, LS-8 had cracking occurring later in the test. During initial loading the strands have enough space inside the sheath to elongate without transferring load the grout through the sheath. However, as the later stages of the load test are reached, the strand has elongated sufficiently so that it contacts the sheath and transfers load to the grout. This causes the later grout cracking.
- The presence of the grout had no measurable effect on the axial stiffness of the stay.
- The load tests indicate that a relatively low level of axial load above the grout injection load is required to cause the grout to crack. These results confirm the findings from the inspection of the Pasco-Kennewick Bridge discussed in Chapter One. Thus it can be concluded with reasonable confidence that in most cable stayed bridges that use the two-barrier system, the grout is cracked along the full length of the stay cables.

Chapter Eight
Large-Scale Test Series:
Accelerated Corrosion Tests

Introduction

This chapter presents the methodology and results for the accelerated corrosion tests performed as a part of the large-scale test series. The general test philosophy, assembly, grouting and load tests are covered in Chapter Seven while the analysis and discussion are covered in Chapter Nine. There were a total of eight large-scale test specimens. The specimens and variables were as follows:

- LS-1: Bare strand
- LS-2: Bare strand
- LS-3: Bare strand coated with temporary corrosion protection (TCP) prior to grouting
- LS-4: Bare strand coated with TCP prior to grouting
- LS-5: Bare strand coated with TCP prior to grouting. Grout improved with silica fume.
- LS-6: Epoxy-coated strand
- LS-7: Galvanized strand
- LS-8: Greased and sheathed strand

Load tests and additional loads applied during the accelerated corrosion test were carried out on all stay specimens except for LS-1 and LS-3.

Reference System for Specimens

Each stay specimen was composed of twelve 12.7-mm diameter prestressing strands which were approximately 9.5 m in length (see Figure 0.1). In addition, each stay specimen had two anchor heads and two deviator rings. Because a thorough examination was required at the end of the accelerated corrosion test, a referencing system was devised so that corrosion encountered could be easily referenced to a standard location. This standard location was the same in all of the

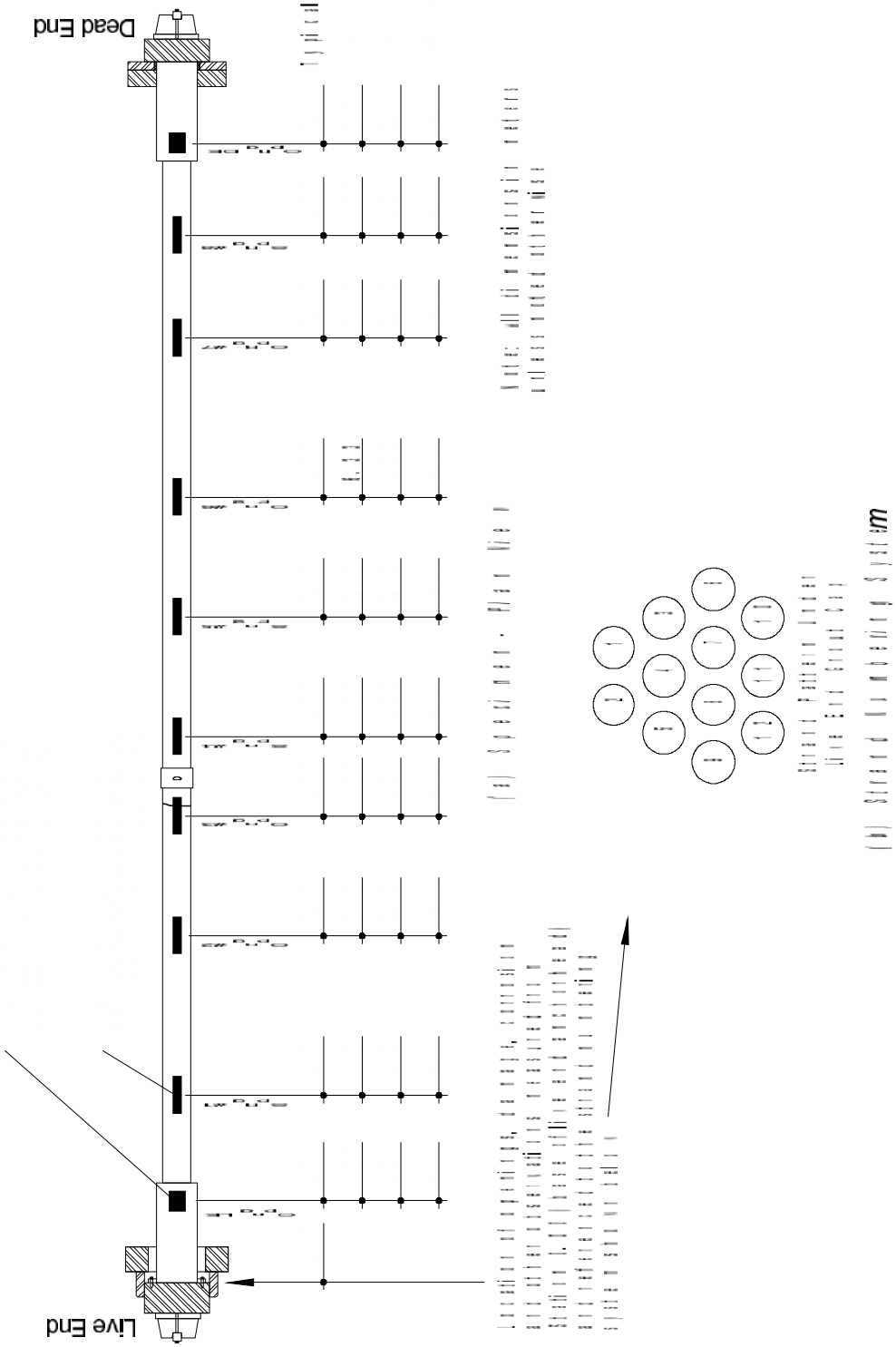

Figure 0.1 - Sheathing Breaks and Standard Referencing System for Large Scale Specimens.

specimens so that comparison of results could be made between various specimens. The reference location chosen was the base of the live end anchor head. The live end anchorage was at the bottom of the slope during injection. All measurements made on the specimen such as sheathing breaks, individual sheathing damages, and corrosion were referenced to this point. For example, if corrosion was found at 2.00 meters from the inside face of the live end the location would be designated Sta 2.00. During assembly the anchor heads were oriented so that the stand pattern was always as shown in the figure. This allowed each strand to be assigned a number based on its location in the bundle pattern.

Sheathing Breaks

The primary purpose of the accelerated corrosion test was to determine the effectiveness of the grout in providing secondary corrosion protection if the primary corrosion protection (external sheathing) is somehow damaged and the grout is exposed. Therefore, a pattern of openings or "breaks" were made in the exterior sheathing of each specimen to permit ponding of a salt solution on the surface of the exposed grout.

After the completion of the load tests a total of 10 openings were made in the sheathing on the top side of each specimen (Figure 0.1). Eight of the openings were in the free length and two were in the transition length. The openings in the free length were placed along the length at somewhat regular intervals while the transition openings were placed in the transition length near the deviator ring, mainly because this was the most accessible area of the transition. The opening dimensions and orientation were selected to mimic, to a degree, the longitudinal splits which occurred in the Luling Bridge (see discussion in Chapter One).

The openings in the free length were designated with the numbers 1 through 8 while the dead end and live end transition were designated with DE and LE, respectively. Opening 3 was placed at the joint in the grout between the first and second lifts. A grout leak occurred at the live end of LS-7 during injection of the first lift which caused the level of the grout to drop approximately 300 mm from its intended location. As a result, opening 3 for this specimen was adjusted so that it coincided with the grout joint. Opening 2 in the same specimen was moved correspondingly in the same direction. The location of opening 6 was inadvertently made in an incorrect location in LS-3. Specimens LS-1 and 6 were constructed in reaction frames which required the use of a thicker anchor plate under the anchor heads. This resulted in LS-1 and 6 being 50 mm longer than the other specimens which accounts for the slight differences in the opening locations.

Epoxy-Coated Strand (LS-6): Damage and Repair

The manufacturing process as well as the requirements and specifications for the manufacturing of epoxy-coated strand are discussed in Chapter Three. This section covers only the requirements for inspection and repair of damage. The application of intentional damages and subsequent repair of the epoxy-coated strands in specimen LS-6 are covered as well.

Specifications and Recommendations

Because epoxy-coated strand is a recent development, there is limited experience with its use. However, even though the epoxy coating used on strand is much tougher than the coating used on reinforcing bars, inspection techniques and repair of field damage are still of major concern considering the wide spread field damage problems which have been encountered in the use of epoxy-coated reinforcing bars.[66] Field damage and repair of epoxy-coated reinforcing bars has been studied extensively and there are established inspection and repair methods available to the users. One might think that the technology used in epoxy-coated reinforcing could be directly transferred to epoxy-coated strand. However, while the manufacturing process is quite similar, the epoxy-coating used for strand is much tougher than that used for bars.[79] In addition, the transportation and installation of epoxy-coated strand is quite different from bar. The strand is generally transported on reels which makes protection during handling much easier than for bars. Thus, there are really no additional handling requirements compared to a reel of bare strand. Generally, the strand is fed directly from the reel into its final position which gives the strand much less handling than a bar. Combined with the toughness of the epoxy, this makes the likelihood of damage much less than for coated bars.

In 1993, PCI Ad Hoc Committee on Epoxy-Coated Strand[94] published a committee report which gave guidance for the use of epoxy-coated strand. The report covered handling and installation of the strand so that damage is minimized. However, inspection and repair/rejection of damaged strand was not addressed.

ASTM A 882 - 92[7] gives specific recommendations for the manufacturing of the epoxy-coated strand and the continuity of the coating. Specifically, the specification requires that the coating be “free of holes, voids, cracks, and damaged areas discernible to the unaided eye” and allows for rejection of strand which does not meet these (and other) requirements. The coating may have up to two holidays (pin hole in coating not discernible to the unaided eye) per 30 meters but the holidays must be patched. It there are more holidays, then the strand must be rejected and corrective action taken to resolve the manufacturing problem. The specification goes on to say that damage due to handling is to be repaired in accordance with the recommendations of the manufacturer of the

patching material. There are no other recommendations made concerning inspection or repair procedures such as the maximum allowable area of damage past which the strand would be rejected or milestones in the construction process at which inspection of the strand would be appropriate.

Based on the lack of information on the performance of damaged epoxy-coated strand, it was decided that the strands in the epoxy-coated strand specimen would be intentionally damaged and that some of the damaged areas would be repaired using the repair kit supplied by the manufacturer.

As-Received Condition

Coating Thickness

The thickness of the epoxy coating was measured using a thumbwheel pull-off magnetic gage. The measurements were taken at approximately Sta 2.50 at the crown (Figure 0.2) of all six outer wires of each strand. The measured thicknesses are presented in Table 0.1 and indicated that the coating thickness is within tolerance allowed by ASTM A 882 - 92 which specifies coating thicknesses from 0.64 mm to 1.14 mm.

PTI *Recommendations for Stay Cable Design, Testing and Installation* requires that the nominal thickness be within the range of 0.64 to 1.00 mm. Again, all of the measured thicknesses presented in Table 0.1 are within these limits. However, the PTI specification has an optional provision that if the purchaser requires it, the strand supplier must specify a nominal thickness of coating for the size and type of strand involved. Then, a fairly tight tolerance is applied so that all strand supplied on that order must have coating thicknesses within plus or minus 0.063 mm of that nominal. This uniformity is specified to ensure that the teeth of the wedges will extend through the epoxy and seat properly. No nominal thickness was requested for the epoxy-coated strand order used in the large-scale tests. However, it was anticipated that while the supplier would select a nominal thickness, a reasonable coating tolerance would be maintained. It is noted that the average thickness for the coating on the strands was 0.78 mm (only slightly higher than the 0.76 mm thickness cited by Moore[79] and Dorsten et al[40]). If this actual average of 0.78 mm is used, only 7 of the 12 strands measured were within the tolerance recommended by the PTI specifications. In contrast, Moore and Dorsten et al cited a tolerance of ±0.13 mm with a nominal thickness of 0.76 mm. The source of these requirements was not given. If the coating thicknesses are compared using this tolerance then all of the measured thicknesses satisfy the cited requirements.

Importantly, there were no problems experienced with the seating of the wedges.

Table 0.1 - Summary of Epoxy Coating Thickness as Received (mm).

Strand	Six readings; one at crown of each outer wire*						Average
1	0.81	0.86	0.91	0.81	0.74	0.71	0.81
2	0.86	0.76	0.86	0.86	0.74	0.86	0.83
3	0.86	0.81	0.86	0.76	0.76	0.74	0.80
4	0.86	0.84	0.81	0.76	0.76	0.86	0.82
5	0.84	0.81	0.76	0.71	0.71	0.74	0.76
6	0.76	0.86	0.86	0.76	0.74	0.74	0.79
7	0.76	0.81	0.81	0.76	0.76	0.71	0.77
8	0.74	0.79	0.81	0.74	0.76	0.71	0.76
9	0.84	0.79	0.79	0.74	0.81	0.79	0.79
10	0.76	0.81	0.84	0.76	0.66	0.69	0.75
11	0.69	0.76	0.81	-	-	-	0.76
12	0.71	0.79	0.81	0.81	0.79	0.71	0.77
Average Coating Thickness							0.78

* Reading taken at 2.4 m from live end anchor head.

Cavities

A thorough visual inspection of the coating was performed prior to assembly in which cavities were found in the epoxy at somewhat regular intervals (Figure 0.3). The cavities would not have constituted holidays because the underlying strand was not exposed. Several selected locations of the strand which had these cavities were sectioned and the thickness of the coating at the cavity was measured with a portable microscope. The minimum thickness found was 0.13 mm and generally ranged between 0.13 mm and 0.26 mm. The cavities were *only* found on the coated and filled strand. After a thorough examination it was determined that there were no cavities on the coated strand. The minimum thickness allowed by ASTM A 882 - 92 is 0.64 mm. A brief survey indicated that there were about 6 to 26 of these cavities per meter of length of strand with the average being closer to six. The cavities were found only in the area between the outer wires and not on the crown of the strand.

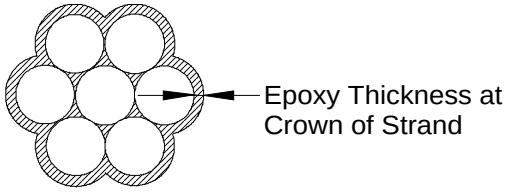

Figure 0.2 - Crown Thickness of Epoxy-Coated Strand.

The manufacturer indicated that the cause of the cavities was a problem with the manufacturing process which can be alleviated by adjusting the process.[46] The reason that the cavities form can be illustrated by examining Figure 0.4. The bare strand is de-stranded prior to entering the fluidized bed of electrically charged particles. The particles are attracted to the grounded strand and melt onto the surface of each individual wire with approximately the same coating thickness (Figure 0.4a). While the epoxy is still fluid, the wires are re-stranded, creating a temporary geometric incompatibility. During closure, the outside wires approach the center wire,

where an air pocket may form in the epoxy in the interstitial space (Figure 0.4b). If the process parameters are not adjusted optimally then the air bubble leaves a cavity at the epoxy surface as it exits the epoxy (Figure 0.4c).

As noted previously, the cavities were only found between the outer wires and not at the crown of the strand. The manufacturer indicated that the minimum coating thickness specified in ASTM A882 includes an allowance for abrasion and damage; because the cavities are located between the wires and not at the crown, they are protected from abrasion and damage.[46]

Figure 0.3 -Section Through Epoxy-Coated and Filled Strand at a Cavity.

The manufacturer also indicated that a coating thickness as low as 0.17 mm on a single wire is able to meet the "prequalification tests" of ASTM A882 using the same epoxy formulation as used on the 7-wire strand.[46] For these reasons, the manufacturer believes that these cavities are not cause for rejection of the epoxy-coated strand.[46]

Intentional Damage and Repair of Coating

Damage and Repair Matrix

Three different sizes of coating damage were selected to determine the influence of damage area on corrosion. The smallest consisted of a cut made to the surface of the strand with a utility knife. This

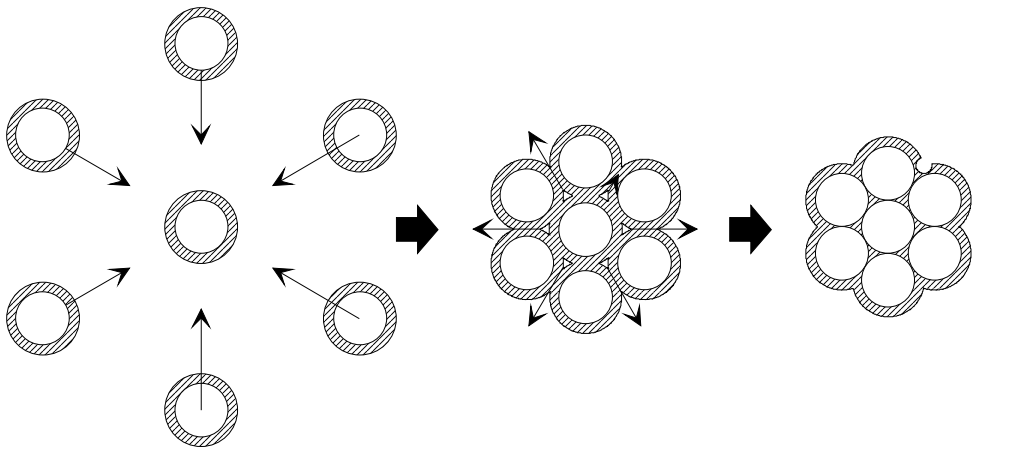

Figure 0.4 - Cause of Cavity in Surface of Epoxy Coated Strand.[46]

exposed a small area of strand at the base of the cut. The other two opening were made by removing a square section of epoxy with the arbitrarily chosen sizes of 3.2 mm and 6.4 mm per side. The exposed areas of strand are shown in Figure 0.5.

A systematic approach was taken to the layout of the damaged areas (Table 0.2). The top layer of strands (1 and 2), one interior strand (4), and two strands on the bottom layer (10 and 12) were selected for damage at the sheathing openings. The damage was varied in intensity along the length with the live end half of the specimen left unrepaired and the dead end half of the specimen repaired.

Figure 0.5 - Three Sizes of Damage Made to Epoxy Coating: Cut, 3.2-mm square, and 6.4 mm square (middle). Repaired Damages Shown at Bottom.

Several of the strands were also damaged midway between the openings (Table 0.3). Since strands 1 and 2 were extensively damaged at all of the openings, they were only damaged between openings in two locations. The top layer of strands were the most accessible to the chlorides introduced at the openings. Thus, the strands most likely to have corrosion occur between an

Table 0.2 - Summary of Intentional Damage to LS-6 and LS-8 Under Sheath Openings.

Strand*	Opening (Station)									
	LE (0.62)	1 (1.42)	2 (2.64)	3 (3.56)	4 (4.17)	5 (5.08)	6 (6.02)	7 (7.24)	8 (7.98)	DE (8.74)
1	6.4	C	3.2	6.4	-	CR	3.2R	6.4R	-	6.4R

2F	6.4	C	3.2	6.4	-	CR	3.2R	6.4R	-	6.4R
3	-	-	-	-	-	-	-	-	-	-
4F	6.4	C	3.2	6.4	-	CR	3.2R	6.4R	-	6.4R
5F	-	-	-	-	-	-	-	-	-	-
6	-	-	-	-	-	-	-	-	-	-
7	-	-	-	-	-	-	-	-	-	-
8F	-	-	-	-	-	-	-	-	-	-
9F	-	-	-	-	-	-	-	-	-	-
10	6.4R	-	6.4R	3.2R	CR	-	6.4	3.2	C	6.4
11	-	-	-	-	-	-	-	-	-	-
12F	6.4R	-	6.4R	3.2R	CR	-	6.4	3.2	C	6.4

* Strands with F indicate coated and filled for LS-6.

Key to Table 0.2 and Table 0.3:
C - Single cut.
3.2 - 3.2-mm square opening.
6.4 - 6.4-mm square opening.
R - indicates repaired damage.

Table 0.3 - Summary of Intentional Damage to LS-6 and LS-8 Between Sheath Openings.

Strand*	Between Opening: (Station)						
	1-2 (2.03)	2-3 (3.10)	3-4 (3.99)	4-5 (4.62)	5-6 (5.54)	6-7 (6.63)	7-8 (7.60)
1	-	6.4	-	-	-	6.4	-
2F	-	6.4	-	-	-	6.4	-
3	6.4	6.4	6.4	6.4	6.4	6.4	6.4
4F	-	-	-	-	-	-	-
5F	6.4	6.4	6.4	6.4	6.4	6.4	6.4
6	6.4	3.2	C	-	CR	3.2R	6.4R
7	C	C	C	-	CR	CR	CR
8F	C	C	C	-	CR	CR	CR
9F	6.4	3.2	C	-	CR	3.2R	6.4R
10	-	-	-	-	-	-	-
11	6.4	6.4	6.4	6.4	6.4	6.4	6.4
12F	-	-	-	-	-	-	-

* Strands with F indicate coated and filled for LS-6.

opening would be the top layer. In addition, three other strands were selected to have the maximum size damage between each opening. They were strands 3 and 5 which are one layer from the top on the outside and strand 11 which is in the middle of the bottom layer. These were the other two areas which could possibly have had a significant exposure to chlorides introduced at the openings. It was hypothesized that if the solution did travel, it would seep along the length of the stay between the

sheath and outside surface of the grout. Strands 6 and 9 had varying degrees of damage while strands 7 and 8 had only cuts. In these four strands the damaged areas in the dead end half of the stay were repaired.

As much as possible, the damages in the coated strand were mirrored by the damages in the coated and filled strand.

Repair of Damages

Armstrong Patch Kit M-181 along with instructions for use were provided by the strand manufacturer for repair of damaged areas and patching the cut ends. The patch kit was manufactured by Morton Thiokol, Inc., Armstrong Products Company. It is described as a two-part epoxy system which is used to patch steel cable coated with C-701 (epoxy-coating designation) and is to be applied in accordance with the following instructions:

1. Clean areas requiring repair to remove grease, oil, and dirt. Loose or damaged coating should be removed with surface grinding prior to cleaning.
2. Mix material 1:1 by volume and blend thoroughly until a uniform color is achieved.
3. Apply by brush, roller, or spray. Application below 12.8°C is not recommended. If necessary, thin with xylol.
4. Coating will be tack free in two to three hours at 25°C, and full cure is achieved in three to five days at 25°C. Care must be exercised in handling parts before they are fully cured.

These instructions were followed in the repair of those intentionally damaged areas selected for repair. Immediately after mixing it was noted that the epoxy was somewhat watery which resulted in a very thin coat of epoxy over the strand when the material had cured. The specifications require that the repaired area should meet the requirements of the original coating including thickness. However, to achieve this would have required several coats of repair material. It is unlikely that more than one coat would be applied in the field so the repair was made with one coat.

Repair of Cut Ends

The ends of the strands were repaired as shown in Table 0.4. The patch repair method consisted of painting the patching compound onto the end of the strand in accordance with the following procedure:

1. Prepare patching compound by mixing equal parts a “Part A” and “Part B” in a clean metal container.
2. Blend thoroughly until a uniform color is achieved.
3. Allow mixed compound to set at room temperature until compound starts to thicken, approximately 2 hours.
4. Grease, oil and dirt should be removed from cable ends prior to applying the patching compound.
5. Apply compound liberally to cable ends with a small bristled brush (see Figure 0.6).
6. Allow patching compound to cure.

The procedure as indicated was followed when patching the ends of the strands. However, the material did not “thicken” in two hours as suggested by the instructions. The patch was applied at two hours after the epoxy was mixed which resulted in a rather thin coat of epoxy over the ends. The material actually took approximately six hours to thicken to a state which would give a thick coating.

The caps were also applied in accordance with the manufacturer’s instructions:

1. Fill the Flo-Cap approximately one-third full of the epoxy patching material.
2. Insert the strand end approximately two-thirds the depth of the Flo-Cap. The patching compound will ooze out of the cap sealing the interstices of the cable.
3. Allow the patching compound to cure.

The instructions were followed as written. The capping was carried out immediately after the epoxy was mixed since the instructions did not give a time frame. This is likely how it would be done in the field.

Table 0.4 - Techniques Used to Repair Cut Ends of Strand.

Repair	Live End		Dead End	
	Filled	Unfilled	Filled	Unfilled
Patch	2, 12	1,10	2, 12	1 10
Cap	4, 9	3, 7	4, 9	3, 7
None	5, 8	6, 11	5, 8	6, 11

Figure 0.6 - Repair of Cut Ends of Epoxy-Coated Strands.

Greased and Sheathed Strand (LS-8): Damage and Repair

The manufacturing process as well as the requirements and specifications for the manufacturing of greased and sheathed strand are discussed in Chapter Three. This section covers only the requirements for inspection and repair of damage. The application of intentional damages and subsequent repair of the greased and sheathed strands in specimen LS-8 are covered as well.

Specifications and Recommendations

PTI *Recommendations for Stay Cable Design, Testing and Installation* indicate that during the manufacturing process an owner's representative shall be given free access to the manufacturing process to inspect the greased and sheathed strand for compliance with the specifications.[28] In addition, "Any damaged polyethylene sheath on the strand shall be rejected. At the manufacturer's option, such strand shall be replaced or, alternatively, may be stripped of sheathing, recleaned, resheathed and resubmitted for acceptance testing including fatigue test in accordance with the requirements of this specification." This provides a specific method of damage control at the manufacturing facility.

However, the recommendations also indicate that upon inspection prior to installation "it should be expected that sheathed strands will be completely free of damage to the sheathing. If any damage is found, a qualified engineer shall determine either repair of the sheathing, or replacement of the strand." There are no specific recommendations for repair methods. In addition, the specification allows "a certified engineer" to determine the course of action and not the owners representative.

PTI *Specification for Unbonded Single Strand Tendons* requires that the sheathing shall be inspected for damage.[92] In non-corrosive environments small damaged areas are acceptable. However, in corrosive environments "damaged areas shall be repaired by restoring the corrosion preventive coating in the damaged area, and repairing the sheathing. Repairs of sheathing shall be watertight, and must be approved by the engineer of record." A repair method is suggested in which a tape with moisture-proof adhesive is used. It is recommended that the tape be wrapped around the sheathing at least twice.

As-Received Condition

PTI *Recommendations for Stay Cable Design, Testing and Installation* require a minimum thickness of 1.00 mm for the sheathing. The mill report gave the following characteristics for the sheathing:

	Mill Certificate	**PTI Recommendations**
• Melt Index:	1.4	1.0 maximum
• Density:	0.950 g/cm^3	0.941-0.955 g/cm^3
• Tensile Yield:	20.7 MPa	20.7- 31.1 MPa

These were all within the tolerances allowed by the PTI recommendations except for the melt index. The grease was certified to be in compliance with the requirements for corrosion preventive coatings specified by PTI *Specification for Unbonded Single Strand Tendons*.

Since the sheathing is removed at the anchor head there is no need to tightly control the tolerances on the sheathing. Measurements were not taken of the sheath thickness using the magnetic pulloff device. As a substitute, several random samples were selected from the strand supplied for specimen LS-8. The strands were cut and the thickness of the sheathing was measured with a portable microscope. The thickness ranged from a minimum of 1.11 mm to a maximum of 2.20 mm which satisfies the PTI Recommendations.

Intentional Damage and Repair of Sheathing

Based on the PTI specifications for unbonded tendons and discussions with VSL personnel, a damage repair systems was used which consisted of the application of tape with moisture proof adhesive.[69] The tape selected was Scotch brand No. 838 "Tedlar" Plastic Film tape as manufactured by 3M. The tape was described as a "Tedlar" tape with an acrylic adhesive developed for weather-resistant applications. Possible uses listed by the manufacturer were outdoor seals of building panels and similar severe exposure applications. Physical properties were given as follows:

• Adhesion to Steel	46 N/100 mm	ASTM D-3330
• Tensile strength at break:	420 N/100 mm	ASTM D-3759
• Elongation at break:	194%	ASTM D-3759
• Total tape thickness:	0.0864 mm	ASTM D-3652
• Temperature use range:	-72°C to 107°C	

The damage sizes and patterns were identical to that used on the epoxy-coated strand (see Table 0.2 and Table 0.3). The method of repair was: to cut and remove the section of sheathing; fill exposed space with grease (salvaged from unused strand); wrap area once with tape using an overlap that resulted in a total of two layers of tape covering the sheathing at any location; wrap the same area in the opposite direction in the same manner. Thus, at any location, the sheathing was covered by 4 layers of tape. The repair extended approximately 30 mm beyond the damage in each direction.

Test Setup and Procedure

Each reaction frame was placed in the prone position in the equipment storage building at Ferguson Structural Engineering Laboratory for the duration of the corrosion test as well as post-mortem examination. After the reaction frame had been moved into place, the sheathing openings were traced onto the sheathing for cutting. Photographs were taken of the sheathing prior to cutting the openings to retain a record of the crack locations and identification numbers.

A router was used to cut a trough tracing the outline drawn on the sheathing. The plunge depth of the router was set so that a thin layer of PVC remained between the bottom of the router bit and the grout surface. A utility knife was then used to cut the rest of the thickness of PVC. This procedure minimized damage to the grout surface during removal of the PVC. Acrylic dams were cut to fit the outline of each opening and were fastened to the sheathing using silicone caulk (Figure 0.7). After the caulk had cured the ponding of the salt solution was initiated. The time from removal of the sheathing to the application of the salt solution was generally five days to a week.

Figure 0.7 - Acrylic Dams for Ponding Salt Solution on Surface of Grout.

A solution of 5% (by weight) sodium chloride was mixed using tap water. Prior to initiating the first wet cycle, photographs were taken of the surface of the grout. The surface of the grout was moistened with salt solution and the half-cell potential was measured. The dam was filled with solution to a depth of approximately 25 mm with salt solution and the half-cell potential was measured again.

One week after the first wet cycle was started, the axial load test apparatus was installed on specimens LS-2, 4, and 5 through 8 and additional load was applied. The axial stress was increased from $0.30F_{ULT}$ to $0.45F_{ULT}$ for ten cycles and was held for one minute at each load level. After the cycles were completed the load level was returned to $0.30F_{ULT}$. Specimens LS-1 and LS-3 remained at $0.30F_{ULT}$ throughout the duration of the accelerated corrosion test.

Two weeks after the first wet cycle was initiated the first dry cycle was started. With the solution still in the dam, the half-cell potential was measured. The solution was removed from the dam and the half-cell potential was measured again. Photographs were taken of the grout surface after the solution had been removed.

There were a total of three wet cycles and three dry cycles performed, alternately, for a total test period of three months.

The equipment storage building where the specimens were housed during the corrosion test was not climate controlled other than small gas heaters in isolated locations. In addition, there was no insulation in the roof or walls. As a result the temperature inside the building varied with the ambient conditions. The specimens were housed in the building for a total of approximately four months. For three of the months the specimens were undergoing the accelerated corrosion test. The remainder of the time was specimen preparation and the delay between the end of the corrosion test and post-mortem examination. The monthly average of the daily temperatures are shown in Table 0.5. Austin has a fairly temperate climate and is not subject to wide seasonal swings in temperature.

Therefore, temperature fluctuations were not considered to have significantly affected the results of the corrosion tests.

Effect of Sheathing Breaks

Prior to the application of additional axial load and cutting openings in the sheathing, the grout remained uncracked, as determined by visual observations made through the transparent sheathing. On specimens LS-1 and 3 (no additional load applied) it was found following the cutting of the openings in the sheathing that the exposed area of grout dried and localized shrinkage cracking occurred. The cracks were oriented both perpendicular and parallel to the axis of the stay. Depending on the ambient humidity, the cracking usually occurred within 2 to 3 days after the sheathing had been opened locally and only occurred in and around the opening in the sheathing. Selected cracks were measured and it was found that the crack widths were in the range of 0.03 to 0.09 mm in width.

On specimens LS-2, 4, and 5 through 8, the sheathing openings were made after the load test had been performed. While the spacing of the cracks varied depending of the type of strand used, in all cases cracking perpendicular to the stay axis developed during the axial load test. When the load was reduced back to dead load level, the cracks closed so that they were not visible to the unaided eye. When the openings in the sheathing were made for the corrosion test, these pre-

Table 0.5 - Ambient Temperature Conditions for Austin Area.[81]

Specimen	Month	Monthly Average of Daily Temperature		
		High	Low	Average
LS-1 and LS-3	first	22	7	14
	second	18	8	13
	third	17	7	12
	fourth	19	7	13
LS-2 and LS-4	first	23	12	18
	second	28	15	21
	third	29	19	24
	fourth	35	24	29
LS-5	first	18	7	13
	second	19	8	14
	third	22	12	17
	fourth	27	14	20
LS-6	first	35	23	29
	second	32	20	25
	third	28	17	22
	fourth	23	13	18

LS-7	first	19	9	14
	second	18	7	13
	third	19	8	14
	fourth	22	12	17
LS-8	first	23	13	18
	second	19	9	14
	third	18	7	13
	fourth	19	8	14

existing cracks opened to widths similar to specimens LS-1 and 3. Figure 0.8 shows the typical progression of crack growth after removal of the sheathing.

Grout Precompression Test

Precompressed of pc grout in stay cables has occasionally been used to improve the effectiveness of the grout in providing corrosion protection.[110] This procedure requires that the stay be stressed to a level of dead load plus anticipated live load (3% to 8% of F_{ULT} depending on the type of bridge[44]) just prior to grouting. After the grout has been injected and is sufficiently cured the load is lowered back to dead load level.

(a) Full Width of Sheath Opening Immediately After Sheath Removal.

(b) Close-up of Left Side of Sheath Opening Immediately After Sheath Removal.

(c) Close-up of Left Side of Sheath Opening 1 day After Sheath Removal.

(d) Close-up of Left Side of Sheath Opening 5 days After Sheath Removal.

Figure 0.8 -Grout Shrinkage Cracks. Longitudinal Cracks Visible in (c); Longitudinal and Transverse Cracks Visible in (d).

The precompression is intended to prevent the grout from going into tension under normal traffic loads, thus preventing cracking of the grout. If the sheathing is intact, then the grout (and the main tension element) is protected from the environment and the question of grout cracking is irrelevant. However, if the sheathing is broken the question becomes: does the precompressed grout provide better protection than grout that is not?

Test Method

Testing precompression of grout was not in the original scope of the series so it could not be thoroughly investigated as a viable method for improving corrosion protection. However, as an alternative, an abbreviated test of precompression was conducted on LS-5 (Bare strand with TCP and silica fume grout).

Consistently, it was found in all other specimens of large-scale test series that when the sheathing was broken and the grout was exposed to the outside air, the grout would shrink and crack. The concept of this variation in the standard test was to precompress the grout in LS-5 after the load tests had been completed but before the openings in the sheathing had been made. After the grout had been precompressed, the sheathing would be removed in only one location. This area would

then be monitored for grout shrinkage and cracking. After a few days the stress level would be brought back to the normal test level and the regular test procedures would be continued. This gave a qualitative measure of the effectiveness of the precompression while affecting only one location in the large-scale specimen. The following procedures were used to conduct the test of precompression:

- Specimen LS-5 was assembled, stressed and grouted using the standard procedures. Lateral and axial load tests were conducted.
- At the end of the load test the load was reduced from $0.30F_{ULT}$ to $0.24F_{ULT}$. This would correspond to the level of precompression applied if the expected live load on the specimen was $0.06F_{ULT}$.
- The sheathing was removed at opening 4 using same method as for the other openings.
- Crack widths were measured immediately and photos were taken of the exposed surface of the grout. At this time the cracks were not visible to the unaided eye.
- Crack widths were measured and photos were taken again 24 hours later. New cracks were noted and measured.
- Crack widths were measured and photos were taken again 5 days after the sheathing was removed.
- The load in the specimen was returned to $0.30F_{ULT}$ and the accelerated corrosion test was resumed.

Results

The progression of crack growth which occurred after the sheathing was removed was very similar to that of the specimens in which the grout was not precompressed. In the initial examination of the grout surface through the portable microscope, a total of ten pre-existing cracks (due to the axial load increase from $0.30F_{ULT}$ to $0.45F_{ULT}$) were present as single lines with no visible width (the cracks appeared about as wide as the divisions in the scale of the microscope). The cracks were oriented perpendicular to the stay axis and were fairly evenly spaced. Within 24 hours the pre-existing cracks had grown to a width of 0.025 mm. Two new cracks perpendicular to the stay axis had formed and a single crack parallel to the axis had formed which extended the full length of the opening. These cracks also had a crack width of 0.025 mm. At the end of five days the perpendicular crack widths were in excess of 0.05 mm in width while the longitudinal crack was as large as 0.08 mm in some locations. No other new cracks had formed.

This experiment indicated that the precompression was ineffective in controlling local shrinkage cracking of the grout.

Visual Monitoring During Test

During the accelerated corrosion tests the surface of the grout was monitored periodically for the appearance of corrosion or other significant events. Corrosion product appeared on the surface of the grout during the accelerated corrosion test in specimens LS-1 through LS-4 (standard grout), LS-5 (silica fume grout), and LS-8 (greased and sheathed). In all instances, the appearance of corrosion product was a definite indication that significant corrosion activity was occurring on either strand 1 or 2 (top layer of strand) just below the surface of the grout.

Half-Cell Potential Readings

Half-cell potentials were taken with a saturated calomel reference electrode (SCE) during each cycle change at each sheathing opening using the arrangement shown in Figure 0.9. There were two sets of readings taken at each cycle change. One set of readings (denoted as "dry") was taken on the grout surface at three locations per sheathing opening and another set of readings (denoted as "wet") was taken with the electrode submerged in the salt solution. Procedures outlined in ASTM C 876-87[9] were used to take readings. ASTM C 876-87 suggests the use of a wetted sponge on the end of the electrode to maintain good electrical contact with the underlying concrete. However, this was not necessary because the surface of the grout was wetted with the salt solution prior to taking the reading and the porous tip of the electrode was placed directly onto the surface of the moistened grout for the reading.

Average, high, and low values of the dry half-cell potential (HCP) readings at the beginning of the first and last wet cycles are presented in Table 0.6. The moisture content of the grout at that time was in equilibrium with the ambient air humidity. Similarly, Table 0.7 shows the dry HCP values taken at the ends of the first and last wet cycle when the grout was in a saturated state after having been soaked in salt solution for two weeks.

When the HCP values in the tables are compared it becomes obvious that there is a large difference between the readings. González, et al. found that the difference in the half-cell potentials between saturated and dry concrete of similar properties can be as high as 700 mV.[54] Consequently, half-cell potential measurements can vary widely depending on the moisture content of the concrete or grout. As the moisture content changes so does the electrical resistance of the circuit formed when the HCP measurement is taken. This explains why the values of HCP measured on the saturated grout are more negative than those measured on the dried grout. The relative change of the

wet or dry value with time is of some interest because it can indicate the change in the level of corrosion activity with time.

ASTM C876-87 recommends using the method of interpretation shown in Table 0.8 to determine the probability of corrosion being present. Unfortunately, the interpretation was based on tests conducted on concrete samples and is not necessarily appropriate for grout. However, there was no information found in the literature which could be used to interpret the results of the half-cell test on grout. Anodic polarization tests conducted as a part of this test program are reported in Chapter Six and gave HCP in the range of -190 to -210 mV_{SCE} for noncorroding single strands in cracked portland cement grout. While this does not agree totally with the standard interpretation of the HCP, it does give some confidence that HCP above this range indicate that significant corrosion is probably not present.

The half-cell potentials for the entire test period are included in Appendix C. Analysis and discussion of the half-cell tests are presented in Chapter Nine.

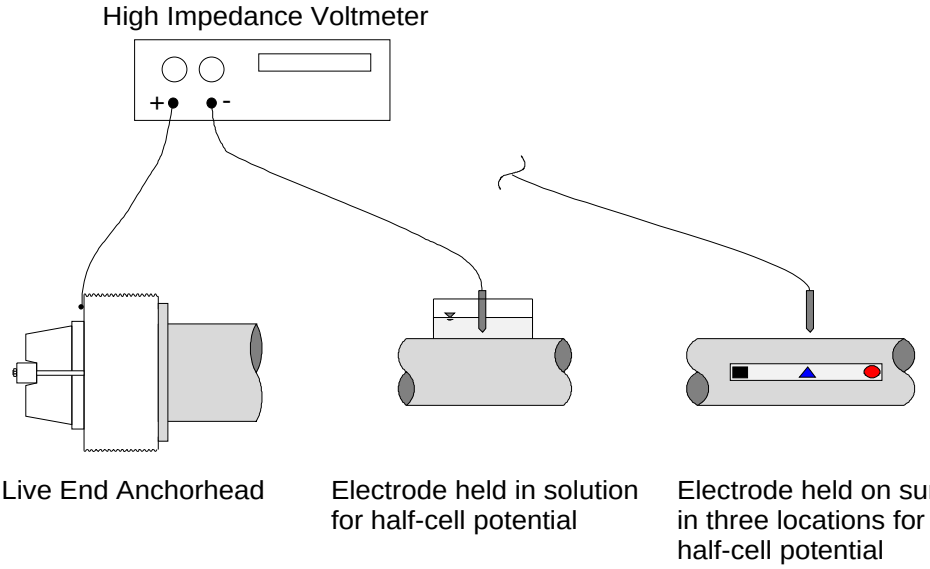

(a) Measurement Technique

(b) Half-cell Potential Measurement on "Dry" Grout Surface.

Figure 0.9 - Large Scale Specimen - Half-Cell Potential Measurement.

Table 0.6 - Summary of Half-Cell Potentials Measured at the Beginning of First and Last Wet Cycles (mV_{SCE}).

Specimen	Potential at Beginning of First Wet			Potential at Beginning of Last Wet		
	Average	High	Low	Average	High	Low
LS-1	-140	-120	-180	-210	-130	-370
LS-2	-120	-90	-160	-220	-120	-370
LS-3	-140	-120	-180	-270	-140	-460
LS-4	-110	-80	-150	-270	-160	-380
LS-5	-130	-110	-160	-240	-170	-350
LS-6	-170	-150	-190	-300	-210	-440
LS-7	-520	-390	-710	-730	-660	-920
LS-8	-150	-130	-180	-380	-220	-480

Table 0.7 - Summary of Half-Cell Potentials Measured at the End of First and Last Wet Cycles(mV_{SCE}).

Specimen	Potential at End of First Wet			Potential at End of Last Wet		
	Average	High	Low	Average	High	Low
LS-1	-300	-150	-710	-570	-460	-810
LS-2	-290	-120	-540	-600	-490	-810
LS-3	-580	-220	-800	-590	-420	-750
LS-4	-690	-540	-810	-660	-460	-830

LS-5	-680	-510	-930	-690	-630	-780
LS-6	-650	-420	-970	-670	-480	-920
LS-7	-1060	-1030	-1130	-1060	-1040	-1070
LS-8	-350	-300	-470	-380	-210	-480

Table 0.8 - ASTM C876-87 Interpretation of Results of Half-Cell Potential.

Probability of Corrosion	Measured Half-Cell Potential (mV)	
	Saturated Calomel Electrode SCE	Copper-Copper Sulfate, CSE
Less than 10% if potential is less negative than:	-130	-200
More than 90% if potential is more negative than	-280	-350
Uncertain if potential is between	-130 and -280	-200 and -350

Visual Inspection and Rating Corrosion

Following the completion of the accelerated corrosion tests, the specimens were disassembled and the components were visually inspected for corrosion. When corrosion was found on a strand it was rated according to the outline given in Table 0.9 which was adapted from Poston's work on the corrosion of prestressing strands in bridge decks.[93] The rating system was used to quantitatively compare the extent of corrosion between specimens.

There were two different corrosion phenomena evaluated. The first was the corrosion on the outside of the strand. This generally occurred to the greatest extent on the outside of one of the two strands in the top layer which were nearest to the opening in the sheathing. The corrosion would typically not follow a single wire around the strand but instead would travel along the length of the strand with the heaviest corrosion occurring on the side of the strand facing the sheathing opening. The second type of corrosion evaluated occurred between the outer six wires and the center wire. This corrosion was labeled "interstitial corrosion." Typically this corrosion would travel along the strand, sometimes for the full free length. The corrosion was mostly confined to one or two of the interstitial spaces once it had initiated.

Other components of the specimens were evaluated in terms of the amount of corrosion found during the post-mortem evaluation. These components consisted of anchor heads, deviator rings, and prestressing wedges. However, instead of applying a rating system to these items, they were visually rated and descriptive summaries were made of the level of damage.

Post-Mortem Examination

The post-mortem examination consisted of alternately taking visual observations and disassembling the specimen. It was necessary to proceed with caution with the disassembly for two reasons. The first was that some item of interest might be destroyed if the specimen was taken apart too hastily. The other reason was that the behavior of the complete system was being examined. Therefore, every component had to be closely inspected. While the disassembly of each specimen was similar, there were several minor adjustments made in the process before the most efficient and careful method was determined. The following is an outline of the procedure used for disassembly:

- Grout was removed and the strand bundle was visually inspected and rated between Sta 1.22 to 8.15. Samples of grout were taken for chloride and carbonation tests. Carbonation tests were performed immediately while chloride tests were performed at a later date.

Table 0.9 - Evaluation and Rating System for Corrosion Found on Strand During Visual Inspection (adapted from Poston[93])

Code	Meaning	Description	Rating
		Exterior Surfaces	
NC	No Corrosion	No evidence of corrosion	0
D	Discoloration	No evidence of corrosion, but some discoloration from original color	1
VL	Very Light	Surface corrosion less than 6-mm long at a location; no pitting	2
L	Light	Surface corrosion greater than 6-mm long at a location but less than 12-mm long; no pitting	3
M	Medium	Surface corrosion greater than 12-mm long at a location but less than 25-mm long, and/or shallow pits in the early stages of formation	4
H	Heavy	Surface corrosion greater than 25-mm long, but less than 50 mm long at a location and/or presence of pitting	5
VH	Very Heavy	Surface corrosion greater than 50-mm long at a location and/or presence of deep pitting	6*(L/50) L=length of corrosion

Interstitial Spaces			
L	Light	Surface corrosion less than 50-mm long; no pitting	2
M	Medium	Mild pitting corrosion less than 50-mm long	4
H	Heavy	Heavy pitting corrosion 50-mm long or greater	6*(L/50) L=length of corrosion

- Strand bundle was torch-cut at approximately Sta 8.15. Live end was pulled out from frame and the strands were saw-cut at Sta 1.22. This left the transition areas intact for post-mortem examination after removal from frame (Figure 0.10).
- Strands were examined and rated again in the areas that were not previously visible between Sta 1.22 and 8.15, especially the interstitial spaces between the outer and inner wires.
- Sheathing and grout were removed in length A (Figure 0.10). Exposed strands were saw-cut at location 1 and the strands were examined and rated.
- Sheathing and grout were removed in length C and a saw-cut was made in 2 and 3.
- Strands in length C were examined and rated.
- Deviator ring was saw-cut (length B) at diametrically opposed locations and the short strand bundle was removed for examination. The deviator was examined as well.
- Grout caps and underlying grout were removed.
- Hydraulic ram and strand coupler were used to pull individual strands and wedges from anchor head. The strand and wedges usually came out intact and undamaged for subsequent examination.

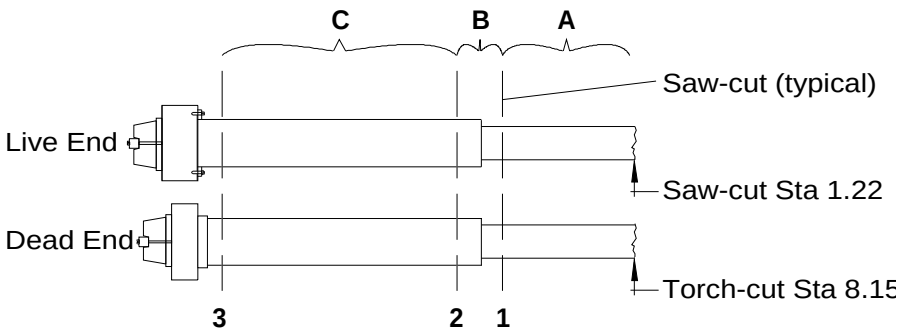

Figure 0.10 - Post-Mortem Examination of Transition Region.

Detailed records were kept of the findings and observations noted during the post-mortem examination. A summary of these observations is presented in Appendix C. The summary is divided into four components. The first component is the listing of corrosion observations and ratings for the exterior of the strands. The second component is the listing of corrosion observations and ratings for interstitial corrosion of the strands. These two lists were compiled using the rating systems shown in Table 0.9. The third component is the description of the corrosion on the prestressing wedges and at the strand/wedge interface. The final component is the description of corrosion on the anchor heads and deviator rings. In addition to observations recorded, photographs were taken of unusual or interesting findings.

Grout

Removal of the grout was initiated at Sta 1.22 and continued along the stay free length to Sta 8.15. Grout was removed carefully from the strand bundle using a hammer and cold chisel. On all of the specimens except LS-7 (Galvanized) the grout was removed with very little effort. It was observed that each of the specimens had cracks in the grout at regular intervals (20 mm to 130 mm depending on the type of strand used) which formed “disks” of grout. These disks of grout were easily removed by striking lightly with a hammer. In areas where gentle removal was necessary the chisel was used to remove small pieces at a time.

The grout in LS-7 (galvanized) was much more difficult to remove because it adhered to the zinc layer on the surface of the strand. Zinc is very reactive in the presence of the fresh cement paste. This reaction must have caused some type of bond between at the grout/strand interface. When the surface of the grout was struck with the hammer the grout would fracture away from the surface so that a thin layer of grout was left on the strand. Further hammering only damaged the surface of the strand. The best way to remove the grout was to detension the stay with the grout in

place. This removed the grout fairly cleanly from the surface of the strand. Unfortunately, this method of disassembly did not allow chloride and carbonation samples to be taken.

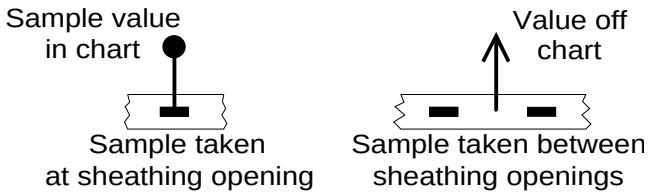

Figure 0.11 - Legend for Chloride Content Charts.

Joint Between Grout Lifts

The large-scale specimens were placed in a sloped orientation, and the grout was injected in two lifts of approximately equal lengths. In the planning stages of the test program, the grout joint at the interface between the two lifts was thought to be an area where the corrosion protection of the grout would be compromised. On the contrary, post-mortem examination of the specimens revealed that the joint was "tight" (no voids or other discontinuities were found).

Chloride Tests

To the extent possible, samples of grout were preserved during the examination process to be tested later for acid-soluble chloride content. The grout samples were taken from the top and bottom side of the stay cross-section at each opening in the sheathing and midway between openings. The results are presented graphically in Figure 0.12 through Figure 0.16. The legend for the charts is shown in Figure 0.11. In addition, samples were taken from the grout between strands under the deviator rings and also from the grout under the grout caps. These results are presented in Table 0.10. Note that a chloride content reading below 0.005% indicates that no detectable chlorides were present in the sample.

Caution is necessary when interpreting the results of the chloride tests for several reasons. The first reason is that the sampling method was somewhat unconventional. Normally, concrete is sampled by drilling to the desired level and the pulverized sample is then tested. This gives a reasonable measure of the chlorides that have permeated through the concrete to that depth. In cracked concrete the drill can be centered over the crack and drilled to the desired sample depth. Even in grout samples taken from post-tensioning ducts the grout can be drilled out to the specified depth as in concrete sampling. However, this sampling method was not possible because the grout layer was too thin to be drilled. Consequently, the grout was sampled by chipping small sections from the area where the grout was in contact with the strand, presumably to obtain the chloride level at the surface of the strand. Pieces of the grout in the area of the strand were then chipped, pulverized, and tested for acid soluble chlorides. This method of sampling may have led to contamination of samples used to test for acid soluble chlorides. Because of this potential for contamination the results of the chloride tests should be looked at as approximate.

Table 0.10 - Chloride Test Results at Grout Caps and Deviator Rings(% cement weight).

Specimen	Live End		Dead End	
	Grout Cap	Deviator Ring	Grout Cap	Deviator Ring
LS-2	0.004	n/s	n/s	n/s
LS-4	0.005	n/s	0.13	n/s
LS-5	0.012	0.14	0.026	0.11
LS-6	n/s	0.35	0.0078	0.22
LS-7	0.005	0.13	0.015	n/s
LS-8	no grout cap	0.15	no grout cap	0.39

n/s = not sampled

Originally the chloride test was not going to be conducted because of the irregular sampling method. In fact tests were not conducted on LS-1 and 3 for this reason. However, it was decided that the chloride test would at least indicate the *presence* of chlorides. Even though the

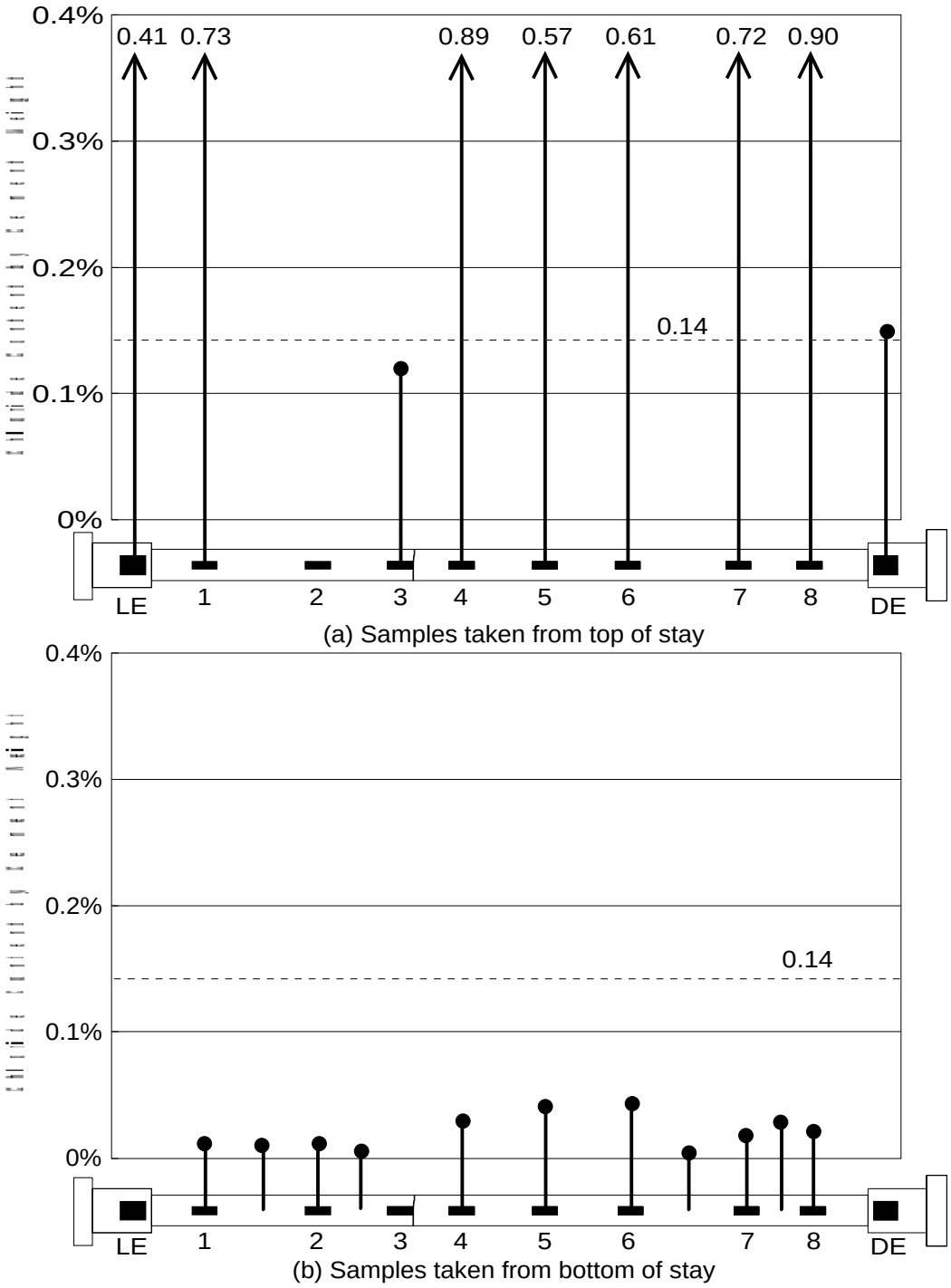

Figure 0.12 - Grout Chloride Content for Specimen LS-2.

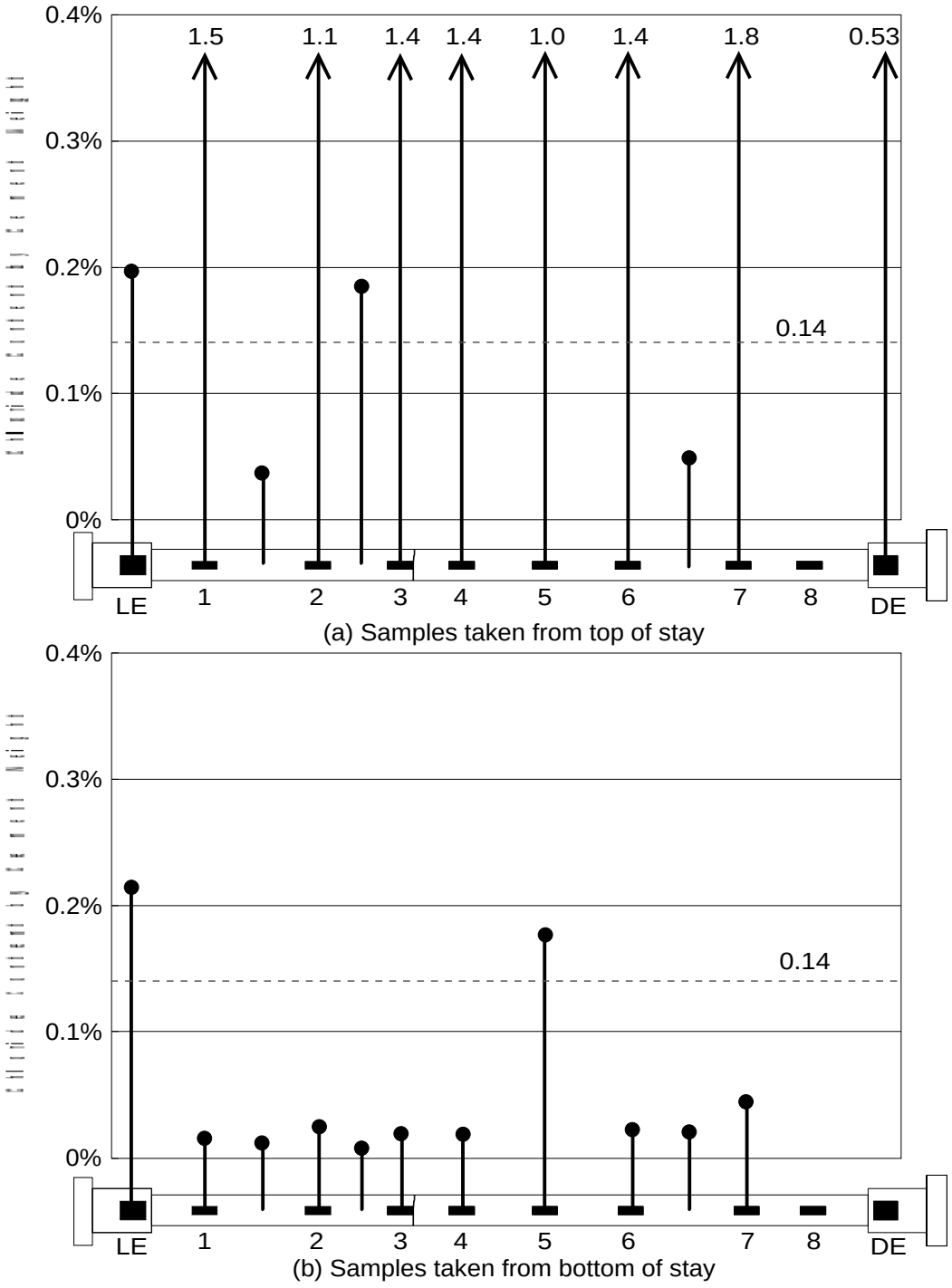

Figure 0.13 - Grout Chloride Content for Specimen LS-4.

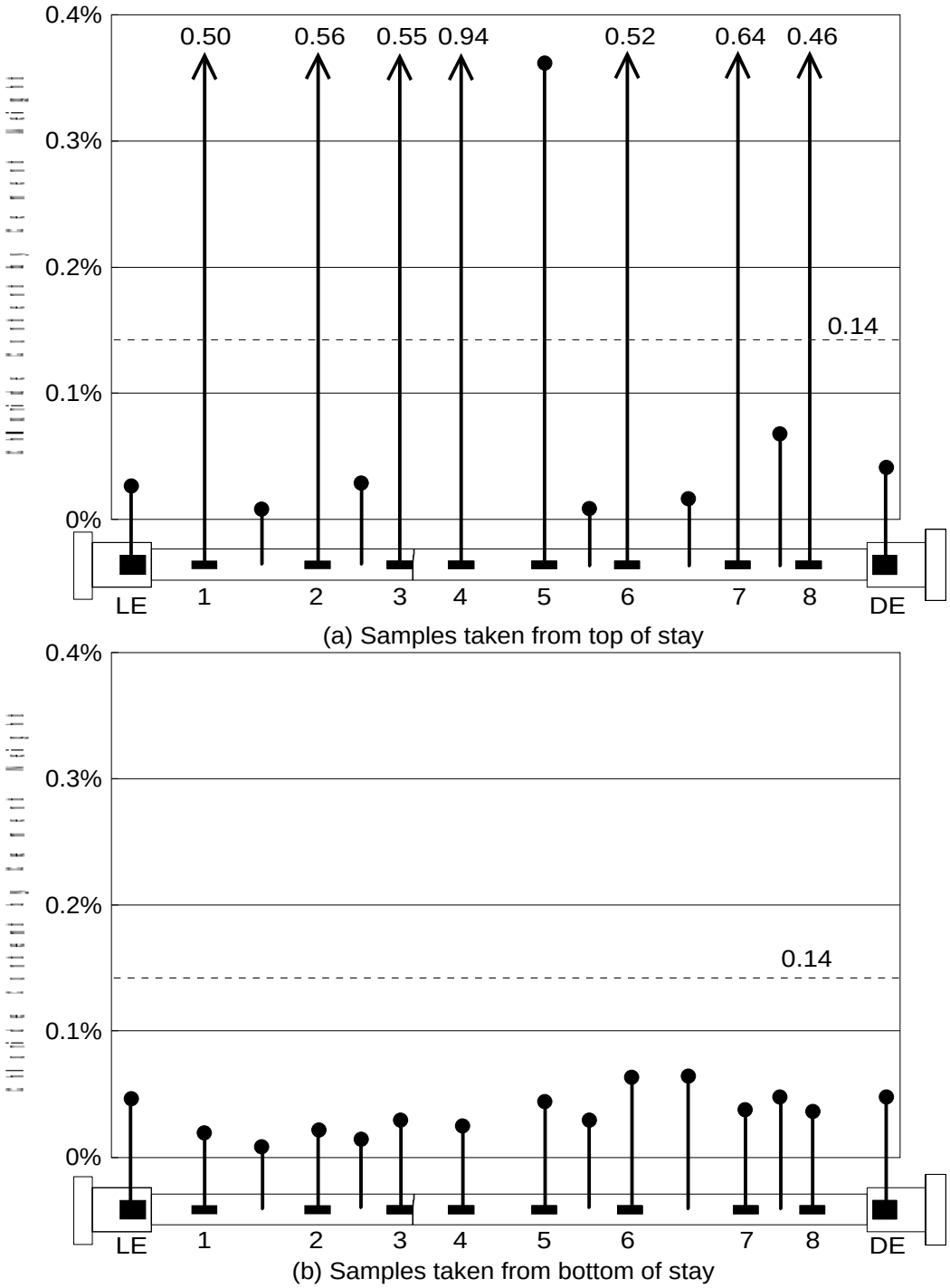

Figure 0.14 - Grout Chloride Content for Specimen LS-5.

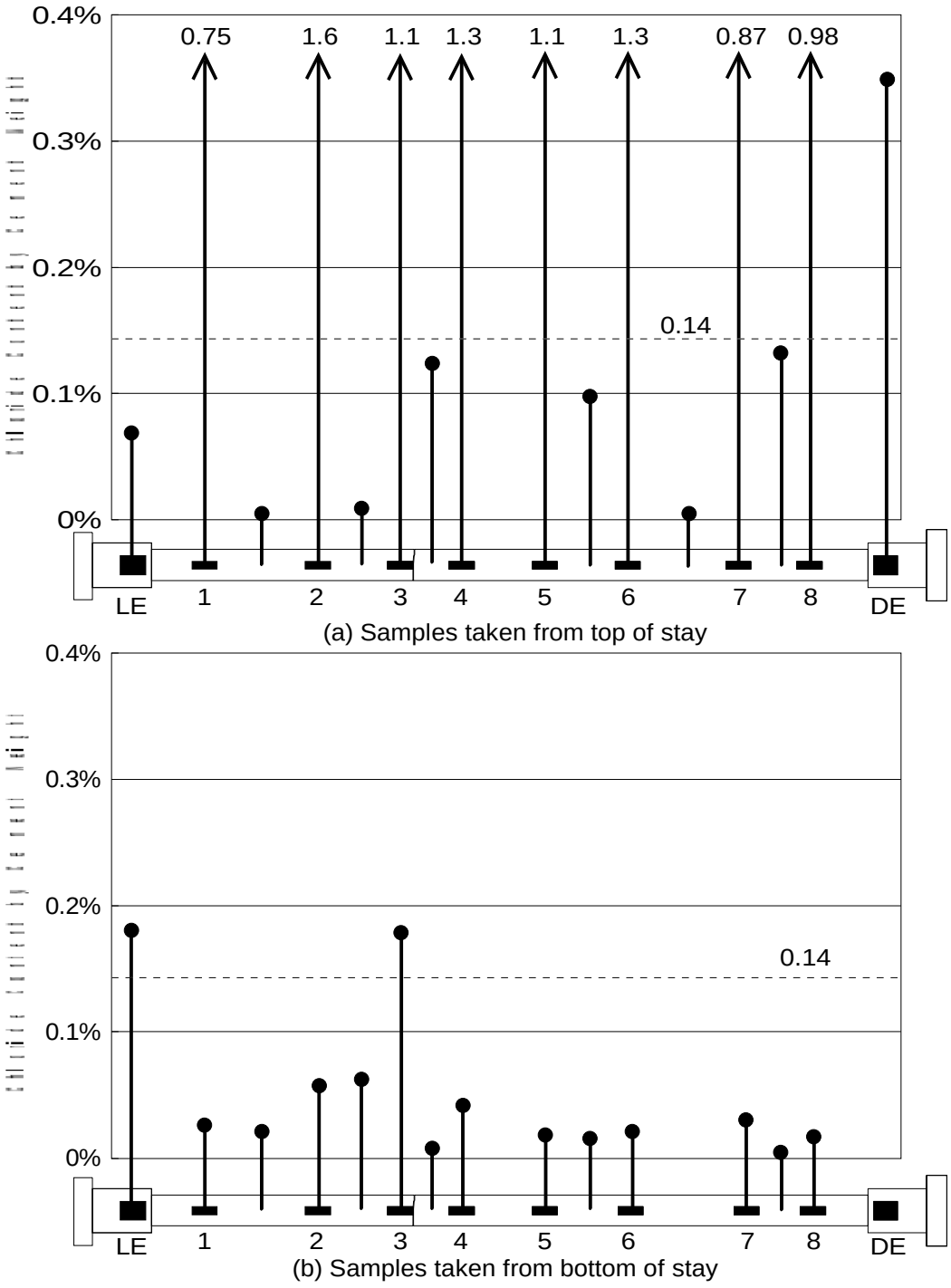

Figure 0.15 - Grout Chloride Content for Specimen LS-6.

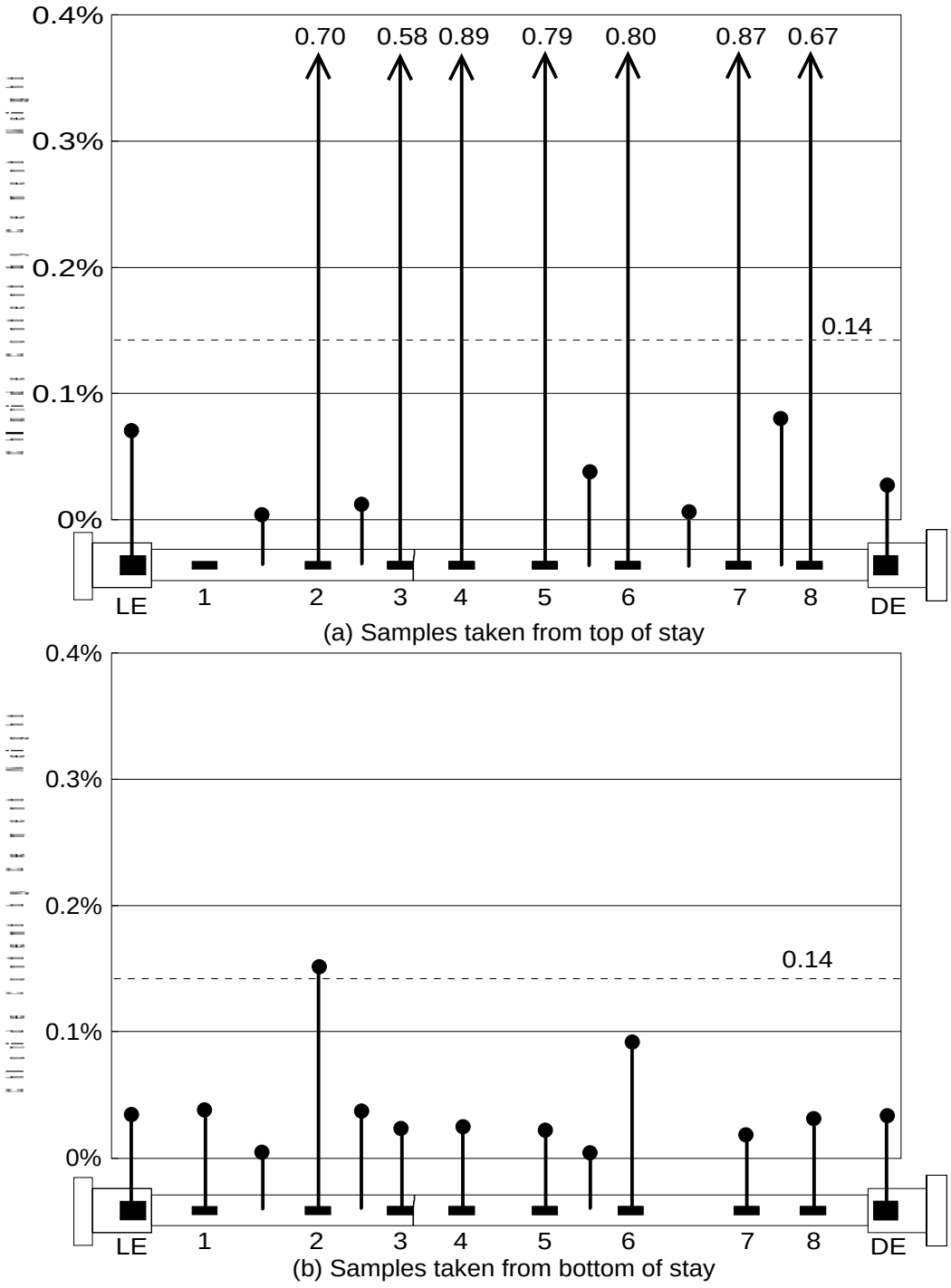

Figure 0.16 - Grout Chloride Content for Specimen LS-8.

level of chlorides present may not be accurate, the fact that they were present can be of value in determining how far and to what extent the chlorides have penetrated into the specimens.

As was discussed in Chapter Two, the threshold level of chloride content is a somewhat controversial issue. Researchers have found widely varying values of chloride content which have initiated corrosion activity of steel in concrete. Kahhaleh found in an extensive literature review that reported critical ranges fell between 0.14% and 0.35% by weight of cement.[66] To provide a benchmark for evaluating the chloride contents, the lower limit of this range is plotted on the chloride results for the large-scale specimens (Figure 0.12 - Figure 0.16).

Chloride tests were conducted on the grout taken from strand interstices in two locations on specimen LS-5. The sample for one of the tests was taken from strands 10, 11, and 12 midway between opening 1 and the live end deviator ring. The second sample was taken from strands 1, 2, and 3 in the same area. Both samples had a chloride content of 0.10% by cement weight which indicated that chlorides had permeated the strand interstitial spaces.

Carbonation Tests

Carbon dioxide, over time, penetrates concrete and grout through the pore structure.[22, 66, 99] The carbon dioxide combines with the moisture in the pore structure to form carbonic acid which neutralizes the alkalinity of the grout reducing the pH to less than 9. Generally, carbonation in solid concrete or grout occurs slow enough so that it does not become a problem over the life of the structure. However, carbonation becomes a problem in cracked grout because carbon dioxide is allowed to penetrate much more quickly into the crack than it does through the matrix. Carbonation can then occur on the crack face. If the crack extends down to the steel then the area where the crack intersects the steel can lose the protective alkaline environment. This coupled with the oxygen and moisture which are available through the crack can lead to the initiation of corrosion.

The faces of the cracks in the grout were tested for carbonation at selected locations during the course of the grout removal. It was necessary to test the grout immediately upon removal so that the grout did not carbonate significantly after it had been removed. The tests were performed by spraying a 1% (by weight) phenolphthalein solution on the crack face. If the solution turns red then the pH is above 9 and if the solution remains colorless then the pH below 9 and is considered carbonated.[37]

The results of the carbonation tests indicated that in nearly all of the cases in which a pre-existing crack in the free length (the length of the stay between deviator rings) was exposed by an opening in the sheathing, the grout had carbonated down to the level of the strand. Figure 0.17 shows the typical result of a carbonation test on the face of a crack in the grout. It should be noted that the thickness of the grout layer varied along the free length from 6.4 mm at the midspan to 12.7 mm at the deviator ring. The deviator ring assembly held the sheathing concentric with the strand bundle, but away from the deviator ring the sheathing was allowed to sag down onto the helical spacer. In the openings in the transition sheathing (LE and DE) the grout cover over the strand was approximately 30 mm. In this area the maximum depth that the carbonation front reached into the grout crack was approximately 12 mm. Selected cracks in grout away from the sheathing openings were tested for carbonation. There were no cases in which the crack faces had carbonated to a significant depth.

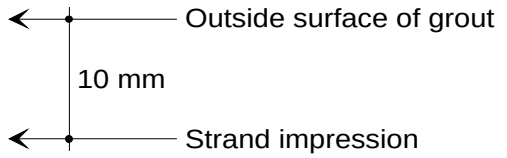

Figure 0.17 - Carbonation of Grout Crack Face as Indicated by Phenolphthalein.

Bare Strand Systems (LS-1 through 4)

Overall Performance

Considering the short time duration of the test, the extent and nature of the corrosion was quite extensive. Figure 0.18 shows the typical progression of corrosion through the three months of wet/dry cycling and post-mortem examination. The shrinkage cracks in the grout allowed the rapid ingress of chlorides to the surface of the strands to initiate corrosion activity very quickly. It was found that in many cases corrosion product would appear on the surface of the grout midway through the second wet cycle. In addition to corrosion of the strands in specimens LS-1 through LS-4, corrosion was also found, to some degree, on all of other components used to construct the stay.

While corrosion was found in many areas on these specimens, the most intense activity occurred on the strands directly under the opening in the sheath where chlorides, moisture and oxygen were plentiful. There were three conditions which, either in conjunction or separately, contributed to the occurrence of corrosion. The first and most common condition was the cracking of the grout. As discussed previously, cracking occurred at all openings in the sheathing. The second condition was the presence of air pockets. Because of the thin cover over the strand in the

area where the sheathing was removed, air pockets, even if small, would leave a portion of the underlying strand unprotected. The third condition which promoted corrosion was the exposure of the helical wrap at the opening. It was not possible to place the spacer in the same location with exactly the same pitch on every specimen. Therefore, the spacer was not exposed at the same openings in every specimen. When the spacer is exposed at a sheathing opening, a direct path is formed for the chlorides, moisture and oxygen to the surface of the strand through the interface between the spacer and grout. This is especially true if air was trapped adjacent to the helical wrap during grout injection.

The observations taken during post-mortem examination at each of the openings in LS-1 through 4 are shown in Table 0.11. The table indicates during which cycle corrosion product appeared on the surface of the grout. The table also indicates if there were any voids exposed or if the helical spacer was exposed at any of the openings. The corrosion evaluation of the strands in the top layer is also given (strands 1 or 2). Finally, for openings which did have corrosion occur the tables indicate if the corrosion was caused *only* by the presence of the voids or helical spacer. For instance, in Table 0.11(a) at opening number 2 the helical wrap was exposed but corrosion did not occur only at the spacer. This indicates that the corrosion was also caused by the shrinkage cracks.

Corrosion at Grout Cracks

An example of the corrosion at the base of a grout crack is shown in Figure 0.19. The outline of the crack is visible in the remaining grout and is in line with the most intense area of corrosion. Away from the crack location the intensity of the pitting corrosion decreases. In some areas a greenish-white corrosion was noted which was still moist when the grout was removed. Usually within a day the corrosion product would dry and the remaining deposit would be red or black.

Corrosion at Air Pockets

Air pockets in the grout which coincided with the openings in the sheathing in some cases left the underlying strands completely unprotected or at most covered with a thin layer of grout. In most cases the underlying strands corroded almost immediately upon initiating the accelerated corrosion test. The area of air pockets exposed at each of the sheathing openings are tabulated in Table 0.11 along with an indication if the void was the only cause of corrosion at the opening. The table indicates that in the first four specimens there were only two locations in which the corrosion

(a) During First Wet Cycle.

(b) Midway Through 2nd Wet Cycle.

(c) Corroded Strands Uncovered During Post-Mortem Examination.

Figure 0.18 - Corrosion Product on Surface of Grout During Accelerated Corrosion Test (Specimen LS-5 opening 5)

Table 0.11 - Summary of Observations at Sheathing Openings for Specimens LS-1 through 4.

(a) Specimen LS-1 (Bare strand with no additional load applied).

Open-	Staining became	Helical	Area of air	Corrosion	Corrosion	Corrosion

ing	visible on surface during:	spacer exposed?	pockets exposed(mm^2)	Evaluation (length-mm)	occur only at voids?	occur only at spacer?
DE	none	n/a	0	none	n/a	n/a
1	none	N	0	VH(280)	n/a	n/a
2	2nd wet	Y	0	VH(165)	n/a	N
3	2nd wet	N	0	VH(280)	n/a	n/a
4	2nd wet	Y	0	VH(250)	n/a	N
5	none	N	0	VH(280)	n/a	n/a
6	none	Y	0	VH(280)	n/a	N
7	none	Y	0	VH(280)	n/a	N
8	none	N	0	none	n/a	n/a
LE	none	n/a	0	none	n/a	n/a

(b) Specimen LS-2 (Bare strand).

Open-ing	Staining became visible on surface during:	Helical spacer exposed?	Area of air pockets exposed(mm^2)	Corrosion Evaluation (length-mm)	Corrosion occur only at voids?	Corrosion occur only at spacer?
DE	none	n/a	690	none	n/a	n/a
1	none	N	0	H	n/a	n/a
2	none	N	0	none	n/a	n/a
3	2nd wet	N	0	VH(50)	n/a	n/a
4	none	N	0	none	n/a	n/a
5	none	N	0	none	n/a	n/a
6	none	N	0	none	n/a	n/a
7	2nd wet	Y	0	VH(200)	n/a	Y
8	none	N	0	none	n/a	n/a
LE	none	n/a	100	none	n/a	n/a

(c) Specimen LS-3 (Bare strand with TCP and no additional load applied).

Open-ing	Staining became visible on surface during:	Helical spacer exposed?	Area of air pockets exposed(mm^2)	Corrosion Evaluation (length-mm)	Corrosion occur only at voids?	Corrosion occur only at spacer?
DE	none	n/a	0	L	n/a	n/a
1	none	N	0	VH(140)	n/a	n/a
2	2nd wet	Y	15	VH(220)	Y	Y
3	2nd dry	N	0	VH(280)	n/a	n/a
4	2nd wet	N	0	VH(220)	n/a	n/a
5	none	N	0	none	n/a	n/a
6	2nd wet	Y	15	VH(64)	Y	N
7	2nd wet	N	0	VH(130)	N	n/a
8	2nd dry	Y	90	H	Y	Y
LE	none	n/a	0	none	n/a	n/a

(d) Specimen LS-4 (Bare strand with TCP).

Open-ing	Staining became visible on surface	Helical spacer	Area of air pockets	Corrosion Evaluation	Corrosion occur only at	Corrosion occur only at

	during:	exposed?	exposed(mm^2)	(length-mm)	voids?	spacer?
DE	none	n/a	0	none	n/a	n/a
1	2nd wet	N	0	VH(280)	n/a	n/a
2	2nd wet	N	30	VH(260)	N	n/a
3	2nd wet	N	0	VH(280)	n/a	n/a
4	none	Y	0	none	n/a	n/a
5	none	N	0	none	n/a	n/a
6	none	Y	0	none	n/a	n/a
7	1st wet	N	165	VH	n/a	n/a
8	none	Y	90	VH(178)	Y	n/a
LE	none	n/a	0	none	n/a	n/a

Figure 0.19 - Typical Corrosion at Base of a Grout Crack.

at the openings were caused solely by the air pocket. An example of the corrosion at an air pocket is shown in Figure 0.20.

Corrosion at Helical Spacer

Corrosion of the helical spacer consistently occurred very rapidly when it was exposed at an opening. In fact, in all eight specimens the helical spacer corroded to some degree at every location that it was exposed by an opening in the sheathing. In some cases the strand that was directly under the spacer would corrode. The helical spacer was responsible for initiating corrosion on the underlying strand at four sheathing openings in the first four specimens. Figure 0.21 shows opening 7 on LS-2 at the completion of the wet/dry cycles and after the grout has been removed. Corrosion of the wire is apparent as the polyester coating has been undercut by the corrosion. The underlying strand is corroded most intensely at the areas under the spacer and diminishes away from the spacer. This is a strong indication that the corrosion on the strand was initiated under the spacer, probably in the contact region.

Interstitial Corrosion

In addition to examining the exterior surface of the strand, alternate wires were removed from the outside six wires of the strand to expose the interstitial space between the outer wires and the center wire. It was found that the spaces between the wires were mostly filled with grout. In some locations corrosion was also found in these spaces (Figure 0.22). The corrosion was not limited to the area under the sheathing openings but was also found to some degree in the interstitial spaces under the wedges and the deviator ring, and intermittently in both transitions and the free length.

Anchor Heads and Deviator Rings

Strand/wedge sections were removed from the anchor head using a hydraulic ram. This allowed the section to be removed with the grout still intact. Visual inspection of the section indicated that the grout had, without fail in the first four specimens, filled solidly all of the spaces between the strand and wedge (Figure 0.23). In some cases, when the wedges were removed from the strand, there was corrosion present at the interface between the strands and wedges (Figure 0.24). When viewed closely it was found that the corrosion product was mainly between the teeth marks in the strand (see Figure 0.25).

Figure 0.20 - Example of Corrosion Initiated by Air Pocket(LS-5, Opening 8).

(a) After Completion of Wet/Dry Cycles.

(b) During Post-Mortem Examination.

Figure 0.21 - Corrosion of Helical Spacer and Underlying Strand (LS-5, Opening 3).

The specimens which had the worst corrosion of the strand/wedge interface were LS-2 and LS-4 at the dead end. Note that additional load was applied to these specimens during the corrosion test.

In some locations when the wedges were removed for inspection there was black corrosion product present which would turn red after being exposed to the air for several hours. Black product

is indicative of corrosion in a restricted oxygen environment.[66] The product has been identified as Fe_3O_4 (magnetite) which is formed when the complex ferrous chloride ion is exposed to air. Further oxidation produces the more familiar and more stable red rust Fe_2O_3.

Figure 0.22 - Corrosion in the Interstitial Space of Bare Strand.

Figure 0.23 - Example of Removed Wedge/Strand Section.

Figure 0.24 - Corrosion at the Interface Between the Strand and Wedge.

Figure 0.25 - Corrosion Between Tooth Marks on Strand.

The anchor heads typically had medium to light surface corrosion which covered the exposed area. The corrosion was particularly heavy in the area under the flange of the transition sheathing.

The interface between the strand and deviator ring was found to be slightly corroded at isolated locations. Generally, if corrosion was present on the strand it was not directly under the contact point between the deviator ring but just adjacent to the deviator ring (Figure 0.26). When the strands were removed from the deviator ring there was very little corrosion on the inside surface of the deviator ring (Figure 0.27). Figure 0.27 also shows the typical nature of the corrosion on the

deviator ring for the first four specimens. The corrosion was heavy and usually covered more than 50% of the outside area.

Improved Grout (LS-5)

Specimen LS-5 had 5% silica fume added to the grout to determine if the addition would improve the corrosion protection provided by the grout. The performance of LS-5 was very similar to that of the first four specimens. The grout cracking (due to axial load or shrinkage caused by the openings in the sheathing) did not differ extensively from the cracking observed in the other specimens. As a result, significant corrosion occurred at eight of the ten sheathing openings. Two of those were due to an air pocket and one was caused by the helical spacer (Table 0.12). Behavior of the anchor head and deviator ring were similar to LS-1 through LS-4.

Table 0.12 - Summary of Observations at Sheathing Openings
Specimen LS-5 (Bare strand with TCP and Improved Grout).

Open-ing	Staining became visible on surface during:	Helical wrap exposed?	Area of air pockets exposed(mm^2)	Corrosion Evaluation (length-mm)	Corrosion occur only at voids?	Corrosion occur only at spacer?
DE	none	n/a	0	none	n/a	n/a
1	none	N	0	M	n/a	n/a
2	2nd wet	N	0	VH(200)	n/a	n/a
3	2nd wet	Y	0	VH(250)	n/a	Y
4	1st wet	N	0	VH(280)	n/a	n/a
5	2nd wet	N	0	VH(280)	n/a	n/a
6	none	Y	0	VH(90)	n/a	N
7	none	N	10	VH(100)	Y	n/a
8	2nd wet	N	320	VH(130)	Y	n/a
LE	none	n/a	0	none	n/a	n/a

Figure 0.26 - Corrosion of Strand Adjacent to Deviator Ring.

Figure 0.27 - Typical Condition of Inside Face of Deviator Ring.

Epoxy-Coated System (LS-6)

Overall Performance

The use of epoxy-coated strand provided a significant improvement in corrosion protection over the bare strand systems. Between the anchor heads, only two instances of surface corrosion were found. Both occurred at unrepaired, intentionally damaged areas. Both of these were in unrepaired intentional damages which were made in strands 1 and 2 (Figure 0.28). These were the strands closest to the opening in the sheathing and would have had the highest concentration of chlorides.

Several epoxy-coated (not filled) strands were selected from the transition length of the Live End anchorage. These strands were opened to allow examination for interstitial corrosion. Corrosion was found in several of the strands as shown in Figure 0.29. It was unclear from the examination whether the corrosion was present prior to the test or occurred during the corrosion test. Several sections of the strand were sampled as received from the manufacturer and were found to be corrosion free. This would seem to indicated that the corrosion occurred during the test. Selected coated and filled untested strands were examined in the same manner. No interstitial corrosion was found.

Anchor Heads and Deviator Rings

Special wedges are required to grip epoxy-coated strand. The teeth on the wedges are deeper than those on standard wedges so that they can cut through the epoxy coating and embed in the surface of the strand. One concern with this system is the reduction in effectiveness of the coating when using these types of wedges. The protective barrier is broken at each tooth on the wedge exposing the strand to corrosion at a very critical location.

Short sections of strand were extracted from the anchor head with wedges attached. Corrosion was found on some of the strands and the associated wedges. The corroded strands had product around the area where the teeth were embedded in the steel (Figure 0.30). Corrosion product was also found under the epoxy coating between the tooth marks (Figure 0.31). This configuration was typical in those grip regions (where the wedge bites into the strand) which had corrosion.

The grip regions at the Live End did not suffer as extensive corrosion as did the Dead End. The corrosion was cataloged by recording the number of tooth marks in the grip region of each strand which had corrosion. There were a total of 57 instances of corrosion on 10 of the 12 strands

Figure 0.28 - Corrosion of Strand at Intentional Damage in Epoxy-Coating.

Figure 0.29 - Interstitial Corrosion of Epoxy-Coated Strand (not filled).

Figure 0.30 - Corrosion of Strand at Tooth Mark.

Figure 0.31 - Corrosion Under of Epoxy Coating Between Tooth Marks.

at the Live End. Two of the strands did not have any corrosion. At the Dead End there were 111 spots of corrosion on 7 of 10 strands. The remaining two strands had corrosion at nearly every tooth mark. The most severe corrosion occurred in the top layer of strands and diminished on the lower layers of strand. This was particularly true at the Dead End.

Another area of concern in epoxy-coated strand is the deviator ring. The deviator ring gathers the strand into a tight bundle (in the free length) to reduce weight and wind forces. By necessity the deviator ring places a lateral force on the exterior strands so that they may be deviated slightly. During assembly and stressing this can lead to abrasion between the strand and deviator ring. If the strands have a coating or sheathing then it is possible that they could be damaged in this area. Stay cable suppliers generally line the deviator ring with polyethylene or other type of plastic material to reduce the potential for damage. However, if the sheathing material of the strand is of

similar toughness to the lining material, the potential for mutual damage remains. In these tests the deviator ring was not lined, but was left bare to give the worst case condition for the individual strand protection systems.

Post-mortem examination of the strands in contact with the deviator ring indicated that the epoxy had been damaged in several locations. Nine of the twelve strands were in contact with the deviator rings at each end. Of the total number of contact points (18) there were 5 areas where the epoxy had been damaged at the Dead End and none at the Live End. Of those five, two had been damaged to the extent that the strand was exposed (see Figure 0.32). However, no corrosion had occurred on the exposed strand.

Epoxy-Repair

Epoxy-coating repairs were made in two locations. The first was the repair of the spots which were intentionally damaged. The damaged areas were placed along the length of the strand at selected locations using selected sizes as was discussed previously. There was no corrosion detected during the post-mortem examination at any of these repaired areas. The second location that required repair was the cut end of the strand under the grout cap. There were two techniques used to repair the ends. One was to cover the ends with a cap partially filled with epoxy repair compound (cap method). The other was to apply the compound directly to the end of the strand with a brush (patch method).

The cap method did not prove to be effective in preventing grout or moisture from contacting the end of the strand (Figure 0.33). Most of the ends repaired with the cap method had grout, moisture, and some corrosion present when the cap was removed during post-mortem

Figure 0.32 - Epoxy-Coating Damaged By Contact with Deviator Ring.

Figure 0.33 - Grout in Epoxy Repair Cap.

examination. It appeared as if the grout had seeped into the cap through the space between the cap and outside diameter of the strand. This space should have been filled with the repair compound.

The patch repair method did not perform adequately either. Figure 0.34 shows the repaired end of a strand immediately after removal of the grout. The corrosion was not particularly heavy, but its occurrence did indicated that the repair method did not adequately protect the end of the strand.

Galvanized System (LS-7)

Overall Performance

The use of galvanized strand provided a significant improvement in corrosion protection over the bare strand systems. The post-mortem examination revealed a total of 4 areas in the free length

Figure 0.34 - Corroded End of Strand Repaired with Epoxy Compound.

and 8 areas in the transition length where red rust was found. All of the areas were smaller than 4 mm in length.

Red rust product is an indication of corrosion of the underlying steel. Zinc alloys embedded in hardened cement (concrete or grout) systems in the presence of chlorides produce a white corrosion product which is a combination of zinc hydroxide ($Zn(OH)_2$) and zinc hydroxychloride ($Zn_5(OH)_8CL_2 \bullet H_2O$).[59]

Figure 0.35 shows a typical example of an area where the zinc has been completely lost. Note that the black area is very soft layer of zinc corrosion product which can easily be scraped away. Blackening of the zinc in similar conditions has also been found in other work.[121] However, microscopic examination of the strand under the black corrosion reveals that the steel is uncorroded and in bright condition. Even though the zinc is no longer directly covering the steel in this area the protection is provided galvanically by the remaining zinc. Also note the white zinc hydroxychloride corrosion product surrounding the black corrosion product.

Anchor Heads and Deviator Rings

There was no significant corrosion found on the anchor heads, deviator rings, or wedges. This indicates that the zinc provided galvanic protection for the components as well as the strand. In the grip region there was a total of 7 spots of red rust found between tooth marks (Figure 0.36).

Greased and Sheathed System (LS-8)

Overall Performance

The use of greased and sheathed strand provided a significant improvement in corrosion protection over the bare strand systems. Between the anchor heads there were four locations which suffered corrosion. In all cases the corrosion occurred at an unrepaired intentional damage in the sheathing. Table 0.13 shows the location of the corrosion and the size of the defect where the corrosion occurred. Figure 0.37 shows the corrosion on strand 2. Note that the heaviest area of corrosion is under the damaged area. This was typical of the corrosion except at one site. The corrosion on strand 12 occurred away from the damage in the strand sheath. This is probably because the cathodic reaction supporting the corrosion under the sheath was occurring at the damage site.

Table 0.13 - Location of Corrosion on LS-8.

Strand	Sheathing Opening	Defect
1	2	3.2-mm square
2	3	6.4-mm square
4	1	cut
12	6	6.4-mm square

Figure 0.35 - Example of Loss of Zinc Coating.

Figure 0.36 - Corrosion Between Tooth Marks in Grip Region.

Figure 0.38 shows a section of strand in which the sheath was unintentionally damaged during assembly. There were 3 of these areas found in the sheath during the post-mortem examination. Note that grout has intruded into the sheath through the damaged area. The space between two outer wires and the sheath is normally filled with grease. However, during the process of injection the grout seeped into the sheath and displaced the grease. In some locations the grout intruded up to 230 mm from the damage site.

Figure 0.39 shows the typical damaged area which had been repaired with the waterproof tape. There was no grout or moisture intrusion into any of the damaged areas that had been repaired with this method.

Anchor Heads and Deviator Rings

As noted in Chapter Seven the system devised to seal the strand sheath against the anchor head met with limited success. During the accelerated corrosion test it was noted that salt solution was leaking from the wedge pockets in the anchor head. This solution had to travel from the LE and DE openings in the transition sheathing which were approximately 600 mm away. The strands and wedges through which salt solution had passed corroded severely during the accelerated corrosion test. This is no surprise since there was no protection provided to these areas other than the residual grease.

The anchor heads and tension rings were moderately corroded except for the areas on the anchor heads where the salt solution had leaked. These areas were severely corroded (see Figure 0.40).

The individual sheath was damaged in two locations that were in contact with the deviator ring. One location was at the live end and the other was at the dead end. The damage at the live end was on strand 12 and resulted in no corrosion of the strand. The damage at the dead end was on strand 5 and also resulted in no corrosion of the strand. However, the damaged area on strand 5 did allow the intrusion of grout into the sheath.

Figure 0.37 - Corrosion Under Sheathing.

Figure 0.38 - Intrusion of Grout into Sheathing.

Figure 0.39 - Repaired Damage Location After Completion of Corrosion Test.

Figure 0.40 - Corrosion Damage to Anchor Head on LS-8.

Chapter Nine
Large-Scale Test Series:
Discussion of Results

9.1 Introduction

This chapter presents additional discussion and analysis of the data collected during the accelerated corrosion tests. The methodology and results for the accelerated corrosion tests are presented in Chapter Eight while the general test philosophy, assembly, grouting and load tests are covered in Chapter Seven. There were a total of eight large scale test specimens. The specimens and variables were as follows:

- LS-1: Bare strand
- LS-2: Bare strand
- LS-3: Bare strand coated with temporary corrosion protection (TCP) prior to grouting
- LS-4: Bare strand coated with TCP prior to grouting
- LS-5: Bare strand coated with TCP prior to grouting. Grout improved with silica fume.
- LS-6: Epoxy-coated strand
- LS-7: Galvanized strand
- LS-8: Greased and sheathed strand

Load tests and additional loads applied during the accelerated corrosion test were carried out on all stay specimens except for LS-1 and LS-3.

9.2 Correlation of Corrosion and Variables

Corrosion was evaluated visually using the criteria presented in Section 8.11 of the previous chapter. This system was used on the free length as well as the transition length of the specimen during the post-mortem examination. A numerical rating system was developed to supplement the visual evaluation (also presented in Section 8.11). Each area of corrosion was identified according to the established criteria and was assigned a score. The sum of the numerical scores for each specimen can then be used as a means of comparing the intensity of corrosion in the different

specimens (see Table 9.1 and Figure 9.1). The complete list of corrosion evaluations for the two-barrier systems is included in Appendix C.

This system was most useful on the specimens which used the "two-barrier" corrosion protection system because there was a large amount of corrosion activity associated with these systems. This included LS-5 which was the improved grout specimen. Very little corrosion activity occurred along the free length and transition lengths of LS-6, 7, and 8. Most of that corrosion occurred at areas where the individual protection had been intentionally damaged. For comparison purposes, a rating was assigned to those areas of corrosion and are shown in Table 9.1. Even considering the damaged individual corrosion protection systems, there is a marked contrast when two-barrier specimens are compared (using the rating system) to the specimens with individual protection. The ratings for the individual protection systems (LS-6, LS-7, and LS-8) are presented only for comparison with the two-barrier system. The ratings are so low that differences between the ratings not likely indicate a significant difference in field performance; thus, the ratings should not be used to make comparisons between the individual protection systems.

There were some very interesting trends and correlations discovered when using the rating system to compare the two-barrier systems. Examining the ratings for the two-barrier systems reveals that when considering the exterior corrosion, LS-2 performed the best with a score of 80 followed by LS-5 with a score of 170. When considering the interstitial corrosion, LS-5 performed the best followed by LS-4. Unfortunately, the interstitial corrosion on LS-3 was not inspected so there is no rating available for this specimen. The ratings for the exterior and interstitial corrosion might have been summed to give a total score for each specimen. However, this would have been misleading because the characteristics of the two types of corrosion are quite different. In addition, it would be difficult to correlate the two types of corrosion so that the rating system would be equivalent.

The variables introduced in the first four specimens (LS-1 through 4) were additional axial load and temporary corrosion protection (TCP). When examining the exterior corrosion there is a clear difference between the scores for the specimens with and without TCP. LS-1 and 2 have a score of 290 and 80 respectively while LS-3 and LS-4 have a score of 560 and 600. This seems to indicate that the specimens with TCP corroded more than the specimens without the TCP. However, specimens LS-1 and LS-2 had no voids exposed at the sheathing openings while LS-3 and LS-4 had several openings where air pockets were exposed. This could explain the large difference since most of the exterior corrosion occurred on the strands directly under the sheathing openings.

Table 9.1 - Total Corrosion Ratings for All Systems.

Specimen (LS-1 through LS-5 have bare strand)	Exterior Corrosion	Interstitial Corrosion
LS-1 (no additional load)	290	2900
LS-2	80	2600
LS-3 (with TCP and no additional load).	560	not inspected
LS-4 (with TCP)	600	1500
LS-5 (with TCP and 5% silica fume grout)	170	1300
LS-6 (epoxy-coated strand)	8	*
LS-7 (galvanized strand)	24	0
LS-8 (greased and sheathed strand)	20	0

*Corrosion was found in unfilled strand but was not quantified. No corrosion found in examined filled strand.

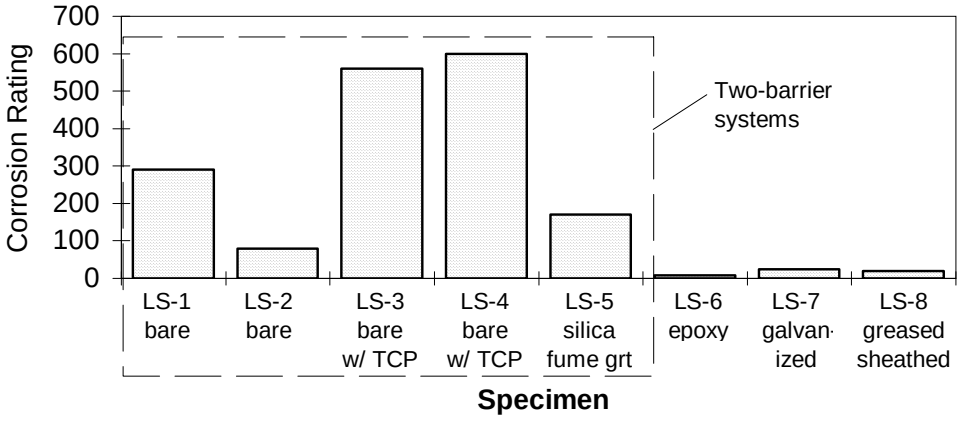

(a) Exterior Corrosion Ratings.

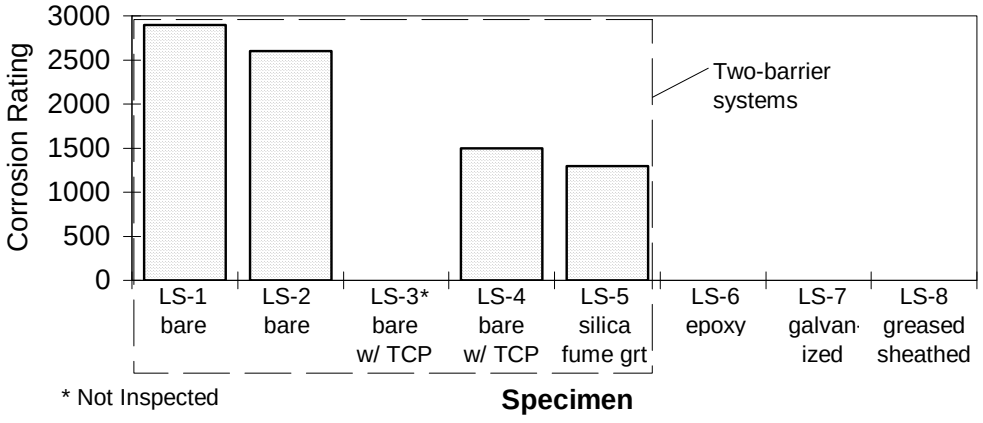

(b) Interstitial Corrosion Ratings.

Figure 9.1 - Comparison of Corrosion Ratings for the Large-Scale Specimens.

Conversely, when considering the interstitial corrosion, the specimens without TCP had more corrosion than those without. It is unlikely that this trend was influenced directly by air pockets. It is possible that the presence of the TCP between the wires provided some level of protection from the interstitial corrosion. Another possibility is that the air pockets in the specimens with TCP initiated corrosion quickly and provided cathodic protection for the nearby interstitial sites.

LS-5 performed best in both exterior and interstitial corrosion compared to the other two-barrier specimens except LS-2. This may have been due to the addition of the silica fume. The added protection was not provided by reduced the cracking. The specimen formed shrinkage cracks at the sheathing openings in the same manner as did the other specimens. The protection was probably provided by the reduced permeability of the grout due to the addition of silica fume. In order for corrosion to proceed uninhibited, the electrolyte (grout) must be sufficiently conductive and oxygen must be available in sufficient quantities to support the cathodic reaction. Fidjestol indicates that the diffusion of oxygen through water-saturated concrete is not influenced by the presence of silica fume.[43] This is because the oxygen transfer is slowed by the presence of water in the pore structure. He suggests that the presence of silica fume might reduce the diffusion of oxygen in unsaturated concrete because of the difference in the pore structure related to the addition of silica fume. However, conductivity was probably more of a factor in controlling the rate of corrosion in LS-5. It has been shown that the use of silica fume greatly decreases the resistivity of the concrete with the resistance increasing by an order of magnitude in some cases.[17, 43] An increase in grout resistivity in a situation where the corrosion rate is under "resistance control" can lead to a reduced corrosion rate (see Chapter Two).

9.3 Performance of Two-Barrier System

In general, a comparison can be made between the systems tested in LS-6, LS-7, and LS-8 and the "two-barrier system." However, the differences in performance between the two systems is vast. For instance, using the rating system presented in Table 9.1 show the corrosion rating for any of the strand barrier systems to be near zero. This indicates a very significant improvement in performance when the additional barrier is added. In retrospect this result seems obvious. However, in the early stages of the test program, when the variables were being investigated it was not anticipated that the grout would perform so poorly. It was anticipated that the grout would provide a better level of performance than was actually experienced and that the improvement in the level of performance provided by the additional barrier would not be so drastic.

9.4 Damage vs. Grout Discontinuities

At a number of openings in the sheathing of each specimen there were unintentional discontinuities in the grout which disturbed the effectiveness of the grout in preventing chlorides from reaching the strand. One of these discontinuities was caused by the helical spacer. The spacer provided a nearly direct conduit to the surface of the strand for the chlorides especially in the case where air had become trapped adjacent to the wrap during grout injection. The second discontinuity was air pockets.

In all of the cases in which an air pocket or the helical spacer coincided with an opening in the sheathing, significant corrosion occurred on the strand at that location.. In some cases corrosion would occur only at these locations. In other cases corrosion would occur when chlorides permeated through the grout cracks to the surface of the strand.

The number of grout discontinuities in the two-barrier specimens are summarized in Table 9.2. Note that the total may not equal the sum of the two categories because in some cases the air pockets and helical spacer were in the same opening and were considered one discontinuity. If the damage ratings in Table 9.1 are compared to the number of grout discontinuities there is a definite trend when considering the exterior corrosion. LS-2 has the lowest rating and the smallest number of discontinuities while LS-4 has the highest number of discontinuities and the highest corrosion rating. Thus, as would be expected, the presence of grout discontinuities affected (significantly in some cases) the corrosion behavior of the specimens. Conversely, LS-5 had 4 discontinuities but still had low corrosion ratings when compared to the other specimens. This, again, is probably due to the reduction in the grout conductivity caused by the addition of silica fume.

Table 9.2 - Grout Discontinuities

Specimen (all with bare strand)	Air Pockets	Helical Spacer	Total
LS-1 (no additional load)	0	4	4
LS-2	0	1	1
LS-3 (with TCP and no additional load).	3	3	3
LS-4 (with TCP)	3	3	5
LS-5 (with TCP and 5% silica fume grout)	2	2	4

9.5 Damage vs. Chloride Levels

The average chloride contents of the grout at sheathing openings 1-8 for specimens LS-2, LS-4, and LS-5 were 0.65, 1.40, and 0.57% by weight of cement. This correlates with the corrosion rating for exterior corrosion, but does not correlate with the interstitial corrosion rating. All three of the specimens were loaded during the accelerated corrosion test. The specimens were loaded during

the wet cycle so it is expected that the ingress of chlorides would occur during this operation. Based on this, it is expected that their chloride contents would be somewhat similar. However, the chloride content of LS-4 was more than twice that of the other two specimens.

The heaviest corrosion of the strands at the strand/wedge interface took place at the dead end of specimens LS-2 and LS-4. Of the grout samples taken from under the grout cap, LS-4 was the highest at a level of 0.13% by weight of cement. All other chloride contents that were sampled under the grout cap were either null or nearly an order of magnitude lower than this level. Unfortunately LS-2 was not sampled at the dead end grout cap. The elevated chloride content at the LS-4 grout cap indicates that the chlorides traveled from the dead end opening through the anchor head and into the grout under the grout cap. The elevated level of chlorides at the strand/wedge interface initiated the corrosion activity found during the post-mortem examination.

9.6 Half-Cell Readings

One area of particular interest was that of correlating the presence and severity of the corrosion with that of the half-cell readings taken during the test. In general, there seemed to be a correlation between the half-cell potential and the presence of corrosion, although it was not wholly consistent. Half-cell potentials are presented in Figure 9.1 through Figure 9.8. Each figure has two plots corresponding to potential readings made with the reference electrode placed directly on the surface of the grout with no solution present (as opposed to submerged in the salt solution). These potential readings gave the best indication of the presence of corrosion both during the test and in the post-mortem examination.

Note that the vertical scale is the half-cell potential taken on the surface of the grout and that each vertical line corresponds to an individual opening in the specimen sheathing as indicated by the schematic at the top of the figure. Three readings were taken at each opening, one at each end and one in the middle. The three potentials were plotted in their respective locations adjacent to the appropriate vertical line; i.e. the reading taken at the left end of the opening was plotted just to the left of the line, the reading taken at the middle of the opening was plotted on the line, and the reading taken at the right of the opening was plotted to the right of the line. These points were then connected with straight lines to make trends more obvious. The plot should not be interpreted to represent a continuous half-cell potential for the length of the specimen.

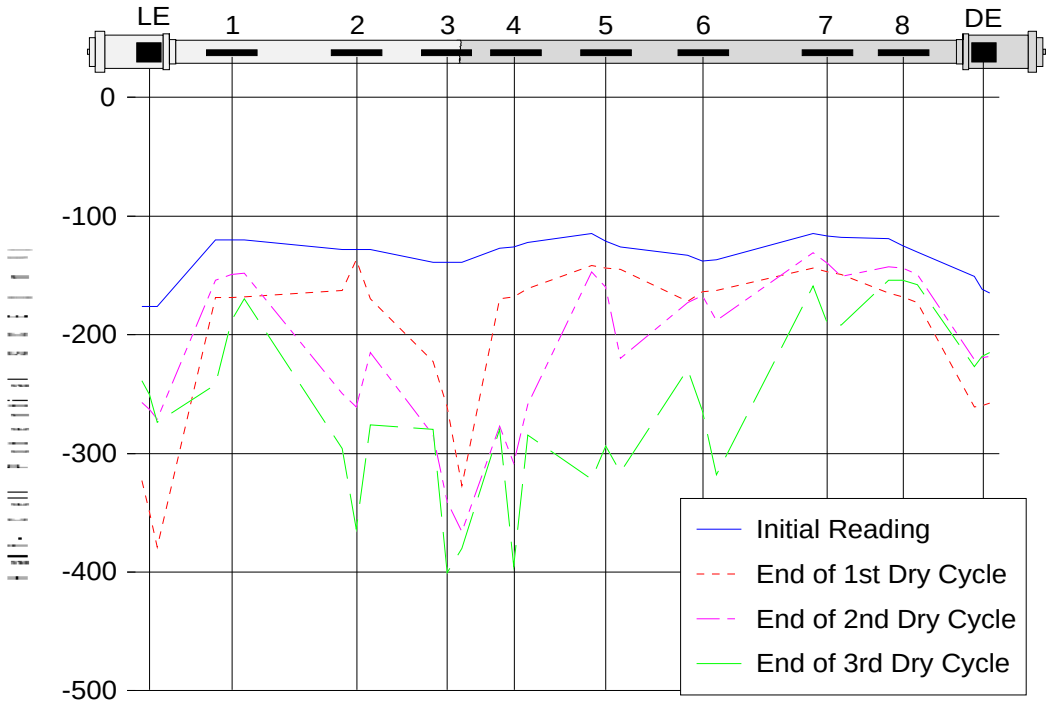

(a) Readings Taken at the Beginning of a Wet Cycle.

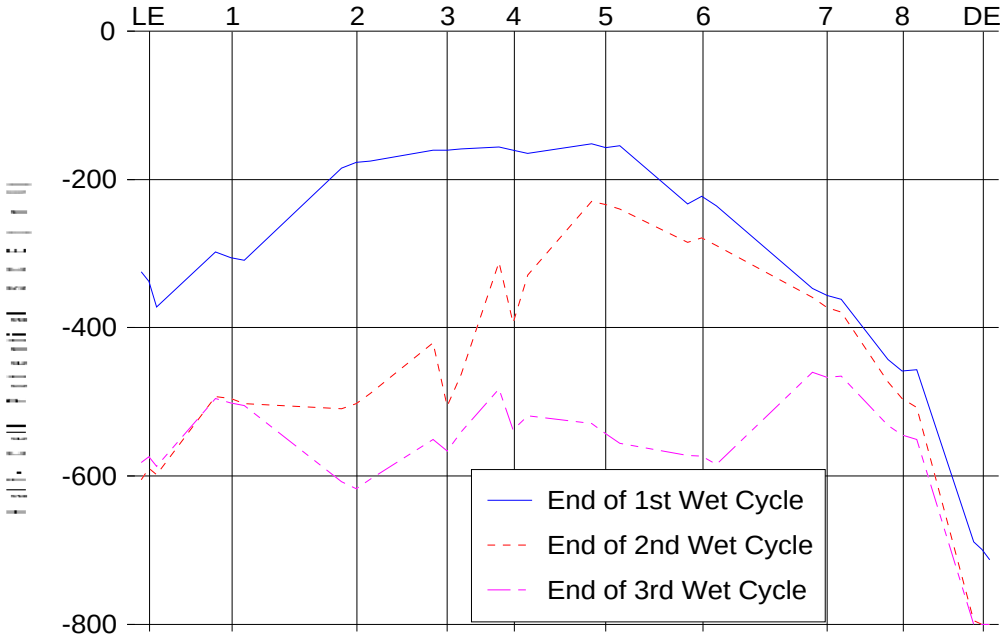

(b) Readings Taken at the End of a Wet Cycle.

Figure 9.1 - Half-Cell Potentials Taken on Grout Surface for Specimen LS-1.

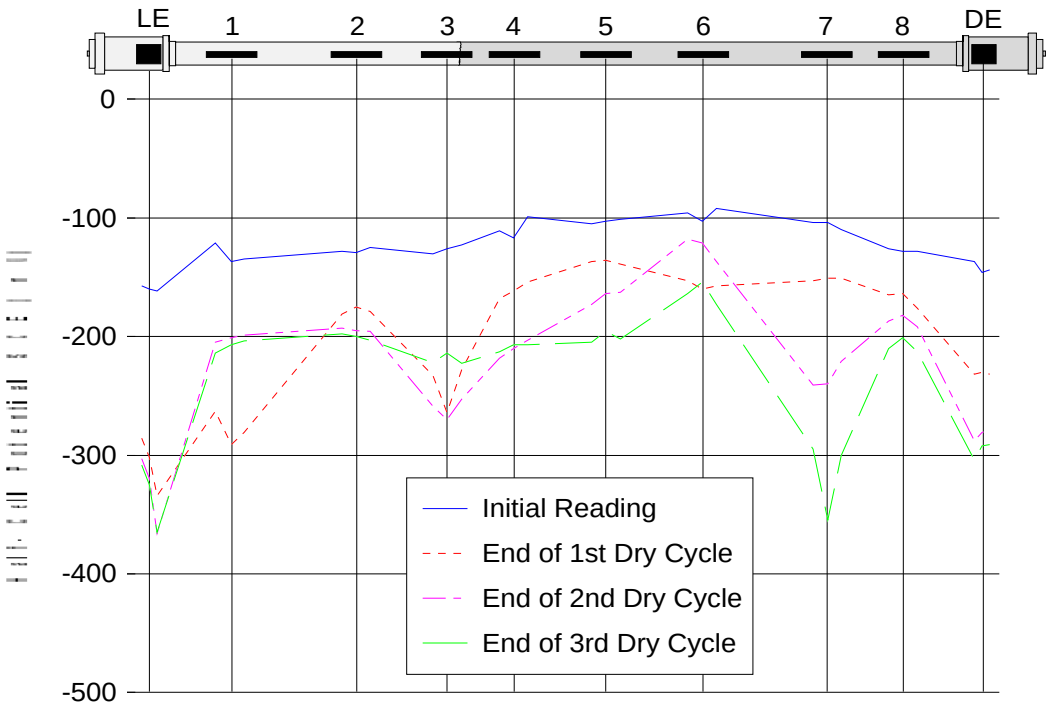

(a) Readings Taken at the Beginning of a Wet Cycle.

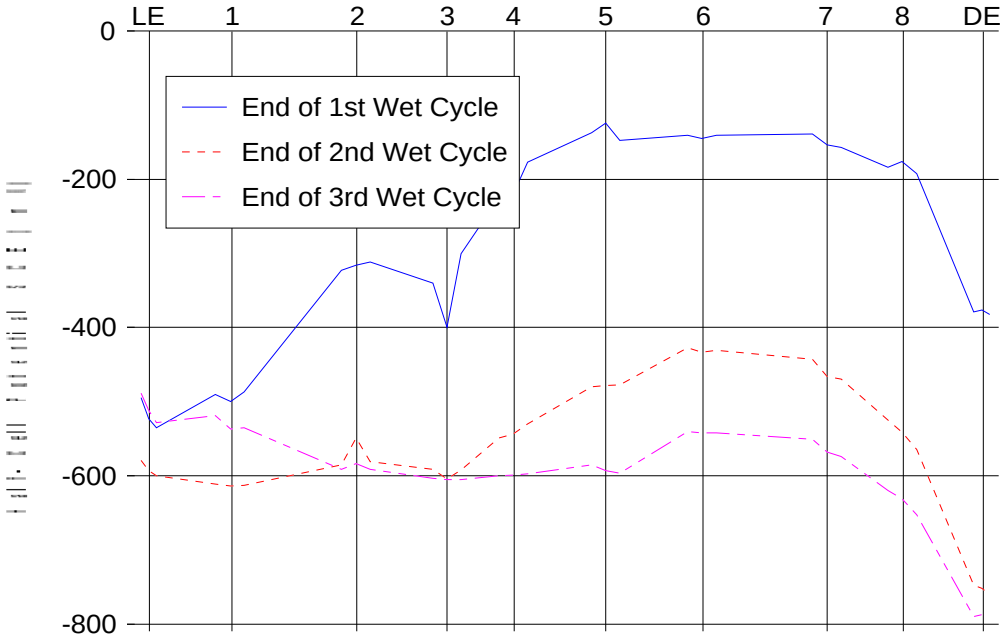

(b) Readings Taken at the End of a Wet Cycle.

Figure 9.2 - Half-Cell Potentials Taken on Grout Surface for Specimen LS-2.

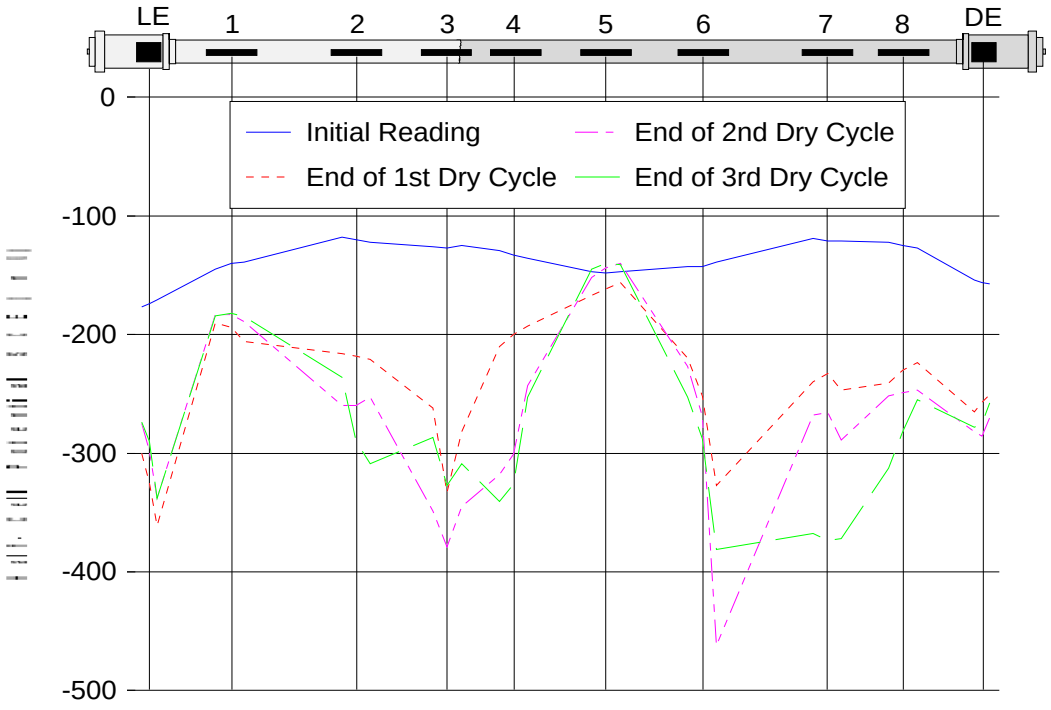

(a) Readings Taken at the Beginning of a Wet Cycle.

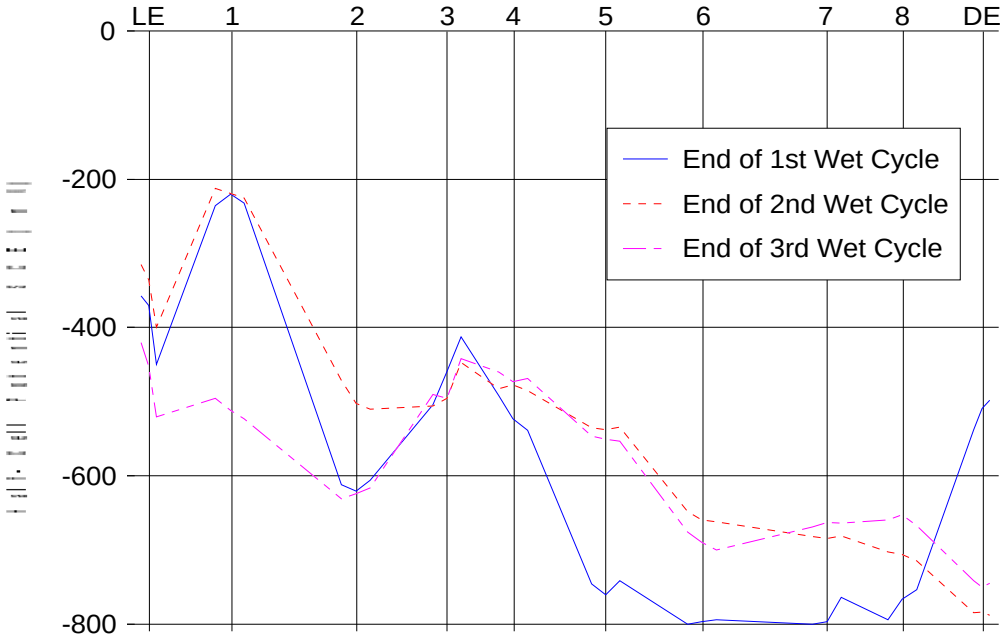

(b) Readings Taken at the End of a Wet Cycle.

Figure 9.3 - Half-Cell Potentials Taken on Grout Surface for Specimen LS-3.

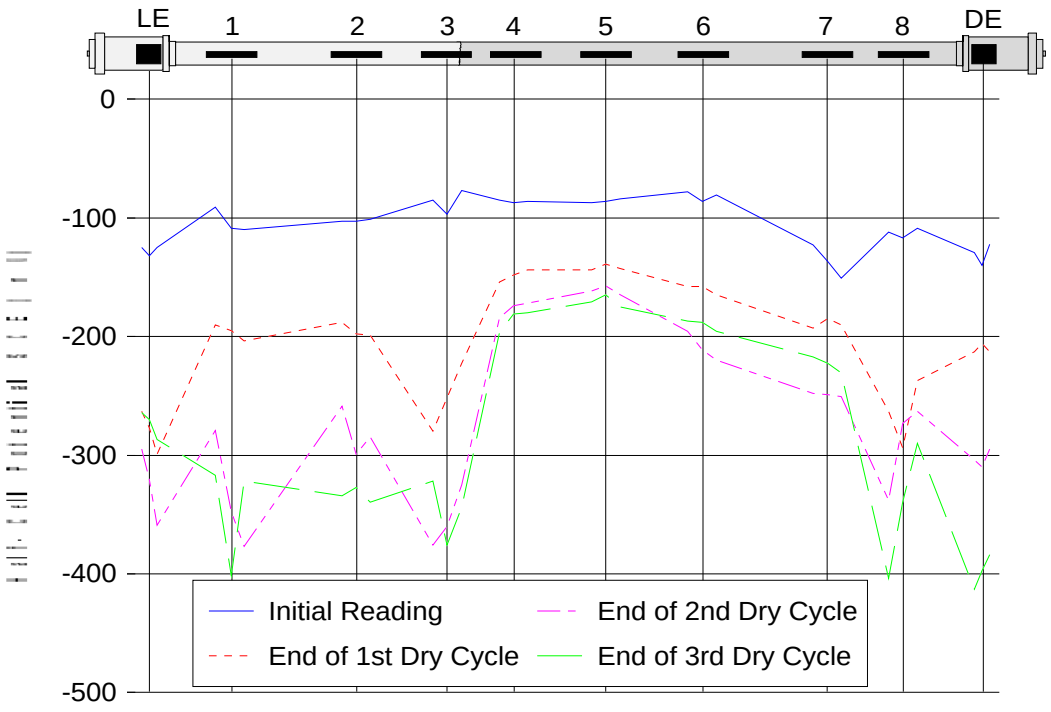

(a) Readings Taken at the Beginning of a Wet Cycle.

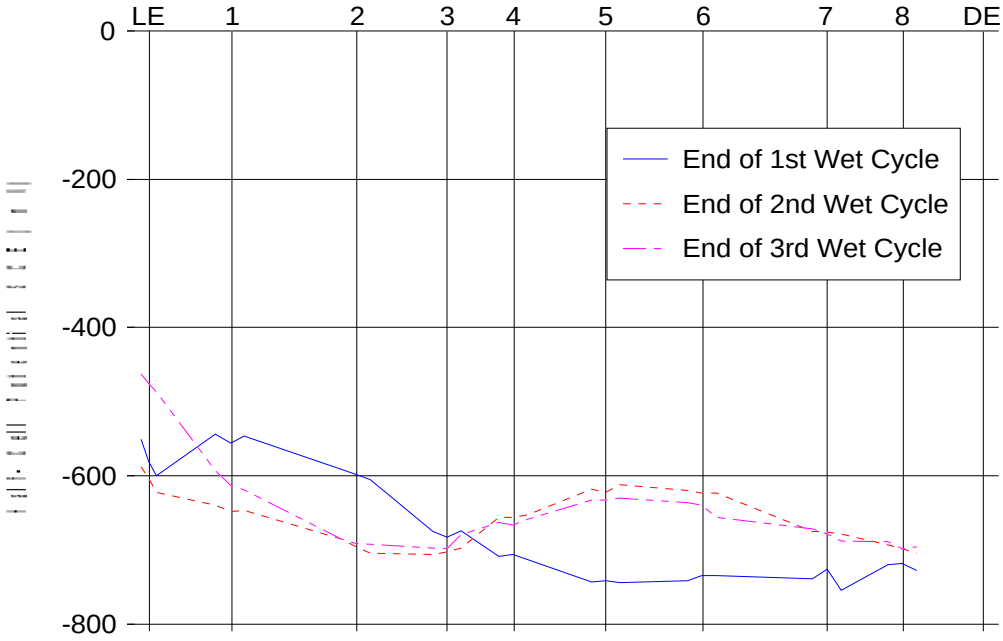

(b) Readings Taken at the End of a Wet Cycle.

Figure 9.4 - Half-Cell Potentials Taken on Grout Surface for Specimen LS-4.

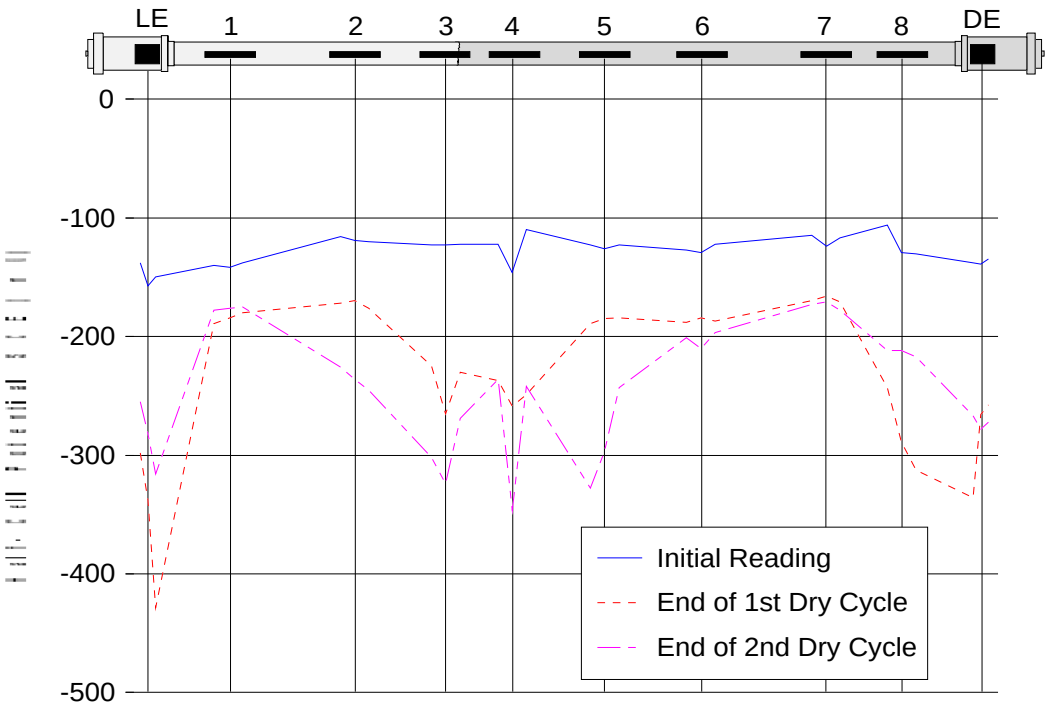

(a) Readings Taken at the Beginning of a Wet Cycle.

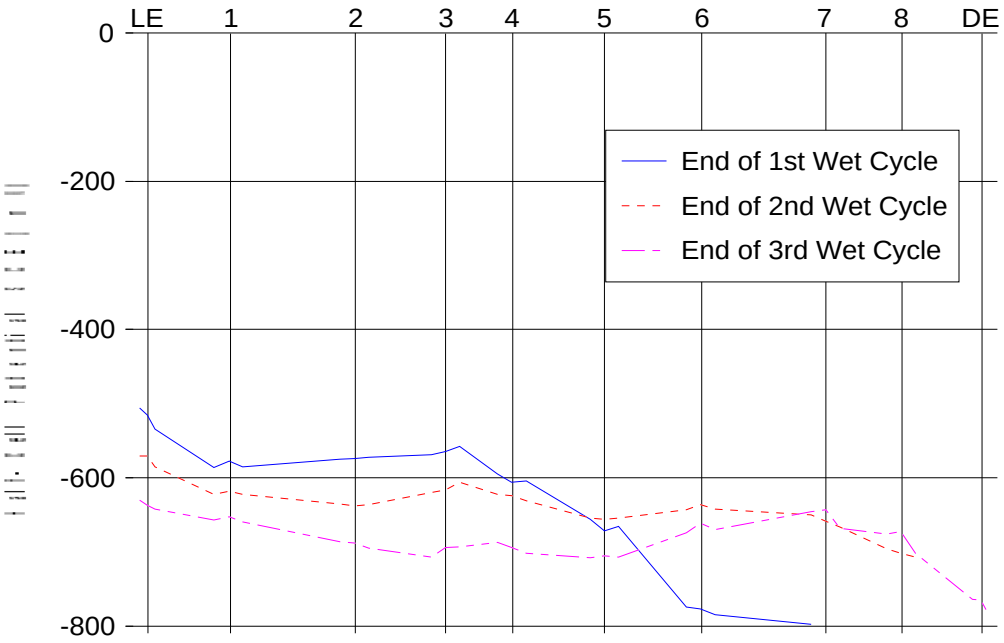

(b) Readings Taken at the End of a Wet Cycle.

Figure 9.5 - Half-Cell Potentials Taken on Grout Surface for Specimen LS-5.

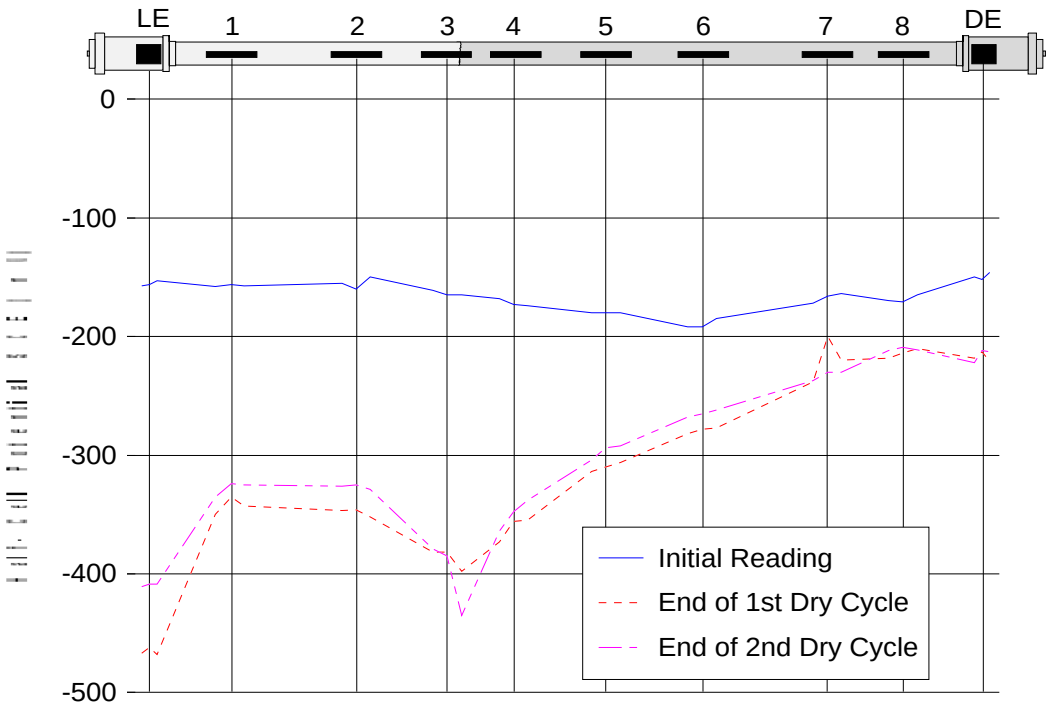

(a) Readings Taken at the Beginning of a Wet Cycle.

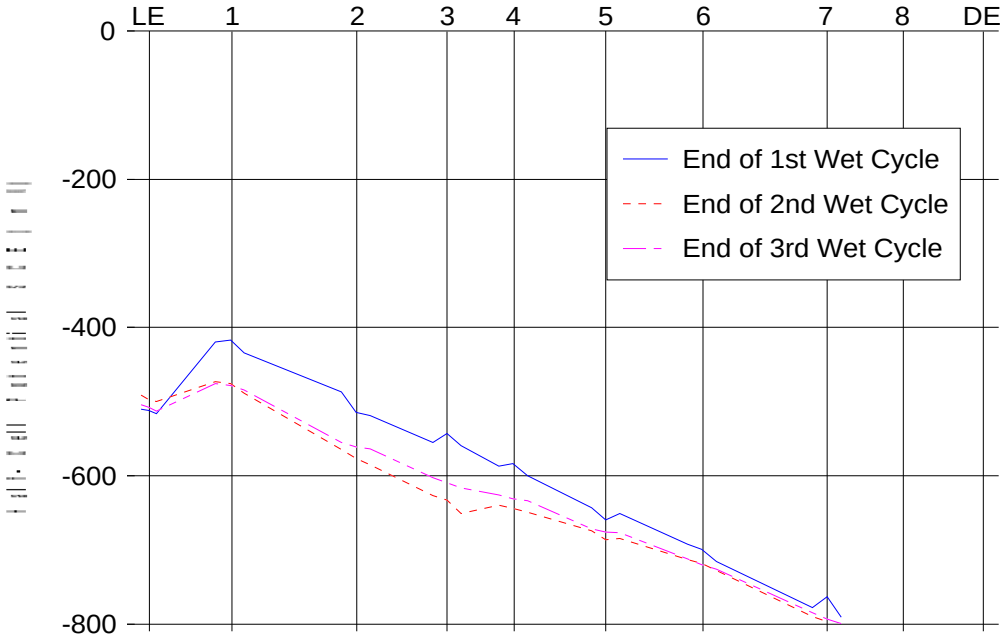

(b) Readings Taken at the End of a Wet Cycle.

Figure 9.6 - Half-Cell Potentials Taken on Grout Surface for Specimen LS-6.

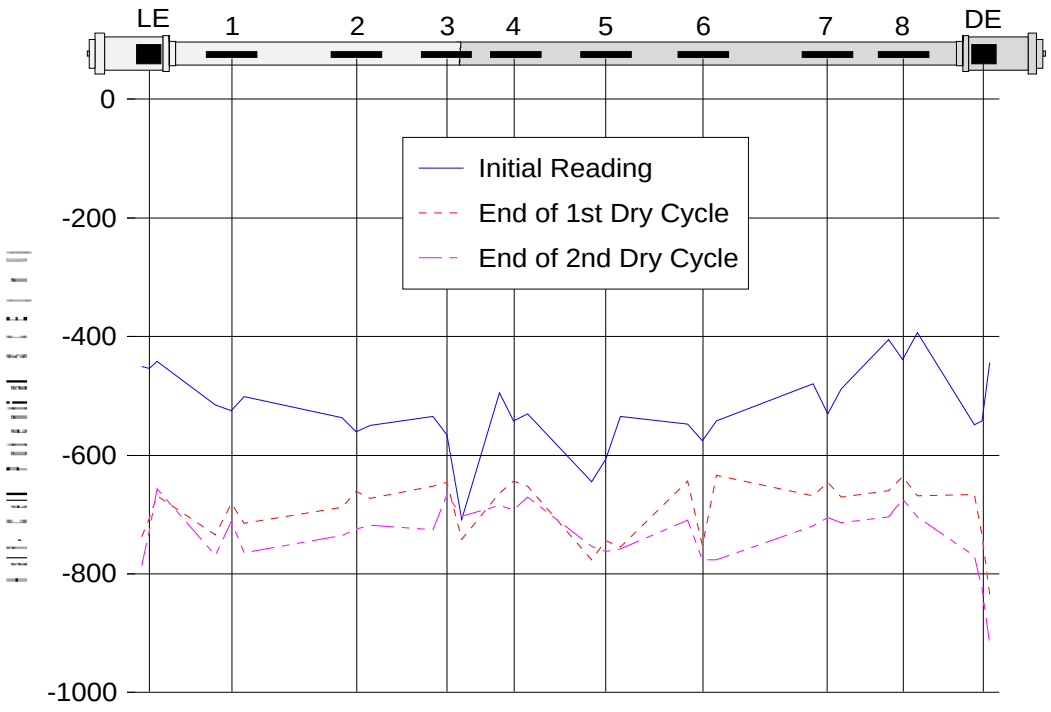

(a) Readings Taken at the Beginning of a Wet Cycle.

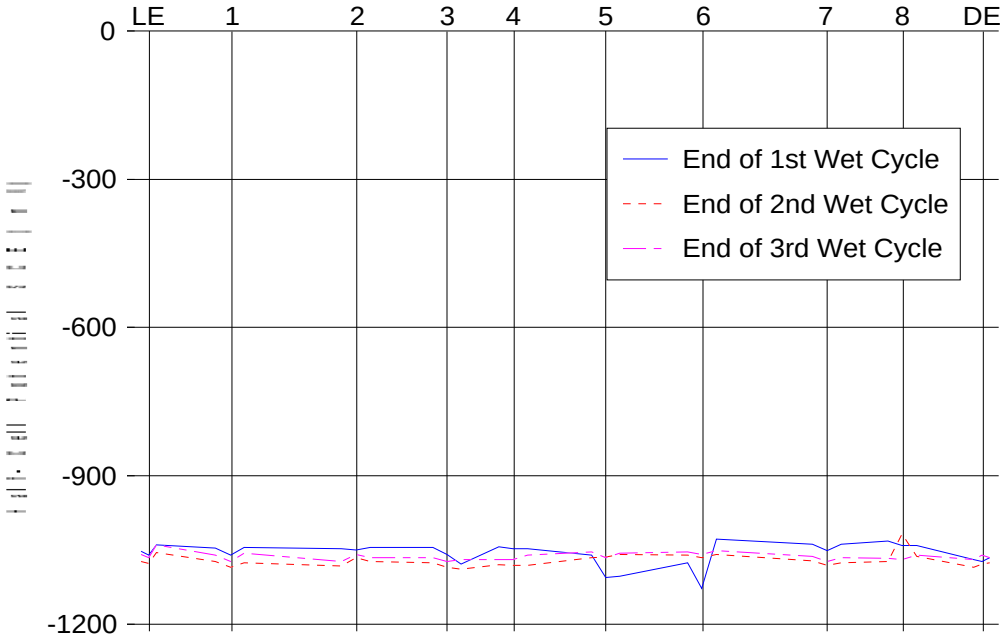

(b) Readings Taken at the End of a Wet Cycle.

Figure 9.7 - Half-Cell Potentials Taken on Grout Surface for Specimen LS-7.

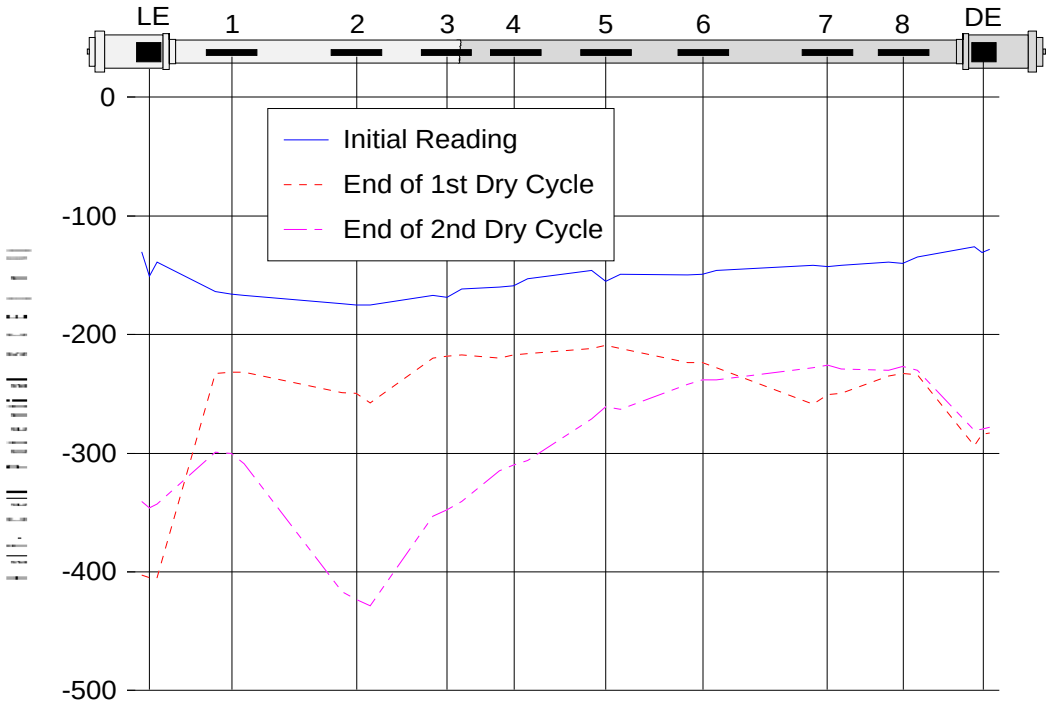

(a) Readings Taken at the Beginning of a Wet Cycle.

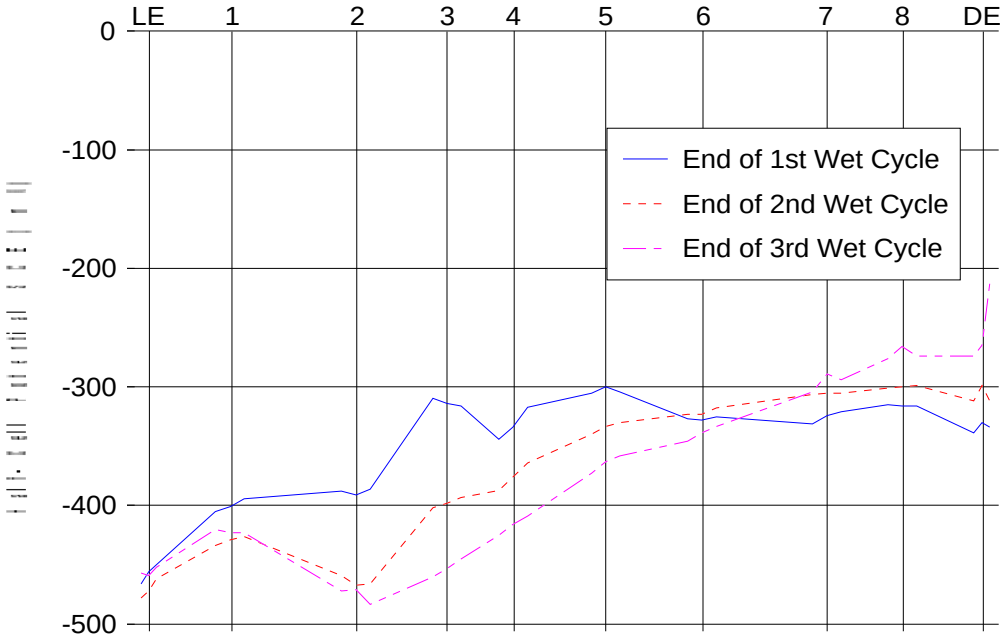

(b) Readings Taken at the End of a Wet Cycle.

Figure 9.8 - Half-Cell Potentials Taken on Grout Surface for Specimen LS-8.

Plot (a) of each figure gives the readings taken at the beginning of a wet cycle after a two-week dry cycle. The grout moisture content at this point is most likely to match that encountered in the field. Plot (b) gives the readings taken at the end of the wet cycle. The grout in this case is saturated after having been ponded with salt solution for two weeks. Hime indicates that the half-cell potential in concrete often represents the chemistry of the solution in contact with the steel and may not correlate to corrosion at all.[60] He suggests that if chloride ions are present they complex with the ferrous ions and lower their concentration, thus making the potential more negative. In addition, González et al. found that the half-cell potential of concrete can be influenced by the moisture content.[54] The greater the moisture content, the more negative is the potential. It is likely that the very negative potentials read on the saturated grout reflected the "chemistry" and moisture content of the grout rather than the presence of active corrosion. Therefore, plot (a) is the most useful of the two and will be discussed further in the following sections.

9.6.1 Specimens LS-1 through LS-5

The initial readings made on LS-1 through 5 indicated that the half-cell potential for the uncorroded prestressing strand was in the range of -120 to -150 mV_{SCE}. This differs somewhat from the Modified Accelerated Corrosion Test Method (modified ACTM) reported in Chapter Six. In those tests the half-cell potential was consistently between -190 and -220 mV_{SCE}. In both cases the grout was cracked, so this should not have caused the difference in the two sets of readings. In the modified ACTM the specimens were immediately immersed in the salt solution after removal of the sheathing. Therefore, there was no opportunity for the moisture content of the grout to drop below that in the sealed system. In the large-scale tests the initial half-cell potential readings were taken on the surface of the grout several days after the removal of the sheathing. This allowed the loss of moisture from the grout in the area of the opening where the half-cell potentials were taken. As discussed previously, the half-cell potential becomes more negative as the moisture content increases due to the increased conductivity. This explains the difference in the half-cell potentials between the large-scale tests and the modified ACTM.

Another common occurrence for the two-barrier specimens was that the half-cell potentials at the DE and LE openings were in the range of -200 to -350 mV_{SCE} at the end of the test period and in some cases less than -400 mV_{SCE}. In the free length these values generally indicated the presence of corrosion. However, very little exterior or interstitial corrosion was found on the strands in area of the DE or LE openings. The deviator rings were within 100 mm of the points where the half-cell potentials were taken at these openings. During post-mortem examination it was found that the deviator rings were severely corroded and were likely the cause of the negative potentials at the LE

and DE openings. As a result, the half-cell readings in the LE and DE openings did not necessarily reflect the activity on the strands locally and most likely were dominated by the depressed potential at the deviator rings.

Distribution of Half-Cell Potentials. The half-cell readings for openings 1-8 in specimens LS-1 through 4 are plotted in Figure 9.9. The distribution of readings gives an indication of the range of potentials for which corrosion may be expected.

No corrosion was found at any of the openings which had a half-cell potential more positive than -150 mV_{SCE}. However, there was significant overlap in the range between -150 and -250 mV_{SCE}. There were 33 data points which were in this range and which had no corrosion on the underlying strand. In contrast, there were 18 data points which had potentials in this same range but had significant corrosion.

The average initial half-cell potentials taken prior to the initiation of the accelerated corrosion test for LS-1 through 4 were -126, -116, -132, and -99 mV_{SCE}, respectively. There was no corrosion on the strand at the time these readings were taken.

These half-cell potentials corresponded reasonably well to the ranges given in ASTM A876.[9] ASTM suggests that for potentials more positive than -130 mV_{SCE} there is less than 10% probability of corrosion. For potentials more negative than -280 mV_{SCE} there is more than 90% probability of corrosion. If the potential is between these limits then the probability of corrosion is uncertain. The data shown in the figure indicate that there were no uncorroded locations which had a final reading more negative than -250 mV_{SCE}. This corresponds reasonably well to the more negative limit of the standard. There were very few readings more positive than -150 mV_{SCE} so a trend in this range could not be established. However, the trend of the locations which did have corrosion indicates that there would be a low probability of corrosion at sites which had readings more positive than -150 mV_{SCE}. Finally, between -150 and -250 mV_{SCE} there would be some uncertainty whether there was corrosion or not.

Increase in Potential During Test. The half-cell potential at opening 1 and 3 of LS-2 at the end of the test were more positive than the potentials taken during the test. This indicated that the corrosion in these openings may have ceased or slowed during the test causing an increase in potential. Post-mortem examination of the specimen revealed a significant amount of interstitial corrosion in the strands between opening 1 and 5. It is likely that the activation of this interstitial corrosion had the effect of cathodically protecting the exterior of the strands in opening 1 and 3, thus reducing or eliminating the corrosion.

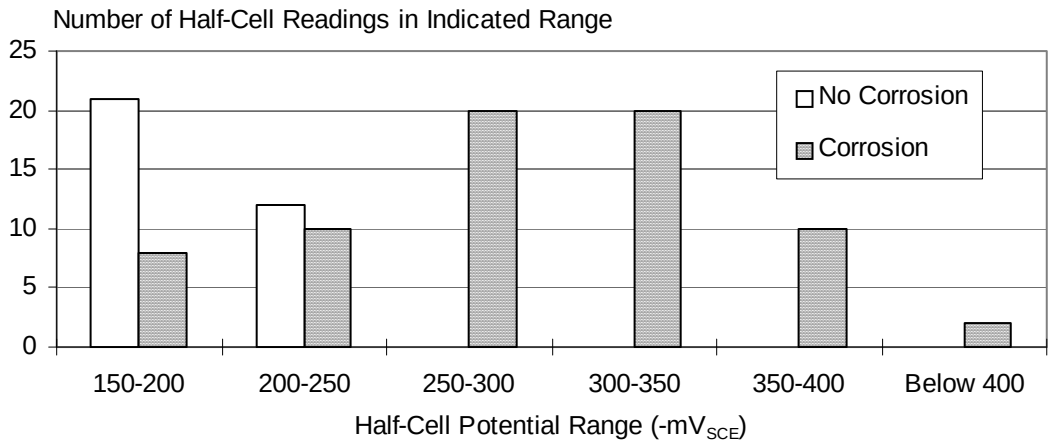

Figure 9.9 - Distribution of Half-Cell Readings After the Third Dry Cycle for LS-1 through LS-4.

Effect of Interstitial Corrosion. If the potentials for specimen LS-2 at openings 1, 2, and 3 are compared to the potentials in 4, 5, and 6 there is a difference of approximately 50 mV in the readings between the two groups of openings at the end of the 1st dry cycle. In addition, a significant amount of interstitial corrosion was found in the strands under openings 1, 2, and 3. It is possible that the interstitial corrosion was causing the slightly more negative readings than at openings 4, 5, and 6 which were found to have minimal interstitial corrosion. One difficulty in using the half-cell readings to make a distinction between the two types of corrosion is that both types of corrosion activity will give more-negative half-cell potentials if either or both are present.

9.6.2 LS-6 Epoxy-Coated Strand

The epoxy-coated strand had only two locations between the anchor heads where corrosion was found. Both of these locations were at intentional damages. It is interesting to note that even with this minimal amount of corrosion, the half-cell potentials were very negative compared to the readings taken in LS-1 through LS-5. The half-cell readings started in the range of -150 to -200 mV_{SCE} which was slightly more negative than the values in for the uncoated strands. At the end of the test they had dropped to more negative than -300 mV in openings 1 through 4 and were between -200 and -300 mV at openings 5 through 8. The only opening which had significant corrosion was opening 2 at the damaged area on strands one and two.

Kahhaleh cited field studies that have shown that there is no correlation between half-cell readings and visual bar ratings on epoxy-coated reinforcing based on ASTM A876.[66] Perenchio et al. found half-cell potentials in the range of -330 to -430 mV_{SCE} for undamaged, non-corroding epoxy-coated strand embedded in concrete.[89] The epoxy-coated strand were made by the same

manufacturer as the strands used in these tests. This range is similar to the range of readings taken in openings 1 through 4.

Figure 9.10 shows a schematic close-up of the strand/wedge interface for an epoxy-coated strand. During the stressing operation when the strand is released the teeth of the wedge pierce the epoxy and penetrate the strand. This causes the epoxy to flow into the spaces between the wedge teeth. In addition, the seating action disrupts the bond between the epoxy and the strand in the area between the teeth. It is also possible that the seating action opens a small space between the teeth and the epoxy allowing access of chlorides, moisture and oxygen. This mechanism explains the corrosion shown in Figures 8.30 and 8.31 in Chapter Eight.

9.6.3 LS-7 Galvanized Strand

The half-cell potentials for the galvanized strand were initially between -550 and -600 mV_{SCE} with the exception of opening 8. At the end of the first and second cycles, the potentials had dropped to the range of -650 to -750 mV_{SCE}. Yeomans reported half-cell potentials on galvanized reinforcing in concrete taken during accelerated corrosion tests.[131] The initial values prior to the application of salt solution were approximately -580 mV_{SCE}. When sufficient chlorides had reached the level of the steel the values dropped to -980 mV_{SCE}; although the potentials did increase to approximately -600 mV_{SCE} over time depending on the severity of the conditions.

In general, the initial potentials agree with Yeomans' results. However, the very negative

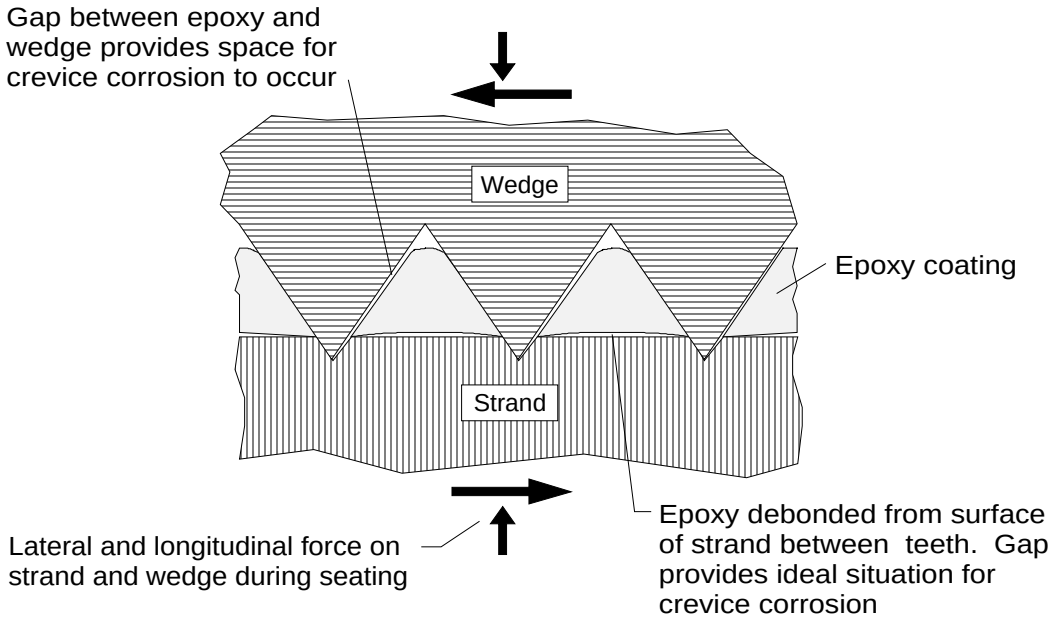

Figure 9.10 - Corrosion Mechanism at Strand/Wedge Interface of Epoxy-Coated Strand.

potential obtained by Yeomans after the initiation of zinc corrosion is much more negative than the potentials encountered in this study. One explanation is that the zinc-iron alloy on the surface of the strand may be different from that of the reinforcing steel in Yeomans' tests. Yeomans indicates that the free corrosion potential of pure zinc is around -1065 mV_{SCE} while that of steel is -540 mV_{SCE}. The potentials of the zinc-iron alloys vary between these two potentials. It is possible that the layer of galvanizing had an alloy higher in iron content than that of the reinforcing steel in Yeomans' test, thus leading to the difference in potentials.

9.6.4 LS-8 Greased and Sheathed

LS-8 had corrosion in four locations between the anchor heads: openings 1, 2, 3, and 6. All four were in areas where the strand sheath was intentionally damaged. Ignoring DE and LE potentials, the half-cell readings for 1, 2, and 3 are all more negative than -300 mV_{SCE}. Opening 6 has a final half-cell potential of -250 mV_{SCE}. This more positive reading may be due to the location of the corrosion at this opening. The corrosion did not occur on the strand directly under the strand sheath damage. It occurred approximately 100 mm away from the opening.

The initial half-cell readings were between -150 and -200 mV_{SCE} , similar to the readings for the epoxy-coated strand. It is likely that the greased and sheathed strand and the epoxy-coated strand behaved similarly.

9.7 Crevice Corrosion in Wedges

The post-mortem examination revealed that consistently the strands and wedges were completely encased in grout. The passivating effect of the grout made the presence of chlorides necessary for corrosion to occur in and around the prestressing wedges. Chloride tests on samples of uncontaminated grout indicated that there were no detectable chlorides present in the grout prior to the corrosion test. Therefore, the salt solution must have moved from the DE and LE openings (where the salt solution was applied) to the anchorage region during the wet cycles.

Figure 9.11 shows the schematic of one possible mechanism by which the chlorides could have traveled to the anchorage from the transition openings. During the wet cycles it was visibly noted that the solution placed in the DE and LE opening would seep into the grout/sheathing interface and slowly migrate towards the anchor head as shown in the figure. During the application of additional load midway between the wet cycles the salt solution could have been drawn into the interface between the strand and the anchor head. The solution then permeated into the wedge-strand interface and initiated corrosion. In some cases the solution eventually made its way into the grout under the grout cap as indicated by the high chloride content found in some samples. This situation might be even worse in inclined stays, where gravity would assist downward migration.

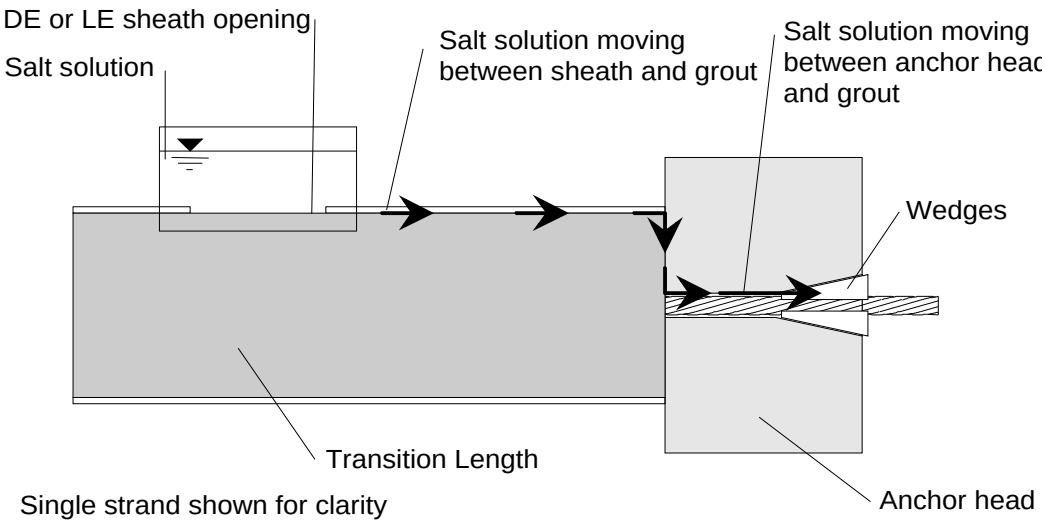

Figure 9.11 - Schematic of Chloride Transport Mechanism.

Post-tensioning is applied with a hydraulic ram. After the proper level of stress had been reached the wedges were placed around the strands in the anchor head and the strands are released. Upon release the strands shorten and pull the wedges into the beveled holes in the anchor head. The wedges are forced against the strand while the teeth on the wedges bite into the strand to keep it from slipping relative to the wedge. This causes local deformations in the strand in the area of the teeth as shown in Figure 9.12. These deformations can affect the corrosion behavior of the strand in two modes. The first mode is by the plastic deformations in the crystal lattice caused by the deformations. Cold-worked or plastically deformed steel can is generally more susceptible to corrosion.[123] This susceptibility is probably heightened by the nearby areas of undeformed strand. The second is that the small spaces created by the close contact between the strand and wedges provide excellent cavities for chlorides, moisture, and oxygen to gather. The confined space allows the corrosion to transform into crevice corrosion (mechanism discussed in Chapter Two); thus accelerating the corrosion process.

One additional factor is the difference in the metallurgy between the wedges and strand which can result in an acceleration of corrosion due to the potential difference in the two metals.

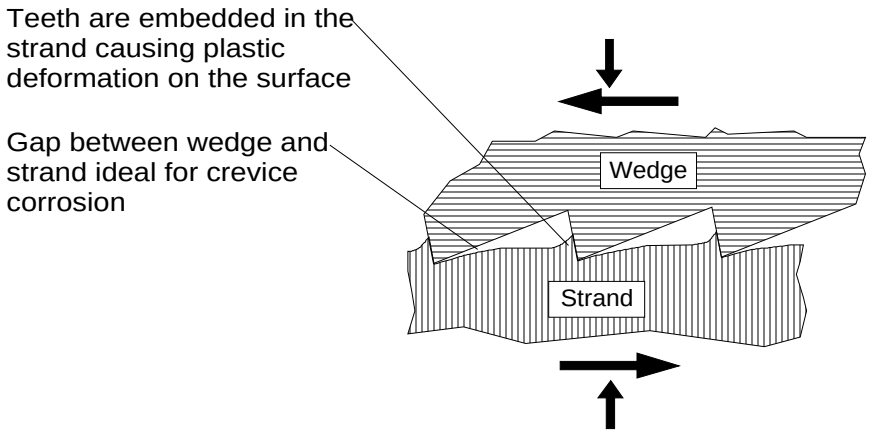

Figure 9.12 - Schematic of Strand/Wedge Interface.

9.8 Conclusions

Four large-scale stay cable specimens have been subjected to an artificially severe environment with the purpose of providing a comparison of the relative effectiveness of the currently used corrosion protection systems. Openings were made in the sheathing which represented accidental breaks in an actual stay. The exposed surface of the grout was then ponded with salt water. In addition to providing a basis with which to compare the improved systems, the testing uncovered many interesting behavioral tendencies. The most important of these is that within two to three days of cutting an opening in the sheath the grout in the immediate vicinity of the opening would shrink and crack.

This finding essentially voids the concept that a stay system which has bare strand with or without TCP in a PE sheath, and is injected with portland cement grout is a “two-barrier system.” At any location where a break in the sheathing occurs the grout will probably crack, allowing immediate access of air and moisture and also chlorides or pollutants, if present. As a result, the strands in the vicinity of the sheath opening corroded almost immediately. This effectively reduces the two-barrier system to a one-barrier system. The second level of protection that the grout is intended to provide, is rendered ineffective.

In addition to the corrosion of the strands at the sheathing openings, corrosion also occurred away from the openings. The salt solution migrated away from where it was ponded at the openings in the sheathing. High chloride levels as well as corrosion were found in the anchorage region of the specimens. Especially disturbing was the corrosion found at the strand-wedge interface.

Due to the poor performance of the two-barrier system under these artificially severe test conditions, four additional specimens were tested using improved corrosion protection systems.

Three of the specimens had an additional layer of protection added to the individual strands: epoxy-coating, galvanizing, and greasing and sheathing. The fourth specimen used grout which was improved with silica fume. In addition, there was no additional protection provided for the strand.

While the three systems which used an additional barrier provided a substantial increase in corrosion protection, the improved grout provided only a slight improvement. It is hypothesized that this slight improvement was due to a reduced corrosion rate caused by the increased ohmic resistance of the grout.

Each of the three improved systems provided a substantial increase in the level of protection over the two-barrier system in the accelerated corrosion tests. However, there were some differences in the behavior of the specimens. Each protection system had its strong and weak points with respect to performance under the accelerated corrosion test.

LS-6 Epoxy-Coated Strand:

- Epoxy-coated strand provided excellent corrosion protection where the coating was intact. However, interstitial corrosion was found on the epoxy-coated (unfilled) strand in several locations. This finding supports the requirement in PTI recommendations that only the epoxy-coated and filled strand should be used in stay cables.
- Epoxy was tough and durable. Intentional damage was very difficult to inflict , even with a sharp utility knife. This toughness can reduce accidental coating damage during installation in field-assembled stays. In this specimen, there were no locations where the epoxy was unintentionally damaged during assembly.
- Corrosion occurred in a few of the intentionally damaged areas that were not repaired. However, the coating was well bonded to the strand and no undercutting of the coating was noted in the areas around the exposed strand where the coating was still intact. This characteristic reduces the tendency for the corrosion to spread.
- Repair methods need improvement. Even when mixed in accordance with the instructions the epoxy repair material was thin and watery. The repair did not give a substantial coating thickness. While no corrosion was found in the free length at the repairs, the coating is not likely to provide adequate protection. When used to attach the plastic caps to the ends of the strands the epoxy repair material did not prevent grout from intruding into the cap, nor did it protect the ends of the strand from corrosion when painted on the exposed end of the strand.

- In some locations the epoxy coating was damaged in the contact area between the strand and the deviator ring.
- Corrosion occurred in several locations at the strand/wedge interface. Damage was noted adjacent to the wedge tooth marks were the epoxy had debonded from the strand.

LS-7 Galvanized Strand

- Provided excellent corrosion protection in all areas of stay including the grip region. In addition, the galvanic action of the zinc protected other stay components as well.
- Increase in bond indicated that the zinc layer on the outer surface had corroded significantly when the grout was fresh. This corrosion process produces hydrogen which may lead to hydrogen embrittlement of the strand if not controlled.

LS-8 Greased and Sheathed Strand

- Sheathing provided excellent protection when intact.
- Significant corrosion occurred at areas where strand sheathing was damaged and not repaired. In one location the corrosion product was found under the sheathing away from the damage. The recommended repair procedure with Tedlar tape worked very effectively.
- When the areas selected for intentional damage were being cut it was noted that the PE was soft and easily cut. Special precautions would be necessary in the field to prevent damage to the sheathing during installation.
- Couplings that connected the strand sheathing to the anchor head, and that were designed to keep grout and salt solution away from the greased strand, did not perform as intended. Grout penetrated the coupling and leaked through the strand opening in the anchor head. The connection between the coupling and the strand sheath was inaccessible for inspection during the installation of the second anchor head because the area was covered by the transition sheathing. These couplings should be carefully designed for ease of installation and inspection, and ability to prevent grout intrusion.

Chapter Ten
Conclusions and Recommendations

10.1 Summary

In recent years questions have been raised concerning the effectiveness of stay cable corrosion protection systems. Severe corrosion problems have been encountered with older locked-coil strand systems in which complete replacement of the cables was required in at least two cable-stayed bridges. In more recent years, the two-barrier system (prestressing strand or wire main tension element inside a polyethylene (PE) sheath injected with portland cement grout) has become popular and has been used worldwide. This system has performed satisfactorily in that there have been no serious recorded problems requiring stay replacement. However, the system has only been in use for the last twenty-five years in major vehicular bridges and the majority of the bridges in the US have been constructed in the last fifteen years. In addition, at this time, no stay cables which use this two-barrier system have been fully inspected or replaced. As a result, there is limited field data available on the in-service performance of this system. There were only two experimental studies found in the literature which examined the effectiveness of corrosion protection of stay cables. An extensive survey of owners, designers, constructors, and stay suppliers was carried out to document current opinions and concerns. The survey results are reported in Chapter Four.

An inherent characteristic of the two-barrier system is that it does not allow non-destructive visual inspection while in service. There are no NDE systems currently available which are sufficiently reliable to inspect the main tension elements for loss of section due to corrosion.

Two bridges have had reported problems with cracked PE sheathing in service. Minor corrosion of the main tension element at a break in the PE sheathing was encountered on one of these bridges during a recent inspection. In addition, there have been serious corrosion problems encountered in a number of recent fatigue acceptance tests.

In response to these concerns the stay cable suppliers have been introducing “improved” corrosion protection systems in the form of individual barriers for the main tension elements. Such systems include epoxy-coated strand, greased and sheathed strand (with or without galvanizing of strand), and galvanized strand or wire. In addition, alternate materials for injection such as petroleum wax and polyurethane have been used to replace portland cement (pc) grout. In some cases the injection material has been eliminated altogether.

To address these concerns an experimental program was developed to study the effectiveness of the corrosion protection provided by the basic two-barrier system and several of the "improved" systems. The objectives of the program were:

- Develop and implement a rational and objective evaluation of the two-barrier corrosion protection system.
- Evaluate several improved corrosion protection systems.
- Provide a basis for continued objective research in this area.

While the ability of intact PE to prevent the ingress of moisture and pollutants is well documented, the performance of the pc grout as the secondary barrier is not. The focus of the first part of the study was on the protection provided by the pc grout as a secondary barrier after an accidental but realistic breach of the PE barrier. If the PE cracks, how well does the pc grout protect the main tension elements?

In order to test the effectiveness of grout in providing corrosion protection, it was necessary to develop a suitable grout mix. It was decided to optimize the pc grout mix in terms of two properties of the fresh grout: bleed under pressure and fluidity. Corrosion inhibiting admixtures were also tested in this series to determine their effect on the fresh properties. The results of this study are presented in Chapter Five.

Several of the grout mixes developed in the grout test were tested using the Modified Accelerated Corrosion Test Method (ACTM). The results are presented in Chapter Six. The specimens were composed of single seven-wire strands covered with a layer of grout. The specimens were then immersed in salt solution and a potential was applied to the strand to accelerate the ingress of the chlorides. The grout was precracked in all of the Modified ACTM specimens prior to initiating the accelerated corrosion testing.

The large-scale tests investigated the entire stay cable system including the anchorage. A total of eight specimens were tested, each of which was composed of 12 12.7-mm diameter seven-wire prestressing strands placed inside transparent sheathing to aid in visual observation of grout injection and corrosion tests. In addition, each specimen had two anchor heads and two deviator rings. The specimens were assembled and loaded to 30% of their ultimate strength ($0.30F_{ULT}$) to simulate dead load conditions in the field. The stays were then injected with grout in an inclined position using typical field grouting procedures. After the grout had cured, additional axial load as well as lateral load were applied to selected specimens. These loads were intended to represent the effects of live loads and wind or light earthquake loads respectively. The accelerated corrosion

portion of the test consisted of cutting simulated breaks in the sheathing, exposing the grout. Salt solution was then ponded on the exposed grout to test its effectiveness in protecting the underlying strand from corrosion. The salt solution was applied in two week wet/dry cycles for a total test duration of three months. The stay specimens were then disassembled and subjected to a "post-mortem" examination.

10.2 Stay Cable Survey Trends

The stay cable survey covered many aspects of the design, construction, and installation of stay cables. The following trends were pertinent to the corrosion protection and durability.

10.2.1 Corrosion Protection

For corrosion protection the following items were very highly rated in the All category of respondents (the "All" category indicates that the responses from all respondents were considered):

- Parallel wire or parallel strand are preferred over wire rope, bridge strand, or locked-coil cables when considering the ease with which corrosion protection is provided.
- Greased and plastic sheathed galvanized tension element.
- Epoxy coated and filled tension element.
- Some type of blocking system (numerous systems mentioned all with about the same rating).
- HDPE external sheath.
- System: greased and individually sheathed galvanized tension element, with wax or cement grout and external HDPE.
- Portland cement grout is felt to be an adequate corrosion protective system and the grout is believed to completely encase the tension elements, although European respondents doubt the adequacy of the grout.
- Galvanizing, epoxy coating or greased and sheathed monostrand are preferred.

10.2.2 Inspectability/Durability

For inspection and durability the following items were very highly rated in the All category of respondents:

- Multiple protection and limited visual inspection but other monitoring options (electrical/magnetic).
- The entire stay should be replaceable as opposed to individual elements of the stay.

- Stay life expectancy is bimodal with a large group favoring 26-50 years and another favoring 76-100 years. Average stay life expectancy is 60 years.

The survey indicated that the trend toward the use of prestressing wire, strand and bar will continue. In addition, the use of structural rope, locked-coil strand and structural strand will continue to decrease. There is a lack of confidence in blocking materials for providing corrosion protection, in that blocking compounds were given ratings in the range of 59% to 64%. Conversely, much more confidence is placed in individual protection systems such as epoxy-coating and greased, sheathed and galvanized with ratings of 76% and 84%, respectively. This may indicate a lack of confidence in the ability to properly install or inspect blocking compounds. Whereas, individual protection systems are installed in the factory and can be visually inspected prior to installation.

One surprising result was the low rating of 63% given to galvanizing as an individual corrosion protection barrier. It is interesting to note that while this system has been used successfully for years in suspension bridges, it is given a relatively low rating for use in cable-stayed bridges. The results from another question asking for the rating of stay systems contradicts this opinion. The rating given for galvanized tension elements with wax blocking compound and HDPE sheathing was 73%. This indicates that the respondents felt that the galvanizing alone is not sufficient but that it should be used with other systems. Another contradiction was the rating of 77% given to galvanizing alone for temporary corrosion protection. This rating was higher than for epoxy-coating or greasing and sheathing.

Stays without an external sheath were rated very low at 23%. This indicates that the respondents overwhelmingly believe that an external sheathing should be used. The highest rated external sheath was HDPE at 80%.

10.3 Conclusions

10.3.1 Portland Cement Grout Series

The portland cement grout series measured the fresh and hardened properties of portland cement grout with various admixtures and water/cement ratios. Tests included fluidity, bleed, bleed under pressure, initial set time, cube strength and pH. The primary goal of the test series was to develop a grout mix which had minimum bleed and still remained fluid. The following findings were made:

- An optimum mix design was developed which met the designated criterion for bleed under pressure.

- Corrosion inhibitors that were added to the optimum mix design did not adversely affect the properties of the grout. The only significant effect was the reduction of the set time caused by the calcium nitrite. However, this had the beneficial effect of offsetting the delay in set time caused by the anti-bleed admixture used in the optimum grout mix.
- Silica fume was used in conjunction with the anti-bleed admixture to produce a reduced-bleed silica fume grout. This mix was used in the "improved grout" specimen in the large-scale tests (LS-5).

10.3.2 Modified ACTM

The Modified Accelerated Corrosion Test Method was used to test the durability of several grout mix designs. The grout was placed around a seven-wire prestressing strand using a PVC mold. After curing the grout was flexurally precracked and a section of the PVC pipe was removed, exposing the resulting crack. The specimen was then immersed in a 5% salt solution and anodically polarized at +600 mV_{SCE}. This accelerated the migration of the chlorides through the exposed crack in the grout to the surface of the steel to initiate corrosion. The time necessary for the chlorides to penetrate the grout was termed time-to-corrosion. The times-to-corrosion of grouts with various admixtures were compared and ranked. The following findings were made:

- The optimum anti-bleed grout developed in Chapter Five had a time-to-corrosion 30% less than that of a standard grout (w/c = 0.40 and no admixtures). Based on these results it can be concluded that the use of the anti-bleed admixture can reduce the effectiveness of cracked grout in providing corrosion protection.
- The use of calcium nitrite reduced the effectiveness of cracked grout in providing corrosion protection. The reduction in time-to-corrosion was 27 percent.
- The use of Rheocrete 222 slightly improved the effectiveness of cracked grout in providing corrosion protection. However, the increase in time-to-corrosion was 4 %, which is not really significant considering the scatter of the data.
- The use of silica fume improved the effectiveness of cracked grout in providing corrosion protection. The increase in time-to-corrosion was 45 percent. The silica fume mix was selected and used in the "improved grout" specimen in the large-scale tests.
- Several potentiodynamic tests were conducted. There was no strong indication from these tests that would indicate an effect from grout ohmic resistance. However, average corrosion currents recorded prior to the time-to-corrosion indicated that there may be

some effect from the difference in polarization. No conclusion can be drawn at this point. Further investigation with more sophisticated equipment is required.

10.3.3 Large-Scale Test Series

10.3.3.1 Grout Injection

The large-scale specimens were placed in a sloped orientation, and the grout was injected in two lifts of approximately equal lengths. In the planning stages of the test program, the grout joint at the interface between the two lifts was thought to be an area where the corrosion protection of the grout would be compromised. On the contrary, post-mortem examination of the specimens revealed that the joint was "tight" (no voids or other discontinuities were found).

Despite precautions taken and considering the ideal laboratory conditions, there was still a significant problem with air pockets forming in the specimens. Air pockets formed to some degree in all but one of the large-scale specimens. It is hypothesized that the air pockets formed because of the thickening effect of the anti-bleed admixture. Air is trapped as the grout is being injected but the grout is too thick to allow the air to rise to the top of the lift before it reaches initial set.

10.3.3.2 Additional Lateral Load Tests

Preliminary Analysis:

- Flexural stresses are significantly reduced at the anchor head when a damper is used.
- Moment was found to be rather insensitive to the presence of grout. This is because of the small cross sectional area of grout relative to the area of the strand bundle.

Load Tests:

- Audible cracking occurred on four of the six specimens tested with no discernible effect on the stiffness. In addition, the measured midspan load-displacement relationship was linear. These results confirm the analysis which suggests very little contribution from the grout to flexural stiffness.
- Cracking caused by lateral loads is not significant when compared to the cracking caused by additional axial loads simulating live load effects.

10.3.3.3 Additional Axial Load Tests

- Cracking occurred almost immediately upon lift off in all of the specimens. It is suspected that the grout already had tensile shrinkage strains from autogenous shrinkage.
- Specimen LS-7 (galvanized strand) had more narrow closely-spaced grout cracks during the application of additional axial load than the other specimens. This indicated that

there was improved bond between the galvanized strand and grout. This was probably due to the chemical reaction between the zinc and wet grout.

- Specimen LS-8 (greased and sheathed) had wide cracks at large spacings. This indicated poor bond between the strand and grout. While all of the other specimens had cracking occur only during the early stages of the load test, LS-8 had cracking also occur later in the test. During initial stages of the additional loading the strands have enough space inside the individual sheaths to elongate without transferring load to the grout through the individual sheath walls. However, as the later stages of the additional axial load test are reached, the strand has elongated sufficiently so that it transfers load through the sheath to the grout. This causes the later grout cracking.
- The presence of the grout had no measurable effect on the axial stiffness of the stay.
- The additional live load tests indicate that a relatively low level of axial load above the grout injection load (stay dead load level) is required to cause the grout to crack. These results confirm the findings from the inspection of the Pasco-Kennewick Bridge discussed in Chapter One. Thus it can be concluded with reasonable confidence that in most cable stayed bridges which use the two-barrier system, the grout is cracked along the full length of the stay cables.

10.3.3.4 Grout Precompression Test

Testing precompression of grout was not in the original scope of the series so it could not be thoroughly investigated as a viable method for improving corrosion protection. However, as an alternative, an abbreviated test of precompression was conducted on LS-5 (Bare strand with TCP and silica fume grout). This experiment indicated that the precompression was ineffective in controlling local shrinkage cracking of the grout.

10.3.3.5 Corrosion test

Eight large-scale stay cable specimens were subjected to an artificially severe environment with the purpose of providing a comparison of the relative effectiveness of the currently used corrosion protection systems. Openings were made in the sheathing which represented accidental breaks in an actual stay. The exposed surface of the grout was then cyclically ponded with salt water. In addition to providing a basis with which to compare the improved systems, the testing uncovered many interesting behavioral tendencies. The most important of these is that within two to three days of cutting an opening in the sheath the grout in the immediate vicinity of the opening would shrink and crack.

This finding essentially voids the concept that a stay system which has bare strand with or without TCP in a PE sheath, and is injected with portland cement grout is a "two-barrier system." At any location where a break in the sheathing occurs the grout will probably soon crack, allowing immediate access of air and moisture and also chlorides or pollutants, if present. As a result, in the four specimens with the "two-barrier system" the strands in the vicinity of the sheath opening corroded almost immediately. This effectively reduces the two-barrier system to a one-barrier system. At any location where the sheathing could be lost, the grout will shrink and crack (or most likely existing live load cracks will open) providing access for pollutants, moisture and oxygen to the strands. Thus, the second level of protection provided by the grout is rendered ineffective.

In addition to the corrosion of the strands at the outer sheathing openings, corrosion also occurred away from the openings. The salt solution was able to migrate away from the openings in the outer sheathing where it was ponded. High chloride levels as well as corrosion were found in the anchorage regions of the specimens. Especially disturbing was the corrosion found at the strand/wedge interface.

Another interesting finding was that the half-cell potential (HCP), taken with the saturated calomel electrode on the grout surface, gave a reasonable indication of the presence of corrosion. However, it is not recommended that the HCP be used in routine inspection. The test requires that the sheathing be removed at the location where the reading is being taken. In order to get useful results, HCP readings must be taken at close spacings, both along the length and around the circumference. This would require that the sheathing be broken at each reading location, which would compromises the stay corrosion protection.

Due to the poor performance of the two-barrier system under these artificially severe test conditions four additional specimens were tested using improved corrosion protection systems. Three of the specimens had an additional layer of protection added to the individual strands. These layers were epoxy-coating, galvanizing, and greasing and sheathing. The fourth specimen used grout which was improved with silica fume but had no other additional protection provided for the strand.

While the three systems which used an additional barrier provided a substantial increase in corrosion protection, the improved grout did not provide much improvement. There was a slight improvement in this specimen based on the visual inspection performed during the post-mortem examination. It is hypothesized that this was due to a reduced corrosion rate caused by the increased ohmic resistance of the grout.

Each of the three improved systems which used an additional barrier provided a substantial increase in the level of protection over the two-barrier system in the accelerated corrosion tests.

However, there were some differences in the behavior of the specimens. Each protection system had its strong and weak points with respect to performance under the accelerated corrosion test.

LS-6 Epoxy-Coated Strand:

- Epoxy-coated strand provided excellent corrosion protection where the coating was intact. However, interstitial corrosion was found on the epoxy-coated (unfilled) strand in several locations. This finding supports the requirement in PTI recommendations that only the epoxy-coated and filled strand should be used in stay cables.
- Epoxy was tough and durable. Intentional damage was very difficult to inflict , even with a sharp utility knife. This toughness can reduce accidental coating damage during installation in field-assembled stays. In this specimen, there were no locations where the epoxy was unintentionally damaged during assembly.
- Corrosion occurred in a few of the intentionally damaged areas that were not repaired. However, the coating was well bonded to the strand and no undercutting of the coating was noted in the areas around the exposed strand where the coating was still intact. This characteristic reduces the tendency for the corrosion to spread.
- Repair methods need improvement. Even when mixed in accordance with the instructions the epoxy repair material was thin and watery. The repair did not give a substantial coating thickness. While no corrosion was found in the free length at the repairs, the coating is not likely to provide adequate protection. When used to attach the plastic caps to the ends of the strands the epoxy repair material did not prevent grout from intruding into the cap, nor did it protect the ends of the strand from corrosion when painted on the exposed end of the strand.
- In some locations the epoxy coating was damaged in the contact area between the strand and the deviator ring.
- Corrosion occurred in several locations at the strand/wedge interface. Damage was noted adjacent to the wedge tooth marks were the epoxy had debonded from the strand.

LS-7 Galvanized Strand

- Provided excellent corrosion protection in all areas of stay including the grip region. In addition, the galvanic action of the zinc protected other stay components as well.
- Increase in bond indicated that the zinc layer on the outer surface had corroded significantly when the grout was fresh. This corrosion process produces hydrogen which

may lead to hydrogen embrittlement of the strand if not controlled.

LS-8 Greased and Sheathed Strand

- Sheathing provided excellent protection when intact.
- Significant corrosion occurred at areas where strand sheathing was damaged and not repaired. In one location the corrosion product was found under the sheathing away from the damage. The recommended repair procedure with Tedlar tape worked very effectively.
- When the areas selected for intentional damage were being cut it was noted that the PE was soft and easily cut. Special precautions would be necessary in the field to prevent damage to the sheathing during installation.
- Couplings that connected the strand sheathing to the anchor head, and that were designed to keep grout and salt solution away from the greased strand, did not perform as intended. Grout penetrated the coupling and leaked through the strand opening in the anchor head. The connection between the coupling and the strand sheath was inaccessible for inspection during the installation of the second anchor head because the area was covered by the transition sheathing. These couplings should be carefully designed for ease of installation and inspection, and ability to prevent grout intrusion.

10.4 Recommendations

- Based on the results of the tests and the information gathered in the literature review it is recommended that pc grout *not* be considered a corrosion protection barrier. While its use in stay cables may have other benefits, it should not be considered as an effective corrosion barrier. In addition, elimination of the pc grout improves the inspectablility and eases the replacement of the stay cable should it be required.
- The use of an additional individual barrier (such as epoxy-coating and filling, greasing and sheathing, or galvanizing) on the strand or wire main tension element is strongly recommended. When properly constructed an appropriate individual barrier provides a much improved backup system (in case the external sheath is damaged) compared to pc grout. In addition, for field assembled stays, individual barriers eliminate the need for temporary corrosion protection since permanent protection is installed on the strand or wire at the factory.
- It is strongly recommended that epoxy-coated unfilled strand should not be used in stay cable construction.

- The repair system for the epoxy-coated strand should be modified so that an effective thickness of repair material is deposited on the surface of the strand.
- If epoxy-coated strand is used in stay cables, addition effective protection (other than pc grout) must be provided for the strand in the area where the wedge teeth penetrate the epoxy. This protection should be provided immediately after the strands have been stressed.
- If pc grout is to be used in stays with greased and sheathed strands, care must be used in designing and installing the seal between the sheath and anchor head to ensure that grout/moisture do not seep into this area where the strands are unprotected.
- When epoxy-coated or greased and sheathed strand are used, deviator ring details should be used which preclude the possibility of damage to the epoxy or sheathing in the contact area is eliminated.
- Revisions to the Post-Tensioning Institute's *Recommendations for Stay Cable Design, Testing and Installation* are included in Appendix D.

10.5 Future Research

- Additional investigation of the variation of the ohmic resistance of pc grout with different admixtures is needed to validate the usefulness of the Modified ACTM.
- There are many different combinations of materials available for use in stay cables. Additional large-scale specimens need to be tested to determine the effectiveness of these systems. One set of tests could be conducted on a prefabricated wire or strand stay using a socket type anchorage such as the HIAM system. In addition, different injection materials should be tested such as petroleum wax, polyurethane, and epoxy.
- Another area which needs study is the problems which have occurred with the fatigue acceptance tests. The effect of different grouts and admixtures on corrosion fatigue resistance should be tested systematically.
- Assuming the validity of claims that new galvanizing processes eliminate the problem of hydrogen embrittlement, galvanized strand use shows great promise especially when combined with greased and sheathed applications. Such application should be investigated with further tests.

References

1. **ACI Committee 222**, "Corrosion of Metals in Concrete," *American Concrete Institute Manual of Concrete Practice*, Part 1, Committee Report ACI 222R-85, American Concrete Institute, Detroit, 1987.

2. **ACI Committee 224**, "Cracking of Concrete Members in Direct Tension," *American Concrete Institute Manual of Concrete Practice 1987*, Committee Report ACI 224.2R-86, American Concrete Institute, Detroit, 1987.

3. **ACI Committee 318**, *Building Code Requirements for Reinforced Concrete (ACI 318-89) and Commentary-ACI 318-89,* American Concrete Institute, Detroit, November 1989.

4. **Aitcin, P.C., Ballivy, G. and Parizeau, R.,** "The Use of Condensed Silica Fume in Grouts," *Innovative Cement Grouting*, ACI SP-83., Welsh, J. P., Ed, American Concrete Institute, Detroit, 1984.

5. **Allen, B.,** "Grouting of Post-Tensioning Ducts Alsea Bay Bridge," unpublished report, February 20, 1990.

6. **American Society for Testing and Materials**, "Standard Practice for Heat-Joining Polyolefin Pipe and Fittings," ASTM A2657-90, Philadelphia, PA, 1990.

7. **American Society for Testing and Materials**, "Standard Specification for Epoxy-Coated Seven-Wire Prestressing Steel Strand," ASTM A882-92, Philadelphia, PA, 1992.

8. **American Society for Testing and Materials**, "Standard Specification for Seven-Wire Prestressing Steel Strand," ASTM A416-92, Philadelphia, PA, 1992.

9. **American Society for Testing and Materials**, "Standard Test Method for Half-Cell Potentials of Uncoated Reinforcing Steel in Concrete," ASTM A876-87, Philadelphia, PA, 1987.

10. **American Society for Testing and Materials**, ASTM C109-90 *Compressive Strength of Hydraulic Cement Mortars (Using 2-in. or 50-mm Cube Specimens),* Philadelphia, PA, 1990.

11. **American Society for Testing and Materials**, ASTM C191-92 *Time of Set for Hydraulic Cement by Vicat Needle,* Philadelphia, PA, 1992.

12. **American Society for Testing and Materials**, ASTM C939-87 *Flow of Grout for Preplaced-Aggregate Concrete (Flow Cone Method),* Philadelphia, PA, 1987.

13. **American Society for Testing and Materials**, ASTM C940-87 *Expansion and Bleeding of Freshly Mixed Grouts for Preplaced-Aggregate Concrete in the Laboratory,* Philadelphia, PA, 1987.

14. **American Society for Testing and Materials**, ASTM C953-87 *Time of Set of Grouts for Preplaced-Aggregate Concrete in the Laboratory*, Philadelphia, PA, 1987.

15. **Beeby, A. W.**, "Cracking, Cover, and Corrosion of Reinforcement," *Concrete International*, February 1983.

16. **Berke, N. and Rosenberg, A.,** "Technical Review of Calcium Nitrite Corrosion Inhibitor in Concrete.," *Concrete Bridge Design and Maintenance: Steel Corrosion in Concrete*, Transportation Research Record 1211, Transportation Research Board, Washington, D.C., 1989.

17. **Berke, N. S.,** "Resistance of Microsilica Concrete to Steel Corrosion, Erosion, and Chemical Attack," *Fly Ash, Silica Fume, Slag, and Natural Pozzolans in Concrete: Proceedings, Third International Conference, Trodheim, Norway*, ACI SP-114, Malhotra, V. M., Ed., 1989.

18. **Berke, N. S., Shen, D. F. and Sundberg, K. M.,** "Comparison of Current Interruption and Electrochemical Impedance Techniques in the Determination of Corrosion Rates of Steel in Concrete," *The Measurement and Correction of Electrolyte Resistance in Electrochemical Tests,* ASTM STP 1056, L. L. Scribner and S. R. Taylor, Eds., American Society for Testing and Materials, Philadelphia, 1990, pp. 191-201.

19. **Birdsall, B.,** Readers Write, *Civil Engineering*, American Society of Civil Engineers, Vol. 58, No. 9, September 1988.

20. **Buergi, P.** "Recent Approaches to Corrosion Protection in Stay Cable Design," IABSE Symposium, Leningrad, September 11-14, 1991.

21. **Bureau BBR, Ltd.**, Product Information Pamphlet (not dated).

22. **CEB General Task Group No. 20,** *Draft CEB-Guide to Durable Concrete Structures, Bulletin D'Information No. 166*, Comite Euro-International du Beton, Switzerland, May 1985.

23. **Chalbert, A., Jartoux, P. and Villette, P.,** "The Introduction of Unbonded Greased or Waxed Tendons," International Association of Bridge and Structural Engineers Symposium, Helsinki, June 6-10, 1988.

24. **Chauvin, A.,** "Developments in the Technology of Bridge Stays," Tenth International Congress of FIP, New Dehli, India, February, 16-20, 1986.

25. **Cherry, B. W. and Price, S. M.,** "Pitting, Crevice and Stress Corrosion cracking Studies of Cold-Drawn Eutectoid Steels," *Corrosion Science*, Vol. 20, No. 11-12, 1980 pp. 1163-1184.

26. **Chou, G. K. and Hover, K. C.**, "Cathodic Protection for Prestressed Structures," *Concrete International,* January, 1987.

27. ***Civil Engineering* Staff,** "Brighter Future for Stay Cables," *Civil Engineering*, American Society of Civil Engineers, Vol. 58, No. 10, October 1988.

28. **Committee on Cable-Stayed Bridges,** "Recommendations for Stay Cable Design, Testing, and Installation," Post-Tensioning Institute, August 1993.

29. **Concrete Society's Design Group**, "Grouting Specifications," *Concrete* (London), Vol. 27, No. 4, July-August 1993

30. **Construction Technology Laboratories, Inc.,** "Combined Axial-Flexural Fatigue Tests of 37-Strand Stay Cable Specimen for the Clark Bridge, Alton Illinois," September 1992.

31. **Construction Technology Laboratories, Inc.,** "Fatigue and Static Tests of 31-Strand Stay Cable Specimen for the Burlington Bridge, Burlington, Iowa," October 1991.

32. **Construction Technology Laboratories, Inc.,** "Fatigue and Static Tests of 17-Strand Stay Cable Specimen for the Clark Bridge, Alton, Illinois," September 1992.

33. **Construction Technology Laboratories, Inc.,** "Fatigue and Static Tests of 46-Strand Stay Cable Specimen for the Clark Bridge, Alton, Illinois," September 1992.

34. **Cook, A. R.,** "High Strength Galvanized Wire in Prestressed Concrete," *Galvanized Reinforcement for Concrete - II,"* International Lead Zinc Research Organization, 1981.

35. **Cornet, I. and Bresler, B.,** High Strength Galvanized Wire in Prestressed Concrete," *Galvanized Reinforcement for Concrete - II,"* International Lead Zinc Research Organization, 1981.

36. **Demers, J. G. and Simonsen, O. F.,** "Montreal Boasts Cable-Stayed Bridge," *Civil Engineering,* ASCE, August 1971.

37. **Department of Structural Engineering Technical University of Denmark,** *Durability of Concrete Structures, Bulletin D'Information No. 152*, CEB-RILEM International Workshop, Copenhagen, April 1984

38. **Diederichs, U. and Schütt, K.,** "Silica Fume Modified Grouts for Corrosion Protection of Post-Tensioning Tendons," *Fly Ash, Silica Fume, Slag, and Natural Pozzolans in Concrete: Proceedings, Third International Conference, Trodheim, Norway,* ACI SP-114, Malhotra, V. M., Ed., 1989.

39. **Domone, P. L. and Tank, S. B.,** "Use of Condensed Silica Fume in Portland Cement Grouts," Fly Ash, Silica Fume, Slag, and Natural Pozzolans in Concrete: Proceedings, Second International Conference, Madrid, Spain, ACI SP 91-61, Malhotra, V. M., Ed., 1986.

40. **Dorsten, V., Hunt, F. F. and Preston, H. K.,** "Epoxy Coated Seven-Wire Strand for Prestressed Concrete," *Journal of the Prestressed Concrete Institute,* July-August 1984.

41. **Dywidag**, Product Information Pamphlet (not dated).

42. **Engelke, P.** "State of the Art Grout Injection Techniques for Prestressed Concrete," *Beton- und Stahlbetonbau,* Vol. 81, No. 6, June, 1986 (in German).

43. **Fidjestol, P.,** "Reinforcement Corrosion and the Use of CSF-Based Additives," Concrete Durability: Katherine and Bryant Mather International Conference, ACI SP-100, Scanlon, J. M., Ed, 1987

44. **Figg Engineering**, personal communication with Mr. Denny Pate, July 8, 1993.

45. **Florida Wire and Cable Product Information** (not dated)**.**

46. **Florida Wire and Cable, Inc.,** personal communication with Mr. Bob McCrossen, March 13, 1995, and subsequent letter, August 3, 1995.

47. **Fontana, M. G.,** *Corrosion Engineering,* McGraw-Hill Book Company, New York, 1986.

48. **Frank, K. H.**, Personal conversation.

49. **Freyssinet**, Product Information Pamphlet, May 1994.

50. **Funahashi, M., Wagner, J. and Young, W. T.,** "Cathodic Protection Developments for Prestressed Concrete Components," Report No. FWHA-RD-94-001, Federal Highway Administration, July 1994.

51. **Gautefall, O. and Havdahl, J.** "Effect of Condensed Silica Fume on the Mechanism of Chloride Diffusion into Hardened Cement Paste," *Fly Ash, Silica Fume, Slag, and Natural Pozzolans in Concrete: Proceedings, Third International Conference, Trodheim, Norway,* ACI SP-114, Malhotra, V. M., Ed., 1989.

52. **Ghorbanpoor, A. and Makathanapalli, S. C.,** "Grout for Post-Tensioning Bridge Structures," Draft FHWA report, May 1992.

53. **Gimsing, N. J.,** *Cable Supported Bridges-Concept and Design*, John Wiley and Sons, New York, 1983.

54. **González, J. A., Benito, M., Feliu, S., Rodriguez, P. and Andrade, C.,** "Suitability of Assessment Methods for Identifying Active and Passive Zones in Reinforced Concrete," *Corrosion,* Vol. 51, No. 2, February, 1995

55. **Grant, A.,** Personal Correspondence, March 15, 1995.

56. **Hack, H. P., Moran, P. J. and Scully, J. R.,** "Influence of Electrolyte Resistance on Electrochemical Measurements and Procedures to Minimize or Compensate for Resistance Errors," *The Measurement and Correction of Electrolyte Resistance in Electrochemical Tests, ASTM STP 1056,* L. L. Scribner and S. R. Taylor, Eds., American Society for Testing and Materials, Philadelphia, 1990, pp. 5-26.

57. **Hampejs, G., Jungwirth, D., Morf, U. and Timiney, P.,** "Prestressing Materials and Systems: Galvanisation of Prestressing Steels," *FIP Notes,* 1991/4.

58. **Hartt, W. H., Kumria, C. C. and Kessler, R. J.,** "Influence of Potential, Chlorides, pH, and Precharging Time of Embrittlement of Cathodically Polarized Prestressing Steel," *Corrosion*, Vol. 49, No. 5, May 1993.

59. **Hime, W. G. and Machin, M.,** "Performance of Variances of Galvanized Steel in Mortar and Concrete," *Corrosion*, Vol. 49, No. 10, October, 1993.

60. **Hime, W. G.,** "The Corrosion of Steel - Random Thoughts and Wishful Thinking," *Concrete International,* October 1993.

61. **Hope, B. B. and Ip, A. K.,** "Grout for Post-Tensioning Ducts," *ACI Materials Journal,* July-August 1988.

62. **Isecke, B. And Miletz, J.,** "Risk of Hydrogen Embrittlement in High-Strength Prestressing Steels Under Cathodic Protection," Steel Research, Vol. 64, No. 1, January 1993, pp. 97-101.

63. **Isecke, B.,** "Collapse of the Berlin Congress Hall Prestressed Concrete Roof," *Materials Performance*, NACE, December, 1982.

64. **Jones, D. A.,** *Principles and Prevention of Corrosion*, MacMillan Publishing Company, New York, 1992.

65. **Jungwirth, D. and Windisch, A.**, "Coating of Tendons," FIP - 12th International Congress, Washington, D.C., June 2, 1994

66. **Kahhaleh, K. Z.**,"Corrosion Performance of Epoxy-Coated Reinforcement", Ph.D. Dissertation, Department of Civil Engineering, The University of Texas at Austin, Austin, TX, May 1994.

67. **Kittleman, W. M., Davis, R. T., Hamilton, H. R., Frank, K. H. and Breen, J. E.,** "Evaluation of Agents for Lubrication and Temporary Corrosion Protection of Post-Tension Tendons," *Research Report 1264-1*, Center for Transportation Research, University of Texas at Austin, August 1993.

68. **Klodt, D. T.,** "Studies of Electrochemical Corrosion and Brittle Fracture susceptibility of Prestressing Steel in Relation to Prestressed Concrete Bridges," Proceedings, 25th Conference NACE, March 10-14, 1969.

69. **Lapsley, D.**, VSL Corporation, Personal Correspondence, August 23, 1994.

70. **Leonhardt, Andra and Partners, Consulting Engineers, GmbH**, "Investigation of Cracks in the Polyethylene Pipes," Report to the Louisiana State Department of Transportation on the Luling Bridge, State Project No. 700-19-29, May 1986.

71. **Locke, C. E.,** "Corrosion of Steel in Portland Cement Concrete: Fundamental Studies," *Corrosion Effect of Stray Currents and Techniques for Evaluating Corrosion of Rebars in Concrete, ASTM STP 906*, V. Chaker, Ed., American Society for Testing and Materials, Philadelphia, 1986, pp. 5-14.

72. **Maeda, Y.,** "Cable-Stayed Steel Bridges - Developments and Perspective," The 1985 International Engineering Symposium on Structural Steel, AISC, 1985.

73. **Manning, D. G,** "Durability of Prestressed Concrete Highway Structures," NCHRP Synthesis of Highway Practice 140, Transportation Research Board, November, 1988.

74. **Manzanarez, R., Sein, C. and Smith, D.,** "Beyond Engineering: the Politics of Maracaibo," *Civil Engineering*, American Society of Civil Engineers, Vol. 61, No. 3, March 1991.

75. **Matsui, S. and Fukumoto, Y.,** "Environmental Tests to Reproduce Corrosion on Cement-Grouted Cables of Cable-Stayed Bridges," *Bridge Management 2,* Thomas Telford, London, 1993.

76. **ME 349 Corrosion Engineering Class Notes**, Professor Z. Eliezer, University of Texas at Austin, Fall 1992.

77. **Mehta, K. P.,** *Concrete in the Marine Environment,* Elsevier Applied Science, New York, 1991.

78. **Mehta, P. K. and Gerwick, B. C.,** "Cracking-Corrosion Interaction in Concrete Exposed to Marine Environment," *Concrete International,* October 1982.

79. **Moore, M.**, "Use of Epoxy Coated Prestressing Strand in Concrete Bridge Structures," FIP - 12th International Congress, Washington, D.C., June 2, 1994.

80. **MSC,** "New System Offers Enhanced Corrosion Protection for Bridge Stay Cables," *Modern Steel Construction,* July 1991.

81. **National Oceanic and Atmospheric Administration,** "Local Climatological Data Monthly Summary, Austin," U.S. Department of Commerce, National Climatic Data Center, Asheville, North Carolina, November, 1993 through April 1995.

82. **Naudts, A.,** "Grouting Trends," *Civil Engineering,* American Society of Civil Engineers, October 1989.

83. **Neville, A. M.,** *Properties of Concrete,* Pitman Publishing, London, 1981.

84. **Novokshchenov, V.,** "Brittle Fractures of Prestressed Bridge Steel Exposed to Chloride-Bearing Environments Caused by Corrosion-Generated Hydrogen," *Corrosion,* NACE International, Vol. 50, No. 6, June 1994.

85. **Otaola, M.,** "Replacing Corroded Cables on a Cable-Stayed Bridge," *Civil Engineering,* American Society of Civil Engineers, Vol. 52, No. 9, September 1982.

86. **Parkins, R. N., Elices, M., Sanchez-Galvez, V. and Caballero, L.,** "Environment Sensitive Cracking of Pre-Stressing Steels," *Corrosion Science,* Vol. 22, No. 5, 1982, pp. 392-405.

87. **PCI Committee on Post-Tensioning,** "Recommended Practice for Grouting of Post-Tensioned Prestressed Concrete," *Journal of the Prestressed Concrete Institute,* November-December 1972.

88. **Perenchio, W. F., Fraczek, J. and Pfeifer, D. W.** "Corrosion Protection of Prestressing Systems in Concrete Bridges," NCHRP Report 313, Transportation Research Board, Washington, D.C., February 1989.

89. **Perenchio, W. F., Fraczek, J. and Pfeifer, D. W.,** "Corrosion Protection of Prestressing Systems in Concrete Bridges," NCHRP Report 313, Transportation Research Board, Washington, D. C., February, 1989.

90. **Podolny, Jr., W. and Scalzi, J. B.,** *Construction and Design of Cable-Stayed Bridges*, John Wiley and Sons, New York, 1986.

91. **Post-Tensioning Institute**, "Recommended Practice for Grouting of Post-Tensioned Prestressed Concrete," *Post-Tensioning Manual Fifth Edition*, Post-Tensioning Institute, Phoenix, 1990.

92. **Post-Tensioning Institute**, "Specifications for Unbonded Single-Strand Tendons," *Post-Tensioning Manual Fifth Edition*, Post-Tensioning Institute, Phoenix, 1990

93. **Poston, R. W.,** "Improving Durability of Bridge Decks by Transverse Prestressing", Ph.D. Dissertation, Department of Civil Engineering, The University of Texas at Austin, Austin, TX, December 1984.

94. **Prestressed Concrete Institute Ad Hoc Committee on Epoxy-Coated Strand**, "Guidelines for the Use of Epoxy-Coated Strand," *Journal of the Prestressed Concrete Institute*, July-August 1993, pp. 26-32.

95. **PSG Corrosion Engineering, Inc.,** "Corrosion Investigation of Stay Cable Wires for Full Scale Cable Stay Test Specimens for Mississippi River Bridge at Burlington," unpublished report, September 1991.

96. **Raharinaivo, A., Bot, H., Creton, B. and Olivie, R.,** "Experimental Use of Galvanized Prestressing Steel for Stiffening the Roquemaure Bridge (France) by Additional Prestressing," *Galvanized Reinforcement for Concrete - II,"* International Lead Zinc Research Organization, 1981.

97. **Ryals, K. K., Breen, J. E. and Kreger, M. E.,** "Fretting Fatigue in External Post-Tensioned Tendons," Research Report 1211-1F, Center for Transportation Research, The University of Texas at Austin, December 1992.

98. **Saul, R. and Svensson, H. S.,** "On the Corrosion Protection of Stay Cables," *Der Stahlbau*, No. 6, pp. 165-176, 1990

99. **Schiessl, P.,** *Corrosion of Steel in Concrete*, Report of the Technical Committee 60-CSC RILEM, Chapman and Hall, New York, 1988.

100. **Schupack, M. and Suarez, M. G.,** "Some Recent Corrosion Embrittlement Failures of Prestressing Systems in the United States," *Journal of the Prestressed Concrete Institute*, March-April, 1982.

101. **Schupack, M.,** "Admixture for Controlling Bleed in Cement Grout Used in Post-Tensioning," *Journal of the Prestressed Concrete Institute*, November-December 1974.

102. **Schupack, M.,** "Durability Study of a 35-year-old Post-Tensioned Bridge," *Concrete International*, February 1994.

103. **Schupack, M.,** "Grouting Aid for Controlling the Separation of Water for Cement Grout for Grouting Vertical Tendons in Nuclear Concrete Pressure Vessels," International Conference on

Experience in the Design, Construction and Operation of Prestressed Concrete Pressure Vessels and Containments for Nuclear Reactors, University of York, England, September, 8-12, 1975.

104. **Schupack, M.,** "Grouting Tests on Large Post-Tensioning Tendons for Secondary Nuclear Containment Structures," *Journal of the Prestressed Concrete Institute,* March-April 1971.

105. **Schupack, M.,** "Protecting Post-Tensioning Tendons in Concrete Structures," *Civil Engineering,* American Society of Civil Engineers, December 1982.

106. **Schupack, Suarez Engineers, Inc,** "Mississippi River Bridge - Luling Grouting of Cable Stays," Status Report No. 3, January 25, 1983.

107. **Schütt, K., Diederichs, U. and Rostásy, F. S.,** "Improvement of Performance of Grouts for Corrosion Protection of Post-Tensioning Tendons by Silica Fume Addition," FIP - 11th International Congress on Prestressed Concrete, Hamburg, June 4-9, 1990.

108. **Shinko Wire Company, Ltd.,** "Test Report on Weather-Resistance of Wrapping Tapes for Cable Stayed Bridges," Report No. SWENH-8603, April 30, 1984.

109. **Stafford, D. G. and Watson, S. C.,** "A Discussion of Some Critical Corrosion Problems in the Cable Elements of Stayed Girder Structures," US-European Workshop on Bridge Evaluation, Repair and Rehabilitation, St. Rémy-lès-Chevreuse, June 1987.

110. **Stafford, D. G. and Watson, S. C.,** "Cables in Trouble," *Civil Engineering,* American Society of Civil Engineers, Vol. 58, No. 4, April 1988.

111. **Subcommittee G01.14 on Corrosion of Reinforcing, Steel and Metal Properties Council**, *Corrosion of Metals in Association with Concrete, ASTM STP 818,* Slater, J. E., Ed., American Society for Testing and Materials, Philadelphia, 1983.

112. **Swait, J. and Funahashi, M.,** "Corrosion Protection Systems for Bridge Stay Cables and Anchorages Volume I: Final Report," Report No. FHWA-RD-91-050, Federal Highway Administration, Washington, D.C., May, 1991, pp. 163.

113. **Takena, K., Miki, C., Shimokawa, H. and Sakamoto, K.**, "Fatigue Resistance of Large-Diameter Cable for Cable-Stayed Bridges," *ASCE Journal of Structural Engineering,* Vol. 118, No. 3, March 1992.

114. **Tanabe, S. and Hosokawa, H.,** "Durability of Cables Stays for Cable-Stayed Bridges," *Structural Engineering International,* IABSE, Vol. 1, No. 1, February, 1991, pp. 60-62.

115. **Tanaka, Y. and Haraguchi, T.,** "Some Aspects of a Cable System for Cable-Stayed Bridges," 4th International Conference on Structural Safety and Reliability, 1985

116. **Technical University of Munich,** "Report on the Dynamic Test with Subsequent Tensile Test on a Cable with End Anchorages 37 Strand 0.6" Diameter; Nominal Ultimate Load 9.64 MN," May 21, 1985.

117. **Technical University of Munich,** "Report on the Dynamic Test with Subsequent Tensile Test on a Cable with End Anchorages 44 Strand 0.6" Diameter; Nominal Ultimate Load 11.47 MN," May 3, 1985.

118. **Thompson, N. G., Lankard, D. and Sprinkel, M.,** "Grouting Technology for Bonded Tendons in Post-Tensioned Bridge Structures," Report No. FWHA-RD-90-102, Federal Highway Administration, October 1990.

119. **Thompson, N. G., Lankard, D. and Sprinkel, M.,** "Grouts for Bonded Post-Tensioned Concrete Construction: Protecting Prestressing Steel from Corrosion," *ACI Materials Journal,* September-October 1993.

120. **Thompson, N. G., Lankard, D. and Sprinkel, M.,** "Improved Grouts for Bonded Tendons in Post-Tensioned Bridge Structures," Report No. FWHA-RD-91-092, Federal Highway Administration, January 1992.

121. **Treadaway, K. W. J., Brown, B. L. and Cox, R. N.,** "Durability of Galvanized Steel in Concrete," *Durability of Reinforcing Steel in Concrete, ASTM STP 713,* D. E. Tonini and J. M. Gaidis, Eds., American Society for Testing and Materials, Philadelphia, 1980, pp. 102-131.

122. **Troitsky, M. S.,** *Cable-Stayed Bridges-An Approach to Modern Bridge Design,* Van Nostrand Reinhold Company, New York, 1988.

123. **Uhlig H. H. and Revie, R. W.,** *Corrosion and Corrosion Control,* John Wiley and Sons, 1985.

124. **VSL**, Product Information Pamphlet, March 1994.

125. **Walther, R., Bernard, H., Malmar, I. and Moïa, P.**, *Cable Stayed Bridges,* Thomas Telford, London, 1988

126. **Woodward, R. J. and Miller, E.,** "Grouting Post-Tensioned Concrete Bridges: the Prevention of Voids," *Highways and Transportation,* Vol. 37, No. 6, June, 1990, pp. 9-17.

127. **Woodward, R. J. and Williams, F. W.,** "Collapse of Ynys-y-Gwas Bridge, West Glamorgan," *Proceedings of the Institution of Civil Engineers,* Vol. 85, No. 1, August 1988, pp. 635-669.

128. **Working Group on Grouting of Tendons in Prestressed Concrete**, *Grouting of Tendons in Prestressed Concrete,* Fédération Internationale de la Précontrainte, FIP Guide to Good Practice, Thomas Telford, Ltd., London, 1990.

129. **Yamaoka, Y. and Tanaka, Y.,** "Comparison of the Mechanisms of Hydrogen Embrittlement and Stress Corrosion Cracking of High Carbon Steel Wire," International Workshop on Prestressing Wire, Denver, October 7-8, 1993.

130. **Yamaoka, Y., Kideyoshi, T. and Kurauchi, M.,** "Effect of Galvanizing on Hydrogen Embrittlement of Prestressing Wire," *Journal of the Prestressed Concrete Institute,* July-August, 1988.

131. **Yeomans, S. R.,** "Corrosion Testing of Black, Galvanized and Epoxy Coated Reinforcing Steel in Concrete," NACE Annual Conference, Paper No. 329, 1993.